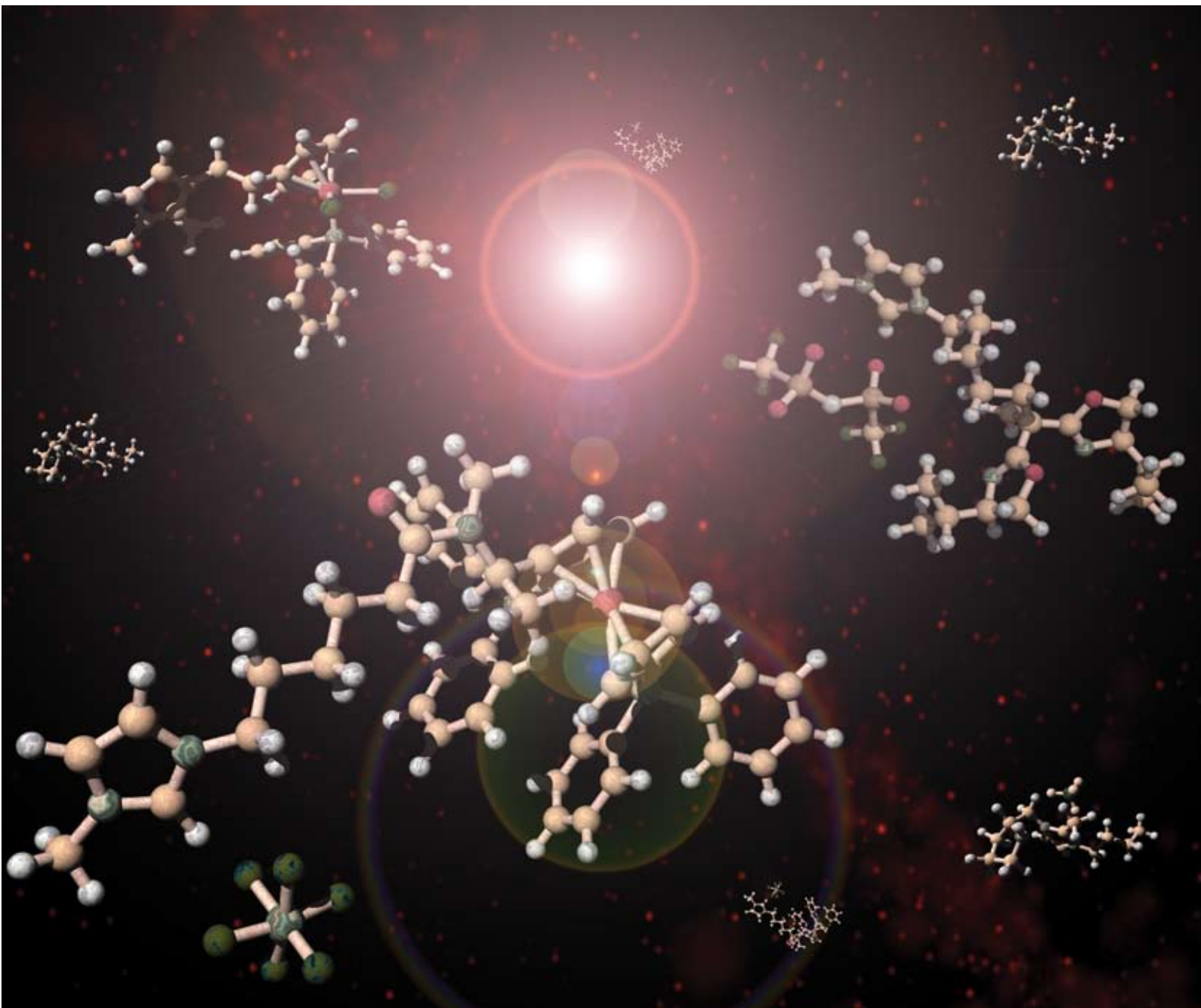


# Green Chemistry

Cutting-edge research for a greener sustainable future

[www.rsc.org/greenchem](http://www.rsc.org/greenchem)

Volume 10 | Number 5 | May 2008 | Pages 473–596



ISSN 1463-9262

Šebesta *et al.*  
Catalysts with ionic tag and their use  
in ionic liquids  
Goto *et al.*  
Enzymatic reactions in water-in-ionic  
liquid microemulsions



1463-9262(2008)10:5;1-D

RSC Publishing



# years of publishing!

## *Green Chemistry...*



- The most highly cited *Green Chemistry* journal, Impact factor = 4.192\*
- Fast publication, typically <90 days for full papers
- Full variety of research including reviews, communications, full papers and perspectives.

Celebrating 10 years of publishing, *Green Chemistry* offers the latest research that reduces the environmental impact of the chemical enterprise by developing alternative sustainable technologies, and provides a unique forum for the rapid publication of cutting-edge and innovative research for a greener, sustainable future

*...for a sustainable future!*

\* 2006 Thomson Scientific (ISI) Journal Citation Reports ®

# Green Chemistry

Cutting-edge research for a greener sustainable future

[www.rsc.org/greenchem](http://www.rsc.org/greenchem)

RSC Publishing is a not-for-profit publisher and a division of the Royal Society of Chemistry. Any surplus made is used to support charitable activities aimed at advancing the chemical sciences. Full details are available from [www.rsc.org](http://www.rsc.org)

## IN THIS ISSUE

ISSN 1463-9262 CODEN GRCHFJ 10(5) 473–596 (2008)



### Cover

See Šebesta *et al.*, pp. 484–496. The image depicts some catalysts with ionic tags, which can be advantageously used in ionic liquids. Molecular models were prepared by POV-Ray (Persistence of Vision Pty, Ltd. (2004) Persistence of Vision Raytracer (Version 3.6) [Computer software]. Retrieved from <http://www.povray.org/download/>).

Image reproduced by permission from Radovan Šebesta, from *Green Chem.*, 2008, **10**, 484.

## CHEMICAL TECHNOLOGY

### T33

Drawing together research highlights and news from all RSC publications, *Chemical Technology* provides a ‘snapshot’ of the latest applications and technological aspects of research across the chemical sciences, showcasing newsworthy articles and significant scientific advances.

## Chemical Technology

May 2008/Volume 5/Issue 5

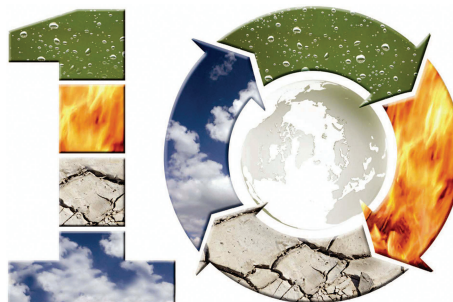
[www.rsc.org/chemicaltechnology](http://www.rsc.org/chemicaltechnology)

## EDITORIAL

### 483

#### Is catalysis in ionic liquids a *potentially* green technology?

Professor Tom Welton discusses the whether catalysis in ionic liquids can be a green technology.



## EDITORIAL STAFF

**Editor**

Sarah Ruthven

**Assistant editor**

Sarah Dixon

**Publishing assistant**

Ruth Bircham

**Team leader, serials production**

Stephen Wilkes

**Technical editor**

Edward Morgan

**Production administration coordinator**

Sonya Spring

**Administration assistants**Clare Davies, Donna Fordham, Kirsty Lunnon,  
Julie Thompson**Publisher**

Emma Wilson

Green Chemistry (print: ISSN 1463-9262; electronic: ISSN 1463-9270) is published 12 times a year by the Royal Society of Chemistry, Thomas Graham House, Science Park, Milton Road, Cambridge, UK CB4 0WF.

All orders, with cheques made payable to the Royal Society of Chemistry, should be sent to RSC Distribution Services, c/o Portland Customer Services, Commerce Way, Colchester, Essex, UK CO2 8HP. Tel +44 (0) 1206 226050; E-mail sales@rscdistribution.org

2008 Annual (print + electronic) subscription price: £947; US\$1799. 2008 Annual (electronic) subscription price: £852; US\$1695. Customers in Canada will be subject to a surcharge to cover GST. Customers in the EU subscribing to the electronic version only will be charged VAT.

If you take an institutional subscription to any RSC journal you are entitled to free, site-wide web access to that journal. You can arrange access via Internet Protocol (IP) address at [www.rsc.org/ip](http://www.rsc.org/ip). Customers should make payments by cheque in sterling payable on a UK clearing bank or in US dollars payable on a US clearing bank. Periodicals postage paid at Rahway, NJ, USA and at additional mailing offices. Airfreight and mailing in the USA by Mercury Airfreight International Ltd., 365 Blair Road, Avenel, NJ 07001, USA.

US Postmaster: send address changes to Green Chemistry, c/o Mercury Airfreight International Ltd., 365 Blair Road, Avenel, NJ 07001. All despatches outside the UK by Consolidated Airfreight.

PRINTED IN THE UK

**Advertisement sales:** Tel +44 (0) 1223 432246; Fax +44 (0) 1223 426017; E-mail [advertising@rsc.org](mailto:advertising@rsc.org)

# Green Chemistry

Cutting-edge research for a greener sustainable future

[www.rsc.org/greenchem](http://www.rsc.org/greenchem)

Green Chemistry focuses on cutting-edge research that attempts to reduce the environmental impact of the chemical enterprise by developing a technology base that is inherently non-toxic to living things and the environment.

## EDITORIAL BOARD

**Chair**

Professor Martyn Poliakoff  
Nottingham, UK

**Scientific Editor**

Professor Walter Leitner  
RWTH-Aachen, Germany

**Associate Editors**

Professor C. J. Li  
McGill University, Canada

**Members**

Professor Paul Anastas  
Yale University, USA  
Professor Joan Brennecke  
University of Notre Dame, USA  
Professor Mike Green  
Sasol, South Africa  
Professor Buxing Han  
Chinese Academy of Sciences,  
China

Dr Alexei Lapkin  
Bath University, UK  
Professor Steven Ley  
Cambridge, UK  
Dr Janet Scott  
Unilever, UK  
Professor Tom Welton  
Imperial College, UK

## ADVISORY BOARD

James Clark, York, UK  
Avelino Corma, Universidad  
Politécnica de Valencia, Spain  
Mark Harmer, DuPont Central  
R&D, USA  
Herbert Hugl, Lanxess Fine  
Chemicals, Germany  
Roshan Jachuck,  
Clarkson University, USA  
Makato Misono, nite,  
Japan

Colin Raston,  
University of Western Australia,  
Australia  
Robin D. Rogers, Centre for Green  
Manufacturing, USA  
Kenneth Seddon, Queen's  
University, Belfast, UK  
Roger Sheldon, Delft University of  
Technology, The Netherlands  
Gary Sheldrake, Queen's  
University, Belfast, UK

Pietro Tundo, Università ca  
Foscari di Venezia, Italy

## INFORMATION FOR AUTHORS

Full details of how to submit material for publication in Green Chemistry are given in the Instructions for Authors (available from <http://www.rsc.org/authors>). Submissions should be sent via ReSource: <http://www.rsc.org/resource>.

Authors may reproduce/republish portions of their published contribution without seeking permission from the RSC, provided that any such republication is accompanied by an acknowledgement in the form: (Original citation) – Reproduced by permission of the Royal Society of Chemistry.

© The Royal Society of Chemistry 2008. Apart from fair dealing for the purposes of research or private study for non-commercial purposes, or criticism or review, as permitted under the Copyright, Designs and Patents Act 1988 and the Copyright and Related Rights Regulations 2003, this publication may only be reproduced, stored or transmitted, in any form or by any means, with the prior permission in writing of the Publishers or in the case of reprographic reproduction in accordance with the terms of licences issued by the Copyright Licensing Agency in the UK. US copyright law is applicable to users in the USA.

The Royal Society of Chemistry takes reasonable care in the preparation of this publication but does not accept liability for the consequences of any errors or omissions.

The paper used in this publication meets the requirements of ANSI/NISO Z39.48-1992 (Permanence of Paper).

Royal Society of Chemistry: Registered Charity No. 207890



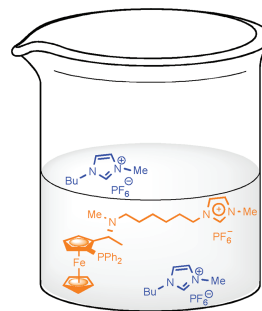
## CRITICAL REVIEW

484

**Catalysts with ionic tag and their use in ionic liquids**

Radovan Šebesta,\* Iveta Kmentová and Štefan Toma

Homogenous supported catalysts combine features of both homogeneous and heterogeneous catalysis. Ionically-tagged catalysts in ionic liquids offer several advantages, such as high catalytic activities and selectivities, easy product isolation and catalyst recyclability.



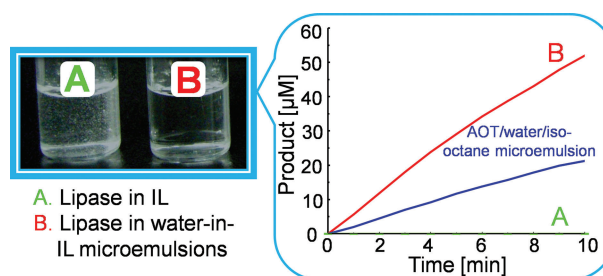
## COMMUNICATION

497

**Water-in-ionic liquid microemulsions as a new medium for enzymatic reactions**

Muhammad Moniruzzaman, Noriho Kamiya, Kazunori Nakashima and Masahiro Goto\*

Enzymes can be solubilized in ionic liquids (ILs) by the formation of water domains in a hydrophobic IL with an anionic sodium bis(2-ethyl-1-hexyl) sulfosuccinate (AOT) surfactant. The catalytic activity of one of the enzymes studied (lipase PS) became higher than in microemulsions of AOT in isooctane.



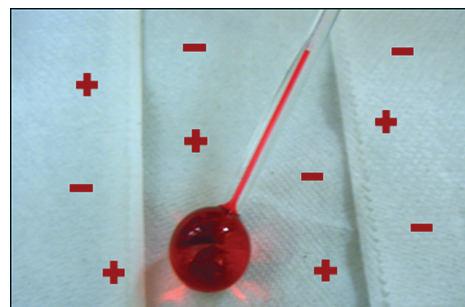
## PAPERS

501

**Ionic liquids for liquid-in-glass thermometers**

Héctor Rodríguez, Margaret Williams, John S. Wilkes and Robin D. Rogers\*

Ionic liquids can constitute a potentially green alternative to the fluids currently used in liquid-in-glass thermometers, additionally allowing for a high degree of customization of these devices.

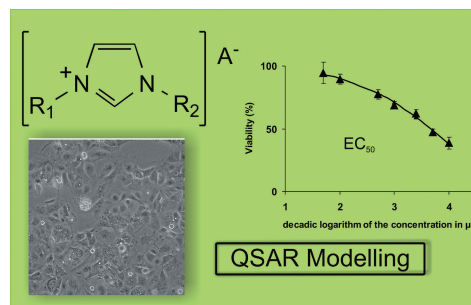


508

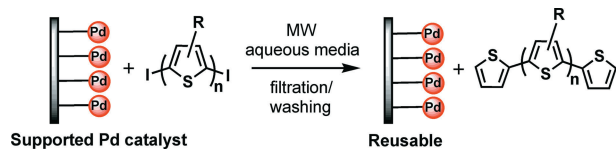
**Cytotoxicity of selected imidazolium-derived ionic liquids in the human Caco-2 cell line. Sub-structural toxicological interpretation through a QSAR study**

Andrés García-Lorenzo, Emilia Tojo, José Tojo, Marta Teijeira, Francisco J. Rodríguez-Berrocal, Maykel Pérez González and Vicenta S. Martínez-Zorzano\*

A group of imidazolium-derived ILs was tested for their cytotoxicity in the Caco-2 human cell line. Using the experimental data we developed a QSAR model which was used to elucidate the structural factors that govern the toxicity of these compounds.



517

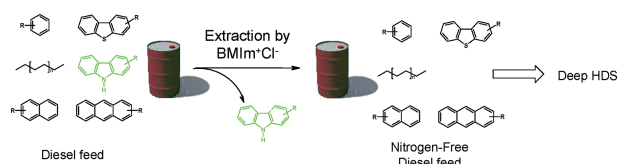


### Microwave-assisted synthesis of oligothiophene semiconductors in aqueous media using silica and chitosan supported Pd catalysts

Silvia Alesi,\* Francesca Di Maria, Manuela Melucci, Duncan J. Macquarrie, Rafael Luque and Giovanna Barbarella

Highly pure thiophene semiconductors were prepared by an innovative microwave-assisted methodology based on Suzuki coupling, using silica and chitosan supported palladium catalysts in aqueous media.

524



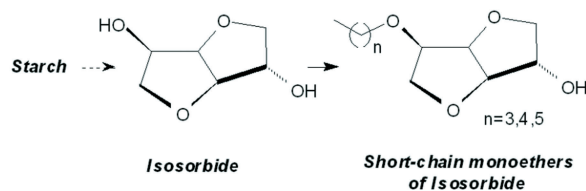
### Selective extraction of neutral nitrogen compounds found in diesel feed by 1-butyl-3-methyl-imidazolium chloride

Li-Li Xie, Alain Favre-Reguillon,\* Xu-Xu Wang, Xianzhi Fu, Stéphane Pellet-Rostaing, Guy Toussaint, Christophe Geantet, Michel Vrinat and Marc Lemaire\*

BMIm<sup>+</sup>Cl<sup>-</sup> have been used for the selective extraction of neutral N-compounds found in diesel feed. Elimination of such HDS inhibitors could lead to improvement of the deep HDS process.

532

Renewable resource  $\rightarrow$  Original polar head  $\rightarrow$  Efficient hydrotropes

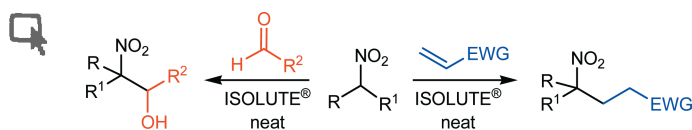


### Isosorbide as a novel polar head derived from renewable resources. Application to the design of short-chain amphiphiles with hydrotropic properties

Ying Zhu, Morgan Durand, Valérie Molinier and Jean-Marie Aubry\*

The potential use of isosorbide, an original diol readily obtained by the double dehydration of sorbitol, has been investigated for the synthesis of novel amphiphilic species.

541



### ISOLUTE<sup>®</sup> Si-carbonate catalyzes the nitronate addition to both aldehydes and electron-poor alkenes under solvent-free conditions

Roberto Ballini,\* Giovanna Bosica, Alessandro Palmieri, Ferdinando Pizzo and Luigi Vaccaro

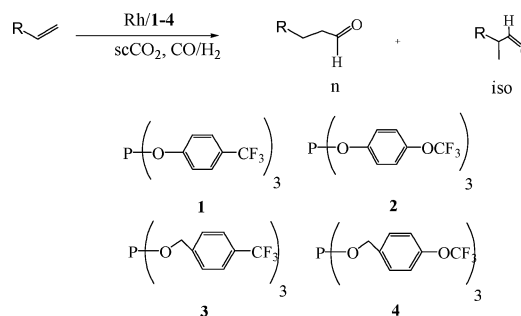
Commercially available ISOLUTE<sup>®</sup> Si-carbonate catalyzes both nitroaldol and Michael reactions, from nitroalkanes and under solvent-free conditions, yielding nitroalkenols and  $\gamma$ -nitro-functionalized carbonyl and cyano derivatives

545

**New rhodium catalytic systems with trifluoromethyl phosphite derivatives for the hydroformylation of 1-octene in supercritical carbon dioxide**

Clara Tortosa Estorach, Arantxa Orejón and Anna M. Masdeu-Bultó\*

Hydroformylation of 1-octene in supercritical carbon dioxide was performed using new soluble rhodium-phosphite catalytic systems.

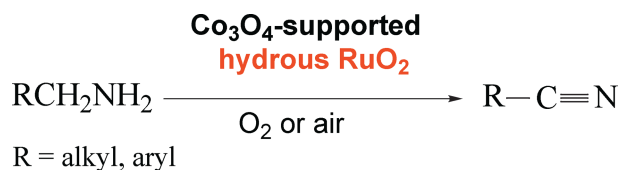


553

**Hydrous ruthenium oxide supported on  $Co_3O_4$  as efficient catalyst for aerobic oxidation of amines**

Feng Li, Jing Chen, Qinghong Zhang and Ye Wang\*

The hydrous  $RuO_2$  catalyst dispersed on  $Co_3O_4$  can catalyse the selective oxidation of amines efficiently by oxygen or air. The catalyst is recyclable and can be operated under solvent-free conditions.

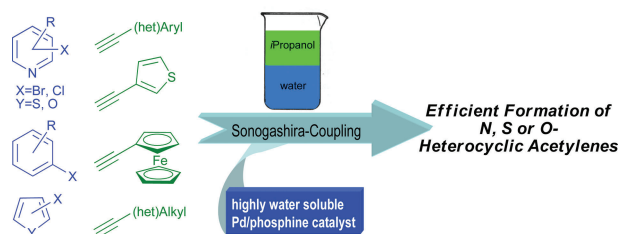


563

**Aqueous/organic cross coupling: Sustainable protocol for Sonogashira reactions of heterocycles**

Christoph A. Fleckenstein and Herbert Plenio\*

The water soluble Pd complex of dicyclohexyl(2-sulfo-9-(3-(4-sulfophenyl)propyl)-9H-fluoren-9-yl)phosphine was used for an efficient copper free and sustainable reaction protocol for Sonogashira cross couplings of heterocyclic aryl chlorides and bromides.

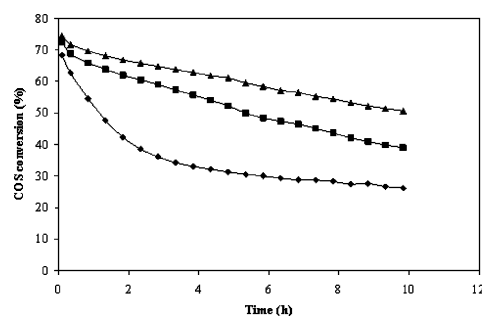


571

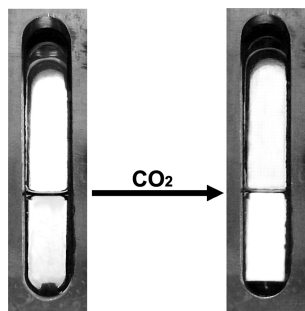
**Purification of chemical feedstocks by the removal of aerial carbonyl sulfide by hydrolysis using rare earth promoted alumina catalysts**

Hongmei Huang, Nicola Young, B. Peter Williams, Stuart H. Taylor and Graham Hutchings\*

$Al_2O_3$  ( $\blacklozenge$ ) is an effective commercial catalyst for COS hydrolysis and addition of  $Y_2O_3$  [ $\blacksquare$  3%, ( $\blacktriangle$ ) 10%] leads to enhancement in catalytic activity as a result of increased basicity.



578

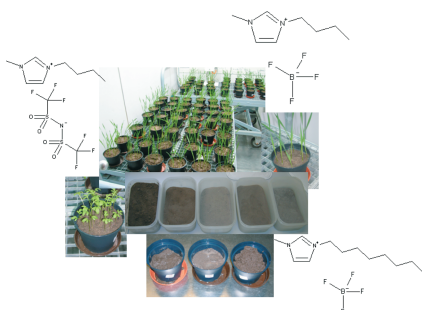


### A new separation method: combination of CO<sub>2</sub> and surfactant aqueous solutions

Xiaoying Feng, Jianling Zhang, Siqing Cheng, Chaoxing Zhang, Wei Li and Buxing Han\*

Phenol and vanadium-8-hydroxyquinoline complexes in aqueous solutions can be separated efficiently by combination of CO<sub>2</sub> and Triton X-100. Also, gold nanoparticles synthesized in Triton X-100 micellar solutions can be recovered by adding CO<sub>2</sub> and the surfactant remains in the solution. This new separation method has wide potential applications.

584

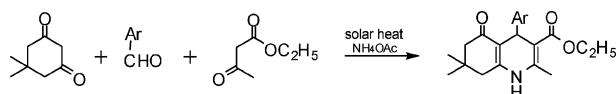


### Imidazolium based ionic liquids in soils: effects of the side chain length on wheat (*Triticum aestivum*) and cress (*Lepidium sativum*) as affected by different clays and organic matter

Marianne Matzke,\* Stefan Stolte, Jürgen Arning, Ute Uebers and Juliane Filser

This study checked the influence of clay minerals and organic matter on the toxicity of imidazolium based ionic liquids for wheat (*Triticum aestivum*) and cress (*Lepidium sativum*). These experiments should help to enlarge the knowledge base on fate and behavior of ionic liquids in the terrestrial environment.

592



### Solar thermochemical reactions: four-component synthesis of polyhydroquinoline derivatives induced by solar thermal energy

Ramadan Ahmed Mekheimer, Afaf Abdel Hameed and Kamal Usef Sadek\*

The synthesis of polyhydroquinoline derivatives *via* a four-component unsymmetric Hantzsch reaction induced by solar thermal energy is reported.




## AUTHOR INDEX

- Alesi, Silvia, 517  
 Arning, Jürgen, 584  
 Aubry, Jean-Marie, 532  
 Ballini, Roberto, 541  
 Barbarella, Giovanna, 517  
 Bosica, Giovanna, 541  
 Chen, Jing, 553  
 Cheng, Siqing, 578  
 Di Maria, Francesca, 517  
 Durand, Morgan, 532  
 Estorach, Clara Tortosa, 545  
 Favre-Reguillon, Alain, 524  
 Feng, Xiaoying, 578  
 Filser, Juliane, 584  
 Fleckenstein, Christoph A., 563  
 Fu, Xianzhi, 524  
 García-Lorenzo, Andrés, 508  
 Geantet, Christophe, 524
- González, Maykel Pérez, 508  
 Goto, Masahiro, 497  
 Hameed, Afaf Abdel, 592  
 Han, Buxing, 578  
 Huang, Hongmei, 571  
 Hutchings, Graham, 571  
 Kamiya, Noriho, 497  
 Kmentová, Iveta, 484  
 Lemaire, Marc, 524  
 Li, Feng, 553  
 Li, Wei, 578  
 Luque, Rafael, 517  
 Macquarrie, Duncan J., 517  
 Martínez-Zorzano, Vicenta S., 508  
 Masdeu-Bultó, Anna M., 545  
 Matzke, Marianne, 584  
 Mekheimer, Ramadan Ahmed, 592  
 Melucci, Manuela, 517
- Molinier, Valérie, 532  
 Moniruzzaman, Muhammad, 497  
 Nakashima, Kazunori, 497  
 Orejón, Arantxa, 545  
 Palmieri, Alessandro, 541  
 Pellet-Rostaing, Stéphane, 524  
 Pizzo, Ferdinando, 541  
 Plenio, Herbert, 563  
 Rodríguez, Héctor, 501  
 Rodríguez-Berrocal, Francisco J., 508  
 Rogers, Robin D., 501  
 Sadek, Kamal Usef, 592  
 Šebesta, Radovan, 484  
 Stolte, Stefan, 584  
 Taylor, Stuart H., 571  
 Teixeira, Marta, 508  
 Tojo, Emilia, 508
- Tojo, José, 508  
 Toma, Stefan, 484  
 Toussaint, Guy, 524  
 Uebbers, Ute, 584  
 Vaccaro, Luigi, 541  
 Zrinat, Michel, 524  
 Wang, Xu-Xu, 524  
 Wang, Ye, 553  
 Wilkes, John S., 501  
 Williams, B. Peter, 571  
 Williams, Margaret, 501  
 Xie, Li-Li, 524  
 Young, Nicola, 571  
 Zhang, Chaoxing, 578  
 Zhang, Jianling, 578  
 Zhang, Qinghong, 553  
 Zhu, Ying, 532

## FREE E-MAIL ALERTS AND RSS FEEDS


Contents lists in advance of publication are available on the web *via* [www.rsc.org/greenchem](http://www.rsc.org/greenchem) – or take advantage of our free e-mail alerting service ([www.rsc.org/ej\\_alert](http://www.rsc.org/ej_alert)) to receive notification each time a new list becomes available.

 Try our RSS feeds for up-to-the-minute news of the latest research. By setting up RSS feeds, preferably using feed reader software, you can be alerted to the latest Advance Articles published on the RSC web site. Visit [www.rsc.org/publishing/technology/rss.asp](http://www.rsc.org/publishing/technology/rss.asp) for details.

## ADVANCE ARTICLES AND ELECTRONIC JOURNAL

Free site-wide access to Advance Articles and the electronic form of this journal is provided with a full-rate institutional subscription. See [www.rsc.org/ejs](http://www.rsc.org/ejs) for more information.

\* Indicates the author for correspondence: see article for details.

 Electronic supplementary information (ESI) is available *via* the online article (see <http://www.rsc.org/esi> for general information about ESI).

# Get straight to the point



**Chemical  
Technology**  
[www.rsc.org/chemicaltechnology](http://www.rsc.org/chemicaltechnology)

**Chemical  
Science**  
[www.rsc.org/chemicalscience](http://www.rsc.org/chemicalscience)

**Chemical  
Biology**  
[www.rsc.org/chembiology](http://www.rsc.org/chembiology)

## Keep track of the latest developments from across the chemical sciences with succinct newsworthy accounts

Online access to *Chemical Technology*, *Chemical Science* and *Chemical Biology* is completely free. With *Research highlights* showcasing articles published across the breadth of RSC journals, *Instant insights* offering whirlwind tours of exciting research areas and leading scientists sharing their opinions in specialist *Interviews*, the magazines are an essential tool for scientists wishing to stay on top of the news and developments in their field and related areas. And all journal articles covered in the news magazines have free online access for a period of eight weeks. Go online now to find out more!

RSC Publishing

[www.rsc.org/journals](http://www.rsc.org/journals)

Registered Charity Number 207890



**Faced with questions?**

- Can I search by structure to find articles?
- Are there any related articles on this topic?
- What groups and relationships are there for this compound?
- Is there any Patent information?
- Can I download files of these structures?
- What's the definition of that term?

**Looking for answers?**

## Use RSC Prospect enhanced HTML journal articles

Linking together related articles by subject ontologies and identified compounds, *RSC Prospect* enhanced HTML articles also provide you with definitions, synonyms, structures and RSS feeds. We've now introduced a structure and sub-structure searching function, widened the compound identifiers to include groups and relationships via the ChEBI (Chemical Entities of Biological Interest) ontology, and included additional features such as an Experimental Data Checker to allow downloading of data for analysis of results. Links to patent information and to compounds in PubChem have also been added.

Hailed as the future of publishing, we add computer readable meaning to our journal articles by applying internationally recognised labels and conventions. We are proud to be leading the way amongst scientific publishers.

*RSC Prospect* - winner of the 2007 ALPSP/Charlesworth Award for Publishing Innovation.



0208106

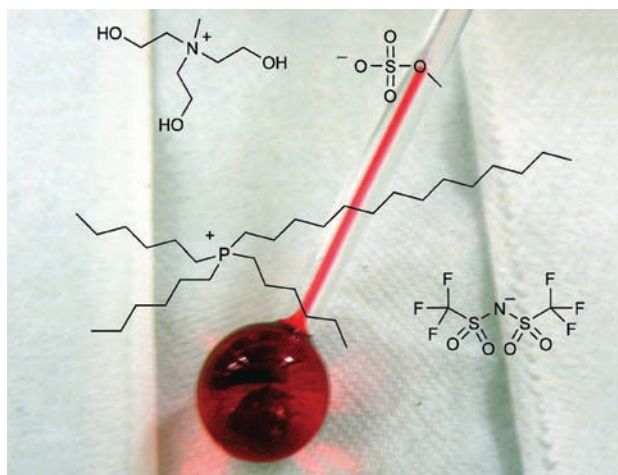
# Chemical Technology

## New role for ionic liquids could take temperature measurement to extremes Designer thermometers rise to new levels

Scientists in Europe and the US have used ionic liquids in liquid-in-glass thermometers as alternatives to mercury and ethanol.

Ionic liquids (ILs) are salts in liquid form and already have a wide range of applications, from use in drug delivery to fuel cells and batteries. Robin Rogers of The Queen's University of Belfast, UK, and his colleagues have now found another role for them. 'We have known the basic properties of ILs and have thought for some time that they should make a great thermometer fluid,' says Rogers. 'We simply had to prove it!'

ILs offer several advantages for thermometers: they have a faster temperature response time compared to mercury and operate over a wider range of temperatures compared to many molecular liquids, including ethanol. Non-toxic ILs can be used and their low volatility reduces their ability to escape into the environment, giving an additional environmental advantage over mercury, which needs to be carefully disposed of if a



thermometer is broken.

To make its thermometers the US team used normally clear ionic liquids coloured red with an IL-dye. This made the liquid level easily visible without affecting the linear relationship between liquid volume and temperature. The thermometers could be adapted for a particular temperature range by changing the make-up of the liquid.

**Ionic liquid thermometers can be adapted for a particular temperature range by changing the liquid's make-up**

#### Reference

H Rodriguez *et al*, *Green Chem.*, 2008, DOI: 10.1039/b800366a

Rogers and colleagues chose an ammonium-based liquid for general applications, as it is economical and non-toxic. They also used an alkylphosphonium-based liquid for a more specialised thermometer with a wider temperature range.

Rogers suggests that the thermometers could have uses both in industry and research and development. 'Specialty thermometers with a suitable liquid range could be interesting for operation under extreme environment conditions,' he says, 'for example, Antarctica and deep sea vents.'

Gary Baker, who also works with ILs, at Oak Ridge National Laboratory, US, says that 'using an IL as a filling fluid toward a new class of liquid-in-glass thermometer nicely illustrates the broad potential of ILs as potentially green replacements for conventional solvents.' He adds that 'the work opens up yet another avenue in engineering science, as ILs continue to find relevance in increasingly diverse areas.'

Sylvia Pegg

## In this issue

### A bright future for solar cells

Dye-sensitised solar cells look to improve their share of the retail market

### Nerve agent detector on a chip

Device performs multistep sequence to detect neurotoxins in droplet of blood

### Instant insight: Detection on the nanoscale

Nicholas Picczonka and Ricardo Aroca use Raman scattering to look at one molecule in a million

### Interview: Having a gas

Gary Hieftje tells Nina Notman about the fun side of science



The latest applications and technological aspects of research across the chemical sciences



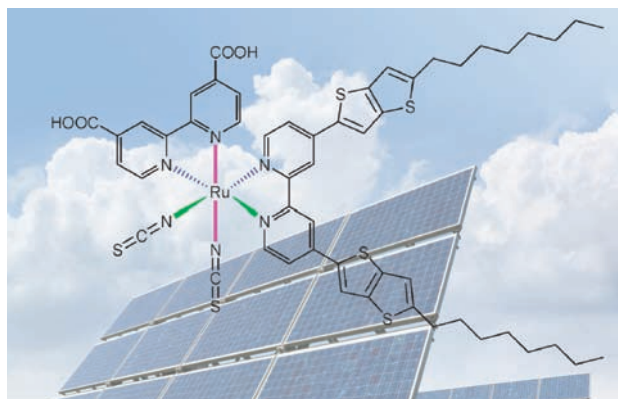
# Application highlights

Dye-sensitised solar cells look to improve their share of the retail market

## A bright future for solar cells

A new efficient light harvesting molecule could lead to cheaper solar cells, claim international scientists.

Developed in the early 1990s, dye-sensitised solar cells are a class of low-cost solar cells which have a layer of titanium dioxide coated with a light-harvesting sensitiser (dye). Peng Wang from Changchun Institute of Applied Chemistry, China, and Shaik Zakeeruddin and Michael Grätzel from Swiss Federal Institute of Technology, Lausanne, Switzerland, and colleagues have made a new sensitiser with a high extinction coefficient – meaning it is excellent at absorbing light. The new sensitiser is a ruthenium complex with highly conjugated ligands containing thiophene rings. Preliminary tests using this sensitiser in a solar cell obtained a power conversion efficiency of 10.53 per cent, which is comparable with the 11.1 per cent achieved by the most efficient dye-sensitised



solar cells reported to date. Grätzel says that this ‘looks very promising’. This conversion may be lower than for commercially available silicon-based solar cells (at 20–25 per cent efficiency) but dye-sensitised solar cells are still desirable as they are hydrophobic and so more stable and robust than silicon-based solar cells, which suffer from water sensitivity.

**Conjugated ligands increase the amount of light absorbed by the ruthenium complex**

**Reference**  
F Gao *et al.*, *Chem. Commun.*, DOI:10.1039/b802909a

The addition of the thiophene rings to the ligands in the ruthenium complex increases the conjugation, and improves the sensitiser’s overall light absorbing capabilities. ‘Less dye is required to extract the same amount of energy from the available light, which translates into immediate cost savings,’ says Kevin Tabor, director of science and research at G24 innovations, Cardiff, UK, a large scale manufacturer of solar cells using Grätzel’s technology. Additionally, the thiophene ring has shifted the absorption band of the sensitiser into the red region. ‘This means further energy uptake over other sensitisers and from an aesthetics perspective, a deeper coloured, almost black solar cell,’ explains Tabor.

Developing a more efficient sensitiser will help towards increasing the market share of this type of solar panel, says Grätzel. *Emma Shiells*

A natural energy source for fluid mixing on the small scale

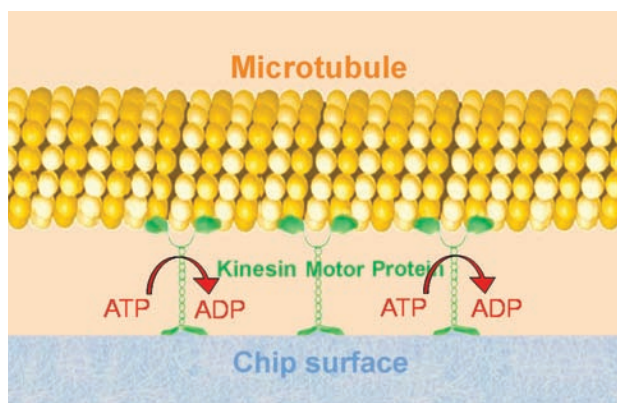
## Cellular power plants fuel molecular motors

Mitochondria have been used to power miniature motors for microfluidics.

Specialised subunits found within many living cells, mitochondria are essentially the cells’ power plants. The structures use glucose to generate adenosine triphosphate (ATP), a multifunctional compound that transports chemical energy within cells. Now Jed Harrison from the University of Alberta, Edmonton, Canada, and colleagues have used mitochondria to synthesise ATP as fuel for molecular motors in microfluidic systems.

Roughly the size of a credit card, microfluidic devices are used to examine fluid flow in structures and channels less than a millimetre across, often being used in disease diagnostics. Using motors allows efficient fluid mixing and transport inside the devices.

ATP has already been used to



power microfluidic motors based on kinesin – a protein that moves as it hydrolyses ATP. Currently, ATP is produced in microfluidics with the enzyme pyruvate kinase, but this is a low energy density fuel, and an improved ATP source is the goal.

Using mitochondria to produce ATP instead, the Canadian team found that these miniature

**On-chip: kinesin moves along microtubules as ATP is hydrolysed**

**Reference**  
J R Wasylcia *et al.*, *Lab Chip*, 2008, DOI: 10.1039/b801033a

machines could power a kinesin motor inside a two-chamber device. ‘Using mitochondria directly avoids the significant challenges associated with creating a synthetic enzyme cascade to duplicate the mitochondrial role,’ explains Harrison. ‘We take advantage of the biomolecular machinery nature has already assembled.’

Harrison adds that, although there are many future challenges for molecular motors, he believes this is the first step towards a system that has a high energy density fuel source and can recycle products back into ATP. ‘And the simplicity of the device is a key point which should ensure its success in labs which are not specialists in microfabrication,’ says Matthieu Piel, who heads a systems cell biology research group at the Curie Institute, Paris, France. *Rebecca Brodie*

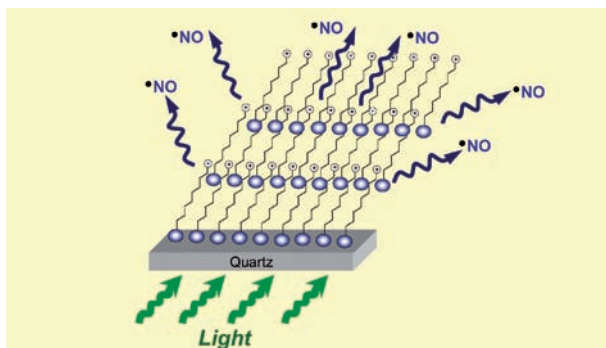


## NO releasing film provides 'significant step' towards molecule-based machines

# Layered film offers NO control

A film that releases one of the body's signalling molecules could find uses from biochemical studies to new materials, say scientists in Italy. Ludovico Valli and co-workers at the Universities of Salento and Catania, have developed a multilayer film that releases nitric oxide (NO) under light stimuli.

NO is more than just an environmental pollutant, it also plays a vital role in a range of biological processes, including blood vessel dilation, neurotransmission and hormone secretion. Therefore, compounds that deliver NO are of great interest for biochemical research. 'But only a limited number of NO photodors have been integrated in appropriate materials,' says team member Salvatore Sortino, explaining the group's motivation.



The researchers incorporated a light-sensitive NO donor molecule into multilayer films. They found that the films were stable in the dark, but when illuminated emitted a nanomolar amount of NO. The NO reservoir size can be varied by changing the number of layers. Also,

**Shining light on multilayer films releases NO on demand**

#### Reference

L Valli, G Giancane and S Sortino, *J. Mater. Chem.*, 2008, DOI: 10.1039/b802126k

increasing the films' light exposure times increases the levels of NO delivered. 'This offers the possibility of accurately controlling NO dosage exclusively by light,' says Sortino, 'making the films ideal for potential studies in biochemical research where precise control of NO release is required.'

Alberto Credi, of the University of Bologna, Italy, whose research interests include photoactive devices and machines, agrees. 'Several molecules will release nitric oxide under light irradiation in homogeneous solution,' says Credi. 'But integrating them into these films represents a significant step towards molecule-based materials and devices for NO delivery with spatial and temporal control.'

Vikki Chapman

## Top tips for better chips

**Lab on a Chip** launches **Chips & Tips** an online resource discussing common problems encountered in the miniaturisation and microfabrication field, with expert advice from David Beebe and Glenn Walker.

- Learn the tricks of the trade
- Post your own tip
- Go online to find out more

RSC Publishing

[www.rsc.org/loc/chips&tips](http://www.rsc.org/loc/chips&tips)

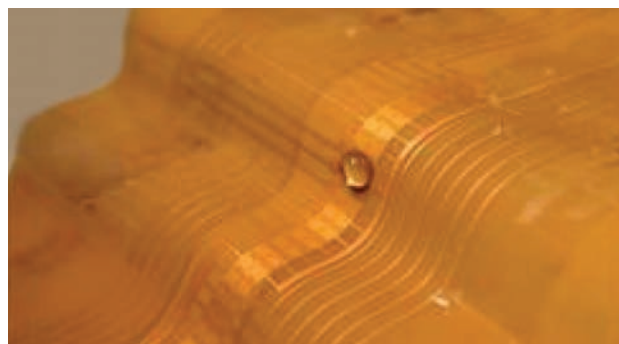
## Fluid movement cycles temperature for DNA studies

# Driving water droplets uphill

Lab-on-a-chip technology could soon simplify a host of applications, thanks to a new way to move droplets up vertical surfaces on flexible chips.

Canadian chemists have developed an all-terrain droplet actuation (ATDA) method to move droplets across chips at a wide range of angles. Aaron Wheeler and colleagues at the University of Toronto say digital microfluidic devices using ATDA could be used to move fluids rapidly between different environments, for example to cycle between heating and cooling.

Wheeler developed ATDA on flexible, water-repellent polyimide surfaces, clad with copper, which can be bent into a variety of shapes including steps, twists and overhangs. The fluid beads are moved by sequentially activating a series of electrode pairs, which is thought to pull the droplet forward by reducing water repellence in front



of the droplet. This process gives the team full control of the droplet, including up and down vertical surfaces.

Wheeler suggests several potential uses for the technique, including PCR (the polymerase chain reaction), which is used in DNA analysis. PCR depends on rapid temperature cycling – and Wheeler showed the method can be used to move fluids between a cooling structure and a hot

**A reduction in water repellence pulls the drop up a stepped surface**

#### Reference

M Abdelgawad *et al*, *Lab Chip*, 2008, DOI: 10.1039/b801516c

plate. The team also showed ATDA devices can be used to extract DNA from a complex organic mixture. By half-immersing the device in the mixture, and driving the water droplet in and out of it, the process could automate a tedious technique molecular biologists use to purify DNA, says Wheeler.

Richard Fair, who studies lab-on-a-chip devices at Duke University, Durham, US, says it is too soon to tell whether all-terrain devices will be useful. 'Demonstrating these applications is kind of cool, but whether ATDA is the best way to do them is another issue,' he says.

Wheeler agrees that the ultimate uses of ATDA are still to be established. 'We're not totally sure what this will be good for but it's been fun to do something new,' he says. 'This certainly isn't the only way to cycle temperature on a lab on a chip device but it's really easy.'  
*James Mitchell Crow*

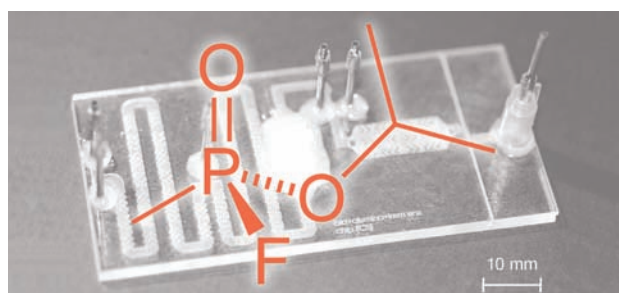
## Device performs multistep sequence to detect neurotoxins in droplet of blood

# Nerve agent detector on a chip

A microfluidic device that can identify exposure to sarin could help identify individuals needing treatment at sites of terrorist attack.

A lab on a chip that can detect traces of sarin and related neurotoxins in a small drop of blood has been made by Nam-Trung Nguyen at Nanyang Technological University in Singapore and colleagues. Nguyen says that the device would allow the first responders to a terrorist strike, such as the 1995 Tokyo subway sarin attack, to quickly distinguish the 'worried well' from genuinely exposed individuals requiring treatment.

'Our device integrates an entire protocol for the detection of trace amounts of nerve gas agents in blood,' says Nguyen. 'One of the challenges is using whole blood as the sample – the device needs to handle several tasks, from blood sample preparation to final optical detection.'



The blood flows through the chip in a sequence of steps. Initially, the blood cells are burst open and the sarin released, before the blood proteins and other particulates are filtered out. The purified mixture is then mixed with a substrate and a chromophore, and passed over an immobilised enzyme. If the sample contains no sarin, the enzyme reacts with the substrate, which then attacks the chromophore, which is detected by an external UV-visible spectrometer. But if sarin is

**Trace amounts of sarin inhibit an enzymatic reaction on the chip**

#### Reference

H Y Tan *et al*, *Lab Chip*, 2008, DOI: 10.1039/b800438b

present it inhibits the enzyme, so the chromophore passes to the detector unchanged.

'The device can also be used to detect organophosphorus insecticides,' adds Nguyen. 'A simple, low-cost device for evaluating the degree of insecticide contamination could be important for rice-producing countries. Together with other future water technologies, our technology could be crucial for securing and providing clean water sources for the population.'

Jonas Berquist studies chip-based blood analysis at Uppsala University, Sweden, and says he is impressed with the number of steps integrated into the device. He points out that the next step would be to remove the need for an external detector. 'For a first screen device, it would be nice to have something easily detected [by eye], like a colour change,' he says.

*James Mitchell Crow*

## Interview

# Having a gas

Gary Hieftje tells Nina Notman about the fun side of science



**Gary Hieftje**

**Gary Hieftje is a distinguished professor at Indiana University and holds the Robert and Marjorie Mann Chair in chemistry. His research interests include fundamental and applied investigations into atomic and molecular absorption, emission, and mass spectrometry and metallomics. Gary is chairman of the Journal of Analytical Atomic Spectrometry editorial board.**

## What motivated you to become a scientist?

As a child I always loved building things like model planes. I also enjoyed making things explode. As with many chemists, these things came together – I would build a model plane and also build something to make it explode mid-flight.

When I was about 8 years old, I used to play with a chemistry set. But the set had a limitation – a small alcohol lamp that didn't get very hot. It was possible using the lamp to bend soft glass but not to do the real glass blowing I wanted to get involved in. So I talked to my uncle who was a plumber and learnt a lot about plumbing. I then used this knowledge to put in a gas line for a Bunsen burner. I was 10 years old when I did it and it was all unknown to my father. When I showed him this bit of glass that I had blown, he asked me where I had done it. I showed him the gas line in the basement and he just about went crazy!

## Do you remember your first experiment?

Making gunpowder was my first real chemical experiment. At first, this was very conventional – a mixture of powdered charcoal, potassium nitrate and sulfur. But my mother complained about the sulfur stink, so I substituted cinnamon for sulfur just out of curiosity. It worked but not quite as well. So I looked in a chemistry book and learnt that potassium perchlorate was a much stronger oxidising agent than potassium nitrate. Potassium perchlorate, charcoal and cinnamon made a wonderful explosion and also smelled pretty good!

## What is hot in atomic spectrometry at the moment?

A lot of things are hot, which is a nice term for people who use plasmas and flames. One area is speciation and a subset of speciation that we are calling metallomics – the study of metals in living things ranging from single cells to whole organisms.

Another hot topic is melding atomic and molecular techniques. People are now using mass spectrometric methods that involve inductively coupled plasma to give elemental and atomic information, and other sources such as electrospray ionisation to yield molecular information.

## How do you see the future of atomic spectrometry?

I see the future in a very positive light. Some people view atomic spectrometry as a stagnant field because we already have such powerful tools. There are good tools, such as inductively coupled plasma mass spectrometry (ICP-MS), but there are still a lot of unknowns and areas where vast improvements are possible. For example, it can be shown on paper that detection using ICP-MS could be improved down to the single atom or ion level. These advances are going to be increasingly important for the areas of nano- and bioscience.

Another important future area for atomic spectrometry is the imaging process. Currently, we take bulk solutions or samples and determine their elemental composition but soon we will also need to determine their atomic placement.

## What is the most exciting project your group is working on at the moment?

The thing I'm most enthusiastic about right now is a new source we have for ambient MS. This technique involves determining samples as they are, everything from a napkin to something on my hand that I have touched. The sample is placed in front of a specialised source, which desorbs the species from the sample surface and ionises them so they can be analysed by MS.

## As a significant role model to young aspiring analytical scientists, what advice can you give on a successful research career?

It's really very easy; work hard and have fun. There is an awful lot of fun in science. I've worked in areas ranging from synthetic organic chemistry to the far reaches of analytical instrument building. I have yet to find an area that isn't exciting once I've learnt enough about it.

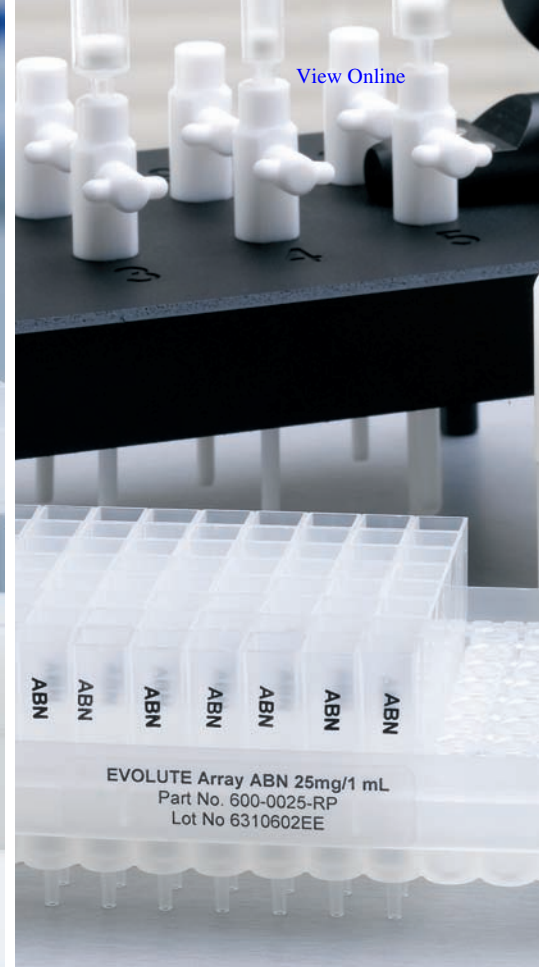
## What research would you most like to be remembered for?

It isn't the research that I want to be remembered for; it is for the students that leave my group. To me research is just a very nice, convenient by-product of the educational process.

## What do you like doing away from work?

I enjoy gin martinis tremendously! I also like skiing, water skiing, swimming and running.





[View Online](#)

IST Sample Preparation • Bioanalysis • Clinical • Environmental • Forensic • Agrochemical • Food • Doping Control

## EVOLUTE® CX **NEW!**

### Mixed-mode selectivity, generic methodology and efficient extraction

EVOLUTE® CX mixed-mode resin-based SPE sorbent extracts a wide range of **basic drugs** from biological fluid samples. EVOLUTE CX removes matrix components such as proteins, salts, non-ionizable interferences and phospholipids, delivering cleaner extracts with reproducible recoveries for accurate quantitation.

## EVOLUTE® ABN

### Minimize matrix effects, reduce ion suppression and concentrate analytes of interest

EVOLUTE® ABN (Acid, Base, Neutral) is a water-wettable polymeric sorbent optimized for fast generic reversed phase SPE. Available in 30  $\mu\text{m}$  columns and 96-well plates for bioanalysis and **NEW 50  $\mu\text{m}$  columns** – ideally suited for environmental, food/agrochemical and industrial analysis as well as forensic and doping control applications.

Contact your local Biotage representative or visit [www.biotage.com](http://www.biotage.com) to request a **FREE** sample.



## Instant insight

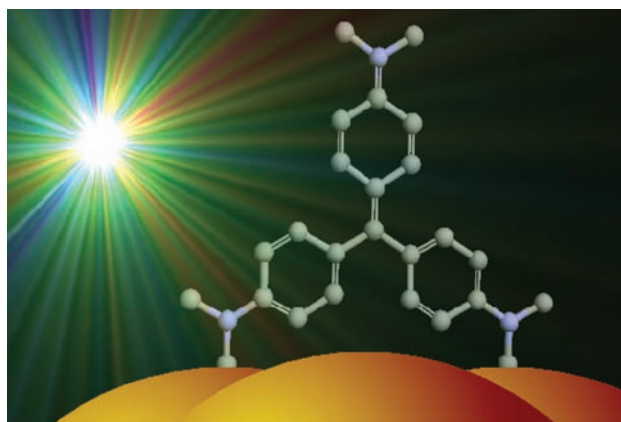
# Detection on the nanoscale

Nicholas Pieczonka and Ricardo Aroca of the University of Windsor, Canada, use Raman scattering to look at one molecule in a million

Single molecule spectroscopy (SMS) uncovers the information and behaviour that is lost when measuring an ensemble of molecules. To be able to detect the spectroscopic signal from a solitary molecule, it must have extraordinary absorption or emission properties. And so, the majority of SMS work has been accomplished by measuring the fluorescence of molecules with exceptional luminescence abilities. But the molecular information and the class of molecules that can be probed through fluorescence are limited.

Raman scattering (RS), the inelastic scattering of light from molecules, is an alternative optical spectroscopy that provides a vibrational spectrum, a true characterisation of any stable electronic state. It is rich in information and can be applied to virtually any type of chemical species. It is not always an efficient process; however its cousin, resonance RS, can be orders of magnitude more intense.

Just over 30 years ago, scientists discovered that a molecule's Raman signal could be greatly enhanced by putting it close to metallic nanoparticles. They found that the source of the enhancement was the intense fields provided by the localised surface plasmon resonances (LSPR), or waves of electrons, that occur when the nanoparticles are excited by light. The new physical phenomenon delivered several new analytical techniques, including surface-enhanced Raman scattering (SERS) and surface-enhanced resonance Raman scattering (SERRS). Several groups expanded the potential for SER(R)S even further



by demonstrating that certain nanostructures provide intense field enhancements, known as hot spots, that are large enough for single molecule detection.

Today, there is a vast body of work that illustrates both the promise and the inherent challenges in SM-SER(R)S. Only two metals (silver and gold) and a handful of nanostructures (aggregated colloids, metal island films and scanning tunnelling microscopy (STM) tips) have demonstrated SM sensitivity. Also, investigations have revealed a very strong dependence between the scattering ability of the molecule and the type of nanostructures that can be used. Molecules that are relatively weak scatterers require nanostructures that can support hot spots, whereas for strong scatterers, single plasmon supporting structures, such as STM tips, will do.

A daunting challenge to SM-SER(R)S is that, in many instances, SM detection depends critically on the structure of the molecule for selective adsorption, particularly onto hot spots. And although ensemble SERS has been observed

for all types of molecular systems, SM-SER(R)S has been observed only for a very limited selection of chemical structures, in particular molecules containing electron-rich moieties.

Scientists are developing a greater understanding of the underlying features of the Raman signal measured for a single molecule. At present, the most common signature that supports the claim that the recorded spectrum comes from a single molecule is fluctuations of the signal. This includes variations in the frequency, bandwidth, relative intensity and, sometimes, an on-and-off behaviour of the spectrum. These dynamics hold a wealth of information that is waiting to be untapped.

The use of plasmon supporting nanostructures for SM-SER(R)S is still at an early stage of development and holds enormous promise for potential applications. The future of SM-SER(R)S will demand a great deal of effort from experimentalists and theorists but this will be justified by the application of SMS in areas of nanoscience and ultrasensitive chemical analysis. The most important implications and fascinating applications may come from the advancement of our understanding of plasmonics. The interaction of molecular systems with confined electromagnetic waves in metallic nanostructures is clearly an exciting subject of study and will no doubt be the source of new knowledge in SM-SER(R)S.

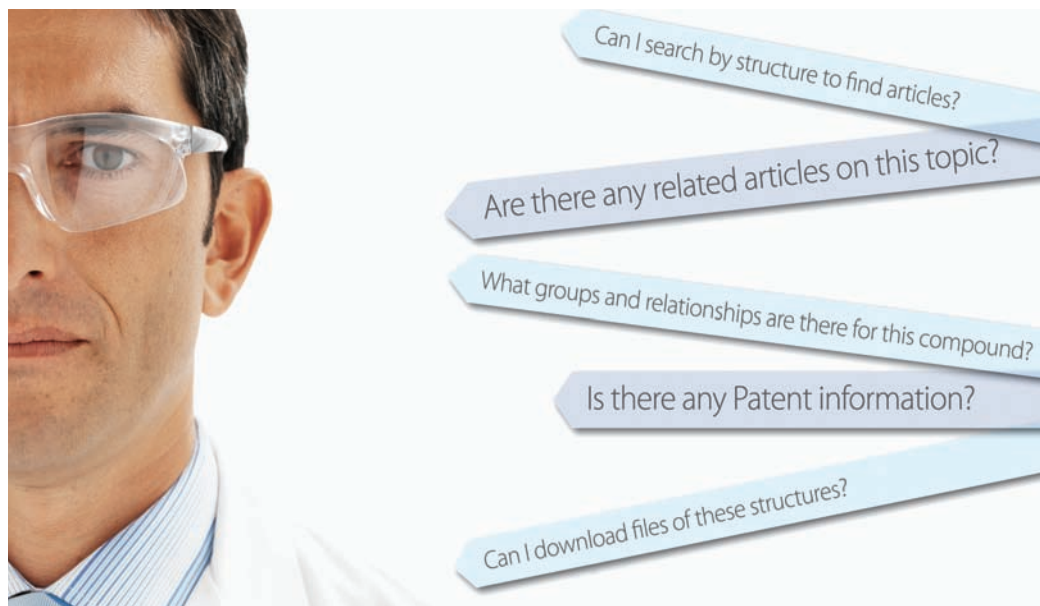
Read Pieczonka and Aroca's tutorial review 'Single molecule analysis by surface-enhanced Raman scattering' in issue 5, a SERS thematic issue of Chemical Society Reviews.

**Reference**

N P W Pieczonka and R F Aroca, *Chem. Soc. Rev.*, 2008, **37**, 946 (DOI: 10.1039/b709739p)

# Essential elements

## Faced with questions?



Finding the answers to questions like these has just become a lot easier, thanks to the latest features introduced for *RSC Prospect* enhanced HTML articles.

Linking together related articles by subject ontologies and identified compounds, *RSC Prospect* enhanced HTML articles already provide you with definitions, synonyms, structures and RSS feeds.

One new feature that we've just introduced is a structure and sub-structure searching function to help you find relevant articles by drawing your own molecule using ChemAxon's MarvinSketch or pasting in a ChemDraw or ISIS/Draw file.

We've also widened the compound identifiers to include groups and relationships via the ChEBI (Chemical Entities of Biological Interest) ontology. Links to patent information in SureChem and to compounds in PubChem have also been added.

Winner of the 2007 ALPSP/Charlesworth Award for Publishing Innovation, *RSC Prospect* was first released in February 2007. There are now more than 1600 articles that have been enhanced with these features.

As Richard Kidd, informatics manager at RSC Publishing says: 'We believe that the application of open and

standard identifiers for both compound and subject matter will transform the future of publishing. We are proud to be leading the way amongst scientific publishers with *RSC Prospect*.'

You can read more about the new features, and view examples of articles, on the website: [www.projectprospect.org](http://www.projectprospect.org)



## Did you know...

RSC Publishing book series provide authoritative insights into critical research, appealing to a broad cross-section of scientists in multiple disciplines. The book series cover new and emerging areas of scientific interest such as Green Chemistry, Energy, Nanoscience & Nanotechnology and Biomolecular Sciences.

Our prestigious Biomolecular Sciences series is devoted to the coverage of the interface between the chemical and biological sciences and has contributions from leading experts in the fields of structural biology, chemical biology, bio- and chemoinformatics, drug discovery and development, chemical enzymology and biophysical chemistry. This month sees the publication of two new titles to join the series.

Written by a team of experts, *Protein-Nucleic Acid Interactions: Structural Biology* bridges the gap between the DNA- and RNA-views of protein-nucleic acid recognition which are often treated as separate fields. *Therapeutic Oligonucleotides* takes a unique look at all the modern approaches and the many advances experienced in the field of protein folding and aggregation during the past 10 years. Both titles are not to be missed, and will serve as ideal reference and state-of-the-art guides at the graduate and postgraduate levels. Look out for more exciting new titles to join the Biomolecular Sciences series later this year.

For more information visit: [www.rsc.org/biomolecularsciences](http://www.rsc.org/biomolecularsciences)

*Chemical Technology* (ISSN: 1744-1560) is published monthly by the Royal Society of Chemistry, Thomas Graham House, Science Park, Milton Road, Cambridge UK CB4 0WE. It is distributed free with *Chemical Communications*, *Journal of Materials Chemistry*, *The Analyst*, *Lab on a Chip*, *Journal of Atomic Absorption Spectrometry*, *Green Chemistry*, *CrystEngComm*, *Physical Chemistry Chemical Physics* and *Analytical Abstracts*.

*Chemical Technology* can also be purchased separately. 2008 annual subscription rate: £199; US \$396. All orders accompanied by payment should be sent to Sales and Customer Services, RSC (address above). Tel +44 (0) 1223 432360, Fax +44 (0) 1223 426017 Email: [sales@rsc.org](mailto:sales@rsc.org)

**Editor:** Joanne Thomson

**Deputy editor:** Michael Spencelayh

**Associate editors:** Celia Clarke, Nina Notman

**Interviews editor:** Elinor Richards

**Web editors:** Debora Giovannelli, Michael Spencelayh

**Essential elements:** Valerie Simpson and Rebecca Jeeves

**Publishing assistant:** Ruth Bircham

**Publisher:** Graham McCann

Apart from fair dealing for the purposes of research or private study for non-commercial purposes, or criticism or review, as permitted under the Copyright, Designs and Patents Act 1988 and the copyright and Related Rights Regulations 2003, this publication may only be reproduced, stored or transmitted, in any form or by any means, with the prior permission of the Publisher or in the case of reprographic reproduction in accordance with the terms of licences issued by the Copyright Licensing Agency in the UK. US copyright law is applicable to users in the USA.

The Royal Society of Chemistry takes reasonable care in the preparation of this publication but does not accept liability for the consequences of any errors or omissions.

Royal Society of Chemistry: Registered Charity No. 207890.

RSC Publishing

# Is catalysis in ionic liquids a *potentially* green technology?

DOI: 10.1039/b805586f

The amount of interest in ionic liquids over the past decade has been simply staggering. This issue of *Green Chemistry* contains a review of the use of catalysts bearing a charged functional group designed to impart better retention of the catalyst in the ionic liquid in biphasic and/or continuous operation. Much, even most, of the activity in this field has centred on the claimed use of ionic liquids as so-called green solvents. This claim has been, to say the least, controversial, and I have seen debates around this get quite animated. Claims and counter claims are made, positions taken and plenty of heat generated, but seldom much light. Although I write from the position of working with ionic liquids, similar debates can be found elsewhere.

Early claims to the greenness of ionic liquids rested on their extremely low vapour pressures. Since the ionic liquids cannot evaporate under typical operating and storage conditions, they cannot leak into the atmosphere, as do most organic solvents that are VOC's. Many people have rightly pointed out that this does not on its own constitute a reason to declare all processes conducted in ionic liquids to be green. They note that ionic liquids are often made from ions that are toxic and that they are usually made by multi-step syntheses, often using the very solvents that they are replacing. Others have countered that ionic liquids can be made to be less toxic, more biodegradable, from more environmentally benign sources and that they can offer process advantages that outweigh the other disadvantages.

Some would say that the thorough way to resolve this issue is to use cradle-to-grave life-cycle analysis. However, to do this requires information about how the particular ionic liquid performs in comparison to the solvent to be replaced in the process in which it is to be used, as well as detailed information about the source, number of recycles possible and disposal of both the ionic liquid and the

replaced solvent. LCA is a lengthy and costly technique, and having performed the analysis the results tell you little about how this or other ionic liquids will perform in other processes. It is very good at providing the information required to make decisions about the final version of an industrial process to be implemented, but it is less able to give guidance about whether some general area of research is worth pursuing.

How does one escape this impasse? First, I would say that it important to recognise what question should be being asked at the beginning of the research process. If one had sufficient information to hand to be able to undertake a detailed LCA there would probably be no need to conduct further studies. The question that is really being asked is whether the technology to be applied offers the *potential* to provide greener chemicals processes. One could try testing this question against the 12 principles of green chemistry. So this is what I have tried to do for catalysis in ionic liquids below using information contained in the review and my background knowledge of the area:

**1. Prevent waste.** Some catalytic ionic liquid processes are more selective and give higher yields of the product than alternative routes. Some catalysts have been designed to be sufficiently retained and stabilized in the ionic liquid solution so that many recycles can be achieved. It is possible to think of ways in which these catalysts can be converted into recoverable forms, but much less is known about this.

**2. Design safer chemicals and products.** If we think of the ionic liquid as the product in this case, they are generally non-volatile and non-flammable liquids and work is already underway to make these from non-toxic materials.

**3. Design less hazardous chemical syntheses.** See 2 above.

**4. Use renewable feedstocks.** There are already ionic liquids made from renewable resources in use. There has been a great

deal of recent activity on the use of ionic liquids as process solvents for biomass derived starting materials.

**5. Use catalysts, not stoichiometric reagents.** Catalysis in ionic liquids does this.

**6. Avoid chemical derivatives.** Catalytic routes often avoid protection/deprotection steps. It is possible that the careful selection of ionic liquid for the process may improve the selectivity of a catalyst and so aid this.

**7. Maximize atom economy.** Some catalytic ionic liquid processes are more selective and give higher yields of the product than alternative routes.

**8. Use safer solvents and reaction conditions.** Ionic liquids are generally non-volatile and non-flammable solvents, work is underway to reduce their toxicity and improve their biodegradability.

**9. Increase energy efficiency.** Ionic liquids have been shown to increase the rates of some reactions, and even act as co-catalysts. Increased rates allow for less energy input.

**10. Design chemicals and products to degrade after use.** There is work in the literature on designing biodegradable ionic liquids.

**11. Analyze in real time to prevent pollution.** Ionic liquids are compatible with most spectroscopic techniques.

**12. Minimize the potential for accidents.** Ionic liquids are generally non-volatile and non-flammable solvents.

So, the answer to the question of whether catalysis in ionic liquids has the potential to provide greener chemicals processes is overwhelmingly yes. It does not mean that it will always provide the greenest process for all products. Solving that problem is what research is for.

## Tom Welton

Professor of Sustainable Chemistry, Imperial College of Science, Technology and Medicine, South Kensington, London, SW7 2AX, UK



# Catalysts with ionic tag and their use in ionic liquids

Radovan Šebesta,<sup>\*a</sup> Iveta Kmentová<sup>b</sup> and Štefan Toma<sup>a</sup>

Received 25th January 2008, Accepted 26th March 2008

First published as an Advance Article on the web 9th April 2008

DOI: 10.1039/b801456f

The concept of homogeneous supported catalysts has emerged as a useful alternative to homogeneous as well as heterogeneous catalysis, possibly combining positive aspects of both. Designing catalysts with respect to not only their catalytic activity but also their physical-chemical properties, appears to be a possible way towards sustainable chemical synthesis. Such tailored catalytic systems would ideally have high catalytic activities and some property enabling their efficient recycling. We reviewed the field of specifically designed ionic catalysts used mostly in ionic liquids.

## Introduction

The notion that catalytic reagents are superior to stoichiometric reagents is one of the green chemistry principles defined by Anastas and Werner.<sup>1</sup> An equally important topic is a search for more environmentally benign alternatives to conventional organic solvents.<sup>2</sup> Ionic liquids have properties that make them promising candidates for performing green processes. In particular, catalytic transformations have been successfully realized in ionic liquids.<sup>3</sup> The use of ionic liquids provides many advantages over conventional solvents in terms of activity, stability and reusability of catalyst or solvent–catalyst system.<sup>4–8</sup> Reusability is a particularly attractive feature for expensive transition metal catalysts, and some organocatalysts as well. Even if the catalyst dissolves well in the ionic liquid, there is often a dramatic decrease in its activity after several runs. The main cause of this decrease is usually catalyst leaching during product extractions from the reaction mixture or during the purification of the ionic phase before recycling. Use of specifically designed or modified catalysts, with physical-chemical properties more similar to that of ionic liquids, may be a possible solution for the problem of catalyst leaching. Incorporation of an ionic moiety into the catalyst structure is probably the most straightforward approach. An important premise being that the ionic tag is catalytically silent and inert in reaction conditions. However, it may not be always the case. Therefore, rational design and optimization of the catalyst structure seems crucial for success. Introduction of an ionic tag is undoubtedly a useful idea, and it was also successfully employed for stoichiometric reagents.<sup>9,10</sup> Ionic catalysts can also be used in classical organic solvents. Owing to their insolubility or immiscibility with such solvents, they can often be easily recovered and reused later.

The aim of this overview is to make a survey of publications dealing with the introduction of an ionic tag into ligands or transition metal complexes as well as organocatalysts. Particular

attention is paid to the relationship between the catalyst structure and the outcome of the catalyzed reaction. Ionic liquids having Brønsted acid or base properties are not covered by this overview. Emphasis is on specifically designed catalysts and their use in ionic liquids, but some important examples of utilization in other media are also mentioned.

The majority of the ionic catalysts contain a cationic tag, which most often is imidazolium or pyridinium ion. The most common way for introduction of such moieties is a nucleophilic substitution of a suitable halogen derivative with 1-methylimidazole or pyridine. Several catalysts also feature an anionic moiety, such as sulfonic or phosphonic acids.

In this review, 1-butyl-3-methylimidazolium and 1-ethyl-3-methylimidazolium cations are denoted as [bmim] and [emim]; 1-butyl-2,3-dimethylimidazolium and 1-hexyl-2,3-dimethylimidazolium as [bdmim] and [hdmim]; 1-butylpyridinium cation is denoted as [bpyr]; *N*-ethyl-3-methylpiccolinium cation is denoted as [epic]. The bis(trifluoromethyl sulfonyl)imide anion is denoted as NTf<sub>2</sub>, and triflate and tosylate as OTf and OTs.

## Catalysts based on transition metal complexes

### Achiral transition metal catalysts

Transition metal complexes with achiral ligands were at the beginning of development of ionically-tagged ligands as a mean of possible immobilization. Most of the work concentrated on hydrogenations, hydroformylations and metatheses.

Chauvin's work from 1996<sup>11</sup> suggested that using cationic ligands/catalyst in ionic liquids may be a good way of catalyst immobilization and recycling. The ligands TPPMS and TPPTS (triphenylphosphane mono and trisulfonate, respectively), initially designed for Ru- or Rh-catalyzed hydrogenations in water, were employed in ionic liquid or ionic liquid/organic solvent systems. These catalysts generally showed low activities in ionic liquids, but catalyst recycling was possible.<sup>12,13</sup> In ionic liquids of type [C<sub>n</sub>mim]pTolSO<sub>3</sub>, the catalyst HRh(CO)(TPPTS)<sub>3</sub> was reported as more active and selective for hydroformylation of hex-1-ene than in [bmim]BF<sub>4</sub>/PF<sub>6</sub>.<sup>14</sup> The results imply that adjusting the properties of reaction medium and conditions for each reaction can offer a good use of these types of catalysts.

<sup>a</sup>Department of Organic Chemistry, Faculty of Natural Sciences, Comenius University, Mlynská dolina, 84215, Bratislava, Slovakia

<sup>b</sup>Auckland Cancer Society Research Centre, School of Medical Sciences, The University of Auckland, Private Bag 92019, Auckland, 1142, New Zealand



A catalyst with an incorporated imidazolium cation, Rh/TPPTI (TPPTI = tri(*m*-sulfonyl)triphenylphosphane 1,2-dimethyl-3-butylimidazolium salt) was used for biphasic hydroformylation of hex-1-ene in [bmim]BF<sub>4</sub>, [bmim]PF<sub>6</sub> or [bdmim]PF<sub>6</sub>. The reaction proceeded slower than with the conventional Rh/PPh<sub>3</sub> catalyst in toluene, but in the instance of TPPTI/Rh it was better retained in the ionic liquid.<sup>15</sup> Also, Cole-Hamilton and co-workers demonstrated the possibility of utilization of TPPTS-derived catalyst.<sup>16,17</sup> Ligand **1** was used with Rh<sub>2</sub>(OAc)<sub>4</sub> as the catalyst precursor for the hydroformylation of non-1-ene in scCO<sub>2</sub>/[bmim]PF<sub>6</sub> biphasic system. No Rh-leaching was observed during the first 9 runs. Throughout the series of runs, isomerisation increased and, after the ninth run, Rh-leaching occurred because of the ligand oxidation from contamination with air during the many openings of the reactor. The scCO<sub>2</sub>/[bmim]PF<sub>6</sub> system was also used for the continuous flow hydroformylation of oct-1-ene with ligand **2**, which allowed easy catalyst/product separation, because both reagents and products have good solubilities in scCO<sub>2</sub>, whereas the metal complex with ligand **2** is retained in the ionic liquid throughout the reaction. The reaction was slow but no catalyst decomposition occurred during 72 h and less than 1 ppm Rh was identified in the product stream (Scheme 1).

Imidazolium-tagged phosphorous ligands **3–5** were tested in biphasic hydroformylation of oct-1-ene using [bmim]PF<sub>6</sub> as solvent. The active catalyst was prepared *in-situ* by mixing Rh(CO)<sub>2</sub>(acac) with two equivalents of the ligand. The reaction was carried out at 100 °C and 30 bar synthesis gas pressure (CO/H<sub>2</sub> 1 : 1) for 1 h. The biphasic hydroformylation under these conditions showed a turnover frequency of 32 mol oct-1-ene per mol Rh per hour and an *n* : *i* ratio of 2.8. No significant leaching of the Rh-catalyst into the organic layer was observed (Scheme 1).<sup>18</sup>

Olivier-Bourbigou and co-workers published Rh-catalyzed hydroformylation of hex-1-ene using cationic phosphane ligands **6–8** (Fig. 1).<sup>19</sup>

Monosubstituted guanidinium triphenylphosphane ligands **6** and pyridinium ligand **7** showed good solubility in [bmim]BF<sub>4</sub>. Ligand **7** displayed better activity and higher selectivities towards linear aldehydes than ligand **6**. However, the retention

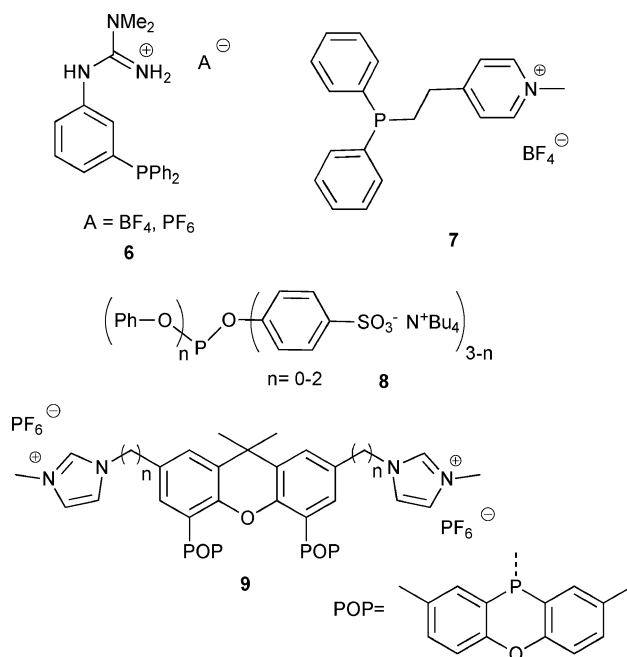
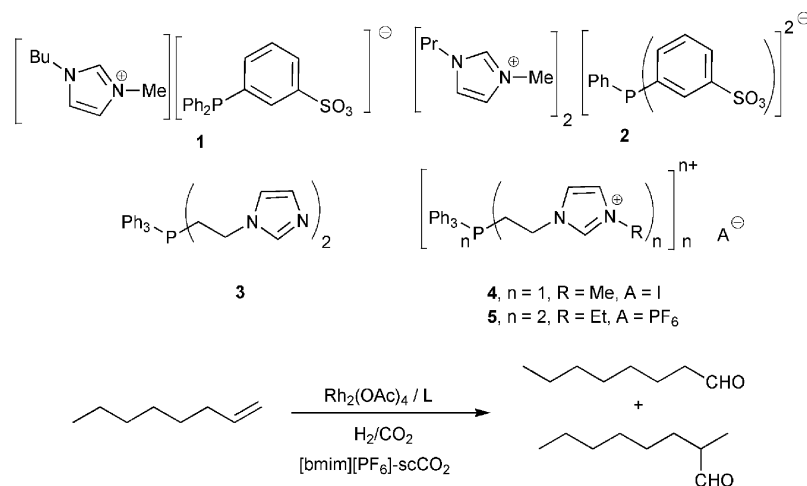


Fig. 1 Achiral ionic phosphanes.

of the Rh-catalyst in ionic liquid phase was more efficient for ligand **6** with BF<sub>4</sub> anion. Ligand **8** showed good catalytic activity and selectivity for linear aldehyde in [bmim]PF<sub>6</sub>, but Rh-leaching and loss of activity was observed in recycling experiments.

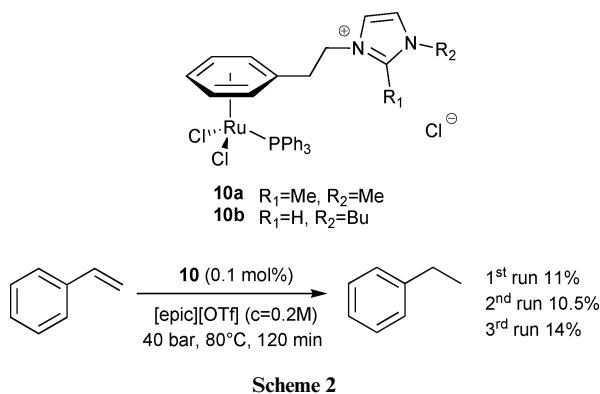
A novel phenoxaphosphano-modified ligand **9** has been prepared and successfully employed in the rhodium catalyzed hydroformylation of oct-1-ene in [bmim]PF<sub>6</sub>. Ligand **9** showed increased activity and good selectivity for the linear aldehyde over series of 7 recycling experiments, without detectable phosphorus (<100 ppb) or rhodium (<5 ppb) leaching during recycling experiments. Furthermore, the catalyst also proved to be stable for more than two weeks under ambient conditions (Fig. 1).<sup>20</sup>

Dyson and co-workers<sup>21</sup> recently reported a ruthenium complex bearing imidazolium functionalized η<sup>6</sup>-arene ligands **10a** and **10b** for biphasic aqueous and ionic liquid hydrogenation of



Scheme 1

styrene. In water, the complexes showed moderate activity, while compound **10b**, when used in [epic][OTf], afforded markedly lower reaction rates (Scheme 2).



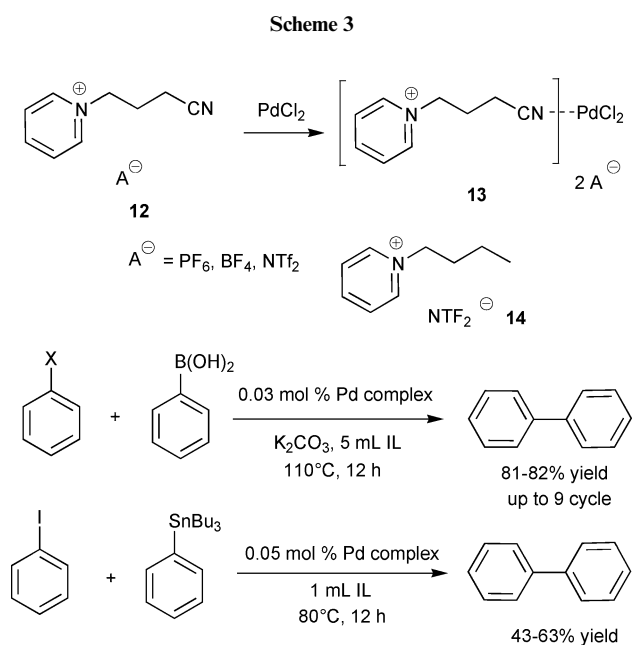
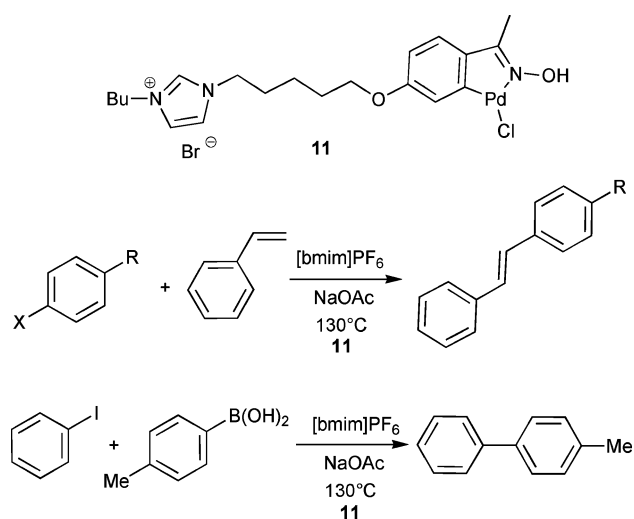
Use of the catalyst **10b** in water resulted in slight leaching of the catalyst into the organic phase, (98% yield in the 1st run, but only 75% yield in the 3rd run), whereas in the ionic liquid/organic system no catalyst loss was observed. In the course of the catalytic runs the color of the aqueous solution changed from orange to brown-purple, but the ionic liquid solution remained orange, and also  $^{31}\text{P}$  NMR spectroscopy revealed that the complex remained unchanged in the ionic liquid.

A modified oxime carbapalladacycle catalyst **11**, with an imidazolium group covalently attached to the rest of the complex, was described by Corma *et al.*<sup>22</sup> The complex **11** was designed to have an increased ionophilicity, with the aim of achieving increased affinity of the catalyst to ionic liquids and to minimize the concomitant leaching of Pd from the complex. Unfortunately, the catalytic activity of this palladium complex was unsatisfactory, providing very low yields (26%) in the coupling of halobenzenes with styrene. A marginal increase in the catalytic activity was observed when the reaction was performed in [bmim][PF<sub>6</sub>]/scCO<sub>2</sub>, which reduced the medium viscosity (26.3% yield).

The complex **11** was also tested in Suzuki coupling with similarly disappointing results (less than 10% conversion). The low activity of complex **11** was attributed to the poor stability of imidazolium ionic liquids in bases due to formation of carbenes by deprotonation of 1-butyl-3-methylimidazolium cation at the 2 position (Scheme 3).

An interesting concept is a modification of the ionic liquid in such a way that it could act both as ligand to a transition metal and as solvent for reaction. Dyson and co-workers<sup>23</sup> synthesized simple nitrile-functionalized *N*-butylnitrile pyridinium ionic liquids, **12**, which reacted with PdCl<sub>2</sub> to form the complexes **13**. All complexes were air-stable, poorly soluble in halogenated solvents and decomposed in acetonitrile. They could be purified by washing with water or alcohols, but decomposed in water or alcohols over prolonged periods of time (Scheme 4).

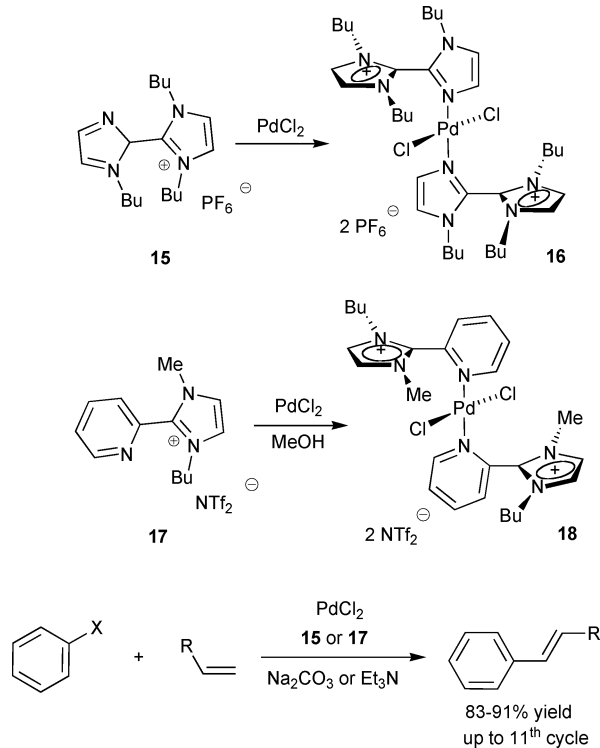
Complexes **13** were evaluated as catalysts in Suzuki and Stille coupling reaction. A very good activity of the catalyst was observed in Suzuki coupling in functionalized ionic liquid, and after 9 times recycling no loss of activity was observed, but in non-functionalized ionic liquid **14** the catalyst solution rapidly lost activity and become inactive after the 5th run.



Shreeve *et al.*<sup>24</sup> described several very effective phosphane-free ionic catalysts, based on an imidazolium moiety, for C–C cross coupling reactions. Substitution at position 2 with imidazole and pyridine led to a useful ligand for Pd and also eliminated the likelihood of side reactions. The monoquaternary product of 2,2'-diimidazole with iodobutane was an ionic liquid that could act both as a solvent and a ligand in the Pd-catalyzed Heck reaction. The palladium complex **16**, prepared from compound **15** and PdCl<sub>2</sub>, gave good to high yields (75–91%) in the coupling of iodo- and chlorobenzene with methyl acrylate and styrene (2 mol% of **16**, Na<sub>2</sub>CO<sub>3</sub>, IL, 100 °C, 4 h). The products were easily separated from the reaction mixture by extraction with diethyl ether. Recovery of the catalyst/ionic liquid could be done simply, by washing with water to remove the sodium salt and drying under vacuum before subsequent use. The high performance exhibited by the catalytic system, even after ten cycles and using the less reactive chlorobenzene, must be highlighted. The ionic liquid supported palladium complex **16**

was found to catalyze the Heck reactions with good recyclability of up to 10 cycles (Scheme 5).

Structurally similar ionic liquids with the pyridyl moiety at C-2 position of imidazolium cation **17** and the resulting Pd-complexes **18** were prepared by the same authors. The Heck cross-coupling reactions using catalyst **18** displayed excellent stability and recyclability of the catalytic system. When each subsequent cycle was carried out with different substrates, high isolated yields were obtained for aryl iodides bearing electron withdrawing and electron donating groups. The catalytic system could be recycled 14 times with different substrates with no apparent loss of catalytic activity (Scheme 5).<sup>25</sup>

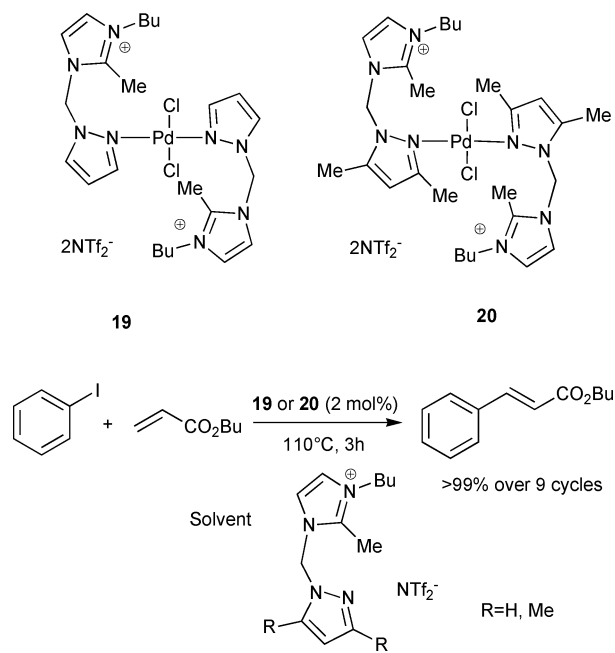


Scheme 5

A number of di- and monoquaternised 2,2'-biimidazolium-based ionic liquids, such as complex **16** have been prepared. The catalyst **16** was demonstrated to be a very efficient and recyclable solvent for Suzuki cross coupling reaction. Coupling products were obtained in high yields (80–90%) up to the 15<sup>th</sup> cycle.<sup>26</sup>

New mononuclear palladium ionic liquid complexes **19** and **20**, based on pyrazolyl- and 3,5-dimethylpyrazolyl-functionalized 2-methylimidazolium salts, have been prepared with anions NTf<sub>2</sub><sup>-</sup> or PF<sub>6</sub><sup>-</sup>. Outstanding stability and activity of these systems was demonstrated in Suzuki, Heck and Sonogashira cross coupling reactions. These ionic liquids serve both as solvent and ligand and the Pd catalyst is part of the ionic liquid in the catalytic system. Decomposition and leaching of the catalyst was markedly reduced in this way (Scheme 6).<sup>27</sup>

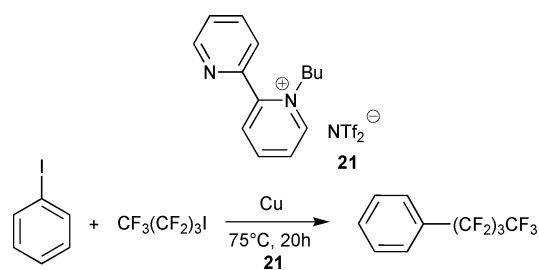
Pd/TPPTS (5 mol%) catalyzes a reaction of allylic acetates with various nucleophiles in [emim]BF<sub>4</sub>/H<sub>2</sub>O (1/2) with or without base under MW irradiation. Excellent yields of products (up to 99%) were obtained together with catalyst recycling for 8 times with a consistent activity. Presence of water and TPPTS



Scheme 6

were essential for reaction, with no reaction occurring without either of them.<sup>28</sup> Bruneau and co-workers<sup>29</sup> recently reported Ru-catalyzed ([CpRu(4,4'-*t*Bu-bipy)(MeCN)][PF<sub>6</sub>]) allylic alkylation of cinnamyl carbonate with different nucleophiles in [hdmim]PF<sub>6</sub> which proceeded under neutral conditions at 50 °C, allowing for a very good conversion, regioselectivity and good recyclability (4 cycles) of the solvent/catalyst system.

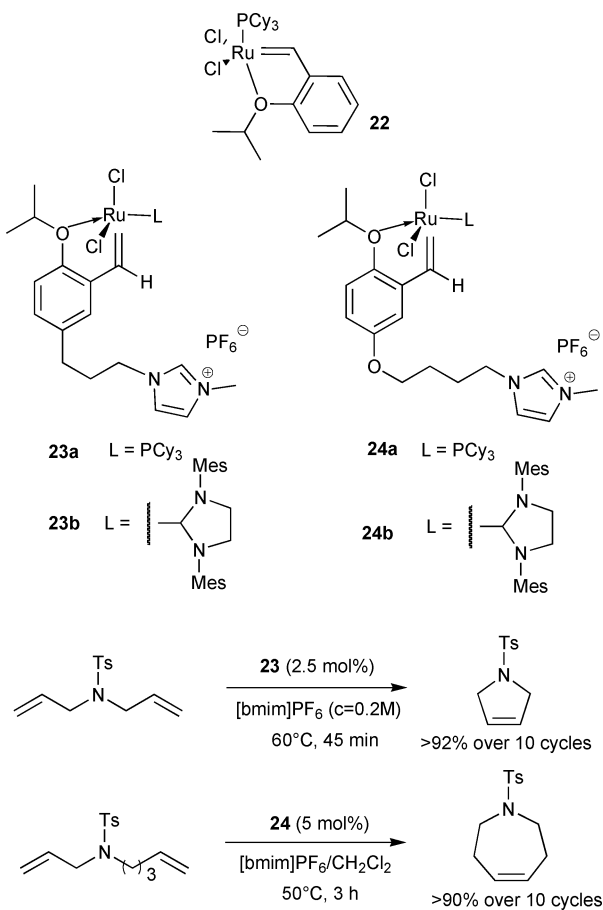
A novel pyridine-based monoquaternary ionic liquid **21** was tested in copper catalyzed cross coupling reaction between perfluoroalkyl halides and aryl iodides. The ionic liquid again acted as a ligand for the perfluoroalkylcopper intermediate, and after isolation of the product by extraction, the catalytic system could be purified and reused as a solvent. No significant loss of ionic liquid was observed, and the regenerated ionic liquid was reused in this way 14 times without any loss of activity (Scheme 7).<sup>30</sup>



Scheme 7

Very good examples of utilization of ionic-tagged catalysts are in Rh and Ru catalyzed olefin metathesis reactions. In 2003, Guillemine and Yao reported independently the synthesis of ionic-liquid-supported catalyst for the ring-closing metathesis (RCM) of olefins, based on Grubbs–Hoveyda catalyst **22**. Prepared catalysts **23** and **24** differ only in the linker between ruthenium and the ionic part.<sup>31,32</sup> The first generation metathesis catalysts **23a** and **24b** are highly active and with remarkable

recyclability in RCM of various diene and enyne substrates in ionic liquid or under biphasic conditions ionic liquid/CH<sub>2</sub>Cl<sub>2</sub> (Scheme 8).



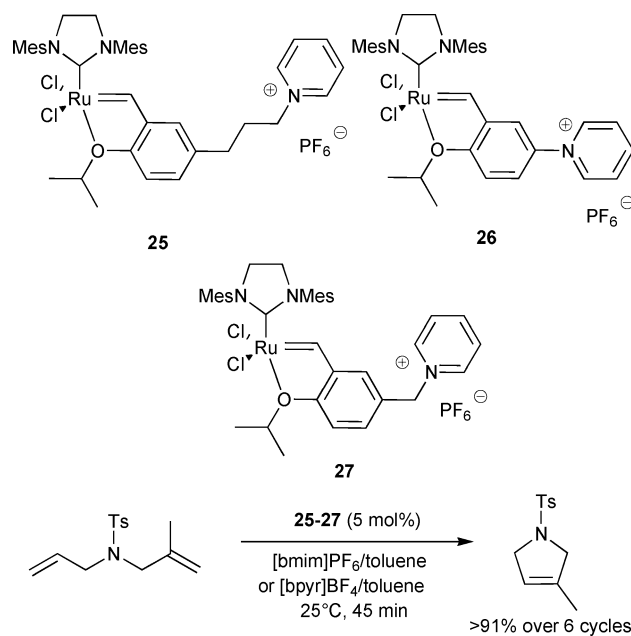
Scheme 8

The ionic catalyst **23a** has a high activity with a remarkable recyclability (92% conversion in the 10th cycle) and can be stored in [bmim]PF<sub>6</sub> for several months without significant loss of activity. The ionic tags were crucial to the recyclability of the catalysts because the unsupported catalysts rapidly lose their activity during the recycle experiments. The Grubbs-Hoveyda catalyst **22** under the same conditions gave low yield after the second, and was completely inactive after the 4th cycle. Also, the catalyst **24a** can be repeatedly recycled and reused as a highly active catalyst for RCM of various diene and enyne substrates in [bmim]PF<sub>6</sub>/CH<sub>2</sub>Cl<sub>2</sub> without significant loss of its activity, and also exhibited a high level of recyclability in the RCM reaction.

The second generation metathesis catalysts **23b** and **24b** can be used for a wide variety of more difficult substrates.<sup>33</sup> Catalyst **24b** is particularly useful for di-, tri- and tetrasubstituted diene and enyne substrates, whereas compound **23b** works well also for range of nitrogen-, oxygen- and sulfur-containing compounds. Moreover, complex **23b** was examined in various solvents at different temperatures ([bmim]PF<sub>6</sub> and [bmim]NTf<sub>2</sub> and [bmim]PF<sub>6</sub>/toluene). Use of a biphasic [bmim]PF<sub>6</sub>/toluene (1/3) medium improved the recycling of the catalyst and it led to very low residual levels of Ru in products. Use of reduced amounts (2.5 mol%) of the catalyst **23a** relative to the substrate

also led to high conversion, even at room temperature. The recycled catalyst/ionic liquid could be reused consecutively in the RCM of another three different substrates, each giving high yields of the respective product, without any replenishment of either the catalyst or the ionic liquid. The catalyst remained highly active even after being recovered from an enyne metathesis.<sup>34</sup>

Grela *et al.*<sup>35</sup> prepared pyridinium-tagged Ru-complexes for olefin metathesis in several media, including room temperature ionic liquids. Complexes **25** and **26** are highly active catalysts for ring closing metathesis of di- and tri-substituted and also oxygen containing dienes in biphasic medium, but the recyclability was disappointing. Catalyst **25** could be reused 6 times with little loss of activity in [bmim]PF<sub>6</sub>/toluene (1/3), but for catalyst **26** the yield was only 6% after 4 runs. Differences of activity and reusability dependent on the counter-anion of the ionic liquid were observed, in favour of the PF<sub>6</sub><sup>-</sup> anion (Scheme 9).



Scheme 9

The second generation metathesis catalyst **27**, modified by attachment of a pyridinium tag to its benzylidene moiety through a CH<sub>2</sub> spacer, allowed the optimum balance between the activity of catalyst and its recyclability, exceeding 98% yield after 6 catalytic runs in the best case (Scheme 10).<sup>36</sup>

Dixneuf *et al.*<sup>37</sup> prepared ruthenium catalysts **28** and **29** for olefin metathesis containing the imidazolium tag linked to the *ortho*-oxygen atom and to the *meta* position of the styrenylidene ligand, and with a methyl group on the imidazolium cation in the C-2 position. The catalysts were investigated in ring closing metathesis of *N,N*-dialkyltosylamine in different ionic liquids. The good activity of catalyst **28** was retained only in the 2nd cycle (90 vs. 89%), then a decrease of activity was observed (75%). Catalyst **29** appeared even less recoverable due to a difficult recoordination of the ligand (Fig. 2).

Yet another way of attaching an ionic tag was reported Consorti and co-workers.<sup>38</sup> They described second generation metathesis catalyst **30**, which has an imidazolium ion linked through the phosphorus atom. The compound **30** was effective



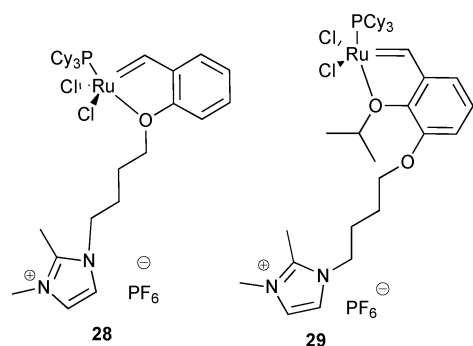
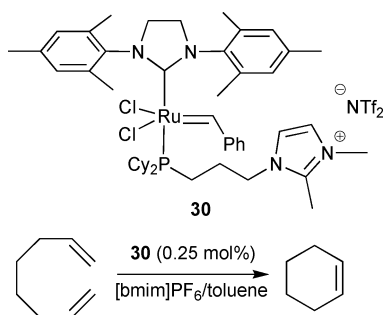


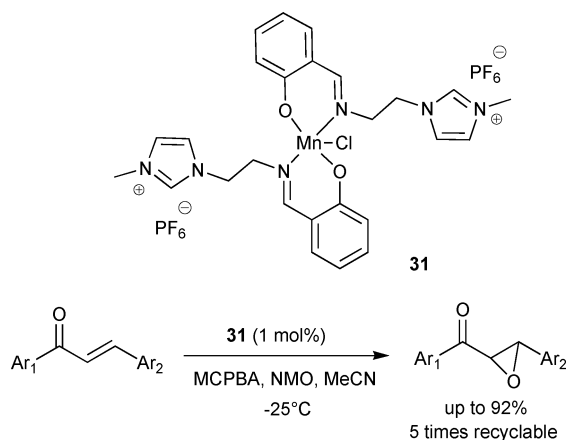
Fig. 2 Metathesis catalysts **28–29**.

in catalyzing the RCM of octa-1,7-diene and other dienes (Scheme 10). In the biphasic system [bmim]PF<sub>6</sub>/toluene, the catalyst **30** was stable for up to eight cycles.



Scheme 10

A new Mn(III)–Schiff base complex with an imidazolium tag was synthesized and employed as an efficient and recyclable catalyst for an epoxidation of chalcones with MCPBA/NMO. Complex **31** was a highly effective epoxidation catalyst affording the corresponding epoxides with excellent yields under mild conditions. This catalyst can be recovered and recycled for at least five runs without loss of activity. In addition, ionic liquid grafted catalysts do not suffer from the extensive mechanical degradation experienced with solid-supported catalysts after operating at high stirring rates (Scheme 11).<sup>39</sup>



Scheme 11

Ionic catalyst **32** is efficient for biphasic atom transfer radical polymerization of methyl methacrylate (MMA). The polymeriza-

tion of MMA at 60 °C was well-controlled, producing polymers with high initiator efficiency and low polydispersity. The catalyst **32** could be easily isolated after reaction by decantation. Recycled complex **32** catalyzed the second run polymerization with similar or even higher activity and improved control. The residual catalyst concentrations in the polymers were in the range 50–100 ppm. The addition of a small amount of silica gel to the polymer solution could further reduce the residual catalyst concentration (Fig. 3).<sup>40</sup>

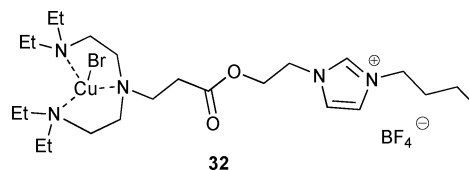
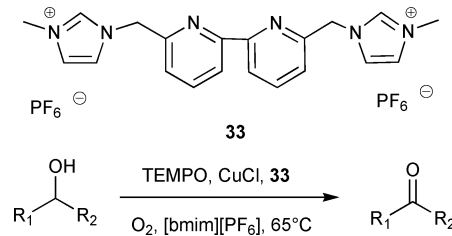


Fig. 3 Copper polymerization catalyst.

A novel imidazolium ionic-liquid-grafted 2,2'-bipyridine ligand **33** has been prepared and successfully employed in the copper-catalyzed selective oxidation of alcohols to the corresponding carbonyl compounds in [bmim]PF<sub>6</sub>. The reaction takes place under mild conditions and the catalytic ionic liquid solution can be recovered and reused without significant loss of catalytic efficiency. If the carbonyl compounds were isolated by distillation the yields were better, 97% yield after the 5th run; but were only 80% after the 5th run when extraction was used (Scheme 12).<sup>41</sup>



Scheme 12

Chauhan and co-workers performed epoxidation of alkenes with hydrogen peroxide by water-soluble iron(III) porphyrin complex **34** in [bmim]Br (Fig. 4). The catalyst could be recycled 5 times, with simple product isolation. The selectivity depended on the substrate, 81% of epoxide formed in the case of cyclooctane, but other oxidation products were formed from styrene and cyclohexene.<sup>42</sup> The catalyst **34** was also used for H<sub>2</sub>O<sub>2</sub>-mediated oxidation of the C=NOH bond in *N*-hydroxyarginine and other oximes to C=O in [bmim]BF<sub>4</sub>. The carbonyl compounds can be easily isolated from the reaction medium, and the catalyst immobilized in ionic liquid can be recycled and reused.<sup>43</sup>

Ionic manganese porphyrin **35** (Fig. 4), with a pyridinium tag embedded in a pyridinium based ionic liquid [bpyr]BF<sub>4</sub>, has been developed as an efficient and recyclable catalytic system for the oxidation of styrene and its derivatives with iodosylbenzene. After five runs the conversion of styrene slightly decreased (from 91% to 71%) but the product distribution varied dramatically from styrene oxide in the 1st run to phenyl acetaldehyde in the 5th run.<sup>44</sup>

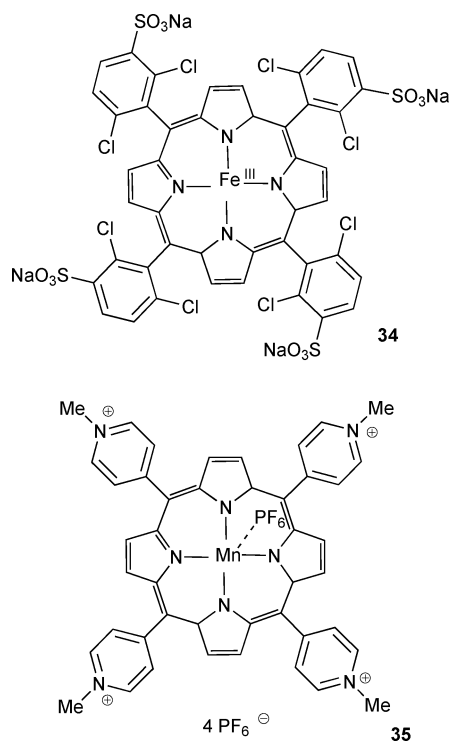


Fig. 4 Porphyrin catalysts.

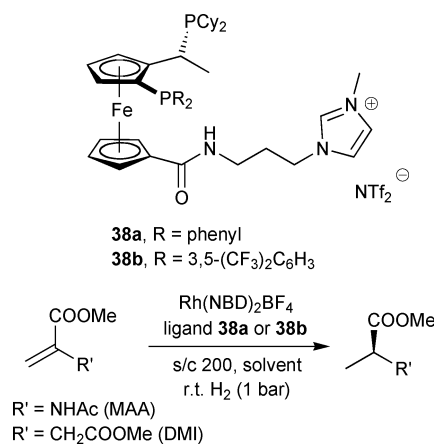
### Chiral transition metal catalysts

Among enantioselective catalysts, chiral transition metal complexes offer the widest range of possibilities in performing desired transformations. Many unmodified transition metal complexes were used in ionic liquids and often excellent results were obtained in such a simple setup.<sup>5</sup> However, it is still highly beneficial, especially in terms of catalyst recycling, to modify an organic ligand in such a manner that the resulting complex interacts more strongly with ionic liquid. In several instances a more active or enantioselective catalyst resulted from introduction of an ionic tag. In the beginning, the majority of work concentrated on asymmetric hydrogenations, but lately other reactions also begin to attract more interest.

Lee and co-workers grafted two imidazolium moieties onto rhodium/bisphosphane complex.<sup>45</sup> Catalyst **36**, produced in

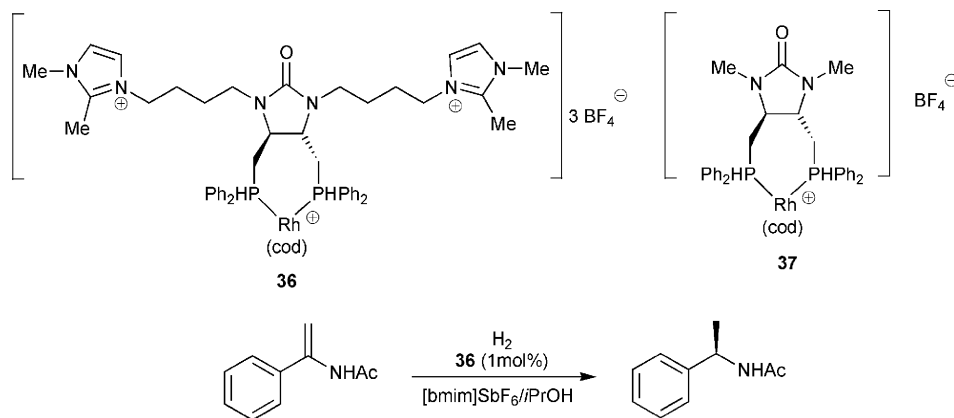
this way, exhibited excellent catalytic activities in asymmetric hydrogenation of enamides. In the two-phase system [bmim]SbF<sub>6</sub>/iPrOH, the enamide was hydrogenated in 97% ee with full conversion within 1h. Catalyst **36** was recycled 4 times with very little loss of catalytic activity (95% ee, 85% conversion in 1h). Hydrogenation with complex **37** resulted in a similarly enantioselective reaction in the first run, but in subsequent runs enantioselectivity and conversion decreased (4th run, 88% ee, 85% conversion in 12h). A control experiment with only 0.5 mol% of complex **37** (96% ee) showed that rhodium leaching is not the sole reason for decrease of catalytic performance. Improved stability of the ionic catalyst **36** in reaction medium was suggested as a possible explanation of its superior catalytic activity (Scheme 13).

Researchers from Solvias and Novartis synthesized modified *Josiphos* ligands with an imidazolium tag **38**.<sup>46</sup> Imidazolium diphosphanes **38** were successfully employed in Rh-catalyzed asymmetric hydrogenation of methyl acetamidoacrylate (MAA) and dimethyl itaconate (DMI) (Scheme 14).



Scheme 14

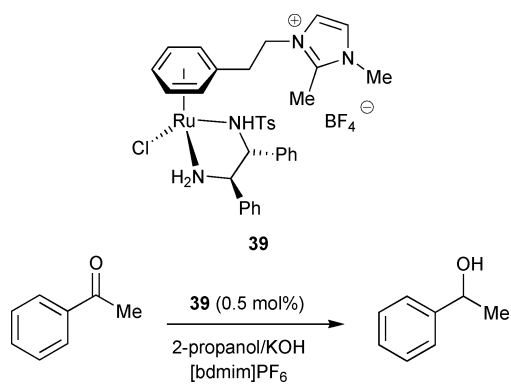
Modified ligands **38** paralleled the behavior of unmodified *Josiphos* ligands in asymmetric hydrogenation in classical organic solvents as well as under biphasic conditions. Reduction of MAA using ligand **38b** proceeded with 99% ee, and for reduction of DMI ligand **38a** was superior (99% ee). Imidazolium-tagged ligands showed much better reusability in *t*BuOMe/[bmim]BF<sub>4</sub>



Scheme 13

biphasic system compared with unmodified *Josiphos* ligands (approx. 15% decrease of TOF for 8th cycle, with constant ee's).

Ruthenium-catalyzed transfer hydrogenation of ketones is an important alternative to classical hydrogenation methods. Several attempts were made to prepare reusable Ru-catalysts with ionic tags. Geldbach and Dyson introduced an imidazolium moiety onto  $\eta^6$ -arene of the Ru-complex.<sup>47</sup> With catalyst **39**, dissolved in [bdmim]PF<sub>6</sub>, acetophenone was hydrogenated in a biphasic system, ionic liquid and propan-2-ol (Scheme 15). When ionic catalyst **39** was used, enantioselectivity was the same (98% ee) as with the traditional *p*-cymene ligand. Recycling of the catalytic system led to decreased conversion (52% in the 4th run compared with 99% in the 1st run) of the reaction, but enantioselectivity remained the same. The decrease in catalytic activity was explained by partial leaching of the catalyst from the ionic liquid due to decomposition of the ruthenium complex.



Ohta and co-workers chose a different approach to functionalization of the Ru-TsDPEN catalyst.<sup>48</sup> They introduced an imidazolium moiety into the diamine part of Ru-complex. Using the catalyst **40**, transfer hydrogenation of acetophenone with formic acid/triethylamine in [bmim]PF<sub>6</sub> proceeded with high enantioselectivity (92% ee) and high conversion (98%). In comparison, classical Ru/TsDPEN (**41**) gave similar results (93% ee, 96% conversion) but after the 4th cycle conversion decreased gradually, whereas catalyst **40** showed slightly better results (63% and 75% conversion, respectively) (Fig. 5).

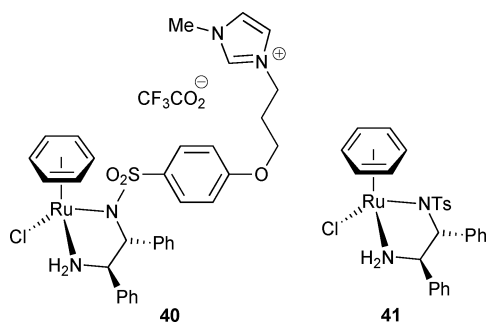


**Fig. 5** Transfer hydrogenation catalysts **40–41**.

Ru-complexes with chiral diamines, such as 1,2-diphenyl-1,2-ethylenediamine (DPEN), are capable hydrogenation catalysts. Chen and co-workers made a sulfonated derivative of DPEN, and used the resulting catalyst in hydrogenation of aromatic

and unsaturated ketones. In a mixture of [emim]OTf/water, enantioselectivities up to 85 and 76% ee, respectively, were obtained.<sup>49,50</sup>

Lin and co-workers prepared two polar phosphonic acid-derived Ru-BINAP systems (**42a**) and (**42b**) for asymmetric hydrogenation of  $\beta$ -ketoesters in ionic liquids (Fig. 6).<sup>51</sup>

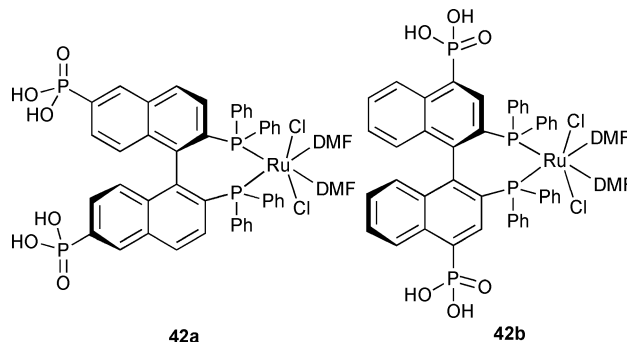
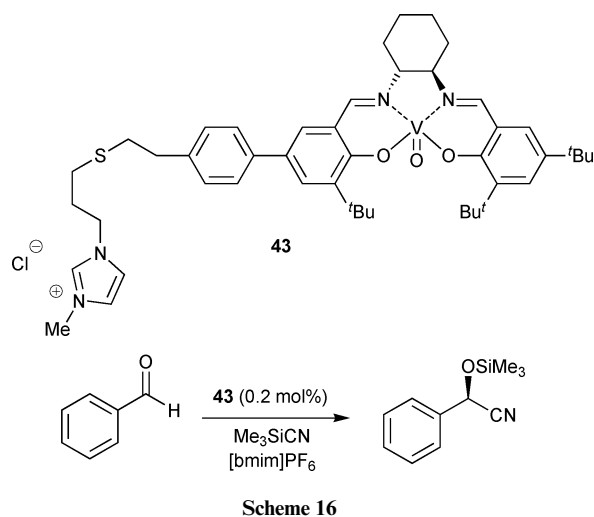


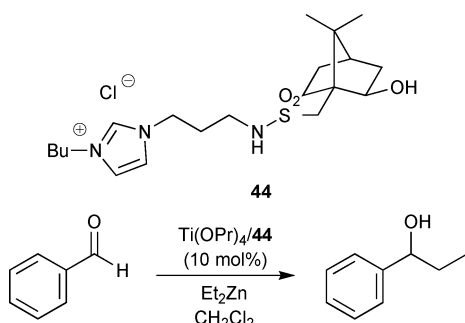
**Fig. 6** Phosphonic acid-derived BINAP complexes.

Several  $\beta$ -ketoesters were hydrogenated with high enantioselectivities using both catalysts **42a** and **42b** in [bmim]BF<sub>4</sub>, [bmim]PF<sub>6</sub> as well as in [bdmim]NTf<sub>2</sub>. Results were comparable with Ru-BINAP system. It was possible to recycle the catalyst in the ionic liquid four times with only small or no decrease in enantioselectivity and conversion.

The chiral vanadyl salen complex was tagged also with an imidazolium ion. Complex **43** catalyzed asymmetric cyanosilylation of benzaldehyde in [bmim]PF<sub>6</sub>. Enantioselectivity of the reaction (57% ee) was significantly lower than that with unmodified vanadyl ligand (89% ee). However, catalytic activity of complex **43** was considerably higher than that of the unmodified catalyst as well as catalyst anchored on silica, activated carbon and single wall carbon nanotubes (Scheme 16).<sup>52</sup>



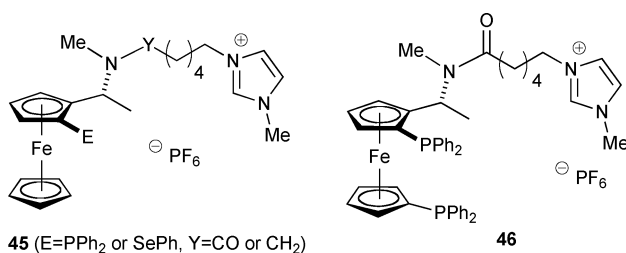
Moreau and coworkers prepared imidazolium-tagged camphorsulfonamide ligands for Ti-promoted asymmetric Et<sub>2</sub>Zn addition to benzaldehyde (Scheme 17).<sup>53</sup> Alkylation of benzaldehyde in the presence of the titanium complex of **44** was performed in CH<sub>2</sub>Cl<sub>2</sub>. Conversions were over 99% in all cases, but enantioselectivities were only moderate (65% ee). Separation



Scheme 17

of the product from the catalyst was achieved by evaporation of the solvent and hydrolysis followed by extraction with diethyl ether, in which the catalyst was not soluble. The catalytic system was used four times without any change in catalytic activity and enantioselectivity.

In our laboratory, we prepared several imidazolium-tagged ferrocene ligands.<sup>54</sup> Ligands **45** and **46** were used in Pd-catalyzed allylic alkylation of 1,3-diphenylprop-2-enyl acetate with dimethyl malonate (Scheme 18).

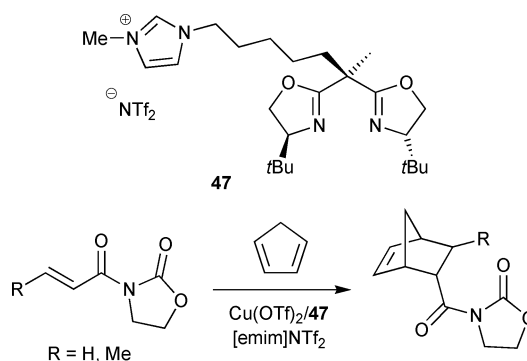


Scheme 18

The highest enantioselectivity (92% ee) was achieved with diphosphine **46** in  $[\text{bmim}]\text{PF}_6$ . Interestingly, this enantioselectivity is higher than that of the corresponding ligand without imidazolium moiety (BPPFA) when used in THF as well as in  $[\text{bmim}]\text{PF}_6$ . Other ionic ligands were inferior. Recycling experiments led to a slight decrease of enantioselectivity and considerable decrease of yield (1st run 94%, 89% ee; 2nd run 57%, 77% ee; 3rd run 16%, 69% ee in  $[\text{emim}]\text{EtOSO}_3$ ).

Imidazolium-tagged bis(oxazoline) **47** has been prepared and used as a chiral ligand in the copper-catalyzed Diels–Alder reaction of *N*-acryloyl and *N*-crotonoyloxazolidinones with cyclopentadiene.<sup>55</sup> Using the ligand **47**, a significant enhancement in rate and enantioselectivity of the reaction in ionic liquid was achieved compared with dichloromethane. Compared with unfunctionalized bis(oxazoline) ligand, similar enantioselectivities were obtained, but with marked rate enhancement in ionic liquid in the case of imidazolium tagged ligand. The catalyst could also be recycled 10 times without loss of activity and enantioselectivity (Scheme 19).

Ligand **47** was also recently used in copper-catalyzed Mukaiyama aldol reaction. Reaction was again faster in ionic



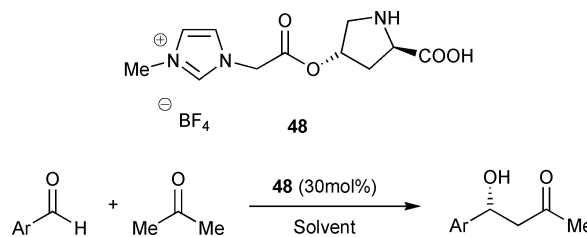
Scheme 19

liquid than in dichloromethane. It was completed in only 2 min and the aldol product was obtained with good enantioselectivity (94% ee). In  $[\text{emim}]\text{NTf}_2$ , the copper complex of **47** was recycled three times with no loss of activity and enantioselectivity.<sup>56</sup> Gavrilov and Reetz prepared imidazolium-tagged phosphate and diamidophosphite ligands. Their Rh and Pd-complexes were efficient catalysts for asymmetric hydrogenation and allylic substitution in organic solvents. Interestingly, hydrogenation in  $[\text{bdmim}]\text{BF}_4$  was less selective than that in dichloromethane (79 vs. 94% ee).<sup>57</sup>

## Organocatalysts

Ionic liquids proved to be useful media for various organocatalytic reactions. Particularly, *L*-proline-catalyzed aldol reactions work well in ionic liquids.<sup>58,59</sup> A smaller amount of the catalyst can be used than in DMSO, although yields of the products decrease significantly in the 3rd recycling. To circumvent these problems, several imidazolium-tagged organocatalysts were reported, even though some of them were tested only in organic solvents. So far, most of the attempts have concentrated on typical organocatalytic reactions such as aldol condensations and Michael additions. But regarding the great progress of organocatalysis, there are without any doubt many possibilities for further research.

Derivatives of *trans*-4-hydroxy-*L*-proline, like compound **48**, are interesting catalysts for the aldol reaction (Scheme 20).<sup>60</sup>



Scheme 20

The catalyst **48** catalyzed the aldol reaction of different aromatic aldehydes with acetone. Reactions were carried out either in excess of acetone or in DMSO at room temperature for 25 h with 30 mol% of the catalyst. The immobilized *L*-proline derivative was a more efficient catalyst than *L*-proline itself under similar conditions and it was possible to reuse it in subsequent experiments. The advantage of the catalyst **48** is also



that volatile starting material can be distilled off and the residue is simply rinsed with dichloromethane to extract the product. The catalyst, which is insoluble in  $\text{CH}_2\text{Cl}_2$ , can be used in the next experiment. The authors did not carry out the reaction in any ionic liquid, nor did they test aldolisation with cyclic ketones. Also, chiral pyrrolidine derivatives **49–54** were recently employed in aldol reaction (Fig. 7).<sup>61</sup>

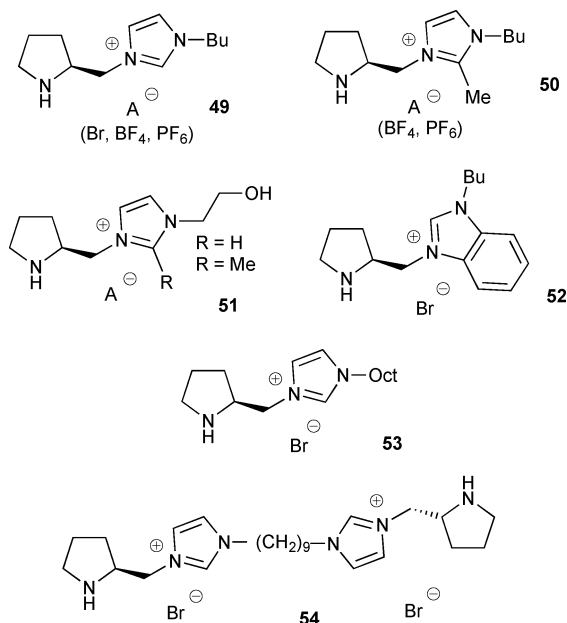
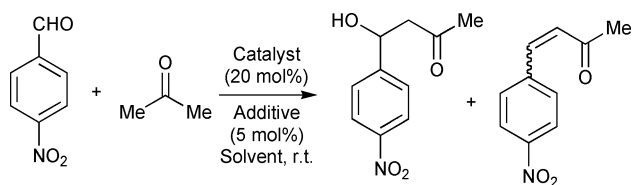


Fig. 7 Pyrrolidine-based ionic catalysts.

Reactions were carried out with *p*-nitrobenzaldehyde and acetone : water 4 : 1 mixture with some additives (Scheme 21). The full conversion of aldehyde was observed, but aldolisation was accompanied with the undesired Claisen–Schmidt reaction. The best catalysts were compounds **49** (with  $\text{BF}_4^-$  anion), **51** and **54**.



Scheme 21

Reactions of aromatic aldehydes can also be performed with cyclic ketones, but it usually requires 1 equivalent of water and 5 mol% of acetic acid as additives. The rate of the reaction depends on the cycle size of ketones. Reactions with cyclopentanone were usually finished after 2–6 h, but cyclooctanone needed 105 h to reach full conversion. Stereoselectivity of the reaction was rather low (*syn/anti* 4.8:1 and 50% ee). Recently, Tromboni *et al.*<sup>62</sup> described two proline-based ionic organocatalysts **55** and **56** (Fig. 8).

The authors performed a thorough study of aldol reaction of *p*-nitrobenzaldehyde with acetone (10 mol excess) catalyzed with compounds **55** and **56** in  $[\text{bmim}]\text{NTf}_2$ . Both catalysts have similar activities and products were isolated in up to 79% yields after

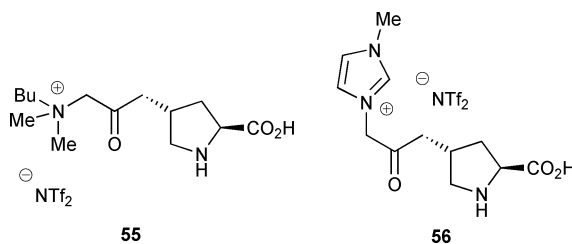
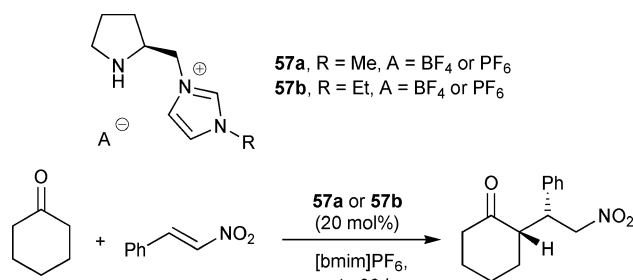


Fig. 8 Proline-derived catalysts.

24 hours using only 5 mol% of the catalyst. Enantioselectivity of the reaction was reasonable (up to 84% ee). They also proved that these catalysts were more efficient in ionic liquids than *L*-proline, with which only medium yield and enantioselectivity was obtained (50% yield, 72% ee). Surprisingly, the product yield decreased to 30% in the 3rd cycle, probably because of catalyst leaching or decomposition during work-up procedure. The residual acetone was distilled off the reaction mixture and the product was isolated by extraction with diethyl ether. The catalytic system was vacuum dried before reuse. Also, Zlotin and co-workers recently used an imidazolium-derived proline catalyst, similar to compound **56**. Aldol reactions of cyclic ketones with aldehydes in water proceeded with high yields, diastereoselectivities as well as enantioselectivities.<sup>63</sup> In our laboratory, we demonstrated that Michael addition of different aldehydes and ketones can be catalyzed by organocatalysts in ionic liquids.<sup>64</sup> The reactions proceeded with high yields and reasonable enantioselectivities, but activity and selectivity decreased after the 2nd run. Xu *et al.*<sup>65</sup> described the first imidazolium-tagged organocatalyst **57** for conjugated addition of ketones to nitroolefins (Scheme 22).



Scheme 22

The activity of the imidazolium-tagged catalyst and enantioselectivity (98%, 99% ee) of the addition reaction in  $[\text{bmim}]\text{PF}_6$  remained high until the 4th recyclization. On the other hand, the reaction with *L*-proline was much slower and the addition product was only isolated in 30% yield and with low selectivity (d.r. 86 : 14, 24% ee).

Luo *et al.*<sup>66</sup> have tested pyrrolidine-based organocatalysts **58** and **59** (Fig. 9) in the same reaction with similar results. The authors used 15 mol% of the catalyst and 5 mol% of TFA as co-catalyst with an excess of cyclohexanone as solvent. Compound **59** was the most efficient catalyst, with excellent yield and selectivity in short reaction time (100% yield, *syn/anti* 99 : 1, 99% ee). Part of the catalyst was probably lost during the work up, because at the 3rd recycle reaction time had to be prolonged to 24 h to obtain similar results.

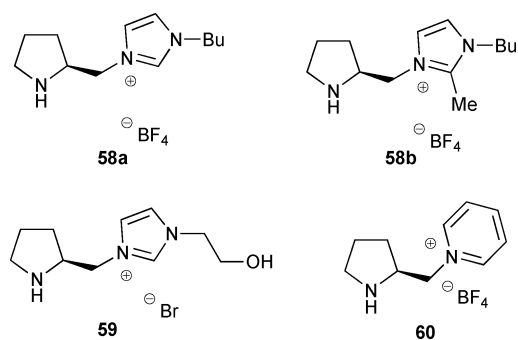


Fig. 9 Pyrrolidine organocatalysts.

Compounds **58–59** with  $\text{PF}_6^-$  anions were less effective. Comparable results were achieved also with substituted  $\beta$ -nitrostyrenes and preliminary experiments proved that addition of aliphatic aldehydes to  $\beta$ -nitrostyrene were also possible. Similarly, Headley and co-workers<sup>67</sup> described pyridinium-based organocatalysts **60**. These compounds effectively catalyzed Michael addition (92% yield, *syn/anti* 99 : 1, 99% ee). The same reaction was catalyzed by pyridinium-derived catalysts described by Xu and co-workers.<sup>68</sup> Catalysts of this type were also effective in desymmetrization of prochiral ketones *via* asymmetric Michael addition reaction to nitrostyrenes.<sup>69</sup>

Liang *et al.*<sup>70</sup> described more complicated ionic-liquid-supported catalysts **61** and **62** (Fig. 10), and employed them in the Michael addition of cyclohexanone to  $\beta$ -nitrostyrene. Reactions were carried out with 2 equivalents of cyclohexanone in several solvents (DMSO,  $\text{CHCl}_3$ ,  $\text{H}_2\text{O}$ ), but the best results were achieved without solvent (97% yield, *syn/anti* 97 : 3, 94% ee). Catalysts could be recycled 3 times in such conditions with good results. The catalyst can be separated by dilution of the reaction mixture with diethyl ether. However no ionic liquid was tested as the solvent.

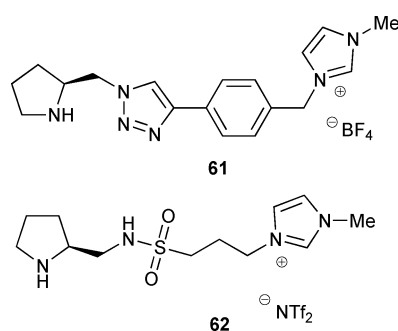
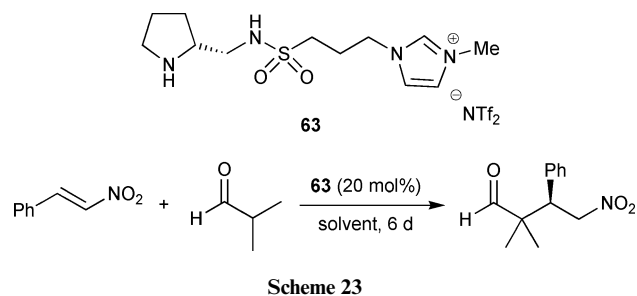


Fig. 10 Catalysts with triazole and sulfonamide linker.

These catalysts also performed well in Michael addition of cyclohexanone to substituted  $\beta$ -nitrostyrenes. The addition of cyclopentanone resulted in a lower yield and selectivity (*syn/anti* 5 : 3, 81 and 77% ee, respectively). The authors also tested addition of acetone (good yields, but low ee) as well as isovaleraldehyde (high *syn/anti* ratio, modest ee).

Sulfonamide derivative **63** is an efficient catalyst for addition of aldehydes to  $\beta$ -nitrostyrene as well (Scheme 23).<sup>71</sup> Catalytic activity of this compound was verified in reaction of  $\beta$ -nitrostyrene with isobutyraldehyde in several conventional organic solvents (MeOH, *i*-PrOH,  $\text{CH}_3\text{CN}$ , THF, DCM,  $\text{CHCl}_3$ , EtOAc, Et<sub>2</sub>O).



Scheme 23

The best yields of the product were obtained in diethyl ether (58%, 82% ee). No decrease of catalytic activity, or selectivity was observed in 3rd recycling. After dilution of the reaction mixture with diethyl ether, the catalyst precipitated and was easily recovered.

Reactions with unbranched aldehydes also proceeded well (50–60% yields) and with high diastereoselectivities (d.r. 96 : 4) and reasonable enantioselectivities (64–73% ee).

Xu and co-workers<sup>72</sup> published very interesting work recently. A range of simple compounds, **64**, were evaluated as catalysts in Michael additions of cyclic ketones to  $\beta$ -nitrostyrenes in DMSO and different polyethylene glycols as the reaction media (Fig. 11). The authors found that the best catalyst (R = Me and A = PhCOO) and polyethylene glycols bigger than PEG 720 form a special pocket, which can wrap (solvate) the cation of the catalyst and thus improve its catalytic activity. The existence of such an entity was proved by ESI MS. Practically full conversion of starting materials was achieved in 12 h with high diastereoselectivity *syn/anti* 97 : 3 as well as high enantioselectivity (97% ee). In DMSO, the reaction was considerably slower (36 hours). The product isolation was simple and the catalyst in PEG was reused in 7 subsequent recyclations, but reaction required a longer time.

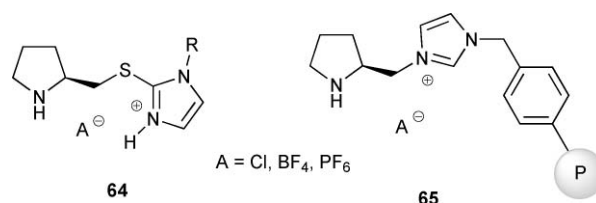


Fig. 11 Catalyst **64** for use in PEG and polymer bound ionic organocatalyst.

Also, polymer bound insoluble catalyst **65** was prepared from a chiral pyrrolidine derivative. It was first connected to imidazole, and the resulting product was alkylated with Merifield resin.<sup>73</sup>

The compound **65** was an excellent catalyst for solvent-free Michael additions giving higher than 90% yields of the products with more than 90% ee, and d.r. usually higher than 95 : 5. L-Proline derivative **66**, immobilized on methylimidazole, is a capable catalyst for Claisen–Schmidt reactions of aromatic aldehydes with acetone. Under solvent-free conditions, yields of unsaturated ketones were higher than 80%, but rather a high amount of catalyst had to be used (20 mol%).

Quinuclidine derivative **67a** (Fig. 12) was used as the catalyst for the Morita–Baylis–Hillman reaction.<sup>74</sup> Several solvents were tested as reaction media but ionic liquids had a negative influence on the reaction. The best results were achieved in methanol

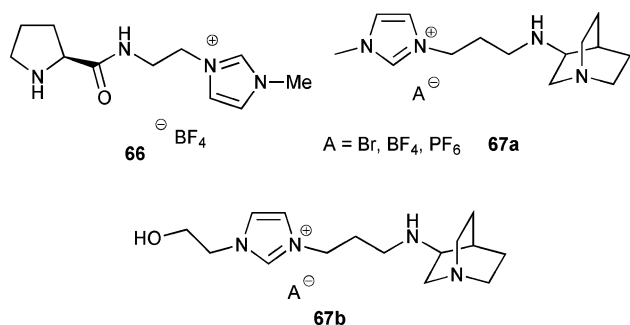
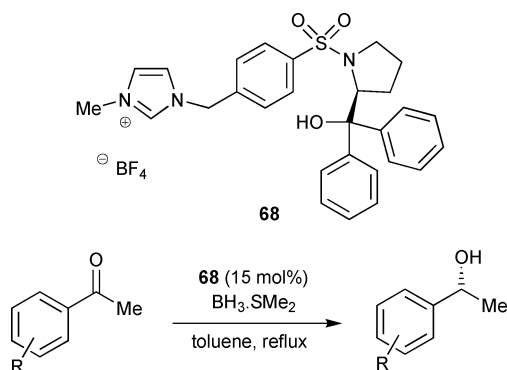


Fig. 12 Prolinamide and quinuclidine catalysts.

(84% yield after 8 h; 74% yield in the 3rd recycle, and in the 6th recycle the reaction time had to be prolonged to 36 h to reach the same yields). Immobilized compound **67a** was as good a catalyst as its soluble counterpart, having a benzyl group instead of imidazolium cation, but the immobilized catalyst can be easily recovered and reused. Later these authors described a similar catalyst **67b** (Fig. 12) with a hydroxyl group in the ionic part. The hydroxyl-derived catalyst displayed better catalytic properties in the Morita–Baylis–Hillman reaction than the original catalyst **67a**.<sup>75</sup>

Liang and co-workers synthesized imidazolium-tagged sulfonamide **68**.<sup>76</sup> The catalyst **68** was effective in mediating borane reduction of aromatic ketones in excellent yields and with enantioselectivities up to 94% ee (Scheme 24). After aqueous work-up, products remained in the organic solvent and the water-soluble catalyst was recycled after drying. In reduction of acetophenone, yield of the product remained unaltered but enantioselectivity decreased from 73 to 65% ee over four recyclings.



Scheme 24

## Conclusion and outlook

Catalysis in general is one of the key strategies towards sustainable chemical synthesis. Furthermore, with many expensive catalysts there certainly is a need for recycling, for environmental as well as economic reasons. Catalyst immobilization is a well-established strategy to achieve recycling. However, heterogeneous systems often suffer from decreased activities, so homogeneous supported catalysts emerge as a valuable concept. We demonstrated in this overview that ionically-tagged catalysts have already proved to be useful alternatives to unmodified

structures. The catalytic activities of these catalysts often parallel or even surpass those of classical catalysts with the added benefit of simplified product isolation and possible catalyst reuse. Published data suggest that careful design and optimization of catalyst structure in connection with each reaction are often crucial for achieving high activities and selectivities throughout recycle experiments. There is a great potential for improvements of catalyst physical and chemical properties by altering both the cation and anion parts of these molecules. The number of possible variations becomes almost uncountable if we also take the ionic liquid media into account. Although great progress has already been achieved in this field, there is still much to be discovered and improved. One of the most important issues seems to be the stability of catalytic system in desired reaction. Several stable and highly active catalysts already exist, which can be recycled even more than 10 times with no or minimal loss of activity. However, a majority of catalysts still fail to achieve these parameters. The usual amount of ionic catalyst used in reactions is a few percent, typically 1–5 mol% for metal catalyzed reactions, but with organocatalysts this number often reaches 20% or even more. These numbers are quite high, especially from the point of view of potential industrial deployment. Using one catalytic system for different reactions or various substrates (even between recycle experiments) is another particularly attractive feature, which is also rather unexplored. Also, only a limited number of enantioselective transformations that use transition metal catalysts have been studied so far. We think that more research effort could be directed towards exploring more challenging asymmetric C–C and C–heteroatom bond forming reactions. In the field of organocatalyzed reactions, the majority of the work with ionically-tagged catalysts concentrates on aldolisations or simple Michael additions. Here, too, it would be beneficial to explore other transformations. We believe that this review can help stimulate further research and development in this exciting area of green chemistry.

## References

- P. T. Anastas and J. C. Werner, *Green Chemistry: Theory and Practice*, Oxford University Press, New York, 1998.
- R. A. Sheldon, *Green Chem.*, 2005, **7**, 267–278.
- P. Wasserscheid and T. Welton, *Ionic Liquids in Synthesis*, Wiley-VCH, Weinheim, 2nd edn, 2007.
- J. Dupont, R. F. de Souza and P. A. Z. Suarez, *Chem. Rev.*, 2002, **102**, 3667–3692.
- C. E. Song, *Chem. Commun.*, 2004, 1033–1043.
- V. I. Parvulescu and C. Hardacre, *Chem. Rev.*, 2007, **107**, 2615–2665.
- S. Liu and J. Xiao, *J. Mol. Catal. A: Chem.*, 2007, **270**, 1–43.
- P. Wasserscheid, and P. Schulz, in *Ionic Liquids in Synthesis*, ed. P. Wasserscheid and T. Welton, Wiley-VCH, Weinheim, 2008, pp. 369–463.
- W. Miao and T. H. Chan, *Acc. Chem. Res.*, 2006, **39**, 897–908.
- M. Vautier, A. Kirchning, and V. Singh, in *Ionic Liquids in Synthesis*, ed. P. Wasserscheid, and T. Welton, Wiley-VCH, Weinheim, 2008, pp. 488–523.
- Y. Chauvin, L. Mussmann and H. Olivier, *Angew. Chem., Int. Ed. Engl.*, 1996, **34**, 2698–2700.
- L. Wei, J. Jiang, Y. Wang and Z. Jin, *J. Mol. Catal. A: Chem.*, 2004, **221**, 47–50.
- T. Suárez, B. Fontal, M. Reyes, F. Bellandi, R. R. Contreras, J. M. Ortega, G. León, P. Cancines and B. Castillo, *React. Kinet. Catal. Lett.*, 2004, **82**, 325–331.
- Q. Lin, H. Y. Fu, F. Xue, M. L. Yuan, H. Chen and X. J. Li, *Acta Phys. Chim. Sin.*, 2006, **22**, 465–469.

- 15 C. P. Mehnert, R. A. Cook, N. C. Dispenziere and E. J. Mozeleski, *Polyhedron*, 2004, **23**, 2679–2688.
- 16 M. F. Sellin, P. B. Webb and D. J. Cole-Hamilton, *Chem. Commun.*, 2001, 781–782.
- 17 P. B. Webb, M. F. Sellin, T. E. Kunene, S. Williamson, A. M. Z. Slawin and D. J. Cole-Hamilton, *J. Am. Chem. Soc.*, 2003, **125**, 15577–15588.
- 18 K. W. Kottsieper, O. Stelzer and P. Wasserscheid, *J. Mol. Catal. A: Chem.*, 2001, **175**, 285–288.
- 19 F. Favre, H. Olivier-Bourbigou, D. Commereuc and L. Saussine, *Chem. Commun.*, 2001, 1360–1361.
- 20 R. P. J. Bronger, S. M. Silva, P. C. J. Kamer and P. W. N. M. van Leeuwen, *Chem. Commun.*, 2002, 3044–3045.
- 21 T. J. Geldbach, G. Laurencyzy, R. Scopelliti and P. J. Dyson, *Organometallics*, 2006, **25**, 733–742.
- 22 A. Corma, H. Garcia and A. Leyva, *Tetrahedron*, 2004, **60**, 8553–8560.
- 23 D. Zhao, Z. Fei, T. J. Geldbach, R. Scopelliti and P. J. Dyson, *J. Am. Chem. Soc.*, 2004, **126**, 15876–15882.
- 24 J. C. Xiao, B. Twamley and J. M. Shreeve, *Org. Lett.*, 2004, **6**, 3845–3847.
- 25 R. Wang, J.-C. Xiao, B. Twamley and J. N. M. Shreeve, *Org. Biomol. Chem.*, 2007, **5**, 671–678.
- 26 J. C. Xiao and J. M. Shreeve, *J. Org. Chem.*, 2005, **70**, 3072–3078.
- 27 R. Wang, M. M. Piekarski and J. N. M. Shreeve, *Org. Biomol. Chem.*, 2006, **4**, 1878–1886.
- 28 M.-c. Liao, X.-h. Duan and Y.-m. Liang, *Tetrahedron Lett.*, 2005, **46**, 3469–3472.
- 29 C. Hubert, J.-L. Renaud, B. Demerseman, C. Fischmeister and C. Bruneau, *J. Mol. Catal. A: Chem.*, 2005, **237**, 161–164.
- 30 J. C. Xiao, C. Ye and J. M. Shreeve, *Org. Lett.*, 2005, **7**, 1963–1965.
- 31 N. Audic, H. Clavier, M. Mauduit and J. C. Guillemin, *J. Am. Chem. Soc.*, 2003, **125**, 9248–9249.
- 32 Q. Yao and Y. Zhang, *Angew. Chem., Int. Ed.*, 2003, **42**, 3395–3398.
- 33 Q. Yao and M. Sheets, *J. Organomet. Chem.*, 2005, **690**, 3577–3584.
- 34 H. Clavier, N. Audic, J.-C. Guillemin and M. Mauduit, *J. Organomet. Chem.*, 2005, **690**, 3585–3599.
- 35 D. Rix, H. Clavier, Y. Coutard, L. Gulajski, K. Grela and M. Mauduit, *J. Organomet. Chem.*, 2006, **691**, 5397–5405.
- 36 D. Rix, F. Caijo, I. Laurent, L. Gulajski, K. Grela and M. Mauduit, *Chem. Commun.*, 2007, 3771–3773.
- 37 C. Thurier, C. Fischmeister, C. Bruneau, H. Olivier-Bourbigou and P. H. Dixneuf, *J. Mol. Catal. A: Chem.*, 2007, **268**, 127–133.
- 38 C. S. Consorti, G. L. P. Aydos, G. Ebeling and J. Dupont, *Org. Lett.*, 2008, **10**, 237–240.
- 39 Y. Peng, Y. Cai, G. Song and J. Chen, *Synlett*, 2005, 2147–2150.
- 40 S. Ding, M. Radosz and Y. Shen, *Macromolecules*, 2005, **38**, 5921–5928.
- 41 X.-E. Wu, L. Ma, M.-X. Ding and L.-X. Gao, *Chem. Lett.*, 2005, **34**, 312–313.
- 42 K. A. Srinivas, A. Kumar and S. M. S. Chauhan, *Chem. Commun.*, 2002, 2456–2457.
- 43 N. Jain, A. Kumar and S. M. S. Chauhan, *Tetrahedron Lett.*, 2005, **46**, 2599–2602.
- 44 Y. Liu, H.-J. Zhang, Y. Lu, Y.-Q. Cai and X.-L. Liu, *Green Chem.*, 2007, **9**, 1114–1119.
- 45 S.-g. Lee, Y. J. Zhang, J. Y. Piao, H. Yoon, C. E. Song, J. H. Choi and J. Hong, *Chem. Commun.*, 2003, 2624–2625.
- 46 X. Feng, B. Pugin, E. Küsters, G. Sedelmeier and H.-U. Blaser, *Adv. Synth. Catal.*, 2007, **349**, 1803–1807.
- 47 T. J. Geldbach and P. J. Dyson, *J. Am. Chem. Soc.*, 2004, **126**, 8114–8115.
- 48 I. Kawasaki, K. Tsunoda, T. Tsuji, T. Yamaguchi, H. Shibuta, N. Uchida, M. Yamashita and S. Ohta, *Chem. Commun.*, 2005, 2134–2136.
- 49 J. Wang, J. Feng, R. Qin, H. Fu, M. Yuan, H. Chen and X. Li, *Tetrahedron: Asymmetry*, 2007, **18**, 1643–1647.
- 50 J. Wang, R. Qin, H. Fu, J. Chen, J. Feng, H. Chen and X. Li, *Tetrahedron: Asymmetry*, 2007, **18**, 847–851.
- 51 H. L. Ngo, A. Hu and W. Lin, *Chem. Commun.*, 2003, 1912–1913.
- 52 C. Baleizao, B. Gigante, H. Garcia and A. Corma, *Tetrahedron*, 2004, **60**, 10461–10468.
- 53 B. Gadenne, P. Hesemann and J. J. E. Moreau, *Tetrahedron Lett.*, 2004, **45**, 8157–8160.
- 54 R. Šebesta, M. Mečiarová, V. Poláčková, E. Veverková, I. Kmentová, E. Gajdošíková, J. Cvengroš, R. Buffa and V. Gajda, *Coll. Czech. Chem. Commun.*, 2007, **72**, 1057–1068.
- 55 S. Doherty, P. Goodrich, C. Hardacre, J. G. Knight, M. T. Nguyen, V. I. Pârvulescu and C. Paun, *Adv. Synth. Catal.*, 2007, **349**, 951–963.
- 56 S. Doherty, P. Goodrich, C. Hardacre, V. Pârvulescu and C. Paun, *Adv. Synth. Catal.*, 2008, **350**, 295–302.
- 57 K. N. Gavrilov, S. E. Lyubimov, O. G. Bondarev, M. G. Maksimova, S. V. Zhegllov, P. V. Petrovskii, V. A. Davankov and M. T. Reetz, *Adv. Synth. Catal.*, 2007, **349**, 609–616.
- 58 P. Kotrusz, I. Kmentova, B. Gotov, S. Toma and E. Solcaniova, *Chem. Commun.*, 2002, **8**, 2510–2511.
- 59 T.-P. Loh, L.-C. Feng, H.-Y. Yang and J.-Y. Yang, *Tetrahedron Lett.*, 2002, **43**, 8741–8743.
- 60 W. Miao and T. H. Chan, *Adv. Synth. Catal.*, 2006, **348**, 1711–1718.
- 61 S. Luo, X. Mi, L. Zhang, S. Liu, H. Xu and J.-P. Cheng, *Tetrahedron*, 2007, **63**, 1923–1930.
- 62 M. Lombardo, F. Pasi, S. Easwar and C. Trombini, *Adv. Synth. Catal.*, 2007, **349**, 2061–2065.
- 63 D. E. Siyutkin, A. S. Kucherenko, M. I. Struchkova and S. G. Zlotin, *Tetrahedron Lett.*, 2008, **49**, 1212–1216.
- 64 P. Kotrusz, S. Toma, H. G. Schmalz and A. Adler, *Eur. J. Org. Chem.*, 2004, 1577–1583.
- 65 D. Xu, S. Luo, H. Yue, L. Wang, Y. Liu and Z. Xu, *Synlett*, 2006, 2569–2572.
- 66 S. Luo, X. Mi, L. Zhang, S. Liu, H. Xu and J.-P. Cheng, *Angew. Chem., Int. Ed.*, 2006, **45**, 3093–3097.
- 67 B. Ni, Q. Zhang and A. D. Headley, *Tetrahedron Letters*, 2008, **49**, 1249–1252.
- 68 D.-Q. Xu, B.-T. Wang, S.-P. Luo, H.-D. Yue, L.-P. Wang and Z.-Y. Xu, *Tetrahedron: Asymmetry*, 2007, **18**, 1788–1794.
- 69 S. Luo, L. Zhang, X. Mi, Y. Qiao and J. P. Cheng, *J. Org. Chem.*, 2007, **72**, 9350–9352.
- 70 L.-Y. Wu, Z.-Y. Yan, Y.-X. Xie, Y.-N. Niu and Y.-M. Liang, *Tetrahedron: Asymmetry*, 2007, **18**, 2086–2090.
- 71 B. Ni, Q. Zhang and A. D. Headley, *Green Chem.*, 2007, **9**, 737–739.
- 72 D. Q. Xu, S. P. Luo, Y. F. Wang, A. B. Xia, H. D. Yue, L. P. Wang and Z. Y. Xu, *Chem. Commun.*, 2007, 4393–4395.
- 73 D.-Q. Xu, L.-P. Wang, S.-P. Luo, Y.-F. Wang, S. Zhang and Z.-Y. Xu, *Eur. J. Org. Chem.*, 2008, 1049–1053.
- 74 X. Mi, S. Luo and J. P. Cheng, *J. Org. Chem.*, 2005, **70**, 2338–2341.
- 75 X. Mi, S. Luo, H. Xu, L. Zhang and J.-P. Cheng, *Tetrahedron*, 2006, **62**, 2537–2544.
- 76 S.-D. Yang, Y. Shi, Z.-H. Sun, Y.-B. Zhao and Y.-M. Liang, *Tetrahedron: Asymmetry*, 2006, **17**, 1895–1900.



# Water-in-ionic liquid microemulsions as a new medium for enzymatic reactions†

Muhammad Moniruzzaman,<sup>a</sup> Noriho Kamiya,<sup>a,b</sup> Kazunori Nakashima<sup>a</sup> and Masahiro Goto<sup>\*a,b</sup>

Received 13th February 2008, Accepted 25th March 2008

First published as an Advance Article on the web 1st April 2008

DOI: 10.1039/b802501k

The insolubility of enzymes in most ionic liquids has been overcome by the formation of aqueous microemulsion droplets in a hydrophobic ionic liquid stabilized by a layer of anionic surfactant sodium bis(2-ethyl-1-hexyl) sulfosuccinate (AOT) in the presence of 1-hexanol as a cosurfactant and the catalytic activity of one of the enzymes studied (lipase PS) became higher than in microemulsions of AOT in isoctane.

Ionic liquids (ILs), representing no measureable vapor pressure, have been proved to be useful as a replacement for ordinary organic solvents to reduce volatile organic compound (VOC) emissions.<sup>1</sup> Not only are ILs more environmentally attractive than organic solvents, but ILs possess many unique physicochemical properties, such as having very good dissolution properties for most organic and inorganic compounds, being non-flammable, fire resistant, having high thermal stability and wide liquid temperature ranges. ILs are also chemically diverse owing to the huge number of possible cation/anion combinations that can be synthesized. The main applications for ILs as a solvent include extraction,<sup>2</sup> organic synthesis<sup>3</sup> and separation<sup>4</sup> and their uses continue to expand.

The technological utility of enzymes can be enhanced greatly by their use in ILs rather than in conventional organic solvents or in their natural aqueous reaction media due to their unique physicochemical properties. The use of ILs has manifested many advantages, such as high conversion rates, high enantioselectivity, better enzyme stability, as well as better recoverability and recyclability.<sup>5-7</sup> However, one important drawback regarding the use of enzymes in ILs is the fact that they are not soluble in most ILs. Although some ILs can dissolve enzymes through the weak hydrogen bonding interactions, they often induce enzyme conformational changes resulting in inactivation. In fact, enzyme powder directly added in ILs needs to be stirred or shaken vigorously to interact with substrates, as there is a possibility of inactivating the enzymes. One of the most effective approaches to affect enzyme solubility in ILs is to add a small amount of water. However, the dissolved enzymes show low

catalytic activity due to their conformational change in ILs.<sup>6</sup> Another attempt to improve the solubility of enzymes was to conjugate lipase with polyethylene glycol (PEG) through chemical modification,<sup>7,8</sup> because PEG shows good solubility in ILs. It has been found that enzyme activity was significantly increased by increasing the solubility in ILs through their modification with comb-shaped polyethylene glycol.<sup>8</sup> However, such a modification is often laborious and time consuming. This is why the feasibility of enzymatic reactions in ILs is very limited. To find an easy way to combine enzyme solubility and activity in ILs is very essential to expand the use of ILs as green solvents.

The insolubility of enzymes in ILs can be overcome by the formation of nano/micrometre-sized aqueous domains in an IL continuous phase (referred to as water-in-IL microemulsions) stabilized by a layer of surfactants. It is well recognized that enzymes can be solubilized in organic solvents by the use of surfactants (generally referred to as water-in-oil microemulsions or reverse micelles) without the loss of their catalytic activity.<sup>9</sup> Enzymes can also be solubilized in organic solvents at very low surfactant concentrations.<sup>10</sup> The polar core of microemulsional systems has the ability to solubilize significant amounts of water, which form water pools. Enzymes solubilized in such water pools are protected from the unfavorable effect of organic solvents by the surfactant layer. Therefore, the new microemulsion in IL is interesting from academic, environmental and practical points of view. However, the formation of IL microemulsions is generally hindered by the insolubility of most conventional surfactants, particularly anionic surfactants such as AOT (sodium bis(2-ethyl-1-hexyl) sulfosuccinate) which has been used extensively to form microemulsions in organic solvents.<sup>11</sup> In our previous study,<sup>12</sup> we reported that AOT could be dissolved in a hydrophobic IL [C<sub>8</sub>mim][Tf<sub>2</sub>N] (1-octyl-3-methyl imidazolium bis (trifluoromethyl sulfonyl) amide) with the aid of 1-hexanol as a cosurfactant and upon addition of a small amount of water, these solutions formed optically transparent aqueous nano-environments. This domain of water is thought to be very suitable for enzymatic reactions in ILs. However, the solubility as well as the activity of enzymes in AOT based water-in-IL microemulsions have not been studied yet.

Here, the objective of the present study is two-fold: first, it is intended to demonstrate that the water domains in the IL microemulsions able to dissolve enzymes. Second, this study addresses the question of whether such a dissolved enzyme shows catalytic activity. In this study, lipase-catalyzed hydrolysis of *p*-nitrophenyl butyrate (*p*-PNB) has been used as a model reaction. *Burkholderia cepacia* lipase (former *Pseudomonas cepacia* lipase,

<sup>a</sup>Department of Applied Chemistry, Graduate School of Engineering, Kyushu University, 744 Moto-oka, Nishi-ku, Fukuoka, 819-0395, Japan. E-mail: mgototcm@mbbox.nc.kyushu-u.ac.jp; Fax: (+81)92-802-2810; Tel: (+81)92-802-2806

<sup>b</sup>Center for Future Chemistry, Graduate School of Engineering, Kyushu University, Japan

† Electronic supplementary information (ESI) available: Experimental details and enzyme solubility study. See DOI: 10.1039/b802501k

also known under its commercial trade name as lipase PS) was chosen because nowadays it is becoming one of the most used enzymes applicable to various processes because of its high activity in hydrolysis as well as in synthesis.<sup>13</sup>

The solubility studies showed that water-in-IL microemulsions can solubilize various enzymes and proteins, whereas the IL alone and water-saturated IL cannot (see the ESI).† The results imply that the water domains in the microemulsions<sup>12</sup> make it possible to solubilize proteins in the IL phase. We also checked the solubilization of one of the enzymes (lipase PS) by fluorescence spectroscopy. This lipase contains 3 tryptophan residues (Trp30, Trp209, and Trp 284) as intrinsic fluorophores being highly sensitive to the polarity of the microenvironment. The fluorescence properties of the tryptophans in lipases microencapsulated in water-in-oil microemulsions have been described in a number of articles.<sup>14</sup> Lipase was dispersed in pure IL as well as in water saturated IL for any residual emission; essentially none was found. With the addition of AOT to form water domains, the lipase dissolved and showed strong fluorescence intensity (Fig. 1). For comparison, we showed spectra of lipase in AOT based microemulsions in isooctane at  $W_0$  (molar ratio of water to AOT) = 10 and bulk buffer solution. The maximum emission wavelength ( $\lambda_{\max}$ ) of lipase in AOT/water/isooctane system was found at 328 nm, which was blue-shifted (generally observed with the decrease in polarity of the environment<sup>15</sup>), relative to the emission peak in water ( $\approx 334$  nm). Similar results have been reported for other lipases dissolved in AOT/isooctane microemulsions.<sup>14</sup> This trend of lipase solubilized in the water domains of AOT based oil microemulsions is well known because the physicochemical properties of water pools are different from those of bulk water. However, the  $\lambda_{\max}$  obtained from the new IL microemulsions is comparable to that of lipase in buffer. The results indicate that the lipase experiences an environment similar to that of bulk buffered water. This notable result can be explained by the large size of water domains formed in the IL microemulsions<sup>12</sup> because Venables *et al.*<sup>16</sup> provided the evidence for bulk-like character for water in large microemulsions.

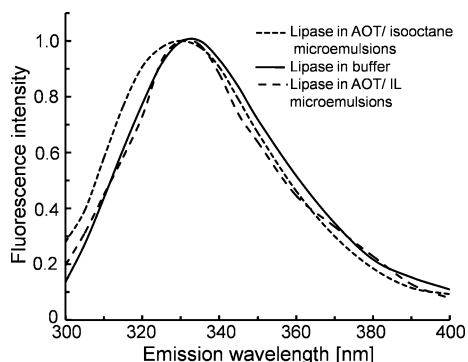


**Fig. 1** Fluorescent emission of lipase in various systems. Experimental conditions: [AOT] = 0.1 M, [lipase] = 0.64  $\mu\text{M}$ ,  $W_0 = 4$  and 10 for microemulsions formed in IL and isooctane, respectively.

Our next aim was to examine the catalytic activity of such a solubilized enzyme in the IL microemulsions. Fig. 2 shows the initial rate of hydrolysis of *p*-NPB as a function of enzyme concentration. As expected, the initial reaction rate was found to be linearly dependent on enzyme concentration. This suggests that

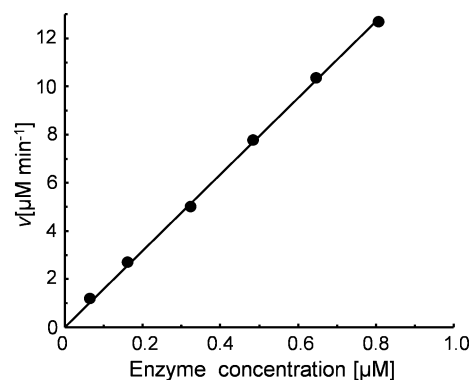


**Fig. 2** Dependence of the initial rate of lipase-catalyzed hydrolysis of *p*-nitrophenyl butyrate on enzyme concentration at 35 °C. Conditions were: [AOT] = 0.15 M, [*p*-NPB] = 0.005 M,  $W_0 = 4$ .

reaction is an enzymatically controlled reaction, *e.g.*, the enzyme is continuously fed with the substrate through the surfactant layer existing within microemulsions. We also investigated the dependence of the initial rate on the concentration of *p*-NPB at a fixed enzyme concentration. The results show that the trend of enzyme activity as a function of substrate concentration is similar to the substrate-saturation trend obtained for enzyme-catalyzed reactions that follow Michaelis–Menten kinetics (data not shown), a common phenomenon found for enzymes microencapsulated in microemulsions formed in organic solvents.<sup>17</sup> The results again confirmed that the reaction is a kinetically controlled enzymatic reaction.

For comparison, the same reaction was also performed in AOT/water/isooctane microemulsions and in water saturated IL. For the hydrolysis in IL, lipase was added to 1 ml IL and was shaken mildly for a few minutes. The supernatant was separated by centrifugation. The lipase activity in the supernatant was assayed in *p*-NPB hydrolysis and found essentially none. However, the hydrolysis rate was faster in the water-in-IL microemulsions than in the water-in-isooctane microemulsions (Fig. 3).

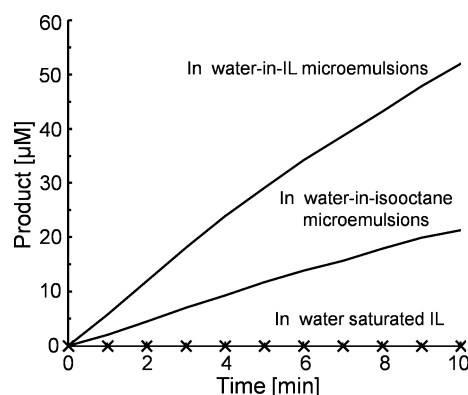


**Fig. 3** Product vs. time kinetic curve for lipase-catalyzed hydrolysis of *p*-NPB at 35 °C. Conditions were: [AOT] = 0.15 M, [lipase] = 0.64  $\mu\text{M}$ , [*p*-NPB] = 0.005 M,  $W_0 = 4$  and 15 for microemulsions formed in IL and isooctane respectively, where buffer pH = 8.0.

The kinetic parameters (maximum reaction rate,  $V_{\max}$  and apparent Michaelis constant,  $K_{m,\text{app}}$ ) for the lipase-catalyzed hydrolysis of *p*-NPB in water-in-IL microemulsions and in AOT/water/isooctane microemulsions were measured. The

**Table 1** Michaelis–Menten parameters for lipase in the hydrolysis of *p*-PNB in IL/water/AOT and isooctane/water/AOT microemulsions at 35 °C. The concentration of lipase (per total volume of the system) was 0.64 μM.  $W_0 = 4$  and 15 for microemulsions formed in IL and isooctane, respectively

Microemulsions system	$V_{\max}/\mu\text{M min}^{-1}$	$K_{\text{m,app}}/\times 10^{-3} \text{ M}$	$V_{\max}/K_{\text{m,app}}/\times 10^{-3} \text{ min}^{-1}$
AOT/water/isooctane	5.3 ± 0.4	4.7 ± 0.6	1.1 ± 0.15
AOT/water/IL	25.0 ± 2.0	7.5 ± 1.5	3.0 ± 0.20

kinetic parameters were obtained from Lineweaver–Burk plots (see the ESI)† and listed in Table 1. The lipase intrinsic activity ( $k_{\text{cat}}/K_{\text{m}}$ , which is proportional to  $V_{\max}/K_{\text{m}}$  as the enzyme concentration is kept constant) in the IL microemulsion was about 3 times higher than that in microemulsions of AOT in isooctane under the given experimental conditions. This enhanced catalytic activity of lipase in water-in-IL microemulsions may be due to (i) aqueous microenvironmental changes (see Fig. 1), (ii) the partition of the substrate or other molecules involved in the reaction between water and IL phases, and (iii) the existence of 1-hexanol as a cosurfactant. Further study will be required to assess the contribution of each of these mechanisms. We believe that the catalytic performances of enzymes in this new microemulsion will be improved by optimizing the physicochemical parameters (*e.g.*, pH, temperature, ionic strength, surfactant concentration and water content ( $W_0$ )). Ongoing work is being conducted to thoroughly characterize the IL microemulsions.

In conclusion, a new approach for carrying out enzymatic reactions in ILs has been reported by forming aqueous nanometre-sized domains comprising AOT as a surfactant. To the best of our knowledge, this is the first report of an enzymatic reaction being conducted in the AOT based IL microemulsions. Therefore, this work opens up new possibilities for studying enzymes in ILs. The IL microemulsions could have advantages over conventional microemulsions (prepared in organic solvents) as reaction media for carrying out biotransformations with polar or hydrophilic substrates such as amino acids,<sup>6a,b</sup> and carbohydrates,<sup>18</sup> which are poorly soluble in most organic solvents (*e.g.*, isooctane and hexane).

## Experimental

For enzymatic reactions in AOT/water/IL/1-hexanol systems, a typical experiment was performed as follows. AOT (1.35 g) was dissolved in an IL (21.23 g) containing 10% (v/v) 1-hexanol (1.46 g). Then, 100 μl Tris-HCl (50 mM) buffer (pH 8.0) was added to prepare a microemulsion. Clear and stable solutions were obtained by vortex mixing and used as stock solutions. 10 μl enzyme solution (2 mg ml<sup>-1</sup>) prepared in buffer was injected into a 0.78 ml stock solution. Following the injection of enzyme solution, the mixtures were shaken mildly for approximately 30 s to obtain a clear and optically transparent solution. The molar ratio of water to AOT ( $W_0$ , calculated by subtracting the independently known amount of water soluble in pure IL without surfactant from the total amount of water<sup>12</sup>) of the microemulsions were adjusted by injecting an appropriate amount of buffer solution. The reaction was commenced by adding 200 μl of *p*-NPB solution (25 mM, 10.46 mg) prepared in above stock solution (2.5 g). For the cases when the amounts of

*p*-NPB solutions were less than 200 μl, stock solution was added to obtain the final reaction volume of 1 ml. All concentrations are given with respect to the total volume of the system.

The lipase activity in microemulsions was measured as the initial reaction rates of hydrolysis. For this purpose, lipase-catalyzed hydrolysis of *p*-NPB was monitored by following the production of *p*-nitrophenol (*p*-NP) with time using a UV-Vis spectrophotometer (Jasco V-570) at 35 ± 0.2 °C. From the slopes of the linear portions of the absorbance *versus* time curves, obtained by least squares fitting, the values of the initial rates ( $v$ ) were measured in μM min<sup>-1</sup> considering the value of the molar extinction coefficient of *p*-NP in each microemulsion (see the ESI).† The monitoring wavelength was 410 nm (see the ESI).† All initial rates were corrected by subtracting the non-enzymic-catalyzed rates of hydrolysis.

Fluorescence emission spectra were recorded using a Perkin Elmer Luminescence Spectrometer with an excitation wavelength at 280 nm, a selective excitation wavelength for tryptophan residues.<sup>14</sup> Excitation and emission band passes were 5 and 10 nm, respectively. All spectra were corrected by subtracting a ‘blank’ spectrum (without lipase). Lipase was added as a solid to produce a concentration of 0.64 μmol dm<sup>-3</sup> (20 μg ml<sup>-1</sup>) based on the total volume of the system. For convenience, each spectrum was normalized to the maximum of the lipase + AOT + water + IL fluorescence in each measurement.

M.M. Zaman would like to thank the JSPS (Japan Society for the Promotion of Science) for financial support (JSPS Postdoctoral Fellowship, P07133) and the necessary funding for this work. The present work is also supported by a Grant-in-Aid for the Global COE Program, ‘‘Science for Future Molecular Systems’’ from the Ministry of Education, Culture, Sports, Science and Technology of Japan.

## Notes and references

- P. Bonhôte, A. P. Dias, N. Papageorgiou, K. Kalyanasundaram and M. Grätzel, *Inorg. Chem.*, 1996, **35**, 1168–1178; P. Wasserscheid and W. Keim, *Angew. Chem., Int. Ed.*, 2000, **39**, 3772–3789; J. G. Huddleston, A. E. Visser, W. M. Reichert, H. D. Willauer, G. A. Broker and R. D. Rogers, *Green Chem.*, 2001, **3**, 156–164; M. J. Earle, J. M. S. S. Esperanca, M. A. Gilea, J. N. C. Lopes, L. P. N. Rebelo, J. W. Magee, K. R. Seddon and J. A. Widegren, *Nature*, 2006, **439**, 831–834; J. L. Anderson, J. Ding, T. Welton and D. W. Armstrong, *J. Am. Chem. Soc.*, 2002, **124**, 14247–14254.
- A. E. Visser, R. P. Swatloski, S. T. Griffin, D. H. Hartman and R. D. Rogers, *Sep. Sci. Technol.*, 2001, **36**, 785–804; S. Chun, S. V. Dzzyuba and R. A. Bartsch, *Anal. Chem.*, 2001, **73**, 3737–3741.
- H. M. Zerth, N. M. Leonard and R. S. Mohan, *Org. Lett.*, 2003, **5**, 55–57; F. van Rantwijk, R. M. Lau and R. A. Sheldon, *Trends Biotechnol.*, 2003, **21**, 131–138; T. Welton, *Chem. Rev.*, 1999, **99**, 2071–2084.
- J. L. Anderson and D. W. Armstrong, *Anal. Chem.*, 2005, **77**, 6453–6462.
- R. A. Sheldon, R. M. Lau, M. J. Sorgedragger, F. van Rantwijk and K. R. Seddon, *Green Chem.*, 2002, **4**, 147–151; R. M. Lau, M. J.

- Sorgedraeger, G. Carrea, F. van Rantwijk, F. Secundo and R. A. Sheldon, *Green Chem.*, 2004, **6**, 483–487.
- 6 (a) M. Eckstein, M. Sesing, U. Kragl and P. Adlercreutz, *Biotechnol. Lett.*, 2002, **24**, 867–872; (b) M. Erbeltinger, A. J. Mesiano and A. J. Russel, *Biotechnol. Prog.*, 2000, **16**, 1129–1131; (c) M. B. Turner, S. K. Spear, J. G. Huddleston, J. D. Holbrey and R. D. Rogers, *Green Chem.*, 2003, **5**, 443–447.
- 7 (a) J. L. Kaar, A. M. Jesionowski, J. A. Berberich, R. Moulton and A. J. Russel, *J. Am. Chem. Soc.*, 2003, **125**, 4125–4131; (b) H. Ohno, C. Suzuki, K. Fukumoto, M. Yoshizawa and Fujita, *Chem. Lett.*, 2003, **32**, 450–451; (c) T. Itoh, E. Akasaki, K. Kudo and S. Sirakami, *Chem. Lett.*, 2001, 262–263; (d) T. Itoh, Y. Matsushita, Y. Abe, S. Han, S. Wada, S. Hayase, M. Kawatsura, S. Takai, M. Morimoto and Y. Hirose, *Chem.-Eur. J.*, 2006, **12**, 9228–9237.
- 8 K. Nakashima, T. Maruyama, N. Kamiya and M. Goto, *Chem. Commun.*, 2005, 4297–4299.
- 9 (a) K. Martinek, A. V. Levashov, Y. L. Khmel'nitskii, N. L. Klyachko and I. V. Berezin, *Science*, 1982, **218**, 889–891; (b) P. L. Luisi and I. J. Magid, *CRC Crit. Rev. Biochem.*, 1986, **20**, 409–474; (c) G. D. Rees, B. H. Robinson and G. R. Stephenson, *Biochim. Biophys. Acta*, 1995, **1257**, 239–248; (d) D. Han, P. Walde and P. L. Luisi, *Biocatalysis*, 1990, **4**, 153–161; (e) P. D. I. Fletcher and B. H. Robinson, *J. Chem. Soc., Faraday Trans. 1*, 1985, **81**, 2667–2679; (f) D. Das, S. Roy, R. N. Mitra, A. Dasgupta and P. K. Das, *Chem.-Eur. J.*, 2005, **11**, 4881–4889; (g) G. Satiyanegara, P. L. Rogers and B. Rosche, *Biotechnol. Bioeng.*, 2006, **94**, 1189–1195; (h) A. Shome, S. Roy and P. K. Das, *Langmuir*, 2007, **23**, 4130–4136.
- 10 V. M. Paradkar and J. S. Dordick, *J. Am. Chem. Soc.*, 1994, **116**, 5009–5010; V. M. Paradkar and J. S. Dordick, *Biotechnol. Bioeng.*, 1994, **43**, 529–540.
- 11 T. De and A. Maitra, *Adv. Colloid Interface Sci.*, 1995, **59**, 95–193.
- 12 M. M. Zaman, N. Kamiya, K. Nakashima and M. Goto, *ChemPhysChem*, 2008, **9**, 689–692.
- 13 K. K. Kim, K. Y. Hwang, H. S. Jeon, S. Kim, R. M. Sweet, C. H. Yang and S. W. Suh, *J. Mol. Biol.*, 1992, **227**, 1258–1262; H. Stamatis, A. Xenakis, E. Dimitriadis and F. N. Kolisis, *Biotechnol. Bioeng.*, 1995, **45**, 33–41.
- 14 E. P. Melo, S. M. B. Costa and J. M. S. Cabral, *Photochem. Photobiol.*, 1996, **63**, 169–175; A. G. Marangoni, *Enzyme Microb. Technol.*, 1993, **15**, 944–949; E. D. Brown, R. Y. Yada and A. G. Marangoni, *Biochim. Biophys. Acta*, 1993, **1161**, 66–72.
- 15 J. R. Lakowicz, *Protein fluorescence, Principles of fluorescence Spectroscopy*, Plenum Press, New York, 1983, pp. 341–381.
- 16 D. S. Venables, K. Huang and C. A. Schmuttenmaer, *J. Phys. Chem. B*, 2001, **105**, 9132–9138.
- 17 C. M. L. Carvalho and J. M. S. Cabral, *Biochimie*, 2000, **82**, 1063–1085; K. Martinek, A. V. Levashov, N. Klyachko, Y. L. Khmel'nitski and I. V. Berezin, *Eur. J. Biochem.*, 1986, **155**, 453–468.
- 18 N. Kimizuka and T. Nakashima, *Langmuir*, 2001, **17**, 6759–6761.



# Ionic liquids for liquid-in-glass thermometers

Héctor Rodríguez,<sup>a,b,c</sup> Margaret Williams,<sup>d</sup> John S. Wilkes<sup>d</sup> and Robin D. Rogers<sup>\*a,b</sup>

Received 9th January 2008, Accepted 22nd February 2008

First published as an Advance Article on the web 19th March 2008

DOI: 10.1039/b800366a

The varied portfolio of applications of ionic liquids (ILs) is broadened in this work by presenting the possibility of their use as thermometric fluids in liquid-in-glass thermometers. Two ILs, namely tris(2-hydroxyethyl)methylammonium methylsulfate ([TEMA][MeSO<sub>4</sub>]) and trihexyl(tetradecyl)phosphonium bis{(trifluoromethyl)sulfonyl}amide ([P<sub>6614</sub>][NTf<sub>2</sub>]), have been selected for the construction of thermometers with ranges of operation tuned to general and speciality applications. The regular expansion of the IL volume with changes in temperature has been tested, and successful prototypes have been built, consisting of liquid-in-glass devices with an approximately spherical reservoir and a capillary tube attached. These devices have the advantage of operating with a fluid of ionic nature and a practically negligible vapor pressure. In addition, the inherent tunability of IL properties is a powerful tool in the possible design of speciality thermometers.

## 1. Introduction

In the last ten years, the scientific and industrial communities have witnessed a formidable burgeoning of interest in and applications of ionic liquids (ILs).<sup>1</sup> These substances, consisting of salts with melting points below the arbitrary mark of 100 °C,<sup>2</sup> initially attracted great interest in the late 1990s as neoteric solvents with a very appealing set of properties for reactions and separations.<sup>3–5</sup> Besides the research into their use as solvents, more recently many other applications have been proposed, for example as lubricants,<sup>6–9</sup> as energetic materials,<sup>10–14</sup> or in polymer science.<sup>15–18</sup>

The high rate of development of the IL field, combined with the controllable variability of their properties, is responsible for the appearance of an important number of novel applications over a broad range of areas. In this vein, we report here the utilization of ILs as alternatives to the traditional filling fluids currently used in the construction of liquid-in-glass (LIG) thermometers for the measurement of temperature.

Various types of temperature sensors are known, including LIG thermometers, bimetallic thermometers, pressure-spring thermometers, resistance thermometers, thermistors, thermocouples, radiometers, and semiconductor devices.<sup>19,20</sup> Depending upon the temperature to be measured, the required accuracy of the measurement, and other factors, such as durability or cost, one type of temperature sensors may be preferable over another. In general, each type presents some advantages, but also specific drawbacks. Thus, bimetallic thermometers are cheap, durable, and easily calibrated, but they require frequent calibration to maintain accuracy and they exhibit slow response times.

Thermocouples, for example, provide a rapid response and are durable and accurate over a broad temperature range; however, these devices require expensive ancillary equipment and electronics to operate. An interesting comparative summary of advantages and disadvantages of the different types of thermometers is provided by Dunn.<sup>20</sup>

Although of limited temperature precision, LIG thermometers deserve a favored place in the lore of thermometry. There are many applications of these types of thermometers, the leading one being the measurement of air temperatures, both indoors and out. Other widespread applications assist medical, biological, veterinary, air conditioning, automotive, chemical and other manufacturing personnel, and engineers employed in a wide range of processing industries in measuring and regulating temperature. Laboratory types of LIG thermometers include clinical standard thermometers, calorimetric thermometers designed to measure temperature differences accurately, and thermometers recommended by organizations such as the American Society for Testing and Materials.<sup>19</sup>

LIG thermometers are simple, with their operation depending on the thermal expansion of a liquid contained in a glass envelope. This holder usually consists of a fine glass bore connected to a fluid reservoir. The desired temperature range is the main criterion in the choice of the thermometric liquid.<sup>19,21</sup>

The most common liquids used in LIG thermometers are the molecular liquids mercury and ethanol. Mercury LIG thermometers are inexpensive, durable, accurate, and easily calibrated. Another advantage of the mercury LIG thermometer is its high temperature range (the upper operating temperature limit for a mercury LIG thermometer is about 350 °C). Several disadvantages are that mercury is not useful in low temperature situations because it freezes at –38.87 °C,<sup>22</sup> that mercury responds slowly in response to changes in temperature, and that mercury is volatile and toxic at low concentrations.<sup>23</sup> Mercury also poses an environmental hazard associated with the storage and disposal of broken mercury thermometers.

For temperature measurements below *ca.* –35 °C, LIG thermometers containing ethanol are commonly used. Ethanol

<sup>a</sup>Department of Chemistry, Center for Green Manufacturing and Alabama Institute for Manufacturing Excellence, The University of Alabama, Tuscaloosa, AL, 35487, USA

<sup>b</sup>QUILL, School of Chemistry and Chemical Engineering, The Queen's University of Belfast, Belfast, Northern Ireland, UK BT9 5AG

<sup>c</sup>Department of Chemical Engineering, University of Santiago de Compostela, E-15883, Santiago de Compostela, Spain

<sup>d</sup>Department of Chemistry, US Air Force Academy, 2355 Fairchild Dr., Suite 2N225, USAF Academy, CO, 80840-6230, USA

has a freezing point of  $-112\text{ }^{\circ}\text{C}$ , and a boiling point of  $78.4\text{ }^{\circ}\text{C}$ .<sup>22</sup> Ethanol has a faster response time and is less hazardous than mercury. However, fluid loss by evaporation is hard to avoid with ethanol and the upper operating temperature of  $78\text{ }^{\circ}\text{C}$  limits the utility of ethanol LIG thermometers over a wide temperature range.

A relatively overlooked feature of ILs is that many have a very wide liquidus range, allowing their use as liquids over a much wider range than most molecular liquids.<sup>3</sup> In addition, ILs may deserve consideration as a green alternative to the hazards and limitations associated with the use of mercury and ethanol as working fluids in LIG thermometers. ILs can be prepared from edible ion combinations,<sup>24</sup> and the volatility of ILs is practically negligible under usual conditions of temperature and pressure,<sup>25</sup> therefore not releasing hazardous vapors. Moreover, the tailoring of their properties by tuning the chemical structures of its constitutive ions allows designing the appropriate IL for a specific desired performance.<sup>26,27</sup> For instance, and in addition to other physical, chemical or biological properties, ILs with the adequate liquid range for a given application can be created by suitable selection and combination of cations, anions and related substituents. Thus, we can think of designing either a standard thermometer operating over conventional temperature ranges (e.g. ambient temperatures and the liquid range of water), or a more specific thermometer for speciality applications operating over a much wider temperature range. Both the standard and speciality approaches have been considered herein as a proof of concept of the versatility potentially offered by ILs as filling fluids in LIG thermometers.

## 2. Results and discussion

### 2.1. Selection of the IL candidates

The choice of ILs for the two types of thermometers is determined by numerous properties. The IL candidates obviously must have suitable melting and decomposition temperatures and appropriate coefficients of expansion. Other relevant properties for the standard thermometer are toxicity, biodegradability, and expense. An ammonium-based IL, tris(2-hydroxyethyl)methylammonium methylsulfate ([TEMA][MeSO<sub>4</sub>]), was selected as candidate for the standard thermometer, since it is reasonably inexpensive and a complete set of toxicological data is available (see Table 1).<sup>28</sup>

For the speciality approach, tetraalkylphosphonium-based ILs have remarkably low glass transition temperatures, and their thermal stability is very good. We selected trihexyl-(tetradecyl)phosphonium bis{(trifluoromethyl)sulfonyl}amide

([P<sub>66614</sub>][NTf<sub>2</sub>]), because it has reported glass transition and decomposition onset temperatures of  $-76\text{ }^{\circ}\text{C}$  and  $400\text{ }^{\circ}\text{C}$ , respectively.<sup>29</sup> The chemical structures of both candidates are displayed in Fig. 1.

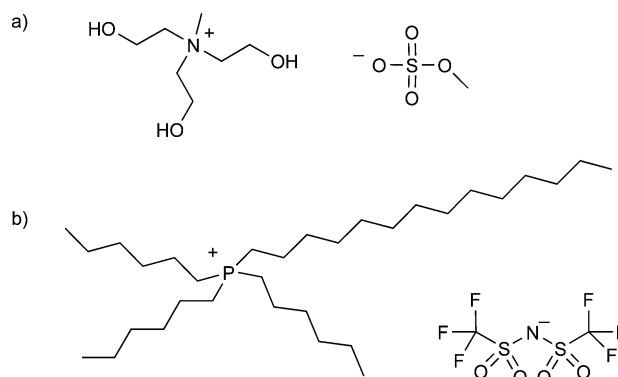


**Fig. 1** Chemical structures of the ILs used in this work: (a) [TEMA][MeSO<sub>4</sub>]; (b) [P<sub>66614</sub>][NTf<sub>2</sub>].

### 2.2. Investigation of the volumetric behavior and IL dyeing

As previously mentioned, the regular variation of the volume of a fluid with changes in temperature is an indispensable requirement for its use in LIG thermometers. Thus, to assess the suitability of the selected IL candidates, a study of their volumetric behavior was imperative. Measurements of density as a function of temperature for both ILs are shown in Table 2.

The graphical representation of the experimental points in a density *versus* temperature plot yields a linear trend to the eye. Indeed, the correlation coefficient ( $R^2$ ) and standard deviation ( $\sigma$ ) of the linear regressions are good for both series:  $R^2 = 0.9991$  and  $\sigma = 5 \times 10^{-4}\text{ g cm}^{-3}$  for [TEMA][MeSO<sub>4</sub>]; and  $R^2 = 0.9998$  and  $\sigma = 3 \times 10^{-4}\text{ g cm}^{-3}$  for [P<sub>66614</sub>][NTf<sub>2</sub>]. However, it was verified that improved linear regressions are achieved when plotting the inverse of the density (*i.e.* the specific volume) against the temperature:  $R^2 = 0.9995$  and  $\sigma = 4 \times 10^{-4}\text{ g cm}^{-3}$  for [TEMA][MeSO<sub>4</sub>]; and  $R^2 = 0.99990$  and  $\sigma = 2 \times 10^{-4}\text{ g cm}^{-3}$  for [P<sub>66614</sub>][NTf<sub>2</sub>]. The numerical difference might seem not very significant, but it acquires relevance from a conceptual point of view, as described below.

The molar volume  $V$  of a substance is given by the quotient of its molecular weight (or formula weight)  $M$  over its density  $\rho$ , eqn (1):

$$V = \frac{M}{\rho} \quad (1)$$

Since  $M$  is a constant for a given substance, the fact that the inverse of its density varies linearly with temperature is equivalent to its molar volume (or its overall volume, for a confined amount of substance) doing so, too. This is conceptually the ideal volumetric behavior of a liquid planned to be used as a thermometric fluid in a LIG thermometer, mathematically expressed as eqn (2):

$$V = a + bT \quad (2)$$

where coefficients  $a$  and  $b$  are constants. Linear fits in the plot of molar volume *versus* absolute temperature are displayed in

**Table 1** Toxicological data set for the IL [TEMA][MeSO<sub>4</sub>]<sup>28</sup>

Parameter	Result
Acute oral toxicity	Not harmful
Skin irritation	Non-irritant
Eye irritation	Non-irritant
Sensitization	Non-sensitizing
Mutagenicity	Non-mutagenic
Biological degradability	Readily biodegradable
Toxicity to <i>daphniae</i>	Not acutely harmful
Toxicity to fish	Not acutely harmful

**Table 2** Density at several temperatures for [TEMA][MeSO<sub>4</sub>] and [P<sub>66614</sub>][NTf<sub>2</sub>], as well as for 1 wt% solutions of the IL-dye [P<sub>66614</sub>]<sub>2</sub>[Direct Red 81] in each

Temperature/K	Density/g cm <sup>-3</sup>			
	[TEMA][MeSO <sub>4</sub> ]	[P <sub>66614</sub> ][NTf <sub>2</sub> ]	[TEMA][MeSO <sub>4</sub> ] + dye	[P <sub>66614</sub> ][NTf <sub>2</sub> ] + dye
277.15	1.3543	1.0465	1.3512	1.0461
288.15	1.3482	1.0391	1.3451	1.0387
303.15	1.3390	1.0282	1.3359	1.0278
313.15	1.3334	1.0214	1.3303	1.0211
323.15	1.3279	1.0144	—	—
333.15	1.3220	1.0074	1.3189	1.0071
353.15	1.3119	0.9943	1.3088	0.9940

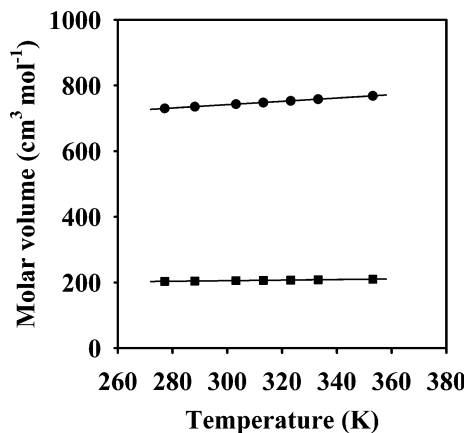
**Fig. 2** Molar volume  $V$  as a function of temperature  $T$  for [TEMA][MeSO<sub>4</sub>] (squares) and [P<sub>66614</sub>][NTf<sub>2</sub>] (circles). The solid lines represent the linear regressions.

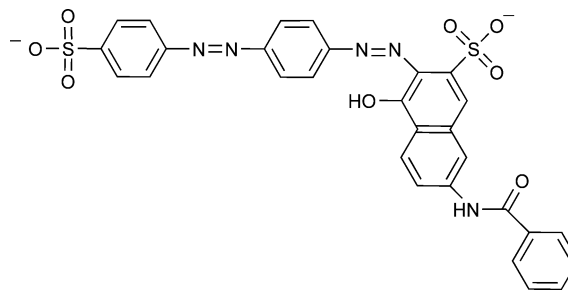
Fig. 2. The equations corresponding to these regressions, strictly valid only within the temperature range of the experimental density measurements (277.15 K to 353.15 K), are given in eqn (3) and (4):

$$(V_{[\text{TEMA}][\text{MeSO}_4]}/\text{cm}^3 \text{ mol}^{-1}) = 179.1 + 0.08724 \times (T/\text{K}) \quad (3)$$

$$(V_{[\text{P}_{66614}][\text{NTf}_2]}/\text{cm}^3 \text{ mol}^{-1}) = 589.4 + 0.5069 \times (T/\text{K}). \quad (4)$$

**Coloration.** Both pure [TEMA][MeSO<sub>4</sub>] and [P<sub>66614</sub>][NTf<sub>2</sub>] are colorless. This is a handicap which would make the visualization of the liquid column in the bore and the reading of the temperature in the IL-based LIG thermometer difficult. To avoid this limitation, while keeping the absolutely ionic nature (and non-volatility) of the filling fluid, it was decided to test the doping of the proposed candidates with another IL with dyeing properties. The IL-dye chosen, [P<sub>66614</sub>]<sub>2</sub>[Direct Red 81], which is a dark red waxy solid at room temperature and atmospheric pressure, provided red color and the cation (two per formula mass) is the same as in [P<sub>66614</sub>][NTf<sub>2</sub>] (see Fig. 1b.). The divalent anion responsible for the color is shown in Fig. 3.

To verify that the effects of the addition of the dye on the volumetric properties of the IL candidates were negligible, 1 wt% solutions of IL-dye in [TEMA][MeSO<sub>4</sub>] or [P<sub>66614</sub>][NTf<sub>2</sub>] were prepared, and the density at several temperatures was measured (Table 2). (A 1 wt% concentration of dye is actually much higher than needed to actually provide an intense red tone to the originally colorless ILs.) The differences between the

**Fig. 3** Chemical structure of the anion of the IL-dye [P<sub>66614</sub>]<sub>2</sub>[Direct Red 81].

pure ILs and the doped ones are extremely small, about  $3 \times 10^{-3} \text{ g cm}^{-3}$  for [TEMA][MeSO<sub>4</sub>] and in the range  $(3 \text{ to } 4) \times 10^{-4} \text{ g cm}^{-3}$  for [P<sub>66614</sub>][NTf<sub>2</sub>]. Thus, the volumetric behavior of the pure ILs remains practically unaltered by the addition of the IL-dye, especially in the case of the more similar phosphonium-based IL. Since these results were obtained for the case of a 1 wt% concentration of dye, it is reasonable to assume that the effect caused by lower concentrations (as they will be ultimately used), will be negligible.

**Liquid range.** The density data in Table 2 do not cover entirely the liquid ranges of the ILs studied, basically due to the limitations of the densitometer used. In principle, there is no guarantee of the validity of extrapolating the regular volume expansion behavior outside this range. In fact, as thermodynamically required, the volume expansivity of a fluid (defined by eqn (5), in subsection 2.3 below) has to diverge to  $+\infty$  when approaching its critical point, therefore implying a clear violation of constant variation in volume with changes in temperature. However, since the critical point is often obscured in ILs under common experimental conditions because of prior decomposition,<sup>25</sup> it may be reasonable to extrapolate the constancy of volume variation with temperature for [TEMA][MeSO<sub>4</sub>] and [P<sub>66614</sub>][NTf<sub>2</sub>] (or their IL-dye doped versions) over most of their liquid range. Therefore, for the design of the standard and speciality thermometers, the total liquid range of each IL was initially considered in the calculations, introducing a safety margin from the solidification and decomposition points to delineate the upper and lower measurable temperatures in each case.

### 2.3. Thermometer design

A classical model consisting of a tube with a bore in liquid communication with a spherical reservoir was chosen for the prototypes to be built, as proof of concept for the IL LIG thermometers. The volume expansivity  $\alpha$  of a pure fluid is a measure of how its volume changes with temperature, and is defined as in eqn (5):<sup>30</sup>

$$\alpha = \frac{1}{V_T} \left( \frac{\partial V_T}{\partial T} \right)_p \quad (5)$$

where  $V_T$  is the total volume,  $T$  is the absolute temperature, and subscript  $p$  indicates constant pressure. Taking into account that the bore of the proposed prototype is cylindrical, with a constant diameter  $D$ , and considering constant pressure in the system, eqn (5) can be rearranged and expressed as eqn (6):

$$\frac{dh}{dT} = \frac{4V\Delta\alpha}{\pi D^2} \quad (6)$$

with  $h$  representing the length of the liquid column in the bore, and  $\Delta\alpha$  being the difference between the volume expansivities of the filling fluid and the glass. Eqn (6) is a classical formula for evaluating the sensitivity of a thermometer, which can be used as a design formula in eqn (7):

$$\Delta h = \frac{4V\Delta\alpha}{\pi D^2} \Delta T \quad (7)$$

However, the application of eqn (7) for the design of the thermometer involves approximations such as the consideration of constant volume of the filling fluid and constant values of the volume expansivities of both the filling fluid and the glass. Since emphasis has been previously put in the linear variation of the volume of the selected ILs with changes in temperature (and therefore a strictly non-constant value of their volume expansivity with temperature), an alternative design method has been preferred, looking for a greater degree of conceptual consistency.

For a reservoir-and-bore thermometer in which the level of the liquid column in the bore is zero at the lowest operational temperature and  $L$  at the highest operational temperature, where  $L$  stands for the total length of the bore, we can write eqn (8):

$$n(V_h - V_l) = \frac{\pi}{4} D^2 L \quad (8)$$

where  $n$  is the number of moles, subscripts  $h$  and  $l$  refer respectively to the states at the highest and lowest operational temperatures, and the second term of the equation obviously corresponds to the total volume of the cylindrical bore. Rewriting the expression in mass terms, and by combination with eqn (2), we obtain eqn (9):

$$\frac{m}{M} b(T_h - T_l) = \frac{\pi}{4} D^2 L \quad (9)$$

where  $m$  represents the mass of IL inside the glass holder, and  $M$  is its formula mass.

On the other hand, for the state of lowest operational temperature, the volume of the reservoir is equal to the total volume of the IL. Therefore, assuming that the reservoir is perfectly spherical, and already considering eqn (2), the balanced

equation is eqn (10):

$$\frac{m}{M} (a + bT_l) = \frac{\pi}{6} \phi^3 \quad (10)$$

with  $\phi$  representing the diameter of the sphere. The actual internal diameter of the spherical reservoir will need to be somewhat smaller, so that the minimum temperature in the scale can be read not exactly at the junction of the tube with the reservoir, but at some point throughout the tube, with a length of liquid column  $x \neq 0$  in the bore. Therefore, considering a perfect junction of sphere and attached cylinder, we have eqn (11):

$$\frac{\pi}{6} \phi^3 = \frac{\pi}{6} \phi_c^3 + \frac{\pi}{4} D^2 x \Rightarrow \phi_c = \left( \phi^3 - \frac{3}{2} D^2 x \right)^{\frac{1}{3}} \quad (11)$$

where  $\phi_c$  represents the corrected internal diameter of the ideal sphere of the reservoir. Adding an extra length  $x'$  to the tube in order to avoid the top reading at the highest operational temperature being coincident with the sealed extreme of the tube, the total length can be calculated as in eqn (12):

$$L_c = L + x + x' \quad (12)$$

where  $L_c$  is the corrected length of the tube.

For a given bore diameter  $D$ , known  $T_h$  and  $T_l$ , and assigning a value to e.g. the length  $L$  of the tube, with eqn (9) and (10), it is possible to calculate the mass  $m$  of IL needed and the internal diameter  $\phi$  of the spherical reservoir. With eqn (11) and (12), and the corresponding estimations of  $x$  and  $x'$ , the diameter of the reservoir and the length of the tube can be corrected, obtaining  $\phi_c$  and  $L_c$ . Therefore, congruent theoretical solutions  $\{m, D, \phi_c, L_c\}$  can be generated by using eqn (9)–(12), and the more convenient combination of these parameters can be chosen. The theoretical values finally selected for each of the approaches considered are summarized in Table 3.

A negligible expansion/contraction of the glass with changes in temperature was considered in the development of eqn (8)–(12). For Pyrex (the borosilicate glass available at the glassblowing workshop for the construction of the prototypes), the linear coefficient of thermal expansion has been reported to be  $3.3 \times 10^{-6} \text{ K}^{-1}$ .<sup>31</sup> The volume expansivity will be approximately the triple of this value, therefore ca.  $9.9 \times 10^{-6} \text{ K}^{-1}$ . With eqn (5) and the data in Table 2, volume expansivities lying in the range (4 to 7)  $\times 10^{-4} \text{ K}^{-1}$  can be found for the IL candidates. Therefore, the volume expansivity of Pyrex represents between 1.4% and 2.4% of the volume expansivity of the ILs in the range of temperatures investigated.

**Table 3** Theoretical values calculated and selected for the design variables of the prototypes of both the standard and speciality approaches considered, according to the procedure described in subsection 2.3

Parameter <sup>a</sup>	Standard thermometer	Speciality thermometer
$m/\text{g}$	5.354	1.278
$D/\text{mm}$	1.2	1.2
$\phi_c/\text{mm}$	22.4	16.0
$L_c/\text{mm}$	340	340

<sup>a</sup> Mass of IL ( $m$ ), internal diameter of the tube ( $D$ ), corrected internal diameter of the ideally spherical reservoir ( $\phi_c$ ), corrected length of the tube ( $L_c$ ).



Eqn (6) and (7) would consider this effect, but they would fail to evaluate the change of volume expansivity of the ILs with temperature. In fact, it can be calculated that  $\alpha$  varies as much as 3.0% for [TEMA][MeSO<sub>4</sub>] and 4.9% for [P<sub>66614</sub>][NTf<sub>2</sub>] from 4 °C to 80 °C. Regardless of this, due to limitations at the glassblowing workshop, the reservoir blown will not be perfectly spherical, and its volume will not be accurately assessed either; so, the actual value will be just an approximation of the theoretical value. Therefore, no further precision is of interest in the designing process, and later testing of the constructed prototypes will be required to check the extent to which their performance agrees with the theoretically expected design considerations.

#### 2.4. Construction and testing of the prototypes

Thick-wall Pyrex tubes with nominal internal diameters of 1.2 mm were selected for the construction of the prototypes. They were cut at the appropriate length, and after that, approximately spherical bulbs were blown at one of the ends, in the glassblowing workshop. Only the external diameter of the bulb could be controlled during the process, so an estimation of the thickness of the glass shell of the reservoir was required in order to approximately match the value of the internal diameter obtained in the theoretical design.

Batches of [TEMA][MeSO<sub>4</sub>] and [P<sub>66614</sub>][NTf<sub>2</sub>] were colored with the IL-dye [P<sub>66614</sub>]<sub>2</sub>[Direct Red 81]. It was found (not unexpectedly) that the IL-dye was much less soluble in [TEMA][MeSO<sub>4</sub>] than in [P<sub>66614</sub>][NTf<sub>2</sub>]. Thus, a very low concentration of dye (62 ppm) was used to color [TEMA][MeSO<sub>4</sub>], whereas for preparation of the colored [P<sub>66614</sub>][NTf<sub>2</sub>], a solution with almost 0.1% of dye (952 ppm) was prepared. Nonetheless, even in the first case, the color intensity was strong.

In Table 2 it was shown that the influence of 1% dye in the density values is higher in [TEMA][MeSO<sub>4</sub>] than in [P<sub>66614</sub>][NTf<sub>2</sub>]. Thus, the fact of using a very low concentration of dye for preparing the colored solution of [TEMA][MeSO<sub>4</sub>] (although the concentrations in both cases are well below the 1% used to produce the data reported in Table 2) enhances the assumption of negligible effect of the dye in the volumetric behavior of the IL candidates.

The colored ILs were introduced in their corresponding customized glass holders through the open extreme of the tube, by means of a double-tipped stainless steel needle, with one tip inside a plastic syringe to which it was connected with a rubber septum, and with the other tip located in the reservoir space, after introduction of the needle across the glass tube from its open end. Due to the difficulties in controlling the weight of the introduced fluid during the filling process, the appropriate amount of thermometric fluid to be placed inside the holder was calculated not by mass, as suggested by the procedure described in subsection 2.3, but by estimation of the length of the liquid column in the bore which should correspond to room temperature (Fig. 4). To remove the bubbles formed during this action, as well as to completely degasify the liquids introduced, both prototypes were placed for several hours in ultrasonic baths. Due to the generally hygroscopic nature of some ILs,<sup>1,32</sup> special care was taken during this period to prevent the ILs from picking up moisture from the atmosphere. Next, the prototypes

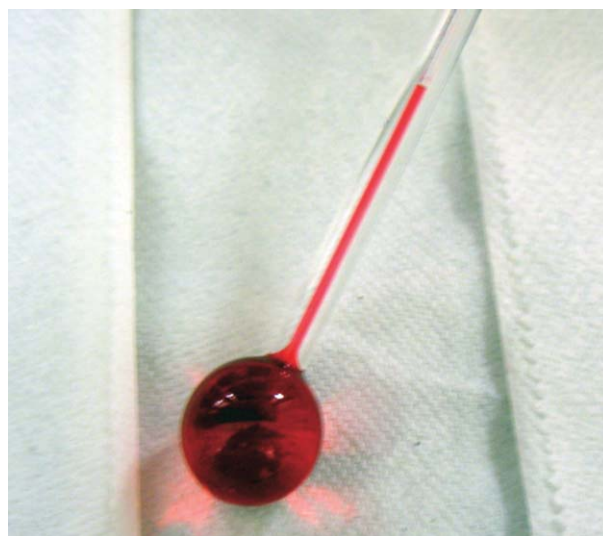


Fig. 4 Colored [TEMA][MeSO<sub>4</sub>] filling the reservoir and part of the bore of the glass holder of the standard thermometer prototype.

were connected to a vacuum line through their open end, and were sealed with a torch.

Once the prototypes were sealed under reduced pressure, calibration was carried out by fixing two points: the ones corresponding to boiling water (100 °C) and melting ice (0 °C). Following recommendations in the literature,<sup>33</sup> the mark at 100 °C was fixed first, by immersing the bulbs of the prototypes in a bath with deionized water in ebullition. Analogously, the mark at 0 °C was fixed by immersing the bulbs in a bath of melting ice. No special control of the atmospheric pressure was carried out during these steps; however a commercial LIG thermometer was placed in parallel in the same baths, and its readings were verified to agree with the supposed temperature (either 100 °C or 0 °C) within the uncertainty of the apparatus. In Fig. 5 the experimental setup for calibration is shown for the standard thermometer.

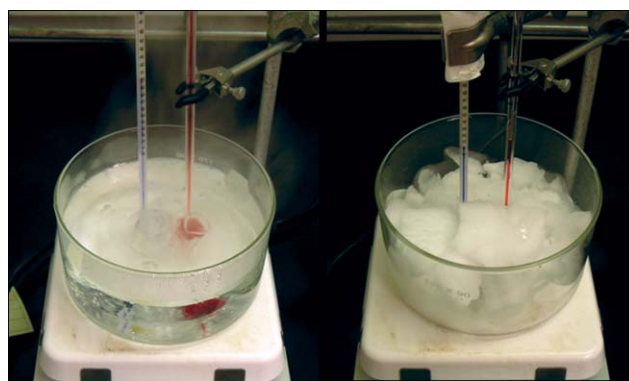


Fig. 5 Experimental setup for the calibration of the standard thermometer with the red-dyed [TEMA][MeSO<sub>4</sub>], in baths of boiling water (left picture) and melting ice (right picture) for determining the marks at 100 °C and 0 °C respectively, while compared with the readings of a commercial LIG thermometer (with blue filling fluid).

With the two reference marks fixed, the rest of the scale could be drawn by equidistant distribution of the degrees. Thus, keeping safety distances between the lowest readable

temperature and the reservoir-bore junction, as well as between the highest readable temperature and the top sealed end of the bore, a scale from  $-40\text{ }^{\circ}\text{C}$  to  $140\text{ }^{\circ}\text{C}$  was assigned to the standard thermometer, and from  $-50\text{ }^{\circ}\text{C}$  to  $300\text{ }^{\circ}\text{C}$  for the speciality thermometer. The validity of the scale was confirmed by placing the bulbs of the graduated prototypes in different organic solvents in ebullition (diethylether, MTBE, acetonitrile, 1-methylimidazole), covering a good range of boiling points. All readings matched the expected temperature within  $\pm 2\text{ }^{\circ}\text{C}$ . The poor precision can be justified by the degree of purity of some of the solvents used (as low as 98% in some case) or to fluctuations in the uncontrolled atmospheric pressure, thus altering the boiling temperature of the solvent.

The IL-based thermometers were found to be kinetically slower than equivalent commercial LIG thermometers. This can be attributed to the much wider diameter of the bore in our prototypes, which implies a much larger amount of thermometric fluid in the liquid column. A professional manufacturing process for the IL thermometers would surely minimize this problem. The work developed herein has basically focused on proving the concept of customized LIG thermometers operating with ILs as filling fluids, rather than on the straight manufacturing of a thermometer ready for commercialization.

### 3. Experimental

The IL [TEMA][MeSO<sub>4</sub>], a colorless viscous liquid synthesized by BASF, was purchased from Fluka with a nominal purity  $\geq 95\%$ , although <sup>1</sup>H and <sup>13</sup>C NMR analyses did not identify any impurity; its water content was measured by Karl–Fischer titration and it was found to be  $< 100\text{ ppm}$ . The preparation and characterization of [P<sub>6614</sub>][NTf<sub>2</sub>] was carried out as described elsewhere.<sup>29</sup>

The IL-dye, [P<sub>6614</sub>]<sub>2</sub>[Direct Red 81], was synthesized by a metathetic reaction, mixing trihexyl(tetradecyl)phosphonium chloride (commercial name CYPHOS® IL 101, from Cytec) and Direct Red 81 (from Sigma–Aldrich, product no. 195251, disodium salt); the mixture was stirred for a minimum of 2 h at room temperature, washed with water, and dried under vacuum while slowly increasing the temperature to a maximum of  $80\text{ }^{\circ}\text{C}$ .

Due to the lack of precise data in the literature for the liquid range of [TEMA][MeSO<sub>4</sub>], differential scanning calorimetry (DSC) and thermogravimetric analysis (TGA) were carried out for this substance in a TA Instruments model 2920 Modulated differential scanning calorimeter (with the sample placed in an aluminium pan and heated at a rate of  $2\text{ }^{\circ}\text{C min}^{-1}$  and cooled at  $5\text{ }^{\circ}\text{C min}^{-1}$  in nitrogen atmosphere) and a TGA 2950 TA Instrument (programmed at a heating rate of  $5\text{ }^{\circ}\text{C min}^{-1}$  and also under nitrogen atmosphere), respectively. In the DSC thermogram, a glass transition temperature  $T_g = -81\text{ }^{\circ}\text{C}$  was observed. Then, [TEMA][MeSO<sub>4</sub>] remains stably liquid from this temperature up to around  $200\text{ }^{\circ}\text{C}$ , where the first symptoms of decomposition were observed in the TGA. No precise onset decomposition temperature could be determined.

A Mettler Toledo DE40 densitometer was used to determine the densities of the pure ILs [TEMA][MeSO<sub>4</sub>] and [P<sub>6614</sub>][NTf<sub>2</sub>], and of their colored mixtures with the IL-dye. The instrument was calibrated using filtered and degassed water (with a resistivity of  $18\text{ M}\Omega\text{ cm}$  at  $25\text{ }^{\circ}\text{C}$ ) through a temperature range from

$4\text{ }^{\circ}\text{C}$  to  $80\text{ }^{\circ}\text{C}$ . Since the IL samples to be examined were viscous in nature, the automated viscosity correction of the apparatus was activated. After calibration, the density of each sample was determined in triplicate at the reported temperatures.

Glassblowing works and construction of the prototypes have already been detailed in section 2.

### 4. Conclusions

Liquid-in-glass prototypes of a standard thermometer and a speciality thermometer, operating over different temperature ranges and oriented to different applications, were successfully built using the ILs [TEMA][MeSO<sub>4</sub>] and [P<sub>6614</sub>][NTf<sub>2</sub>], respectively, as thermometric fluids. Both ILs were selected according to their previously reported properties, and their volumetric behavior as a function of temperature was investigated. Linear variation of the volume with changes in temperature was observed for both ILs, being an ideal result for their utilization as thermometric fluids in LIG thermometers. The drawback of the lack of color of the selected ILs was overcome by doping with an IL-dye, thus providing color and facilitating the reading of the liquid column in the bore, while keeping the completely ionic nature of the fluid. Some difficulties for practical application may arise from, for example, slow response times as a result of the high viscosity of the ILs, especially at low temperatures, or high heat capacity. Nevertheless, this work demonstrates the opportunities of ILs in creating customized devices for the measurement of temperature, designed according to different requirements in parameters such as operational temperature range, price, toxicity, or biodegradability.

### Acknowledgements

The authors thank the PG Research Foundation for financial support of this work. They also want to thank Mr Richard C. Smith, glassblower at The University of Alabama, for fruitful conversations, valuable advice, and glassblowing work. H.R. is grateful to the Ministerio de Educación y Ciencia (Spain) for the award of the FPI grant with reference BES-2004–5311 under project PPQ2003–01326.

### References

- 1 A. Stark and K. R. Seddon, in *Kirk-Othmer Encyclopedia of Chemical Technology*, ed. A. Seidel, John Wiley & Sons, Inc., Hoboken, New Jersey, 2007, vol. 26, pp. 836–920.
- 2 D. R. MacFarlane and K. R. Seddon, *Aust. J. Chem.*, 2007, **60**, 3–5.
- 3 K. R. Seddon, *J. Chem. Technol. Biotechnol.*, 1997, **68**, 351–356.
- 4 J. G. Huddleston, H. D. Willauer, R. P. Swatloski, A. E. Visser and R. D. Rogers, *Chem. Commun.*, 1998, 1765–1766.
- 5 J. D. Holbrey and K. R. Seddon, *Clean Prod. Process.*, 1999, **1**, 223–236.
- 6 Z. Mu, W. Liu, S. Zhang and F. Zhou, *Chem. Lett.*, 2004, **33**, 524–525.
- 7 J. Sanes, F. J. Carrión, M. D. Bermúdez and G. Martínez-Nicolás, *Tribol. Lett.*, 2006, **21**, 121–133.
- 8 L. Weng, X. Liu, Y. Liang and Q. Xue, *Tribol. Lett.*, 2007, **26**, 11–17.
- 9 A.-E. Jiménez and M.-D. Bermúdez, *Tribol. Lett.*, 2007, **26**, 53–60.
- 10 W. Ogihara, M. Yoshizawa and H. Ohno, *Chem. Lett.*, 2004, **33**, 1022–1023.
- 11 C. L. Liotta, P. Pollet, M. A. Belcher, J. B. Aronson, S. Samanta and K. N. Griffith, *US Pat. Appl.*, US 2005–112341 20050422, 2005.

- 12 D. D. Zorn, J. A. Boatz and M. S. Gordon, *J. Phys. Chem. B*, 2006, **110**, 11110–11119.
- 13 A. R. Katritzky, H. Yang, D. Zhang, K. Kirichenko, M. Smiglak, J. D. Holbrey, W. M. Reichert and R. D. Rogers, *New J. Chem.*, 2006, **30**, 349–358.
- 14 M. Smiglak, W. M. Reichert, J. D. Holbrey, J. S. Wilkes, L. Sun, J. S. Thrasher, K. Kirichenko, S. Singh, A. R. Katritzky and R. D. Rogers, *Chem. Commun.*, 2006, 2554–2556.
- 15 H. Ohno, S. Washiro and M. Yoshizawa, *Polym. Prepr. (Am. Chem. Soc., Div. Polym. Chem.)*, 2004, **45**, 309–310.
- 16 M. Radosz, Y. Shen and J. Tang, *PCT Int. Appl.*, WO 2005-US40651 20051110, 2006.
- 17 T. E. Sutto, *J. Electrochem. Soc.*, 2007, **154**, P101–P107.
- 18 H. Nakajima and H. Ono, *Jap. Pat.*, JP 2007–112722 A 20070510, 2007.
- 19 J. F. Schooley, *Thermometry*, CRC Press, Boca Raton, 1986.
- 20 W. C. Dunn, *Introduction to Instrumentation, Sensors, and Process Control*, Artech House, Norwood, 2006.
- 21 B. Wu, J. D. Holbrey, R. G. Reddy and R. D. Rogers, *U. S. Pat.*, No. 6 749 336 B2B, 15 June 2004.
- 22 *Perry's Chemical Engineers' Handbook*, ed. R. H. Perry, D. W. Green and J. O. Maloney, McGraw–Hill, New York, 7th edn, 1999.
- 23 U. S. Environmental, Protection Agency, <http://www.epa.gov/mercury/about.htm> (last accessed: January 4th, 2008).
- 24 G. Fitzwater, W. Geissler, R. Moulton, N. V. Plechkova, A. Robertson, K. R. Seddon, J. Swindall and K. Wan Joo, *Ionic Liquids: Sources of Innovation*, Report Q002, January 2005, QUILL, Belfast, 2005. [Available at: <http://quill.qub.ac.uk/sources> (last accessed: January 4th, 2008)].
- 25 M. J. Earle, J. M. S. S. Esperança, M. A. Gilea, J. N. Canongia, Lopes, L. P. N. Rebelo, J. W. Magee, K. R. Seddon and J. A. Widegren, *Nature*, 2006, **439**, 831–834.
- 26 M. J. Earle and K. R. Seddon, *Pure Appl. Chem.*, 2000, **72**, 1391–1398.
- 27 J. F. Brennecke and E. J. Maginn, *AIChE J.*, 2001, **47**, 2384–2389.
- 28 Sigma–Aldrich, *ChemFiles bulletin*, 2006, vol. 6, number 9, [http://www.sigmaaldrich.com/aldrich/brochure/al\\_chemfile\\_v6\\_n9.pdf](http://www.sigmaaldrich.com/aldrich/brochure/al_chemfile_v6_n9.pdf) (last accessed: January 4th, 2008).
- 29 R. E. Del Sesto, C. Corley, A. Robertson and J. S. Wilkes, *J. Organomet. Chem.*, 2005, **690**, 2536–2542.
- 30 J. M. Smith, H. C. Van Ness and M. M. Abbott, *Introduction to Chemical Engineering Thermodynamics*, McGraw–Hill, New York, 7th edn, 2005.
- 31 W. D. Callister, Jr., *Materials science and engineering: an introduction*, John Wiley and Sons, New York, 7th edn, 2007.
- 32 T. Welton, *Chem. Rev.*, 1999, **99**, 2071–2083.
- 33 W. E. K. Middleton, *A history of the thermometer and its use in meteorology*, Johns Hopkins Press, Baltimore, 1966.

# Cytotoxicity of selected imidazolium-derived ionic liquids in the human Caco-2 cell line. Sub-structural toxicological interpretation through a QSAR study†

Andrés García-Lorenzo,<sup>a</sup> Emilia Tojo,<sup>b</sup> José Tojo,<sup>c</sup> Marta Teijeira,<sup>b</sup> Francisco J. Rodríguez-Berrocal,<sup>a</sup> Maykel Pérez González<sup>b,d</sup> and Vicenta S. Martínez-Zorzano<sup>\*a</sup>

Received 6th December 2007, Accepted 28th February 2008

First published as an Advance Article on the web 19th March 2008

DOI: 10.1039/b718860a

Room-temperature ionic liquids (ILs) are considered green chemicals that may replace volatile organic solvents currently used by industry. However, toxicological effects of ILs are not well known. In this study, we describe the cytotoxicity of selected imidazolium-derived ILs in Caco-2 cells, prototypical human epithelial cells. The most toxic IL was 1-decyl-3-methylimidazolium chloride ([C<sub>10</sub>mim][Cl]), whereas the least toxic was 1,3-dimethylimidazolium methyl sulfate ([C<sub>1</sub>mim][MSO<sub>4</sub>]). Using the toxicological experimental data obtained we developed a Quantitative Structure–Activity Relationship (QSAR) study using the Topological Sub-Structural Molecular Design (TOPS-MODE) approach. The model found showed excellent statistical parameters and from their interpretation, we arrived to some important conclusions such as: For 1-alkyl-3-methylimidazolium chloride derivatives, a correlation between the R<sub>2</sub> alkyl chain length and toxicity was observable. A positive contribution of *p*-chloro substituent in benzyl ring is detected among 1-methylarylimidazolium chloride derivatives. Regarding the contribution of the anion, anion chloride presents a positive contribution to toxicity whereas for compounds [C<sub>1</sub>mim][MSO<sub>4</sub>] and [C<sub>1</sub>eim][ESO<sub>4</sub>], a negative fragment contribution can be detected in anion methyl or ethyl sulfate. The EC<sub>50</sub> values determined for the ILs analysed in this study in Caco-2 cells are lower than the data reported in the literature on the toxicity of classical solvents assessed with cell lines. In conclusion, our results indicate that the possible cytotoxic effect of ILs should be considered in the design and overall evaluation of these compounds. Nevertheless, any toxicity evaluation of ILs should take their bioavailability into account, which will be affected by their low volatility, compared to conventional solvents.

## Introduction

Ionic liquids (ILs) are organic salts that are liquids at low temperature (usually at or below 100 °C).<sup>1</sup> In the last few years, interest in ILs research has dramatically increased and has resulted in the development of a vast number of novel ILs with a wide range of interesting applications.<sup>2</sup>

The most often cited attributes of ILs are their non-volatile properties, which make them potential green substitutes for conventional volatile organic solvents. Other favourable properties include their very good dissolution properties for most organic and inorganic compounds, high intrinsic ionic conductivity,

thermal and oxidative stability, a wide electrochemical window, broad liquid range, excellent heat transfer properties, and efficient absorption/transfer of microwaves.<sup>3</sup>

Another advantage of ionic liquids is that their physical and chemical characteristics can be modified over a wide range by modification of the cation's fine structure and the anion's identity. These variabilities and combinations therefore lead to an enormous number of theoretically accessible ionic liquids.

These chemicals have been widely used as solvents or co-catalysts in a variety of reactions including organic catalysis,<sup>4</sup> biocatalysis,<sup>5</sup> inorganic synthesis,<sup>1</sup> polymerisation,<sup>6</sup> electrochemistry,<sup>7</sup> and traditional extraction processes and gas separation.<sup>8</sup> In addition, there is an increasing use of ILs as engineering liquids for industrial processing,<sup>1</sup> and consequently their utilization in different branches of the chemical industry has quickly expanded.

Although ILs are usually described as green solvents, toxicity research studies have recently received attention and it has been demonstrated that many commonly used ILs have a certain level of toxicity.<sup>2</sup> Recent toxicity studies have documented ILs effects on organisms such as bacteria,<sup>9–16</sup> algae,<sup>17,18</sup> invertebrates,<sup>14,16,17,19–23</sup> fish,<sup>24,25</sup> plants,<sup>26,27</sup> mammalian cell cultures,<sup>11,28,29</sup> or rat.<sup>30,31</sup>

<sup>a</sup>Department of Biochemistry, Genetics and Immunology, University of Vigo, 36310, Vigo, Spain. E-mail: vzorzano@uvigo.es

<sup>b</sup>Department of Organic Chemistry, University of Vigo, 36310, Vigo, Spain

<sup>c</sup>Department of Chemical Engineering, University of Vigo, 36200, Vigo, Spain

<sup>d</sup>Molecular Simulation and Drug Design Group, Chemical Bioactive Center, Central University of Las Villas, Santa Clara, 54830, Villa Clara, Cuba

† This article is dedicated to José Tojo and to Maykel Pérez González in memoriam.



Nevertheless, only a few studies have analyzed the toxicity of ILs on human cell lines.<sup>32–34</sup> These *in vitro* systems have been extremely useful studying the molecular basis of chemical's biological activity, including its mechanisms of toxic action<sup>35</sup> and could facilitate extrapolation of *in vitro* data with regard to possible effects on humans.<sup>36</sup>

Another important challenge in ILs research is to be able to predict the toxicity of compounds that could be ILs by the construction of structure–activity relationship. This information can be used as the basis to design rules in synthesizing ILs with minimal toxicity.

In this connection, Quantitative Structure–Activity Relationship (QSAR) modelling is a potentially useful tool for this propose.<sup>37</sup> This involves the generation of mathematical models that relate the physical–chemical and structural properties of chemicals with their biological effects, by developing models based on the use of a training set of chemicals with known structures and biological activities.<sup>38–40</sup> QSAR studies have been extensively applied for predicting the toxicity of a wide range of chemicals for a diversity of endpoints.<sup>41–43</sup> QSAR modelling can be used for screening purposes and for prioritizing compounds in the early stages of development, and even before they have been synthesized, in virtual applications.<sup>44–46</sup>

In this paper, we report experimental data on the cytotoxicity of selected imidazolium-derived ionic liquids using the Caco-2 human cell line. These data were then used to build a predictive toxicity model based upon QSAR modelling methods.<sup>41,47,48</sup> The model was used to elucidate the chemical and structural factors that govern the toxicity of these compounds.

## Results and discussion

This study investigates the cytotoxicity of selected imidazolium-based ionic liquids in the Caco-2 human cell line including some compounds whose cytotoxicity has not ever been determined. All ionic liquids were prepared as described in previous papers and characterized using FAB mass spectrometry and <sup>1</sup>H and <sup>19</sup>F NMR,<sup>49–58</sup> and are summarized in Table 1.

We have used Caco-2 cells because as Ranke *et al.* suggested,<sup>29</sup> cytotoxicity tests in largely dedifferentiated cancer cell lines such as the one used in this study provide a convenient screening method for obtaining first rough estimates for the toxic potential of chemical substances. Furthermore, Caco-2 cells represent prototypical cells of the human epithelium, and they were chosen because the first contact of an organism with toxic compounds generally takes place in the epithelial cells. During the writing of this manuscript, a new paper has been published describing the effect of ionic liquids on human colon carcinoma HT-29 and Caco-2 cell lines.<sup>34</sup> Among the ILs that we tested, only one compound ([C<sub>8</sub>mim][PF<sub>6</sub>]) was already analysed in the mentioned work. On the other hand, in contrast to this previous study,<sup>34</sup> we develop a QSAR model that could be used to predict the toxicity of the compounds.

For all the ILs investigated, concentration–response curves could be fitted with the linear logistic model and the effective concentration 50 (EC<sub>50</sub>) values were calculated. As examples, dose–response curves for Caco-2 cells exposed to [*p*-ClBnmim][Cl] after 24 and 48 h of incubation are shown in Fig. 1.

The EC<sub>50</sub> values, as well as the decadic logarithm of these data for the ILs tested, are summarized in Table 1. Considering all the ILs assayed, differences in their EC<sub>50</sub> values of more than three orders of magnitude were found. The EC<sub>50</sub> data obtained ranged from 0.03 up to 81.24 mM (from 1.5 to 4.9 in logarithmic form) after 24 h of incubation, and from 0.01 up to 31.69 mM (from 1.0 to 4.5 in logarithmic form) with an incubation time of 48 h. These values are in agreement with those reported by Ranke *et al.*<sup>29</sup> showing a range of cytotoxicity values for imidazolium ILs from about 10 mM to about 0.01 mM.

As it can be seen in Table 1, a reduction in the EC<sub>50</sub> values (indicating an increase in the cytotoxicity effect) for most of the ILs assayed was observed when the exposition time extends from 24 to 48 h. There were only two exceptions: [C<sub>4</sub>mim][MSO<sub>4</sub>] and [C<sub>4</sub>eim][ESO<sub>4</sub>]. This trend of increasing toxicity with increasing exposure time was especially significant for the group of 1-alkyl-3-methylimidazolium chlorides.

**Table 1** Effective concentration (EC<sub>50</sub>) values for different imidazolium-derived ionic liquids tested in Caco-2 cells<sup>a</sup>

Ionic liquid	Exposition time: 24 h				Exposition time: 48 h				
	EC <sub>50</sub>	SD	log EC <sub>50</sub>	R <sup>2</sup>	EC <sub>50</sub>	SD	log EC <sub>50</sub>	R <sup>2</sup>	
I1	[C <sub>4</sub> mim][Cl]	28.69	10.24	4.5	0.96	3.80	0.66	3.6	0.99
I2	[C <sub>6</sub> mim][Cl]	5.24	4.79	3.7	0.89	0.24	0.18	2.4	0.93
I3	[C <sub>8</sub> mim][Cl]	0.54	0.66	2.7	0.92	0.03	0.02	1.5	0.99
I4	[C <sub>10</sub> mim][Cl]	0.03	0.02	1.5	0.91	0.01	0.01	1.0	0.98
I6	[C <sub>6</sub> mim][PF <sub>6</sub> ]	15.67	3.78	4.2	0.97	6.87	1.62	3.8	0.95
I5	[C <sub>8</sub> mim][PF <sub>6</sub> ]	5.12	1.81	3.7	0.94	1.46	0.29	3.2	0.99
I7	[C <sub>1</sub> mim][MSO <sub>4</sub> ]	81.24	24.76	4.9	0.96	31.69	14.53	4.5	0.94
I11	[C <sub>4</sub> mim][MSO <sub>4</sub> ]	20.46	7.88	4.3	0.99	23.34	13.03	4.4	0.96
I13	[Bnmim][MSO <sub>4</sub> ]	16.96	6.71	4.2	0.98	14.13	4.75	4.1	0.99
I8	[C <sub>1</sub> eim][ESO <sub>4</sub> ]	44.11	26.48	4.6	0.94	13.60	5.94	4.1	0.94
I12	[C <sub>4</sub> eim][ESO <sub>4</sub> ]	8.50	11.29	3.9	0.93	13.08	1.99	4.1	0.99
I14	[Bneim][ESO <sub>4</sub> ]	14.08	5.00	4.1	0.97	10.37	0.61	4.0	1.00
I15	[Bnmim][Cl]	30.76	6.41	4.5	0.99	11.09	0.67	4.0	1.00
I9	[ <i>p</i> -FBnmim][Cl]	20.37	7.28	4.3	0.98	2.78	0.99	3.4	0.95
I10	[ <i>p</i> -ClBnmim][Cl]	4.58	0.51	3.7	0.99	1.07	0.12	3.0	0.99

<sup>a</sup> EC<sub>50</sub> values are expressed as mean and standard deviation (SD) calculated from three independent experiments and expressed in mM. log EC<sub>50</sub>: Decadic logarithm of the EC<sub>50</sub> values expressed in μM. R<sup>2</sup> indicates the proportion of variability explained by the fitted equation.

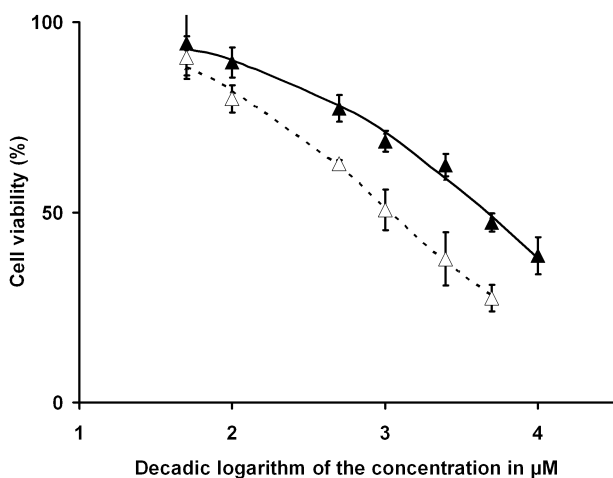


**Fig. 1** Dose–response curves for Caco-2 cells exposed to [p-ClBnmim][Cl] for 24 h (▲) and 48 h (△). Data are the mean and SD of three independent experiments.

Our finding of an increased cytotoxicity of most of the compounds tested in function of the exposure time contrasts with the data reported for some ILs containing tetrafluoroborate in HeLa cells, describing similar or even higher  $EC_{50}$  values after 44 h of incubation in comparison to the values obtained after 24 h.<sup>32</sup> However, in accordance with our results, a trend of increased toxic effect of ILs on the alga *Cyclotella meneghiniana* by increasing the exposure time from one to ten days of culture has been reported.<sup>17</sup>

On the other hand, with the aim of interpreting in a more extensive way the experimental results obtained, we developed a QSAR model using the TOPS-MODE approach.<sup>59–61</sup> This tool permits us to predict the potential contribution of the different sub-structures that constitute the ILs under study.

The model selection was subjected to the principle of parsimony.<sup>62</sup> Then, we chose a function with higher statistical signification but having as few parameters as possible. For that reason, although several models were developed for the spectral moments (TOPS-MODE approach), changing the number of variables in every step of the analysis, the preliminary best model that we found was described with the following equation and followed by the statistical parameters of the regression:

$$-\log(EC_{50}) = -0.928(\pm 0.026) + 2.665(\pm 0.188)\mu_4^{\text{sumB20}} - 4.549(\pm 0.239)\mu_1\mu_{15}^{\text{Dist}} + 2.265(\pm 0.077)\mu_1\mu_1^{\text{Hyd}} \quad (1)$$

$$N = 15, R^2 = 0.989, S = 0.101, F = 332.88, p < 10^{-5}, \text{AIC} = 0.017, \text{LOF} = 0.021, \text{FIT} = 38.111, q_{\text{CV-LOO}}^2 = 0.983, S_{\text{CV-LOO}} = 0.115, q_{\text{CV-Boot}}^2 = 0.934, S_{\text{CV-LGO}} = 0.128, R_{\text{Scram}}^2 = 0.121, q_{\text{Scram}}^2 = -0.478.$$

where  $N$  is the number of compounds included in the model,  $R^2$  is the square of the correlation coefficient,  $S$  is the standard deviation of the regression,  $F$  is the Fisher ratio, AIC is the Akaike's information criterion and FIT is the Kubinyi function. Furthermore, we calculated the validation parameters shown previously like cross-validated squared regression coefficient  $q^2$  and the standard deviation  $S_{\text{CV}}$  of the LOO and bootstrapping procedures. Finally, a scrambling technique verifies models with chance correlations, using  $R_{\text{Scram}}^2$  and  $q_{\text{Scram}}^2$  after that the sequence of response vector has been randomly modified. The procedure

is repeated 300 times and the model show good results from statistical points of view.

The parameter  $q^2$  is used as a criterion of both robustness and predictive ability of the model. Many authors consider high  $q^2$  (for instance,  $q^2 > 0.5$ ) as an indicator or even as the ultimate proof that the model is highly predictive.<sup>63</sup> As we can see, the model proposed by us as the best one presents appropriate values of statistic parameters. Nevertheless, it would be interesting to show the analysis that we carried out to determine the best model with the TOPS-MODE descriptors family.

As we mentioned above, we developed several models for the TOPS-MODE descriptors changing the number of variables in every step of the analysis. In other words, once a model was developed, we calculated their statistical parameters and tested if the addition of a new variable to the model was justified. If it was the case, we compared the results with the previous models and we repeated this analysis whenever we included a new variable.

In this connection, it was very important to calculate some criterion in order to know when to stop the introduction of new variables in the development of the model. Our data set contains only 15 compounds and the maximum number of variables is three for the minimum value of ratio between cases and variables included in the model. It has been reported that this relation is appropriate when there are five cases per variable (5 : 1) as a minimum value.<sup>64</sup> We also applied the Akaike's information criterion and Kubinyi function to determine if a variable should be included in the model. That is to say, if the Akaike's information criterion decreases in value when adding an additional variable and the Kubinyi function increases in value, then, the introduction of this new variable is justified.

The equations that describe the models relative to two variables are shown below with their statistical parameters.

$$-\log(EC_{50}) = -1.023(\pm 0.067) - 3.286(\pm 0.176)\mu_0\mu_8^{\text{Dip}} + 2.649(\pm 0.368)\mu_9^{\text{Hyd}} \quad (2)$$

$$N = 15, R^2 = 0.764, S = 0.447, F = 19.460, p < 10^{-5}, \text{AIC} = 0.301, \text{LOF} = 0.297, \text{FIT} = 8.483, q_{\text{CV-LOO}}^2 = 0.556, S_{\text{CV-LOO}} = 0.687, q_{\text{CV-Boot}}^2 = 0.525, S_{\text{CV-LGO}} = 0.749, R_{\text{Scram}}^2 = 0.086, q_{\text{Scram}}^2 = -0.393.$$

The quality of the statistical parameters for the model with two variables was significantly less adequate than the model reported by eqn (1) and the intercept of the eqn (2) turned out not to be significant. The introduction of this new variable (eqn (1)) conformed to the Akaike's information criterion (decrement from 0.301 to 0.017) and the Kubinyi function (increased from 8.483 to 38.111) was justified. The statistical parameters in model 1 improved with increases in the value of the  $R^2$ ,  $q^2$  and  $F$ , and a decrease in the value of  $S$ . For this reason, we found better results and a more predictive model when introduced a third variable (eqn (1)). In addition, we do not find any compounds that can be considered potential outliers.

On the other hand, in the last few years, considerable progress has been made in identifying structure alerts and critical structural factors aimed at predicting the toxicity of chemicals.<sup>65–68</sup> In particular, computational methods have provided valuable information towards their *early* identification with important implications in the design of safer chemicals.<sup>69</sup> Specifically, in

our case, one can easily write the QSAR model in terms of bond contributions or otherwise structural fragment contributions for the chemicals, and then infer how the latter do influence the toxicity.

Among the ILs evaluated in this study, the most toxic was  $[C_{10}\text{mim}][\text{Cl}]$ , whereas those showing minor toxicity to Caco-2 cells were those containing an alkyl sulfate as anion and a methyl or ethyl group as  $R_1$  substituent ( $[C_1\text{mim}][\text{MSO}_4]$  and  $[C_1\text{eim}][\text{ESO}_4]$  respectively). In this way, our theoretical QSAR model also predicts  $[C_{10}\text{mim}][\text{Cl}]$  (compound I4) as the most toxic, opposed to the alkylsulfate derivatives  $[C_1\text{mim}][\text{MSO}_4]$  and  $[C_1\text{eim}][\text{ESO}_4]$  (compounds I7 and I8 respectively). As can be seen in Fig. 2, anion chloride presents a positive contribution to the studied property for I4. However, for compounds  $[C_1\text{mim}][\text{MSO}_4]$  and  $[C_1\text{eim}][\text{ESO}_4]$ , a negative fragment contribution can be detected in anion methyl or ethyl sulfate.

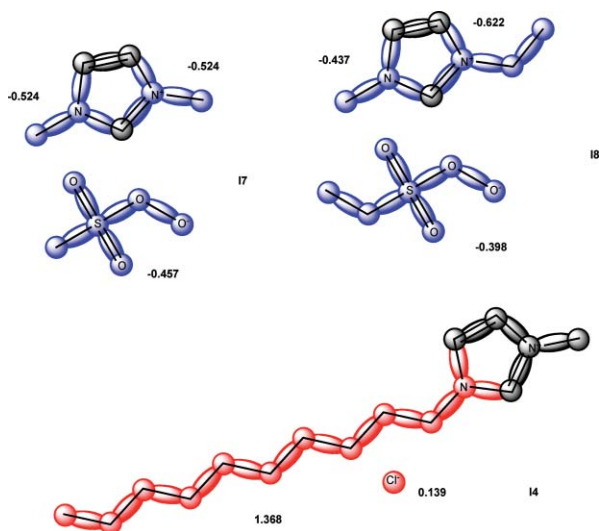


**Fig. 2** Molecular representation of compounds  $[C_1\text{mim}][\text{MSO}_4]$  (I7),  $[C_1\text{eim}][\text{ESO}_4]$  (I8) and  $[C_{10}\text{mim}][\text{Cl}]$  (I4) and corresponding fragment contributions.

To our knowledge, this is the first report about the cytotoxicity of these two methylimidazolium alkyl sulfate derivatives. Regarding other 1,3-dialkylimidazolium-derivatives containing alkyl sulfate as anion we have found only one paper describing an  $\text{EC}_{50}$  value of 1.7 mM for the compound ( $[C_4\text{mim}][\text{MSO}_4]$ ) tested in the IPC-81 rat leukaemia cell line.<sup>70</sup>

To analyse the influence of an aromatic side chain on the toxicity of ILs, methylimidazolium-derived ILs containing an aromatic ring as  $R_2$  substituent were also tested. Among them, three included  $\text{Cl}^-$  as anion  $[\text{Bnmim}][\text{Cl}]$ ,  $[p\text{-FBnmim}][\text{Cl}]$  and  $[p\text{-ClBnmim}][\text{Cl}]$  whereas the other two contained an alkylsulfate as anion  $[\text{Bnmim}][\text{MSO}_4]$  and  $[\text{Bneim}][\text{ESO}_4]$ . For the chloride derivatives, the one containing  $p\text{-ClBn}$  was the most toxic. The same behaviour was found in the model QSAR (Fig. 3).

A positive contribution of  $p$ -chloro substituent in benzyl ring is detected among 1-methylarylimidazolium chloride derivatives. The  $p$ -substitution with the other halogen in compound I9 (fluoro) decreases this effect and in the absence of  $p$ -substituents (compound I15), a negative contribution on property is predicted, in accordance with experimental assays. On the other hand, in comparison with 1-alkyl-3-methylimidazolium chloride

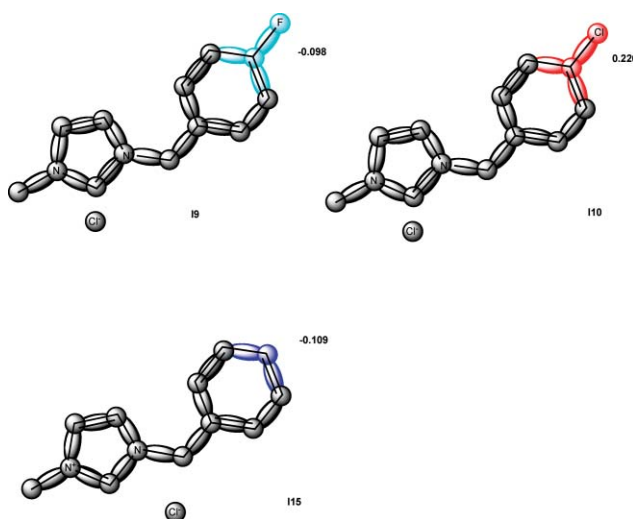


**Fig. 3** Molecular representation of compounds  $[p\text{-FBnmim}][\text{Cl}]$  (I9),  $[p\text{-ClBnmim}][\text{Cl}]$  (I10) and  $[\text{Bnmim}][\text{Cl}]$  (I15) and corresponding fragment contributions.

derivatives, the cytotoxicity of these ILs to Caco-2-cells was similar to that shown for  $[C_4\text{-}C_6\text{mim}][\text{Cl}]$  and lower than that shown for  $[C_8\text{-}C_{10}\text{mim}][\text{Cl}]$ . These results are also detected in the theoretical model. Alkylsubstituents on imidazolium cations with 4 or 6 carbon atoms show a negative contribution to toxicity (compounds I1 and I2) similar to arylsubstituents (compounds I9, I10 and I15), as can be seen in Fig. 4.

However, an increase in the length of the alkyl chain on cation has a positive contribution to Caco-2 cells toxicity (compounds I3 and I4). Concerning the toxicity of the alkylsulfate derivatives  $[\text{Bnmim}][\text{MSO}_4]$  and  $[\text{Bneim}][\text{ESO}_4]$ , their  $\text{EC}_{50}$  values were similar to those shown by  $[C_4\text{mim}][\text{MSO}_4]$  and  $[C_4\text{eim}][\text{ESO}_4]$  respectively. The same predictions are derived from the Fig. 5.

In alkylsulfate derivatives  $[C_4\text{mim}][\text{MSO}_4]$ ,  $[C_4\text{eim}][\text{ESO}_4]$ ,  $[\text{Bnmim}][\text{MSO}_4]$  and  $[\text{Bneim}][\text{ESO}_4]$  (compounds I11, I12, I13 and I14, respectively), a negative contribution to the toxicity activity is detected in alkyl or aryl fragments under imidazolium cations.

In the present work, we observed a decrease in the  $\text{EC}_{50}$  values with an increase in the length of the  $R_2$  alkyl chain for the group of 1-alkyl-3-methylimidazolium chlorides (see data in Table 1). In addition, Fig. 4 allows us to establish a theoretical comparison between 1-alkyl-3-methylimidazolium chlorides. We can see that the alkylsubstituent contribution on studied property increases with the chain length (from  $C_4$  to  $C_{10}$ ).

A similar effect of increased toxicity with a longer  $R_2$  alkyl chain length was found when the following comparisons were established:  $[C_6\text{mim}][\text{PF}_6]$  vs.  $[C_8\text{mim}][\text{PF}_6]$   $[C_1\text{mim}][\text{MSO}_4]$  vs.  $[C_4\text{mim}][\text{MSO}_4]$  and  $[C_1\text{eim}][\text{ESO}_4]$  vs.  $[C_4\text{eim}][\text{ESO}_4]$  (see Table 1). However, in these cases, results are based on the comparison of two ionic liquids only and further testing would be necessary to support this hypothesis.

Our results concerning the influence of the  $R_2$  chain length on toxicity are consistent with data published by other authors describing that the longer the  $n$ -alkyl chain is, the greater the toxicity of the compound is too. This finding was observed for ILs containing  $C_3\text{mim}$  to  $C_{10}\text{mim}$  cations assayed on IPC-81 and C6 rat cell lines,<sup>11</sup> as well as for ILs containing  $C_4\text{mim}$  to

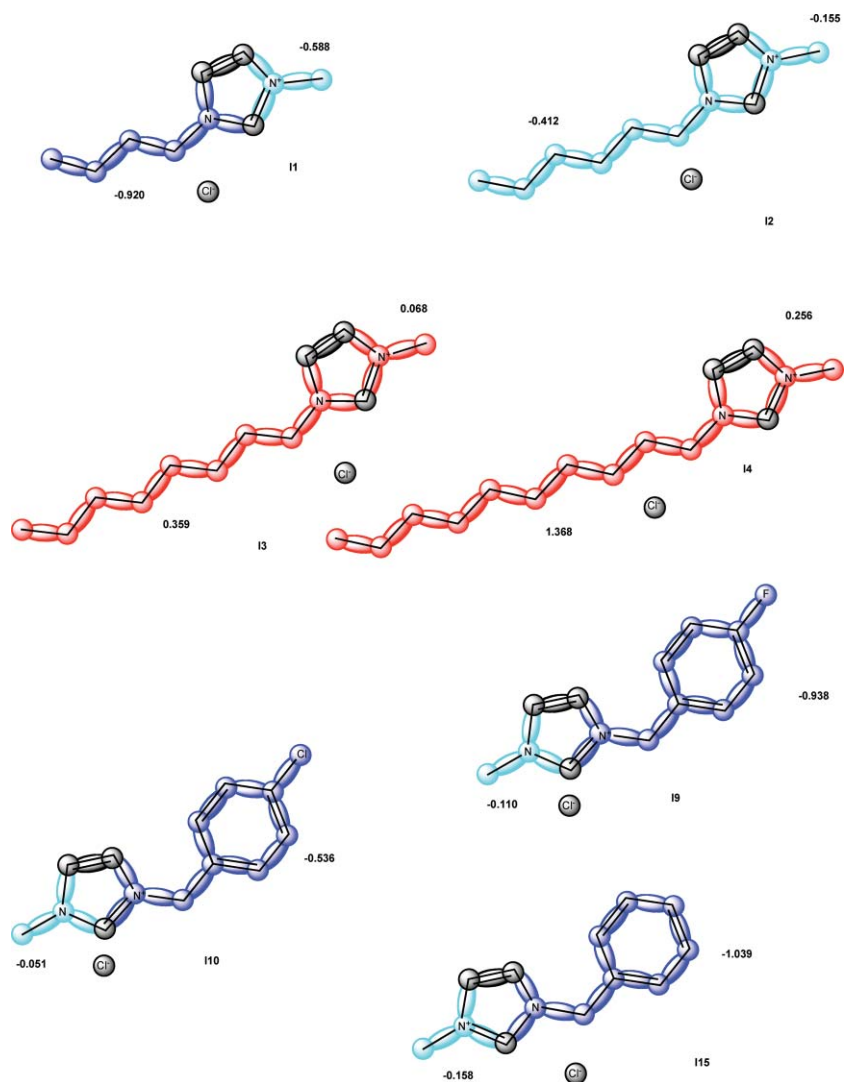


**Fig. 4** Molecular representation of compounds  $[C_4\text{mim}][\text{Cl}]$  (I1),  $[C_6\text{mim}][\text{Cl}]$  (I2),  $[C_8\text{mim}][\text{Cl}]$  (I3),  $[C_{10}\text{mim}][\text{Cl}]$  (I4),  $[p\text{-FBnmim}][\text{Cl}]$  (I9),  $[p\text{-ClBnmim}][\text{Cl}]$  (I10) and  $[Bnmim][\text{Cl}]$  (I15) and corresponding fragment contributions.

$C_{10}\text{mim}$  cations tested on the HeLa human tumour cell line.<sup>32</sup> Additionally, increasing of the toxicity with the length of the alkyl substituent chain on the methylimidazolium cation has also been described for HT-29 and Caco-2 cell lines.<sup>34</sup> The trend of increased toxic effect with increased hydrophobicity of ILs has also been described in other organisms including the marine bacterium *Vibrio fischeri*,<sup>11,15</sup> the nematode *Caenorhabditis elegans*,<sup>19</sup> the crustacean *Daphnia magna*<sup>20</sup> and the snail *Physa acuta*.<sup>21</sup>

In general, ILs with longer alkyl chains are more lipophilic than those with shorter alkyl chains and they can be presumed to have a tendency to be incorporated into the phospholipid bilayers of biological membranes. In this regard, some authors have indicated that the increased toxicity of longer ILs can be attributed to enhanced membrane permeability altering the physical properties of the lipid bilayer.<sup>11,17,32</sup> Furthermore, it has been suggested that the mechanism of toxicity for ILs takes place through membrane disruption because of the structural similarity of imidazolium-derived ILs to detergents, pesticides and antibiotics that attack lipid structure or cationic surfactants

that may cause membrane-bound protein disruption.<sup>15</sup> Recently, Ranke *et al.* have demonstrated that lipophilicity of ILs dominates their *in vitro* cytotoxicity over a wide range of structural variations.<sup>29</sup>

The contribution of the anionic part of the ionic liquids to the observed biological effect was evaluated by comparing the  $\text{EC}_{50}$  values obtained for the cations  $[C_6\text{mim}]^+$  and  $[C_8\text{mim}]^+$ , combined with two different anions ( $\text{Cl}^-$  and  $\text{PF}_6^-$ ). For both cations, a higher toxic effect was found for chloride derivatives. A similar result was described by Stock *et al.* when the inhibitory effects of  $[C_4\text{mim}][\text{Cl}]$  and  $[C_4\text{mim}][\text{PF}_6]$  on the acetylcholinesterase activity were compared.<sup>25</sup> In addition, slightly higher cytotoxicity for the chloride derivative has also been described when the cytotoxicity of  $[C_4\text{mim}][\text{Cl}]$  and  $[C_4\text{mim}][\text{PF}_6]$  on HeLa cells was tested.<sup>32</sup> Several authors have described that varying the anion has only minimal effects on the toxicity of several imidazolium compounds, indicating that ILs toxicity seemed to be related to the alkyl chain branching and to the hydrophobicity of the imidazolium cation and not to the various anions.<sup>11,14,20</sup> In this respect, a recent study using the



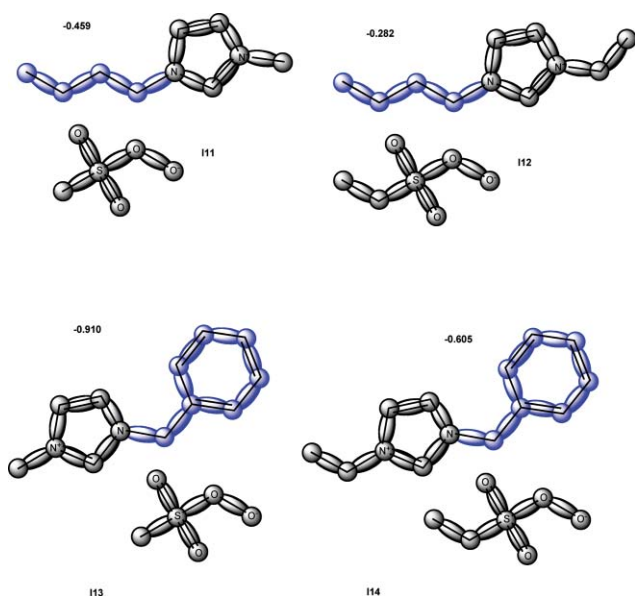


**Fig. 5** Molecular representation of compounds  $[C_4\text{mim}][\text{MSO}_4]$  (I11),  $[C_4\text{eim}][\text{ESO}_4]$  (I12),  $[\text{Bnmim}][\text{MSO}_4]$  (I13) and  $[\text{Bneim}][\text{ESO}_4]$  (I14) and corresponding fragment contributions.

IPC-81 rat leukaemia cell line as test system and including a large pool of anions demonstrated that most of the commercially available anions showed no or only marginal cytotoxic effects. However, anionic moieties with lipophilic and hydrolysable structural elements seem to be of considerable relevance with respect to the toxicity of ionic liquids.<sup>70</sup>

To permit comparisons between the cytotoxicity of ionic liquids and conventional solvents, the following organic solvents: acetone, methanol, acetic acid and benzene were tested with Caco-2 cells in the concentration range from 0.01 to 25 mM. We found that after 24 or 48 h of exposition to these solvents, the cells viability was always higher than 70%. At the same range of final concentrations all the ILs tested in this study were more toxic than the solvents analysed. Based on the data obtained, it was not possible to estimate any effective concentration values for the organic solvents analysed. Similar results were described by Frade *et al.*,<sup>34</sup> when methanol and acetone were tested on Caco-2 and HT-29 cells.

The  $\text{EC}_{50}$  values of the ILs tested in our study were compared to the  $\text{EC}_{50}$  data present in the literature regarding the toxicity of classical industrial solvents assessed with other cell lines. In this regard, the only available data for the same solvents were those reported for methanol and acetone assayed on the IPC-81 rat cell line<sup>11</sup> describing  $\log \text{EC}_{50}$  values higher than 6.0 ( $\text{EC}_{50}$  expressed in  $\mu\text{M}$ ) for both solvents. Furthermore, typical cytotoxicities of mild conventional solvents have been described with  $\text{EC}_{50}$  values of about  $10^6 \mu\text{M}$ .<sup>29</sup> The  $\log \text{EC}_{50}$  values determined for the ILs tested in our study in Caco-2 cells are generally two or three orders of magnitude lower, which indicates that these ILs are more toxic than some commonly used industrial solvents.

## Conclusion

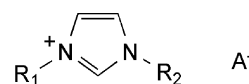
A group of imidazolium-derived ILs have been tested for their biological activity in the Caco-2 human cell line. The results presented in this paper indicate that the cytotoxicity of ILs is

dependent on their chemical structure. In this connection, a QSAR model with good statistical parameters using a TOPS-MODE approach was obtained and a relevant sub-structural analysis from this model was provided. As a consequence, the possible cytotoxic effect of ILs should be considered in the design of these compounds. In this respect, the fact that methylimidazolium alkyl sulfate derivatives have a relatively low cytotoxic effect can be considered as a positive attribute.

## Experimental

### Ionic liquids synthesis

The ILs tested in the present work were synthesized using methods previously described and characterized by  $^1\text{H}$  NMR,  $^{19}\text{F}$  NMR and FAB MS spectrometry. They are cited as: 1-butyl-3-methylimidazolium chloride ( $[C_4\text{mim}][\text{Cl}]$ ),<sup>50</sup> 1-hexyl-3-methylimidazolium chloride ( $[C_6\text{mim}][\text{Cl}]$ ),<sup>50</sup> 1-octyl-3-methylimidazolium chloride ( $[C_8\text{mim}][\text{Cl}]$ ),<sup>50</sup> 1-decyl-3-methylimidazolium chloride ( $[C_{10}\text{mim}][\text{Cl}]$ ),<sup>51</sup> 1-hexyl-3-methylimidazolium hexafluorophosphate ( $[C_6\text{mim}][\text{PF}_6]$ ),<sup>49</sup> 1-octyl-3-methylimidazolium hexafluorophosphate ( $[C_8\text{mim}][\text{PF}_6]$ ),<sup>52</sup> 1,3-dimethylimidazolium methyl sulfate ( $[C_1\text{mim}][\text{MSO}_4]$ ),<sup>53</sup> 1-butyl-3-methylimidazolium methyl sulfate ( $[C_4\text{mim}][\text{MSO}_4]$ ),<sup>54</sup> 1-benzyl-3-methylimidazolium methyl sulfate ( $[\text{Bnmim}][\text{MSO}_4]$ ),<sup>55</sup> 1-methyl-3-ethylimidazolium ethyl sulfate ( $[C_1\text{eim}][\text{ESO}_4]$ ),<sup>56</sup> 1-butyl-3-ethylimidazolium ethyl sulfate ( $[C_4\text{eim}][\text{ESO}_4]$ ),<sup>54</sup> 1-benzyl-3-ethylimidazolium ethyl sulfate ( $[\text{Bneim}][\text{ESO}_4]$ ),<sup>55</sup> 1-benzyl-3-methylimidazolium chloride ( $[\text{Bnmim}][\text{Cl}]$ ),<sup>57</sup> 1-*p*-fluorobenzyl-3-methylimidazolium chloride ( $[p\text{-FBnmim}][\text{Cl}]$ ),<sup>58</sup> 1-*p*-chlorobenzyl-3-methylimidazolium chloride ( $[p\text{-ClBnmim}][\text{Cl}]$ ).<sup>58</sup> Fig. 6 shows a schematic representation of the general structure of the above-mentioned ILs.



$R_1 = \text{Me, Et}$   
 $R_2 = \text{alkyl } C_n (n = 1, 2, 4, 6, 8, 10), \text{Bn, } p\text{-ClBn, } p\text{-FBn}$   
 $A = \text{Cl, PF}_6, \text{MeSO}_4, \text{EtSO}_4$

**Fig. 6** Generic chemical structure of the group of imidazolium-derived ionic liquids tested in this study.

### Other chemicals

The cell culture medium and the supplements were purchased from Biochrom AG. The plastic cellware was provided by Costar. The MTT cell proliferation kit was purchased from Roche. All the other chemicals, of analytical grade, were obtained from Panreac and Sigma.

### Caco-2 cell culture

The Caco-2 human colon adenocarcinoma cell line was obtained from the European Collection of Cell Cultures (ECACC No: 86010202). Cells were routinely grown in 25 or 75  $\text{cm}^2$  plastic flasks in Dulbecco's modified Eagle's medium (DMEM) containing 4.5  $\text{g L}^{-1}$  glucose, 20% foetal calf serum (FCS),

100 units mL<sup>-1</sup> of penicillin, 100 µg mL<sup>-1</sup> of streptomycin, 2 mM L-glutamine, and 1% non-essential amino acids at 37 °C, in a 5% CO<sub>2</sub> humidified atmosphere. The medium was changed every three days and cells were subcultured after reaching 90% confluence by treating them with a solution of 0.05% trypsin/0.02% EDTA in phosphate-buffered saline (PBS).

### Cytotoxicity evaluation

Cytotoxicity was determined using a colorimetric assay with 3-(4,5-dimethylthiazol-2-yl)-2,5-diphenyltetrazolium bromide (MTT) reagent. This assay is based on the conversion of the yellow tetrazolium salt to purple formazan crystals by metabolic active cells.<sup>71</sup> In these experiments, cells were seeded at a density of 10 000 cells well<sup>-1</sup> into 96-well tissue culture plates and grown for 40 h before adding the tested compounds. The ILs, previously diluted in the culture medium, were added to the wells at final concentrations within the range from 1 µM to 100 mM, and cells were incubated for 24 or 48 h. Each plate contained blanks (DMEM medium alone), controls (cells incubated only with medium), and serial dilutions of ILs, with three replicates for each concentration.

After the incubation intervals, 10 µL of the MTT reagent were added to each well and cells were incubated for an additional 4 h period to allow the cleavage of the MTT reagent by viable cell mitochondrial dehydrogenase. Afterwards, 100 µL of the solubilization solution were added and plates were incubated overnight. The absorbance of the solubilized formazan product was then spectrophotometrically quantified in an ELISA microplate reader (Biorad 550) at 570 nm with the reference at 630 nm. The cell viability was expressed as the absorption percentage of exposed cells compared with that of cells incubated with media alone.

The EC<sub>50</sub> values were obtained by fitting dose–response curves, representing cell viability to the base 10 logarithm of the ionic liquid concentration, to a linear logistic model as previously described.<sup>11</sup> Results are expressed as the mean and standard deviation (SD) of three independent experiments. All the statistical analysis were performed using the SPSS program (version 11.5.1).

### QSAR studies

**Data set.** The toxicological property of interest here is the cytotoxicity of the ionic liquids previously synthesized by us and the experimental determination of this was explained above. Then, as usual for others QSAR studies,<sup>72–75</sup> EC<sub>50</sub> values were log-transformed (–log EC<sub>50</sub>), being of practical use in the following QSAR modelling (see Table 1).

**QSAR modelling.** A QSAR modelling approach seeks to uncover relationships between chemical structure and biological activity, most often by a multilinear equation that relates molecular properties of the compounds (*descriptors*) to the desired activity. Here we have resorted to the graphed-based molecular descriptors, spectral moments, designed accordingly to the Topological Sub-Structural Molecular Design (TOPS-MODE) approach and implemented into MODESLAB software available from the internet site: [www.modeslab.com](http://www.modeslab.com). The mathematical details of this approach have been widely reported,<sup>76,77</sup> so we

will limit ourselves to a brief outline highlighting only the most important aspects.

TOPS-MODE codifies the molecular structure by means of the edge adjacency matrix *E*. The *E* matrix is a square symmetric matrix of order *m* whose elements are equal to one if the bonds *i* and *j* are adjacent, that is, they are incident to a common atom, or zero otherwise.<sup>78</sup> The diagonal elements of this matrix are weighted with bond weights aimed at describing the hydrophobic/polarity, electronic and steric features of the molecules. Mainly they mirror fundamental physico–chemical properties that might relate to the biological endpoint. In this work, the weights included the standard bond dipole moments (Dip and Dip2) and the bond distance (Dis), as well as contributions from the following atomic properties: partition coefficient (H), polar surface area (PSA), polarizability (Pol), Gasteiger–Marsilli atomic charges (GM), van der Waals atomic radii (vdW) and molar refractivity (MR). As described previously,<sup>79</sup> the atomic properties are converted into bond weight contributions (*w*(*i,j*)) according to following equation:

$$w(i,j) = \frac{w_i}{\delta_i} + \frac{w_j}{\delta_j}$$

where *w* and *δ* respectively represent the atomic weight and the vertex degree of the atoms *i* and *j*. Spectral moments are then defined as the traces of the different powers of the weighted *E* matrix.

These graph-based descriptors were computed with the Modeslab 1.5 software,<sup>80</sup> from the Simplified Molecular Input Line Entry Specification (SMILES) inputting of the chemical structures.<sup>81–83</sup> Specifically, we have calculated the first 15 spectral moments ( $\mu_1$ – $\mu_{15}$ ) for each bond weight and the number of bonds in the molecules ( $\mu_0$ ), including the hydrogen atoms. As to the modelling technique, we opted for a regression-based approach; in this case, the regression coefficients and statistical parameters were obtained by the Multiple Linear Regression (MLR) analysis implemented in Mobydigs software.

In summary, we adopted the following 3-step procedure for establishing our QSAR model.

#### Step 1: Model set-up

This proceeds as follows.

- (i) Select an appropriate training set of chemicals.
- (ii) Input the molecular structures, through the SMILES codes.
- (iii) Return the spectral-moments descriptors using an appropriate set of bond weights.
- (iv) Find an adequate QSAR model from the training set by a regression-based approach.

#### Step 2: Model evaluation

Assess the performance of the QSAR model, particularly regarding its applicability and predictive power.

#### Step 3: Structural alerts identification

Identify structural alerts to the toxicity based on the bond contributions computed with the final QSAR model.

**Model set-up.** The task is to obtain a mathematical function that best describes the activity, as a linear combination of the predictor  $X$ -variables, with the coefficients  $a_k$ . Such coefficients are to be optimized by means of MLR analysis using the chemicals under study. In most cases, MLR is suitably applied in QSAR studies as long as the problem of selection of variables is faced and solved. In doing so, one should be aware of possible spurious relationships among the variables and multicollinearity. Also, particular care should be taken to avoid *overfitted* models, *i.e.* models with too many included predictor variables. Indeed employing subsets with fewer variables, in general, facilitates model interpretation and may lower the number of random variables selected by chance correlation. Moreover, one should easily detect the presence of influential outliers and then modify the data set accordingly.

**Variable selection.** The variable selection procedure that we have adopted for our QSAR study is the Genetic Algorithm (GA), which is based on the evolution of a population of models.<sup>84</sup> The particular GA simulation conditions applied here are: 1000 generations, 0.5 for the trade-off between crossovers and mutation parameter, 1 smoothness factor and 300 model populations. Further, we followed the principle of parsimony,<sup>62</sup> that is to say, we choose the function with higher statistical significance but having as few descriptors as possible.

**Model evaluation.** Two kinds of diagnostic statistical tools were used for evaluating/enhancing the performance of our regression model: the so-called *goodness of fit* and *goodness of the prediction*. In the first case, attention is given to the fitting properties of the model while in the second case attention is paid to the predictive power of the model (*i.e.* the model adequacy for describing new compounds).

Goodness of fit was assessed by examining the determination coefficient,  $R^2$ , the standard deviation ( $s$ ), the Fisher's statistic,  $F$ . On the other hand, goodness of the prediction was evaluated by means of cross validation (CV), basically leave-one-out (LOO-CV), bootstrapping and scrambling validation techniques. These validation techniques are only applied to final QSAR model.<sup>84</sup>

Besides the classic regression parameters listed above, we adopt other important indices; Kubinyi function (FIT), Akaike's information criterion (AIC) and *Friedman's lack-of-fit function* (LOF).<sup>84</sup> They give enough criteria for comparing models with different parameters; number of variable and number of chemicals.

In summary, a good overall quality of the models is indicated by a large  $F$  (signification of model), FIT and  $\rho$  value; small AIC and LOF (overfitting) values;  $R^2$  (goodness of fit) and  $q^2$  (predictability) values close to one (except in  $R^2_{\text{Scram}}$  and  $q^2_{\text{Scram}}$ , which check random correlations).

**Data reduction.** Outliers are atypical cases, infrequent observations, which do not follow the characteristic distribution of the majority of the data. Deleting a small number of outliers from a QSAR model is acceptable but they should not be removed repeatedly, simply to improve correlation, to prevent final overtrained models. In this work, we employed several criteria for detecting outliers<sup>85</sup> but only Mahalanobis distances, Cook's Distances, standardized and deleted residuals provided atypical results.

**Bond contributions.** One of the greatest advantages of the TOPS-MODE approach, over other traditional QSAR methods, stems from its sub-structural nature. This means that one can transform the QSAR model into a bond additive scheme, and thus describe the biological activity as a sum of bond contributions related to different structural fragments of the molecules. Moreover, one can detect the fragments on a given molecule that contribute positively or negatively to the underlying activity and forward an interpretation of their effects in terms of physico-chemical properties.

Bond contributions are based on the local spectral moments, which in turn are defined as the diagonal entries of the different powers of the weighted  $E$  matrix:

$$\mu_k^T(i) = b_{ii}(T)^k$$

In this equation,  $\mu_k^T(i)$  stands for the  $k$ -th local spectral moment of the bond  $i$ ,  $b_{ii}(T)$  for the diagonal entries of the weighted  $E$  matrix, and  $T$  for the type of bond weight (H, PSA, Dip, vdW, *etc.*). For a given molecule, one can substitute the values of the local spectral moments computed by the previously formulae into the equation below, and thus gather the total contribution to the toxicity of its different bonds:

$$P = a_0 + \sum_k a_k \mu_k^T$$

One should remark here that, since the activity modeled is expressed as  $-\log EC_{50}$ , positive bond contributions decrease the  $EC_{50}$  value and increase the cytotoxicity activity and *vice versa*.

## Acknowledgements

We are grateful to Dr A Vaamonde Liste for his advice in the statistical analysis of data and to Sabela García Oro for her technical assistance.

## References

- 1 H. Zhao, *Chem. Eng. Commun.*, 2006, **193**, 1660–1677.
- 2 D. Zhao, Y. Liao and Z. Zhang, *Clean*, 2007, **35**, 42–48.
- 3 G. A. Baker, S. N. Baker, S. Pandey and F. V. Bright, *Analyst*, 2005, **130**, 800–808.
- 4 C. M. Gordon, *Appl. Catal., A*, 2001, **222**, 101–117.
- 5 N. Jain, A. Kumar, S. Chauhan and S. M. S. Chauhan, *Tetrahedron*, 2005, **61**, 1015–1060.
- 6 P. Kubisa, *Prog. Polym. Sci.*, 2004, **29**, 3–12.
- 7 F. Endres, *ChemPhysChem*, 2002, **3**, 144–154.
- 8 H. Zhao, X. Shuqian and M. Peisheng, *J. Chem. Technol. Biotechnol.*, 2005, **80**, 1089–1096.
- 9 J. Pernak, K. Sobaszekiewicz and I. Mirska, *Green Chem.*, 2003, **5**, 52–56.
- 10 J. Pernak, I. Goc and I. Mirska, *Green Chem.*, 2004, **6**, 323–329.
- 11 J. Ranke, K. Molter, F. Stock, U. Bottin-Weber, J. Poczobutt, J. Hoffmann, B. Ondruschka, J. Filser and B. Jastorff, *Ecotoxicol. Environ. Saf.*, 2004, **58**, 396–404.
- 12 M. Matsumoto, K. Mochiduki and K. Kondo, *J. Biosci. Bioeng.*, 2004, **98**, 344–347.
- 13 J. Cieniecka-Rosonkiewicz, J. Pernak, A. Kubis-Feder, A. Ramani, R. J. and K. R. Seddon, *Green Chem.*, 2005, **7**, 855–862.
- 14 M. T. García, N. Gathergood and P. J. Scammells, *Green Chem.*, 2005, **7**, 9–14.
- 15 K. M. Docherty and C. F. J. Kulpa, *Green Chem.*, 2005, **7**, 185–189.
- 16 D. J. Couling, R. J. Bernot, K. M. Docherty, J. K. Dixon and E. J. Maginn, *Green Chem.*, 2006, **8**, 82–90.



- 17 A. Latala, P. Stepnowski, M. Nedzi and W. Mroziak, *Aquat. Toxicol.*, 2005, **73**, 91–98.
- 18 C. W. Cho, T. P. T. Pham, Y. C. Jeon, K. Vijayaraghavan, W. S. Choe and Y. S. Yun, *Chemosphere*, 2007, **69**, 1003–1007.
- 19 R. P. Swatloski, J. D. Holbrey, S. B. Memon, G. A. Caldwell, K. A. Caldwell and R. D. Rogers, *Chem. Commun.*, 2004, 668–669.
- 20 R. J. Bernot, M. A. Brueseke, M. A. Evans-White and G. A. Lamberti, *Environ. Toxicol. Chem.*, 2005, **24**, 87–92.
- 21 R. J. Bernot, E. E. Kennedy and G. A. Lamberti, *Environ. Toxicol. Chem.*, 2005, **24**, 1759–1765.
- 22 S. Wells and V. T. Coombe, *Org. Process Res. Dev.*, 2006, **10**, 794–798.
- 23 P. Nockemann, B. Thijs, K. Drieska, M. Janssen, H. Hecke, L. Meervelt, S. Kossmann, B. Kirchner and K. Binnemans, *J. Phys. Chem. B*, 2007, **111**, 5254–5263.
- 24 C. Pretti, D. Chiappe, M. Pieraccini, F. Gregori, G. Abramo, F. Monni and L. Intorre, *Green Chem.*, 2006, **8**, 238–240.
- 25 F. Stock, J. Hoffmann, J. Ranke, R. Störmann, B. Ondruschka and B. Jastorff, *Green Chem.*, 2004, **6**, 286–290.
- 26 B. Jastorff, K. Jastorff, P. Mölter, U. Behrend, J. Bottin-Weber, A. Filser, B. Heimers, J. Ondruschka, M. Ranke, H. Schaefer, A. Schröder, P. Stark, F. Stepnowski, R. Stock, S. Störmann, U. Stolte, S. Welz-Biermann, H. Ziegert and J. Thöming, *Green Chem.*, 2005, **7**, 362–372.
- 27 P. Balczewski, B. Bachowska, T. Bialas, R. Biczak, W. M. Wiczorek and A. Balinska, *J. Agric. Food Chem.*, 2007, **55**, 1881–1892.
- 28 J. Ranke, M. Cox, A. Müller, C. Schmidt and D. Beyersmann, *Toxicol. Environ. Chem.*, 2006, **8**, 273–285.
- 29 J. Ranke, A. Müller, U. Bottin-Weber, F. Stock, S. Stolte, J. Arning, R. Stormann and B. Jastorff, *Ecotoxicol. Environ. Saf.*, 2007, **67**, 430–438.
- 30 T. D. Landry, K. Brooks, D. Poche and M. Woolhiser, *Bull. Environ. Contam. Toxicol.*, 2005, **74**, 559–565.
- 31 A. C. Skladanowski, P. Stepnowski, K. Kleszczynski and B. Dmochowska, *Environ. Toxicol. Pharmacol.*, 2005, **19**, 291–296.
- 32 P. Stepnowski, A. C. Skladanowski, A. Ludwiczak and E. LacyD-ska, *Hum. Exp. Toxicol.*, 2004, **23**, 513–517.
- 33 E. A. Hassoun, M. Abraham, V. Kini, M. Al-Ghafri and A. Abushaban, *Res. Commun. Pharmacol. Toxicol.*, 2002, **7**, 23–31.
- 34 R. F. M. Frade, A. Matias, L. C. Branco, C. A. M. Afonso and C. M. M. Duarte, *Green Chem.*, 2007, **9**, 873–877.
- 35 B. J. Blauboer, M. Balls, M. Barratt, S. Casati, S. Coecke, M. K. Mohamed, J. Moore, D. Rall, K. R. Smith, R. Tennant, B. A. Schwetz, W. S. Stokes and M. Younes, *Environ. Health Perspect.*, 1998, **106**, 413–418.
- 36 G. Malich, B. Markovic and C. Winder, *Toxicology*, 1997, **124**, 179–192.
- 37 M. P. González, C. Terán, M. Teijeira and A. H. Morales, *Curr. Med. Chem.*, 2006, **13**, 2253–2266.
- 38 M. P. González and A. H. Morales, *J. Comput. Aided Mol. Des.*, 2003, **17**, 665–672.
- 39 M. P. González and C. Teran, *Bioorg. Med. Chem.*, 2004, **12**, 2985–2993.
- 40 M. P. González and C. Teran, *Bioorg. Med. Chem. Lett.*, 2004, **14**, 3077–3079.
- 41 A. H. Morales, M. P. González and J. R. Briones, *Polymer*, 2004, **45**, 2045–2050.
- 42 M. P. González, C. Terán, Y. Fall, L. C. Diaz and A. H. Morales, *Polymer*, 2005, **46**, 2783–2790.
- 43 A. H. Morales, P. R. Duchowicz, M. A. Cabrera, E. A. Castro, N. Cordeiro and M. P. González, *Chemom. Intell. Lab. Syst.*, 2006, **81**, 180–187.
- 44 E. Molina, H. G. Diaz, M. P. González, E. Rodriguez and E. Uriarte, *J. Chem. Inf. Comput. Sci.*, 2004, **44**, 515–521.
- 45 M. P. González, L. C. Dias, A. H. Morales, Y. M. Rodriguez, L. G. de Oliveira, L. T. Gomez and H. G. Diaz, *Bioorg. Med. Chem.*, 2004, **12**, 4467–4475.
- 46 M. P. González, C. Teran, M. Teijeira and P. Besada, *Bioorg. Med. Chem. Lett.*, 2005, **15**, 2641–2645.
- 47 M. P. González, H. G. Diaz, M. A. Cabrera and R. M. Ruiz, *Bioorg. Med. Chem.*, 2004, **12**, 735–744.
- 48 M. P. González, A. H. Morales and M. A. Cabrera, *Bioorg. Med. Chem.*, 2005, **13**, 1775–1781.
- 49 A. B. Pereiro, E. Tojo, A. Rodriguez, J. Canosa and J. Tojo, *Green Chem.*, 2006, **8**, 307–310.
- 50 E. Gómez, B. González, A. Domínguez, E. Tojo and J. Tojo, *J. Chem. Eng. Data*, 2006, **51**, 696–701.
- 51 A. E. Visser, R. P. Swatloski and R. D. Rogers, *Green Chem.*, 2000, **2**, 1–4.
- 52 J. G. Huddleston, A. E. Visser, R. Matthew, H. D. Willauer, G. A. Broker and R. D. Rogers, *Green Chem.*, 2001, **3**, 156–164.
- 53 A. B. Pereiro, F. Santamarta, E. Tojo, A. Rodriguez and J. Tojo, *J. Chem. Eng. Data*, 2006, **51**, 952–954.
- 54 J. D. Holbrey, W. Matthew, R. P. Swatloski, G. A. Broker, W. R. Pitner, K. R. Seddon and R. D. Rogers, *Green Chem.*, 2002, **4**, 407–413.
- 55 E. Tojo and P. Verdía, in *Chemistry and Sustainable Development 6th ANQUE International Congress of Chemistry*, ANQUE, Madrid, 2006, pp. T2–101.
- 56 E. Gómez, B. González, N. Calvar, E. Tojo and A. Domínguez, *J. Chem. Eng. Data*, 2006, **51**, 2096–2102.
- 57 A. Beyaz, W. S. Oh and V. P. Reddy, *Colloids Surf., B*, 2004, **36**, 71–74.
- 58 E. Tojo, F. Santamarta, J. Tojo and E. Gómez, in *1st International Congress on Ionic Liquids*, DEHEMA Salzburg, 2005, p. 94.
- 59 M. P. González, A. H. Morales and Y. R. Morales, *Internet Electron. J. Mol. Des.*, 2004, **3**, 750–750.
- 60 M. P. González, H. Gonzalez Diaz, R. Molina Ruiz, M. A. Cabrera and R. Ramos de Armas, *J. Chem. Inf. Comput. Sci.*, 2003, **43**, 1192–1199.
- 61 M. P. González, A. H. Morales and I. G. Collado, *Mol. Divers*, 2006, **10**, 109–118.
- 62 D. M. Hawkins, *J. Chem. Inf. Comput. Sci.*, 2004, **44**, 1–12.
- 63 A. Golbraikh and A. Tropsha, *J. Mol. Graphics Modell.*, 2002, **20**, 269–276.
- 64 J. G. Topliss and R. P. Edwards, *J. Med. Chem.*, 1979, **22**, 1238–1244.
- 65 A. H. Morales, M. A. Cabrera, R. D. Combes and P. González M, *Curr. Computer-Aided Drug Des.*, 2005, **1**, 237–255.
- 66 A. H. Morales, M. A. Cabrera Perez, M. P. González, R. M. Ruiz and H. Gonzalez-Diaz, *Bioorg. Med. Chem.*, 2005, **13**, 2477–2488.
- 67 A. H. Morales, M. P. González, D. S. C. MN and M. A. Perez, *Toxicol. Appl. Pharmacol.*, 2007, **221**, 189–202.
- 68 A. H. Morales, M. A. Perez, R. D. Combes and M. P. González, *Toxicology*, 2006, **220**, 51–62.
- 69 R. Benigni, *Chem. Rev.*, 2005, **105**, 1767–1800.
- 70 S. Stolte, J. Arning, U. Bottin-Weber, M. Matzke, F. Stock, K. Thiele, M. Uerdingen, U. Welz-Biermann, B. Jastorff and J. Ranke, *Green Chem.*, 2006, **8**, 621–629.
- 71 T. Mosmann, *J. Immunol. Methods*, 1983, **65**, 55–63.
- 72 M. P. González, L. Dias and A. H. Morales, *Polymer*, 2004, **45**, 5353–5359.
- 73 M. P. González, A. H. Morales and H. Gonzalez-Diaz, *Polymer*, 2004, **45**, 2073–2079.
- 74 M. P. González, A. H. Morales, R. Molina and J. R. García, *Polymer*, 2004, **45**, 2773–2779.
- 75 M. P. González and C. Teran, *Bull. Math. Biol.*, 2004, **66**, 907–920.
- 76 E. Estrada, *J. Chem. Inf. Comput. Sci.*, 1996, **36**, 844–849.
- 77 E. Estrada, *J. Chem. Inf. Comput. Sci.*, 1997, **37**, 320–328.
- 78 E. Estrada, *J. Chem. Inf. Comput. Sci.*, 1995, **35**, 31–33.
- 79 E. Estrada, E. Uriarte, Y. Gutierrez and H. Gonzalez, *SAR QSAR Environ. Res.*, 2003, **14**, 145–163.
- 80 Y. Gutiérrez and E. Estrada, *Modes Lab version 1.0b*, Universidad de Santiago de Compostela, España, 2002.
- 81 D. Weininger, *J. Chem. Inf. Comput. Sci.*, 1988, **28**, 31–36.
- 82 D. Weininger, *J. Chem. Inf. Comput. Sci.*, 1990, **30**, 237–243.
- 83 D. Weininger, A. Weininger and J. L. Weininger, *J. Chem. Inf. Comput. Sci.*, 1989, **29**, 97–101.
- 84 R. Todeschini, and V. Consonni, *Handbook of Molecular Descriptors*, Wiley VCH, Weinheim, Germany, 2000.
- 85 M. Pestana and J. Gageiro, *Análise de dados para Ciências Sociais. A Complementaridade do SPSS*, Edições Silabo, Lisboa, 2000.



# Microwave-assisted synthesis of oligothiophene semiconductors in aqueous media using silica and chitosan supported Pd catalysts

Silvia Alesi,<sup>\*a</sup> Francesca Di Maria,<sup>a</sup> Manuela Melucci,<sup>a</sup> Duncan J. Macquarrie,<sup>b</sup> Rafael Luque<sup>b</sup> and Giovanna Barbarella<sup>a</sup>

Received 5th December 2007, Accepted 7th February 2008

First published as an Advance Article on the web 29th February 2008

DOI: 10.1039/b718776a

We report an innovative heterogeneous procedure for the preparation of highly pure thiophene oligomers *via* microwave-assisted Pd catalysis by using silica- and chitosan-supported Pd complexes. This approach is very efficient and greener than the existing homogeneous methodology as it combines a very efficient reaction with improved catalyst separation. Our new, efficient and cleaner microwave approach smoothly afforded the preparation of coupled products in high yields (up to 87% isolated yield, 30–100 min). Thieryl iodides or activated bromides were employed as starting materials and KF as base. The microwave reaction was carried out in aqueous ethanol. The heterogeneous catalyst can be easily removed from the reaction mixture by filtration and reused in consecutive reactions (up to 4 times).

## 1. Introduction

Oligo- and polythiophenes are semiconductor and fluorescent compounds widely used as active organic materials<sup>1</sup> in electronic and optoelectronic devices including field effect transistors (FETs),<sup>2</sup> light-emitting diodes (LEDs),<sup>3</sup> and photovoltaic cells (PVD).<sup>4</sup> They also act as very sensitive fluorescence sensors for biodiagnostic purposes.<sup>5</sup> The extensive use of such materials as both (opto)electronics and biosensors, requires highly effective and 'user friendly' synthetic approaches for their preparation.

The most widely employed strategy adopted for the preparation of such oligothiophene semiconductors is an organometallic approach,<sup>6</sup> taking advantage of accessible building blocks and Pd or Ni catalysts. Such an approach usually consists of cross-coupling reactions between halogenated thienyls and metalated counterparts in the presence of soluble palladium or nickel complexes (homogeneous catalysis). However, the use of organometallic catalysts in the process presents a number of drawbacks including the presence of by-products either originated by the demetalation or dehalogenation of the starting materials or by homo-coupling or boron-halogen exchange side reactions, as well as the presence of catalyst residues. Such impurities may alter the film deposition processes and therefore the morphology, conductivity and performance of the device prepared. As a consequence, preliminary expensive purification techniques including vacuum sublimation are often required for their successful applications.

In previous work, we demonstrated that the use of microwave-assisted Suzuki-coupling methodologies for the preparation of substituted and unsubstituted oligothiophenes led to higher

reaction rates and minimized the formation of undesired by-products.<sup>7a,b</sup> Along these lines, we envisaged that combining microwave assistance with heterogeneous Pd catalysis<sup>8</sup> could be an interesting way to synthesize highly pure, metal free, thiophene based materials in a very short time.

Suzuki–Miyaura heterogeneous protocols<sup>9</sup> have been reported for the synthesis of biphenyl systems employing palladium supported on various materials including carbon,<sup>10,11</sup> metal oxides, ceramics (perovskites), porous aluminosilicates, as well as on polymers<sup>12</sup> and biopolymers,<sup>13,14</sup> the latter ones offering the advantages of being renewable, biodegradable and having low toxicity.

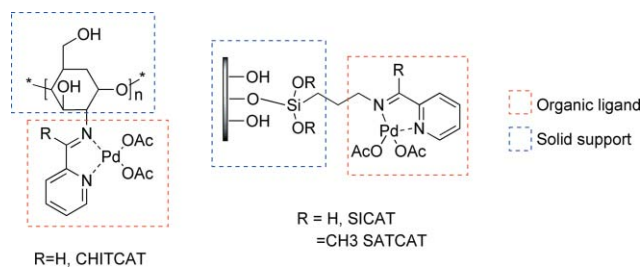
Chitosan and silica based Pd complexes have been demonstrated to be very effective under a wide range of conditions in the Suzuki and Heck couplings, being reusable up to 10 times.<sup>15–17</sup> Such catalysts, comprising bidentate organic ligands, grafted onto the solid support, that complex the active palladium salts, exhibited excellent stability (chemical and thermal), high surface areas, good accessibility and chemical versatility. Moreover, chitosan is a water-tolerant support that will potentially allow reactions to be carried out in aqueous media, and has major advantages in that it can be formed into fibres, films, attached to reactor walls, *etc.* making it ideal for incorporation in different reactor designs (continuous/intensive, *etc.*). On the other hand, silicas can be easily prepared and allow for the robust attachment of organic functionalities and control over their surface chemistries.

Herein, we report for the first time the preparation of thiophene-based materials using a microwave assisted Suzuki coupling methodology using selective and stable chitosan and silica supported palladium complexes (Scheme 1) in aqueous ethanol.

Substituted oligomers containing fused heterocycles into the aromatic backbone can also be prepared in high yields and with a good level of purity in a short period of time, without the need for further purification. Oligomers containing up to six thiophene units have been successfully prepared using this approach.

<sup>a</sup>Consiglio Nazionale Ricerche, CNR-ISOF, Via P. Gobetti 101, I-40129, Bologna, Italy. E-mail: [silvia.alesi@isof.cnr.it](mailto:silvia.alesi@isof.cnr.it); Fax: +39 051 6398349; Tel: +39 051 6398284

<sup>b</sup>Green Chemistry Centre of Excellence, Department of Chemistry, University of York, Heslington, York, UK YO10 5DD. E-mail: [rla3@york.ac.uk](mailto:rla3@york.ac.uk); Fax: +44 1904 432705; Tel: +44 1904 434456



**Scheme 1** Structures of the catalysts used in the present investigation. CHITCAT = chitosan supported Pd complex; SICAT = silica supported Pd complex **1** (R = H); SATCAT = silica supported Pd complex **2** (R = Me).

The proposed protocol can be used as a standard protocol irrespective of the size and substitution of the thienyl, compared to homogeneous Suzuki methodologies which usually require an optimization of the reaction conditions for each substrate.<sup>7a,b</sup>

## 2. Experimental

### 2.1. Materials and methods

All the reactions were carried out under air. All commercially available reagents and solvents were used as purchased without further purification. **10**,<sup>18</sup> **12**<sup>7b</sup> and **15**<sup>19</sup> were prepared by methods described previously. Microwave experiments were carried out in a CEM-DISCOVER model with PC control and monitored by sampling aliquots of reaction mixture that were subsequently analysed by GC/GC-MS using an Agilent 6890 N GC model equipped, with a 7683B series autosampler, fitted with a DB-5 capillary column and an FID detector. Experiments were conducted on a closed vessel (pressure controlled) under continuous stirring. The microwave method was generally power controlled (100 W maximum power input) where the samples were irradiated with the required power output (settings at maximum power) to achieve the desired temperature (80–130 °C). Proton-decoupled <sup>13</sup>C NMR spectra were obtained on a Jeol 400 spectrometer, operating at 100.580 MHz in CDCl<sub>3</sub>. Typically 256 scans were collected for each sample. Chemical shifts were calibrated using the internal CDCl<sub>3</sub> resonance. <sup>1</sup>H NMR spectra were obtained on a Jeol 400 spectrometer, operating at 400.13 MHz in CDCl<sub>3</sub> solvent. Typically 64 scans were collected for each sample. Chemical shifts were calibrated using the internal SiMe<sub>4</sub> resonance.

### 2.2. Synthesis of the catalysts

Supported Pd-catalysts used in the present work were prepared following the already reported procedures,<sup>15–17</sup> obtaining a Pd loading of about 0.5 and 0.2 mmol g<sup>-1</sup> for CHITCAT and SATCAT, respectively, as confirmed by ICP. Diffuse reflectance IR analysis of the materials showed a diagnostic peak at 1638 cm<sup>-1</sup> due to the formation of the pyridylimine unit.

### 2.3. General procedure for CHITCAT and SATCAT catalyzed Suzuki reaction

The microwave oven reactor was charged with halothienyl-derivative or dihalothienyl-derivative (0.2 mmol), dodecane (0.2 mmol), mono- or bithienylboronic derivatives (0.6 mmol

for halides, 1.2 mmol for dihalides), Pd catalyst CHITCAT or SATCAT (0.05 mmol for monohalides and 0.1 mmol for dihalides), KF (0.6 mmol for monohalides and 1.2 mmol for dihalides) and of EtOH–water (1 : 1) (2 mL) for CHITCAT catalyzed procedure or of isopropanol (2 mL) for SATCAT catalyzed one. After 30–100 min of microwave irradiation, a TLC on silica gel showed the absence of starting materials. The solvent was removed, the solid crude was dissolved in CH<sub>2</sub>Cl<sub>2</sub> (Table 4, entries 1, 2, 3; Table 5, entry 1) or in hot toluene (Table 4, entries 4, 5, 6, 7, 8; Table 5, entries 2, 3, 4) and the catalyst filtered off. Then, the organic phase was washed with water (2 × 15 ml), dried on Na<sub>2</sub>SO<sub>4</sub> and the solvent evaporated under vacuum. The shorter oligomers (Table 4, entries 1, 2, 3; Table 5, entry 1) were purified by flash chromatography, while the longer oligomers (Table 4, entries 4, 5, 6, 7, 8; Table 5, entries 2, 3, 4) were purified by washing steps and crystallization.

**2,2':5'2''-terthiophene 7<sup>a</sup>**. Table 4, entry 1, yield 87%; yellow solid, mp 93–95 °C. Flash chromatography: petroleum ether (40–60) purum.  $\delta_{\text{H}}$  (270 MHz, CDCl<sub>3</sub>, Me<sub>4</sub>Si) 7.22 (2H, d, *J* 4.8), 7.18 (2H, d, *J* 3.8 H), 7.08 (2H, s), 7.03 (2H, dd, *J* 3.8);  $\delta_{\text{C}}$  (67.93 MHz, CDCl<sub>3</sub>, Me<sub>4</sub>Si) 137.081, 136.148, 127.851, 124.444, 124.276, 123.650; *m/z* 248.

**2,2':5'2'':5''2'''-quaterthiophene 9<sup>a</sup>**. Table 4, entry 3, yield 83%; yellow solid, mp 210–212 °C. Flash chromatography: petroleum ether (40–60):EtOAc/99:1.  $\delta_{\text{H}}$  (400 MHz, DMSO-d<sub>6</sub>, Me<sub>4</sub>Si) 7.529 (2H, d, *J* 4.8), 7.341 (2H, d, *J* 4.0), 7.297 (2H, d, *J* 3.6), 7.272 (2H, d, *J* 3.6), 7.098 (2H, dd, *J* 3.6); *m/z* 330.

**3',4'-dimethyl-2,2':5'2'':5''2'''-quaterthiophene 11<sup>18</sup>**. Table 4, entry 4, yield 77%; yellow oil. Flash chromatography: petroleum ether (40–60):EtOAc/99:1.  $\delta_{\text{H}}$  (200 MHz, CDCl<sub>3</sub>, Me<sub>4</sub>Si) 7.21 (2H, d, *J* 5.2), 7.16 (2H, d, *J* 3.4), 7.02 (2H, s), 7.01 (t, *J*<sub>3</sub> = 5.0 Hz, 2H).  $\delta_{\text{C}}$  (50 MHz, CDCl<sub>3</sub>, Me<sub>4</sub>Si) 137.33, 137.20, 136.66, 128.10, 127.82, 126.76, 124.39, 123.55, 14.97; *m/z* 358.

**2,2':5'2'':5''2''':5'''2''''-quinquethiophene 13<sup>20</sup>**. Table 4, entry 5, yield 82%; orange solid, mp 251 °C. The crude product was washed with petroleum ether and diethyl ether and finally crystallized from toluene.  $\delta_{\text{H}}$  (400 MHz, DMSO-d<sub>6</sub>, Me<sub>4</sub>Si) 7.51 (2H, d, *J* 5.2), 7.33 (2H, d, *J* 2.8), 7.30 (2H, s), 7.29 (2H, d, *J* 3.6), 7.26 (2H, d, *J* 3.2), 7.10 (2H, dd, *J* 3.2); *m/z* 412.

**3''',4'' - dimethyl - 2,2':5'2'':5''2''':5'''2'''' - hexathiophene 14<sup>19</sup>**. Table 4, entry 6, 7, yield 65%; deep red solid, mp 164–166 °C. The crude product was washed with petroleum ether and diethyl ether and finally CH<sub>2</sub>Cl<sub>2</sub>.  $\delta_{\text{H}}$  (400 MHz, CDCl<sub>3</sub>, Me<sub>4</sub>Si) 7.226 (2H, d, *J* 4.8), 7.182 (2H, d, *J* 3.6), 7.084 (2H, d, *J* 4.4), 7.064 (2H, d, *J* 3.6), 7.028 (2H, dd, *J* 3.2), 7.020 (2H, s), 7.227 (6H, s).  $\delta_{\text{C}}$  (100 MHz, CDCl<sub>3</sub>, Me<sub>4</sub>Si) 137.632, 137.288, 136.527, 136.442, 136.076, 128.347, 128.045, 126.885, 124.665, 124.529, 124.334, 123.862, 15.208; *m/z* 522.

**$\alpha,\omega$ -dihexylhexathiophene 16<sup>21</sup>**. Table 4, entry 8, yield 69%, orange powder, mp: 285–288 °C. The crude product was washed with petroleum ether and diethyl ether and finally CH<sub>2</sub>Cl<sub>2</sub>;  $\nu_{\text{max}}$  (film)/cm<sup>-1</sup> 3085 3060, 2956, 2922, 2873, 2855, 1748, 1596, 1538, 1505, 1466, 1442, 1377, 1221, 1206, 1071, 872, 839, 794, 723, 462; *m/z* 664.

**4,7-Di-2-thienyl-2,1,3-benzothiadiazole 18<sup>22</sup>.** Table 5, entry 1, yield 75%; red solid, mp 123–125 °C. Flash chromatography: petroleum ether (40–60):EtOAc/97:3.  $\delta_{\text{H}}$  (270 MHz, CDCl<sub>3</sub>, Me<sub>4</sub>Si) 8.11 (2H, d, *J* 3.7), 7.86 (2H, s), 7.59 (2H, d, *J* 5.2), 7.21 (2H, t, *J* 4.0);  $\delta_{\text{C}}$  (67.93 MHz, CDCl<sub>3</sub>, Me<sub>4</sub>Si) 152.60, 139.33, 127.99, 127.469, 126.78, 125.96, 125.743; *m/z* 300.

**4,7-Bis(-2,2'-dithiophenyl-5-yl)benzo[1,2,5]-thiadiazole 19.** Table 5, entry 2, yield 47%; violet solid, mp 163–170 °C. The crude product was washed with petroleum ether and diethyl ether and finally CH<sub>2</sub>Cl<sub>2</sub>. MS: 464;  $\delta_{\text{H}}$  (400 MHz, DMSO-*d*<sub>6</sub>, Me<sub>4</sub>Si) 8.11 (2H, d, *J* 3.6), 8.105 (s, 2H), 7.55 (2H, d, *J* 5.2), 7.437–7.434 (4H, m), 7.134 (2H, dd, *J* 3.6).  $\delta_{\text{C}}$  (100 MHz, DMSO-*d*<sub>6</sub>, Me<sub>4</sub>Si) 152.163, 139.230, 137.700, 136.960, 129.273, 129.065, 126.714, 126.149, 125.409, 125.205, 125.179; *m/z* 464.

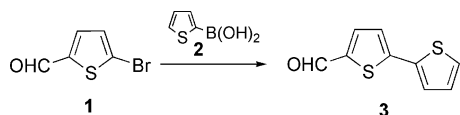
**2,2'-thiene-2,5-diylbisthieno [3,2-*b*]thiophene 20.** Table 5, entry 3, yield 81%; yellow solid, mp 164–166 °C. The crude product was washed with petroleum ether, CH<sub>2</sub>Cl<sub>2</sub> and finally crystallized from toluene.  $\delta_{\text{H}}$  (400 MHz, CDCl<sub>3</sub>, Me<sub>4</sub>Si) 7.37 (2H, d, *J* 4.0), 7.37 (2H, s), 7.23 (2H, d, *J* 5.2), 7.13 (2H, s).  $\delta_{\text{C}}$  (100 MHz, CDCl<sub>3</sub>, Me<sub>4</sub>Si) 139.810, 138.675, 138.161, 136.834, 127.337, 124.531, 119.467, 115.858; *m/z* 360.

**3,3'-dimethyl-5,5'-dithieno [3,2-*b*]thien-2-yl-2,2'-bithiophene 21.** Table 5, entry 4, yield 65%; orange-red solid, mp 182–186 °C. The crude product was washed with petroleum ether and diethyl ether and finally CH<sub>2</sub>Cl<sub>2</sub>.  $\delta_{\text{H}}$  (400 MHz, CDCl<sub>3</sub>, Me<sub>4</sub>Si) 7.36 (2H, d, *J* 5.6), 7.34 (2H, d, *J*<sub>5</sub> 0.8), 7.23 (2H, dd, *J*<sub>3</sub> 5.2, *J*<sub>5</sub> 0.4), 7.06 (2H, s), 2.24 (6H, s).  $\delta_{\text{C}}$  (100 MHz, CDCl<sub>3</sub>, Me<sub>4</sub>Si) 139.77, 138.88, 138.06, 137.52, 137.00, 128.40, 127.12, 126.91, 119.46, 115.65; *m/z* 470.

### 3. Results and discussion

#### 3.1. Optimization of the model reaction

The reaction optimization was performed on two commercially available substrates, namely 5-bromo-2-thiophenecarboxaldehyde **1** and 2-thienylboronic acid derivative **2** (Scheme 2). Supported palladium catalysts were tested under both conventional heating and microwave-assisted conditions. Data are



**Scheme 2** Model reaction between 5-bromo-2-thiophenecarboxaldehyde and 2-thienylboronic acid.

**Table 1** Catalytic performance of different supported Pd complexes in the model reaction (Scheme 2)

Entry	Base	Catalyst	Solvent	MW conditions	<b>3</b> Conversion (%) <sup>b</sup>
1	KF	SICAT	EtOH–H <sub>2</sub> O (1 : 1)	100 W, 60 min, 80 °C	87
2 <sup>a</sup>	KF	CHITCAT	EtOH–H <sub>2</sub> O (1 : 1)	100 W, 2 min, 130 °C <sup>d</sup>	>99
3 <sup>a</sup>	KF	CHITCAT	toluene	100 W, 60 min, 130 °C	8
4 <sup>a</sup>	KF	SATCAT	EtOH–H <sub>2</sub> O (1 : 1)	100 W, 60 min, 80 °C	82
5 <sup>c</sup>	KF	SATCAT	isopropanol	100 W, 60 min, 80 °C <sup>d</sup>	96
6	KF	SATCAT	toluene	220 W, 60 min, 80 °C	20

<sup>a</sup> Carried out with simultaneous cooling. <sup>b</sup> GC conversion. <sup>c</sup> Higher power values did not remarkably improve the reaction conversion. <sup>d</sup> The pressure measured was about 80 and 20 psi for entries 2 and 5, respectively.

summarized in Table 1. Previous reported studies on the Suzuki cross-coupling of thienyl derivatives proved KF was a very suitable base for these systems.<sup>23</sup>

The use of CHITCAT as catalyst and KF as the base in aqueous ethanol (1 : 1) afforded a complete conversion of the starting materials to the coupling product **3** in only 2 min of microwave irradiation at 130 °C (Table 1, entry 2). The same reaction carried out under conventional heating provided a poor 55% conversion after 48 h.

The use of an aqueous environment was also found to be particularly advantageous for an optimum catalytic performance with respect to the use of toluene or other organic compounds as solvents. This can be ascribed to the different solubility of KF in toluene and alcoholic solvents as well as to the more efficient absorption of MW from polar solvents. Medium to high microwave absorbing solvents, including EtOH, isopropanol and water, may allow a more efficient internal heating compared to microwave-transparent solvents (toluene) usually employed in heterogeneous Suzuki reactions.<sup>15–17</sup>

Silica supported palladium catalysts (SICAT and SATCAT) required lower reaction temperatures (80 °C vs 130 °C) but much longer reaction times (60 min) compared to chitosan in order to achieve comparable conversion values.

Clearly, the choice of the catalyst has to take into account several factors including the thermal stability of the boronic-substrates and the size of the target oligomer. Chitosan will possibly be more suitable for stable and smaller substrates compared to silica, in which the porous structure will surely be an attractive feature in reactions with larger molecules.

A hot filtration test (HF) was performed to prove the truly heterogeneous nature of our catalytic reaction (entries 2 and 4, Table 1).<sup>24</sup> The hot reaction mixture (typically less than half way through completion) was filtered off and the liquid filtrate and the solid were recovered separately. Fresh substrates were added both to the liquid filtrate and to the solid and another reaction (under the same conditions) was conducted. The results of the second reuse of CHITCAT are included in Fig. 1. The catalyst was filtered off after 60 s of microwave irradiation (~30% conversion). The reaction mixture without catalyst was then further microwaved for 30 additional minutes and finally quenched. No changes in conversion were observed, excluding the presence of a substantial concentration of palladium leached species in solution. The Pd content in solution was determined using ICP MS. 1.8 ppm Pd was found, confirming that the Pd leaching in the systems was almost negligible.

The catalyst reusability was also investigated under the optimized conditions. The catalyst was filtered off after each reaction

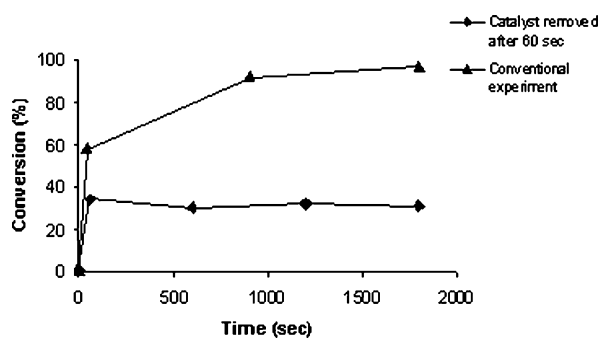


**Fig. 1** Hot filtration test. Effect of removing the chitosan supported palladium catalyst from the second cycle reaction of 2-thienylboronic acid and the 5-bromo-2-thiophenecarboxaldehyde.

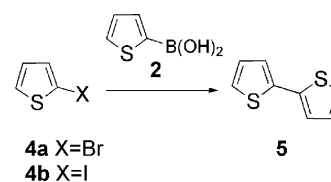
run, washed with aqueous methanol and pure methanol, dried at 90 °C and subsequently reused in another catalytic cycle. Despite an increase in the time of reaction required for complete conversion, the catalysts were reusable up to 4 times preserving more than 95% of the initial catalytic activity (Table 2).<sup>16</sup> The observed slight reduction in catalytic activity with recycling probably can be due to a partial blockage or deactivation of the active sites of the catalyst with the salts and/or by-products from the reaction.

### 3.2. Extension to other substrates

The optimised conditions based on the use of the CHITCAT and SATCAT materials were then extended to various thienyl-based substrates. Several parameters including the nature and number of halogen atoms, functionalization and size of the starting building blocks were investigated. Data are summarised in Tables 3–5.

Iodo-derivatives were found to be more effective than bromo-derivatives in the preparation of bithiophene (Scheme 3), irrespective of the conditions employed (solvent and/or catalyst). Therefore, only thienyl iodides were employed for the synthesis of longer oligomers.

The methodology was then further extended to the preparation of larger ( $\alpha$ - $\beta$  alkyl) substituted oligomers. Results are included in Table 4.



**Scheme 3** Suzuki reaction for the preparation of bithiophene (**5**) from a range of halo-thiophenes.

Terthiophene (**7**) is a useful building block for the preparation of thiophene-based oligomers and polymers.<sup>25</sup> Many synthetic routes to  $\alpha$ -terthienyl have been reported. A previously reported solvent-free microwave assisted Suzuki coupling, provided a maximum isolated yield of 60% starting from 2,5-dibromothiophene<sup>7a</sup>, much lower than that reported in Table 4 starting from the di-iodo derivative.

Quaterthiophene (T4, **9**) is one of the most investigated thiophene derivatives for its photoluminescence<sup>26</sup> and charge transport properties.<sup>27</sup> Terminal alkyl substituted T4 compounds are also of interest as they exhibit liquid crystalline behaviour and enhanced solubility that make them particularly suitable for solution processing.<sup>28</sup> T4 derivatives are usually prepared by using the bi-directional 1 + 2 + 1 approach consisting in the reaction between two equivalents of boronic or halo-thienyl derivative and one equivalent of the corresponding reaction partner.<sup>18</sup> For the preparation of quaterthiophenes **9** and **11**,<sup>18</sup> we chose the reaction between boronic thienyl derivative **2**, and the bifunctional iodo-dimers **8** and **10** that afforded good yields for both unsubstituted and  $\beta$ -methyl substituted T4 compounds (entries 2, 3 Table 4).

Unsubstituted or functionalised  $\alpha$ -quinque- and hexathiophenes were also prepared. Such systems show high self-assembly capability and good charge transport properties in field effect transistors (FET).<sup>19,20</sup>

Two different strategies were employed and compared for both compounds. Quinquethiophene (T5, **13**) was prepared either by adding two boro-functionalized monomers to the diiodoterthiophene (**12**) (+1 strategy, Fig. 2), or by reacting the diiodothiophene (**6**) with two equivalents of borobithiophene (+2 strategy, Fig. 2).

**Table 2** CHITCAT reusability experiments carried out under microwave irradiation with simultaneous cooling

Cycle	Base	Catalyst	Solvent	MW conditions	<b>3</b> (%)
1st	KF	CHITCAT	EtOH–H <sub>2</sub> O (1 : 1)	100 W, 130 °C, 1 min	>99
2nd	KF	CHITCAT	EtOH–H <sub>2</sub> O (1 : 1)	100 W, 130 °C, 30 min	97
3rd	KF	CHITCAT	EtOH–H <sub>2</sub> O (1 : 1)	100 W, 130 °C, 45 min	98
4th	KF	CHITCAT	EtOH–H <sub>2</sub> O (1 : 1)	100 W, 130 °C, 45 min	95

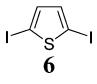
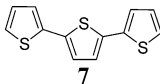
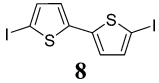
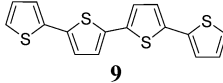
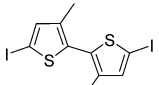
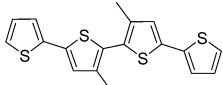
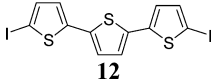
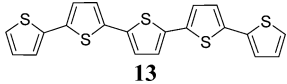
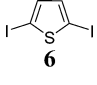
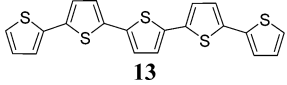
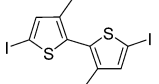
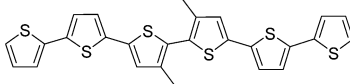
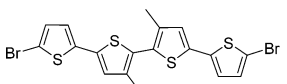
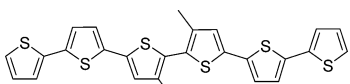
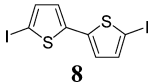
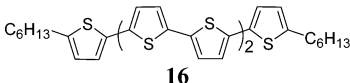
**Table 3** Catalytic performance of various Pd catalysts in the preparation of bithiophene from 2-thienyl bromide and 2-thienyl iodide

Entry	Reagent	Catalyst	Solvent	MW conditions	Yield <b>5</b> (%) <sup>a</sup>
1 <sup>b</sup>	<b>4a</b>	CHITCAT	EtOH–H <sub>2</sub> O (1 : 1)	100 W, 130 °C, 60 min	8
2 <sup>b</sup>	<b>4b</b>	CHITCAT	EtOH–H <sub>2</sub> O (1 : 1)	100 W, 130 °C, 60 min	57
3	<b>4a</b>	SATCAT	isopropanol	100 W, 80 °C, 60 min	36
4	<b>4b</b>	SATCAT	isopropanol	100 W, 80 °C, 60 min	61

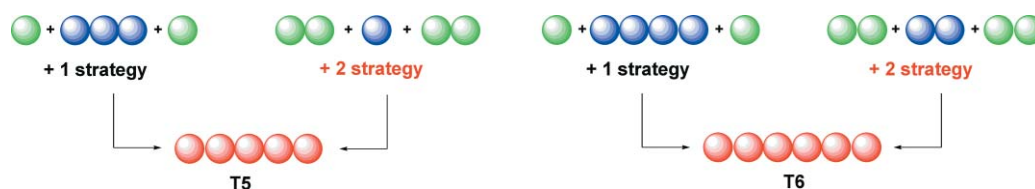
<sup>a</sup> Isolated yield. <sup>b</sup> Carried out with simultaneous cooling.



**Table 4** Preparation of various oligothiophenes derivatives using supported Pd complexes

Entry	Starting material	Product	Catalyst	MW conditions	Yield <sup>b</sup> (%)
1 <sup>a</sup>			CHITCAT	100 W, 30 min, 130 °C	87
2 <sup>a</sup>			CHITCAT	100 W, 100 min, 130 °C	83
3			SATCAT	100 W, 100 min, 80 °C	77
4			CHITCAT	100 W, 100 min, 130 °C	37
5			SATCAT	100 W, 100 min, 80 °C	82
6			SATCAT	100 W, 100 min, 80 °C	65
7 <sup>c</sup>			SATCAT	100 W, 100 min, 80 °C	traces
8			CHITCAT	100 W, 100 min, 130 °C	69

<sup>a</sup> In entry 1, the reaction was carried out with simultaneous cooling. For entry 2 we tried both, with and without simultaneous cooling obtaining similar results (66% after 60 min employing simultaneous cooling). <sup>b</sup> Isolated yield. <sup>c</sup> The dibromo derivative was more soluble than diiododerivative under the reaction conditions.

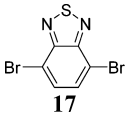
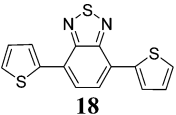
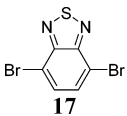
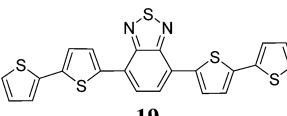
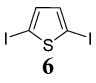
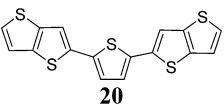
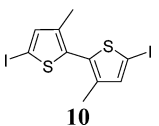
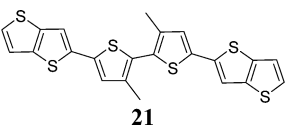
**Fig. 2** Overview of the strategies investigated for the synthesis of T5 and T6 materials.

Similarly, hexathiophene (T6, **14**) was prepared by means of a +2 approach (using the di-iodobithiophene **10**) as well as by the +1 strategy employing di-bromoquaterthiophene **15** as starting material.

The election of the synthetic pathway is usually dependent on many factors including the availability of the starting materials and the formation of by-products such as deborylated thiophenes, homo-coupling and metal-halogen exchange products that have to be removed from the target compounds. The +1 strategy led to by-products easily separated from the reaction

mixture, facilitating the purification of the desired product. However, the starting materials are complex systems, therefore additional synthetic steps are required in order to obtain them. Despite our previous results on homogeneous microwave assisted Suzuki coupling pointing out that the +2 strategy was unfavourable (due to the formation of T4 by-products difficult to remove), it proved to be the most effective for the synthesis of both T5 and T6 oligomers (Table 4, entries 5, 6), as it involves readily available precursors and easily purified products, thus improving the green credentials of the reaction.

**Table 5** Catalytic performance of CHITCAT and SATCAT in the preparation of thiophene based co-oligomers

Entry	Starting material	Product	Catalyst	MW conditions	Yield <sup>a</sup> (%)
1			CHITCAT	100 W, 100 min, 130 °C	75
2 <sup>b</sup>			CHITCAT	100 W, 100 min, 130 °C	47
3 <sup>c</sup>			SATCAT	100 W, 100 min, 80 °C	81
4 <sup>c</sup>			SATCAT	100 W, 100 min, 80 °C	65

<sup>a</sup> Isolated yield. <sup>b</sup> Literature data report 37% yield with a similar compound.<sup>31</sup> <sup>c</sup> The starting material 4,4,5,5-tetramethyl-2-thieno[3,2-*b*]thiophen-2-yl-[1,3,2]dioxaborolane (TTB) was synthesized starting from thieno[3,2-*b*]thiophene<sup>32</sup> following a standard procedure.<sup>7a</sup> To a stirred solution of thienothiophene<sup>31</sup> (200 mg, 1.4 mmol) in fresh distilled THF (16 mL) was added 2.5 M *n*-BuLi in hexane (0.56 mL, 1.44 mmol, 1.01 eq) dropwise at -78 °C under nitrogen atmosphere. After 1.5 h, 0.36 mL (1.82 mmol, 1.3 eq) of 2-isopropoxy-4,4,5,5-tetramethyl-1,3,2-dioxaborolane was added by syringe and the reaction allowed to warm to room temperature. After 12 h of stirring the mixture was poured into water and extracted with diethyl ether. The organic phase was washed with brine and dried over Na<sub>2</sub>SO<sub>4</sub>. The resulting crude product was obtained as a pale yellow oil (317 mg, yield 85%). δ<sub>H</sub>(400 MHz, CDCl<sub>3</sub>, Me<sub>4</sub>Si) 7.76 (1H, d, *J*<sub>5</sub> 0.8), 7.48 (1H, d, *J* 5.6), 7.28 (1H, d, *J*<sub>5</sub> 0.8, *J*<sub>5</sub> 5.6), 1.36 (12 H, s); *m/z* 266.<sup>31</sup>

In the reaction conditions the larger building blocks, including ter- and quaterthiophene, are poorly soluble and consequently less reactive. Moreover, their higher steric hindrance is believed to restrict the oxidative addition to palladium, which is less pronounced than in homogeneous conditions.

Steric effects can also explain why SATCAT and CHITCAT catalyzed reactions show undetectable boron-halogen exchange by-products. The oxidative insertion of Pd in the C–B bond takes place when the C–I bond insertion reaction is very slow. The presence of supported Pd(II) reduces the probability of such insertion therefore minimizing the presence of undesired boron-halogen exchange by-products.

Preliminary investigations on quinque- and hexathiophenes prepared in this way (**13**, **14**, **16**) pointed out that these compounds may display enhanced film forming properties than the same compounds prepared by conventional homogeneous catalysis, due to the higher level of purity obtained using this methodology. Melted homogeneously prepared T5 powder sandwiched between two glasses rendered a viscous fluid containing black solid aggregates which melt at temperatures over 350 °C. Such aggregates can be removed upon purification by vacuum sublimation suggesting they may be residues of the catalyst and/or impurities. No evidence of similar impurities were observed in the preparation of T5 using our heterogeneous protocol (Fig. 3).

Enhanced properties can be expected for all the materials prepared in their use as field effect transistors (FET) and further investigations in this area are currently ongoing.

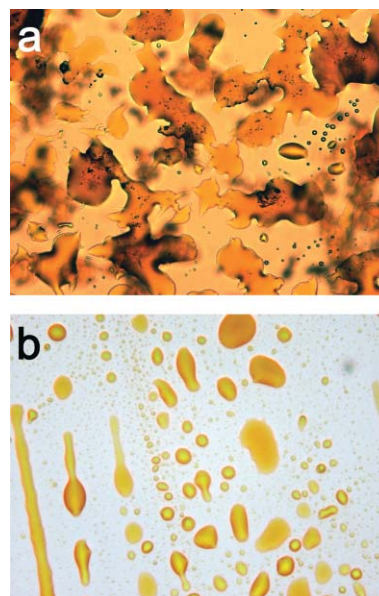


**Fig. 3** Optical microscopy image of melted T5 powder (image size 800 × 800 μm) prepared by (a) conventional homogeneous catalytic method; (b) novel heterogeneously catalyzed protocol.

The optimized protocol was also employed in the preparation of thiophene based co-oligomers containing electron deficient 1,2,3-benzothiadiazole or electron-rich thienothiophene rings. Benzothiadiazole derivatives have been recently proven to have

liquid crystal and semiconducting properties and the polymers have been reported as especially suitable materials for photovoltaic applications.<sup>29</sup> High air stability and charge carrier capabilities have been also recently reported for thienothiophene containing oligomers and polymers.<sup>30</sup> Thienothiophene-thienyl co-oligomers would potentially feature a combination of good  $\pi$ -stacking and charge transport properties (from the thienothiophene system) with the chemical versatility of the thienyl ring.

The benzothiadiazole-based compound (**19**), and the newly synthesized thienothiophene based products (**20** and **21**) were chosen as target compounds. The +2 approach (Fig. 2)—both for odd oligomers (**19** and **20**) and for even oligomer (**21**)—was employed. Data are summarized in Table 5. Our heterogeneously catalysed protocol provided moderate to very good isolated yields to the different synthesized compounds. Product **21** exhibited good solubility in non-polar solvents and highly crystalline cast films, therefore having promising perspectives as active layer in FET.

#### 4. Conclusions

We report a novel, efficient and greener heterogeneous methodology for the preparation of thiophene oligomers and co-oligomers. This useful microwave-assisted protocol does not require a 'one by one' reaction/substrate optimization independently of the size and substitution of the thienyl starting substrates and enables the preparation of extremely pure oligothiophenes in aqueous ethanol. The high level of purity obtained avoids tedious and energy intensive time consuming purification steps and the need to deal with residual metals. Ongoing studies on quinque- and hexathiophenes (**13**, **14** and **16**) pointed out these compounds can display improved filming properties than those prepared by conventional homogeneously catalysed methodologies. Higher charge mobilities in thin film field-effect transistors (FETs) can be expected for all materials prepared employing our microwave approach.

#### Acknowledgements

Thanks to Dr. Matteo Galeotti, Mediteknology srl, for the synthesis of TTB. This work was partially supported by EU Integrated Project NAIMO (No NMP4-CT-2004-500355) and FIRB RBNE03S7XZ\_005 (SYNERGY) project. Financial support from University of Bologna (Progetto Marco Polo) to S.A. is gratefully acknowledged.

#### References

- G. Barbarella, M. Melucci and G. Sotgiu, *Adv. Mater.*, 2005, **17**, 1581–1593.
- M. Mazzeo, V. Vitale, F. Della Sala, M. Anni, G. Barbarella, L. Favaretto, G. Sotgiu, R. Cingolani and G. Gigli, *Adv. Mater.*, 2005, **17**, 34–39.
- A. R. Murphy and J. M. J. Fréchet, *Chem. Rev.*, 2007, **107**, 1066–1096.
- S. Günes, H. Neugebauer and N. S. Sariciftci, *Chem. Rev.*, 2007, **107**, 1324–1338.
- (a) K. P. R. Nilsson and O. Inganäs, *Nature Materials*, 2003, **2**, 419–424; (b) M. L. Capobianco, A. Cazzato, S. Alesi and G. Barbarella, *Bioconjugate Chem.*, 2008, **19**, 171–177.
- F. Babudri, G. M. Farinola and F. Naso, *J. Mater. Chem.*, 2004, **14**, 11–34.
- (a) M. Melucci, G. Barbarella and G. Sotgiu, *J. Org. Chem.*, 2002, **67**, 8877–8884; (b) M. Melucci, G. Barbarella, M. Zambianchi, P. Di Pietro and A. Bongini, *J. Org. Chem.*, 2004, **69**, 4821–4828.
- (a) *Fine chemicals through heterogeneous catalysis*, ed. R. A. Sheldon, and H. van Bekkum, Wiley VCH, 2001; (b) R. B. Bedford, U. G. Singh, R. I. Walton, R. T. Williams and S. A. Davis, *Chem. Mater.*, 2005, **17**, 701–707; (c) J. Ku Cho, R. Najman, T. W. Dean, O. Ichihara, C. Muller and M. Bradley, *J. Am. Chem. Soc.*, 2006, **128**, 6276–6277; (d) J. Y. Shin, B. S. Lee, Y. Jung, S. J. Kim and S.-g. Lee, *Chem. Commun.*, 2007, 5238–5240; (e) H. Oyamada, T. Naito, S. Miyamoto, R. Akiyama, H. Hagio and S. Kobayashi, *Org. Biomol. Chem.*, 2008, **6**, 61–65; (f) Q. Xu, W. Hao and M. Cai, *Catal. Lett.*, 2007, **118**, 98–102.
- L. Yin and J. Liebscher, *Chem. Rev.*, 2007, **107**, 133–173.
- G. Marck, A. Villiger and R. Buchecker, *Tetrahedron Lett.*, 1994, **35**, 3277.
- F.-X. Felpin, T. Ayad and S. Mitra, *Eur. J. Org. Chem.*, 2006, 2679–2690.
- B. M. L. Dioso, I. F. J. Vankelecom and P. A. Jacobs, *Adv. Synth. Catal.*, 2006, **348**, 1413–1446.
- D. J. Macquarrie and J. J. E. Hardy, *Ind. Eng. Chem. Res.*, 2005, **44**, 8499–8520.
- (a) M. J. Gronnow, R. Luque, D. J. Macquarrie and J. H. Clark, *Green Chem.*, 2005, **7**, 552–557; (b) V. L. Budarin, J. H. Clark, R. Luque, D. J. Macquarrie and R. J. White, *Green Chem.*, 2008, DOI:10.1039/b715508e.
- E. B. Mubofu, J. H. Clark and D. J. Macquarrie, *Green Chem.*, 2001, **3**, 23–25.
- S. Paul and J. H. Clark, *Green Chem.*, 2003, **5**, 635–638.
- J. J. E. Hardy, S. Hubert, D. J. Macquarrie and A. J. Wilson, *Green Chem.*, 2004, **6**, 53–56.
- G. Sotgiu, M. Zambianchi, G. Barbarella and C. Botta, *Tetrahedron*, 2002, **58**, 2245–2251.
- G. Barbarella, M. Zambianchi, L. Antolini, P. Ostojia, P. Maccagnani, A. Bongini, E. A. Marseglia, E. Tedesco, G. Gigli and R. Cingolani, *J. Am. Chem. Soc.*, 1999, **121**, 8920–8926.
- M. Melucci, M. Gazzano, G. Barbarella, M. Cavallini, F. Biscarini, P. Maccagnani and P. Ostojia, *J. Am. Chem. Soc.*, 2003, **125**, 10266–10274.
- F. Garnier, A. Yassar, R. Hajlaoui, G. Horowitz, F. Deloffre, B. Servet, S. Ries and P. Alnot, *J. Am. Chem. Soc.*, 1993, **115**, 8716–8721.
- Q. Hou, Y. Xu, W. Yang, M. Yuan, J. Peng and Y. Cao, *J. Mater. Chem.*, 2002, **12**, 2887–2892.
- Other less strong bases, generally used under heterogeneous conditions such as Na<sub>2</sub>CO<sub>3</sub>, K<sub>2</sub>CO<sub>3</sub>, Cs<sub>2</sub>CO<sub>3</sub>, K<sub>3</sub>PO<sub>4</sub> were ineffective.
- H. E. B. Lempers and R. A. Sheldon, *J. Catal.*, 1998, **175**, 62.
- B. J. J. Smeets, R. H. Meijer, J. Meuldijk, J. A. J. M. Vekemans and L. A. Hulshof, *Org. Process Res. Dev.*, 2003, **7**, 10–16.
- H. E. Katz, J. G. Laquindanum and A. Lovinger, *Chem. Mater.*, 1998, **10**, 633–638.
- C. D. Dimitrakopoulos and P. R. L. Malenfant, *Adv. Mater.*, 2002, **14**, 99–117.
- K. R. Amundson, H. E. Katz and A. J. Lovinger, *Thin Solid Films*, 2003, **426**, 140–149.
- (a) Y. Zhu, R. D. Champion and S. A. Jenekhe, *Macromolecules*, 2006, **39**, 8712–8719; (b) R. D. Champion, K.-F. Cheng, C.-L. Pai, W.-C. Chen and S. A. Jenekhe, *Macromol. Rapid Commun.*, 2005, **26**, 1835–1840.
- (a) H.-S. Kim, Y.-H. Kim, T.-H. Kim, Y.-Y. Noh, S. Pyo, M. H. Yi, D.-Y. Kim and S.-K. Kwon, *Chem. Mater.*, 2007, **19**, 3561–3567; (b) M. Medina, A. Van Vooren, P. Brocorens, J. Gierschner, M. Shkunov, M. Heeney, I. McCulloch, R. Lazzaroni and J. Cornil, *Chem. Mater.*, 2007, **19**, 4949–4956; (c) H. Ebata, T. Izawa, E. Miyazaki, K. Takimiya, M. Ikeda, H. Kuwabara and T. Yui, *J. Am. Chem. Soc.*, 2007, DOI: 10.1021/ja074841i.
- E. Bundgaard and F. C. Krebs, *Macromolecules*, 2006, **39**, 2823–2831.
- L. S. Fuller, B. Iddon and K. A. Smith, *J. Chem. Soc., Perkin Trans.*, 1997, **1**, 3465–3470.

# Selective extraction of neutral nitrogen compounds found in diesel feed by 1-butyl-3-methyl-imidazolium chloride

Li-Li Xie,<sup>a,c</sup> Alain Favre-Reguillon,<sup>\*a,b</sup> Xu-Xu Wang,<sup>c</sup> Xianzhi Fu,<sup>c</sup> Stéphane Pellet-Rostaing,<sup>a</sup> Guy Toussaint,<sup>d</sup> Christophe Geantet,<sup>d</sup> Michel Vrinat<sup>d</sup> and Marc Lemaire<sup>\*a</sup>

Received 16th January 2008, Accepted 12th February 2008

First published as an Advance Article on the web 18th March 2008

DOI: 10.1039/b800789f

To produce ultra low-sulfur gasoline and meet the new regulations, the improvement of the HDS reaction by the removal of inhibitors, like nitrogen-containing compounds (N-compounds) commonly found in middle distillates used for diesel feed, could be worth considering.

Liquid–liquid extraction using 1-butyl-3-methyl-imidazolium chloride (BMIm<sup>+</sup>Cl<sup>-</sup>) was found to be a very promising approach for the removal of neutral N-compounds with high selectivity towards sulfur. BMIm<sup>+</sup>Cl<sup>-</sup> was first evaluated using synthetic solution with dibenzothiophene and carbazole as model compounds, and a high selectivity for N-compounds was found. In order to explain the observed selectivity, the extraction of heterocyclic aromatic compounds from a hydrocarbon mixture by BMIm<sup>+</sup>Cl<sup>-</sup> was studied as the function of the toluene/*n*-dodecane ratio. The extraction of sulfur-containing compounds and basic N-compounds decreased when the mass fraction of toluene increased, whereas the extraction of proton donor N-compounds was found to be almost independent of the mass fraction of toluene. We thus assumed that the selective extraction of indole and carbazole by BMIm<sup>+</sup>Cl<sup>-</sup> could be explained both by electron pair acceptor properties of the imidazolium ring and by the binding of the hydrogen-donor group with chloride anion of the RTIL. BMIm<sup>+</sup>Cl<sup>-</sup> was then evaluated using straight-run diesel feed, containing 13400 ppm S and 105 ppm N. An extraction of up to 50% of the N-compounds was obtained in one step, whereas the sulfur concentration reduction was only 5%. The selectivity of the extraction process towards heterocyclic aromatic compounds and polyaromatic compounds using BMIm<sup>+</sup>Cl<sup>-</sup> was further emphasized by two-dimensional GC-MS analysis of the extracted compounds.

## Introduction

The potential of room-temperature ionic liquids (RTILs) as alternative solvents to replace less desirable organic media is currently well recognized. The negligible vapour pressure and the ability to tune their physical and chemical properties, such as hydrophobicity, polarity and solvent miscibility through the appropriate modification of cation and anion has provided the chemist with alternative solvents and reaction media.

The current literature indicates that replacing an organic solvent with an RTIL can bring about remarkable improvements in well-known processes. Among them, RTILs have been explored

as effective solvents in traditional extraction processes<sup>1,2</sup> and gas separation.<sup>3,4</sup>

As a result of the new stringent regulations in transportation fuels, there is a rapid development in the field of separation in the refining industry. RTILs have emerged as alternative solvents for the separation of aromatic hydrocarbons (benzene, toluene, ethylbenzene, and xylenes) from C4 to C10 aliphatic hydrocarbon mixtures.<sup>5–8</sup> RTILs have also been used for the extractive deep desulfurisation of gasoline<sup>9–12</sup> and diesel oil.<sup>13–15</sup>

Aromatic nitrogen compounds (N-compounds), such as pyridine, quinoline, indole and carbazole, naturally present in hydrocarbon feeds are considered as strong inhibitors of the HDS reactions. Furthermore, the reactivity of nitrogen-containing compounds is much lower than that of polyaromatic sulfur compounds,<sup>16</sup> although adsorption is higher. When high levels of desulfurisation are reached, the concentration of refractory sulfur compounds is very low and N-compounds may inhibit the HDS process through competitive adsorption<sup>17</sup> and contribute to the difficulty of meeting the more stringent specifications.<sup>17–23</sup> We could also expect that elimination of HDS inhibitors, such as N-compounds, could lead to improvement in HDS conditions.

The selective removal of N-compounds by non-catalytic processes has already been studied. Basic N-compounds, such as pyridine and quinoline, can be removed using an ion-exchange

<sup>a</sup>ICBMS, Institut de Chimie et Biochimie Moléculaires et Supramoléculaires, Laboratoire de Catalyse et Synthèse Organique, 43 boulevard du 11 novembre 1918, Villeurbanne, F-69622, France, CNRS, UMR 5246, Université Lyon 1. E-mail: favrereg@cnam.fr, marc.lemaire@univ-lyon1.fr

<sup>b</sup>Laboratoire de Chimie Organique, UMR7084, Conservatoire National des Arts et Métiers, 2 rue Conté, 75003, Paris, France

<sup>c</sup>Research Institute of Photocatalysis, Fuzhou University, 350002, Fuzhou, P. R. China

<sup>d</sup>IRCELYON, 2 avenue Albert Einstein, Villeurbanne, F-69626, CNRS, UMR5256, Université Lyon 1, France



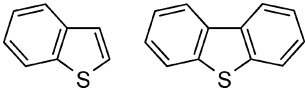
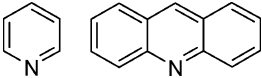
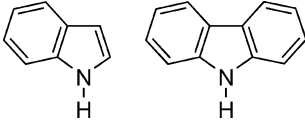
resin,<sup>24,25</sup> by liquid–liquid extraction using volatile carboxylic acid<sup>26</sup> and using RTILs as extracting solvent.<sup>9,27–29</sup> These methods are efficient for the removal of basic N-compounds but none of them seem to be efficient for the removal of the neutral N-compounds, such as indole and carbazole, with the exception of Eßer *et al.* who noticed that indole in *n*-dodecane could be effectively extracted using 1-butyl-3-methyl-imidazolium octylsulfate.<sup>13</sup>

We have already developed new adsorbent material for the selective removal of neutral N-compounds such as indole and carbazole<sup>30,31</sup> and we wish to evaluate RTILs for this selective extraction.

RTILs can be viewed as three-dimensional networks of cations and anions held together by interactions, such as hydrogen bonds, dispersive and Coulombic forces. Due to these strong interactions between the anions and cations, ionic liquids have high viscosities compared to a molecular solvent. Chemists usually attempt to understand solvent effects on chemical processes in terms of the solvent polarity. However, despite a significant amount of experimental measurement of solvent polarity (including spectroscopy,<sup>32–39</sup> chromatography,<sup>40,41</sup> liquid–liquid extraction<sup>42,43</sup> and reactive methods<sup>44</sup>) and modelisation,<sup>45–48</sup> the nature of their interaction with the added solutes needed to be clarified. However, some typical intermolecular solute–RTIL interactions with 1,3-dialkylimidazolium RTILs could be used to explain their properties.<sup>33</sup> For example, the high solubility of toluene in RTILs could be explained by the electron pair acceptor properties of the imidazolium ring ( $\pi$ – $\pi$  interactions)<sup>48,49</sup> and the anionic part of the RTILs appears to control its hydrogen bond acceptor properties.<sup>41,50,51</sup>

Recently, chloride-based RTILs have been used to dissolve native cellulose.<sup>52,53</sup> Chloride based RTILs had high hydrogen bond basicity,<sup>54</sup> suggesting that the chloride anion (with non-bonding electrons), in combination with the imidazolium cation, play a key role in the dissolution of cellulose by disrupting the great number of inter- and intramolecular hydrogen bonds.<sup>55</sup> In the present work, we studied in detail the possible usefulness of hydrogen bond basicity of chloride-based RTILs for the extraction of compounds with a hydrogen-donor group (*i.e.* neutral N-compounds) present in hydrocarbon feeds with a high selectivity towards basic N-compounds and sulfur-containing compounds (S-compounds) (Table 1). It is remarkable that water-miscible chloride-based RTILs have never been used,

**Table 1** Heterocyclic aromatic compounds found in diesel feed stream

S-compounds	
Basic N-compounds	
Neutral N-compounds	

to our knowledge, for the extraction of polar solutes from hydrocarbon feeds.

## Results and discussion

### Solubility of BMIm<sup>+</sup>Cl<sup>–</sup> in the toluene/*n*-dodecane solution

All the experiments were done at 60 °C which is considered to be the temperature of the feed in the industrial process. The loss of solvent in the feed stream is an important factor to be considered in selecting RTILs. Information in the literature on specific properties on RTILs, such as miscibility with aromatic and/or aliphatic hydrocarbons is scarce. The solubility of the BMIm<sup>+</sup>Cl<sup>–</sup> as a function of the toluene/*n*-dodecane ratio for an IL/hydrocarbon ratio of 1/1 was determined (Fig. 1).

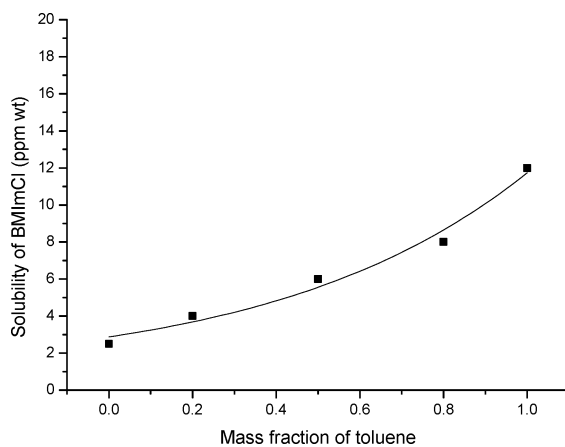


**Fig. 1** Solubility of BMIm<sup>+</sup>Cl<sup>–</sup> as the function of mass fraction of toluene (toluene/*n*-dodecane). Ratio BMIm<sup>+</sup>Cl<sup>–</sup>/hydrocarbon: 1/1, 24 h at 60 °C.

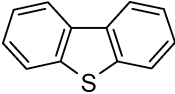
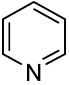
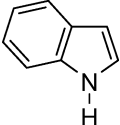
The analytical methods<sup>31</sup> used in this study measured the concentration of total nitrogen in the hydrocarbon feed by chemiluminescence. Thus, the solubility of the BMIm<sup>+</sup>Cl<sup>–</sup> in hydrocarbon could be precisely determined. As expected, a very low solubility of this water-miscible RTIL was observed and measured in pure *n*-dodecane (lower than 3 ppm of BMIm<sup>+</sup>Cl<sup>–</sup>) and the amount of BMIm<sup>+</sup>Cl<sup>–</sup> in the hydrocarbon phase slightly increased with an increase of the mass fraction of toluene.

### Extraction of dibenzothiophene, indole and pyridine from dodecane by BMIm<sup>+</sup>Cl<sup>–</sup>

The extraction was carried out with single component solutions containing 100 ppm of nitrogen in the form of neutral N-compounds (indole), basic N-compounds (pyridine) or 100 ppm of sulfur in the form of S-compounds (dibenzothiophene) (Table 2).

Under those conditions, BMIm<sup>+</sup>Cl<sup>–</sup> was slightly soluble in the hydrocarbon mixture (less than 3 ppm, see Fig. 1), thus the calculated distribution coefficient for indole and pyridine was corrected taking into account the BMIm<sup>+</sup>Cl<sup>–</sup> solubility. Using pure *n*-dodecane, high distribution coefficients of dibenzothiophene and pyridine, comparable to a previous study that used water immiscible 1,3-dialkylimidazolium-based RTIL,<sup>10,12,13</sup> were found. The BMIm<sup>+</sup>Cl<sup>–</sup> showed a higher affinity towards indole and a distribution coefficient of 20.7 was obtained. Such a

**Table 2** Distribution coefficient for extraction of individual compounds with BMIm<sup>+</sup>Cl<sup>-</sup>

Compound	D <sup>a</sup>
	1.2
	1.8 <sup>b</sup>
	20.7 <sup>b</sup>

<sup>a</sup> Individual compounds in *n*-dodecane (100 ppmw), mass ratio *n*-dodecane : RTIL = 1 : 1, reaction time 1 h, 60 °C <sup>b</sup> Corrected value see text.

high distribution coefficient for indole has already been observed by Eßer *et al.*<sup>13</sup> with 1-butyl-3-methyl-imidazolium octylsulfate, but no detail was given about the specific interaction between indole and RTIL. This extraction was further investigated.

#### Influence of the toluene/*n*-dodecane ratio on the extraction efficiency

In order to study the influence of the aromatic content on the extraction efficiency of the RTILs, the extraction was carried out under the same conditions, with single component solutions containing 100 ppm of nitrogen or 100 ppm of sulfur. The toluene/*n*-dodecane ratio was varied and the results obtained for the different compounds are presented in Fig. 2.

The extraction of a single component from a hydrocarbon mixture by BMIm<sup>+</sup>Cl<sup>-</sup> was strongly dependent on the toluene/*n*-dodecane ratio (Fig. 2). The high extraction of heterocyclic aromatic compounds by RTILs has already been reported by several authors. However, most of the extraction of pure compounds from model diesel oil using RTILs have been performed using *n*-heptane,<sup>11</sup> *n*-dodecane,<sup>9,13–15</sup> *n*-tetradecane.<sup>56</sup> However, the diesel oil contained from 25 to 35 wt% of aromatic fraction. It has been suggested that the partitioning of S-compounds from diesel using water insensitive RTILs is more difficult than from gasoline due to the higher content of aromatics.<sup>9</sup> On increasing the mass fraction of toluene in *n*-dodecane, the extraction of dibenzothiophene, pyridine and acridine by BMIm<sup>+</sup>Cl<sup>-</sup> decreased linearly (Fig. 2a–c). The interactions of the RTILs with the aromatic compounds are linked to the electron pair acceptor properties of the 1,3-dialkylimidazolium ring.<sup>48,49,57</sup> From the experimental data obtained with benzothiophene, pyridine and acridine (Fig. 2a–c), we can suppose that in the presence of a high concentration of toluene, toluene will compete with the extraction of heterocyclic aromatic compounds. Thus, when the mass fraction of toluene in the hydrocarbon mixture is increased, the distribution coefficient for heterocyclic aromatic compounds decreases. For acridine (Fig. 2c), no data could be determined for the mass fraction of toluene lower than 0.5

because of the low solubility of acridine in dodecane. However, the same decrease of extraction by BMIm<sup>+</sup>Cl<sup>-</sup> was observed when increasing the mass fraction of toluene.

As expected from the results obtained with indole and pyridine (Table 2), a higher extraction of carbazole compared to the extraction of acridine could be found (Fig. 2c,d). Again no data for carbazole could be determined for a mass fraction of toluene lower than 0.5 because of the low solubility of this compound in dodecane but no decrease of extraction by BMIm<sup>+</sup>Cl<sup>-</sup> was observed when increasing the mass fraction of toluene. From these data we can conclude that BMIm<sup>+</sup>Cl<sup>-</sup> showed a very high affinity for the neutral nitrogen-containing compounds. However, comparison between the extraction of indole (Fig. 2e) and *N*-methylindole (Fig. 2f) as a function of the mass fraction of toluene in *n*-dodecane gave interesting data. On increasing the mass fraction of toluene, the extraction of indole by BMIm<sup>+</sup>Cl<sup>-</sup> remains high, mostly independent of the mass fraction of toluene, although the extraction of *N*-methylindole decreased linearly. From these experiments, we assumed that proton donor molecules (*i.e.* indole and carbazole) could bind to chloride anion and therefore these compounds could be selectively extracted from a hydrocarbon feed. The selectivity of the process was further evaluated on a real straight-run diesel feed stream.

#### Extraction efficiency of BMIm<sup>+</sup>Cl<sup>-</sup> for straight-run feed

BMIm<sup>+</sup>Cl<sup>-</sup> was evaluated with straight-run feed containing 13240 ppm of S and 105 ppm of N. We were not able to decrease the nitrogen content of this feed by using either a strongly acidic ion-exchange resins or a liquid–liquid extraction using diluted acetic acid. From these experiments we can conclude that the feed does not contain basic N-compounds.<sup>31</sup> BMIm<sup>+</sup>Cl<sup>-</sup> was contacted with the straight-run feed with a ratio IL/hydrocarbon feed of 1/10. The total concentration of N and S in the feed were analysed as a function of time. The equilibrium was reached after 1 h of contact at 60 °C, in a batch reactor under continuous stirring. The results are presented in Fig. 3.

More than 50% of the N-compounds were removed from the straight-run feed after a single contact with BMIm<sup>+</sup>Cl<sup>-</sup> with an IL/feed ratio of 1/10 by weight. Under those conditions, the sulfur level was decreased by less than 2%. Therefore, a N/S selectivity higher than 60 can be calculated, according to eqn (3).

#### Regeneration of BMIm<sup>+</sup>Cl<sup>-</sup> and back-extraction of the trapped compounds

Extracted heterocyclic aromatic compounds and coextracted hydrocarbons have a high boiling point and the stripping by distillation cannot be reasonably considered.<sup>13</sup> Back-extraction was carried out using water (50% wt) or methanol (10% wt) that induced the segregation of the solute dissolved in the RTIL phase. The extracted compounds can thus be easily recovered using toluene and BMIm<sup>+</sup>Cl<sup>-</sup> could be quantitatively recovered after vaporisation of the solvent.

To illustrate the capability of chloride-based RTILs to trap the target compounds, two-dimensional gas chromatography has been used. Fig. 4 represents the two-dimensional GC-MS chromatogram of the initial straight-run sample. As already reported

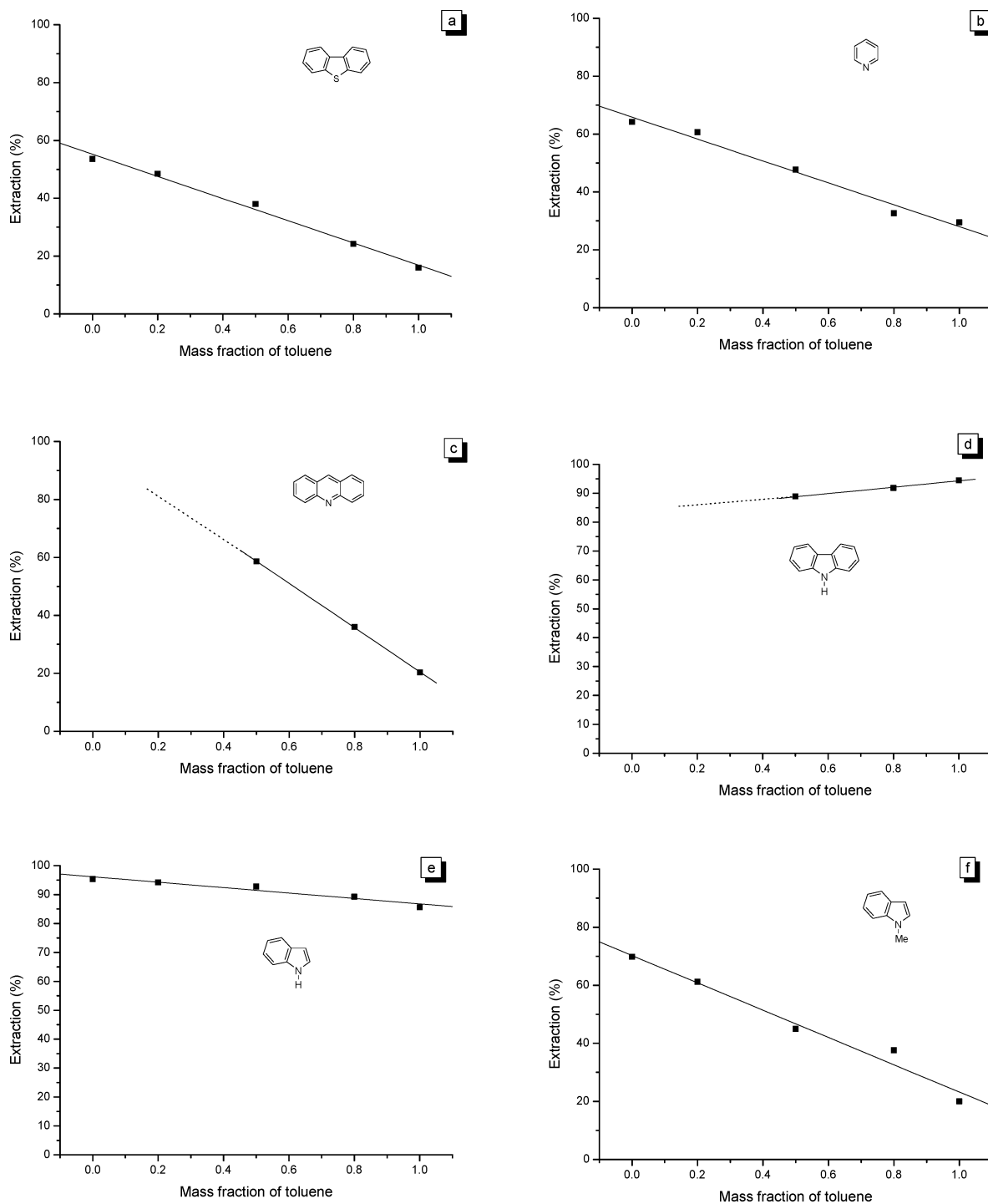


**Fig. 2** Extraction of pure compounds by BMIm<sup>+</sup>Cl<sup>-</sup> as a function of mass fraction of toluene (toluene/*n*-dodecane). Ratio BMIm<sup>+</sup>Cl<sup>-</sup>/hydrocarbon: 1/1, 100 ppm of pure compounds, 24 h at 60 °C.

in the literature,<sup>58–60</sup> this technique enables the separation of the saturate, mono-, di- and triaromatic hydrocarbons in different bands owing to the different interaction of these compounds towards the stationary phase. In many cases, the emphasis is on a group-type characterization only. By the help of the MS detector, linear alkanes in the first band were identified from C8 up to C26. Among triaromatics, it is possible to identify specifi-

cally S-compounds like benzothiophenes, dibenzothiophene and alkyldibenzothiophene since they are present in a relatively high concentration. On the contrary N-compounds can hardly be found.

After extraction by BMIm<sup>+</sup>Cl<sup>-</sup> and back-extraction, the extracted compounds were analyzed and the two-dimensional GC-MS chromatogram is presented in Fig. 5. Concerning

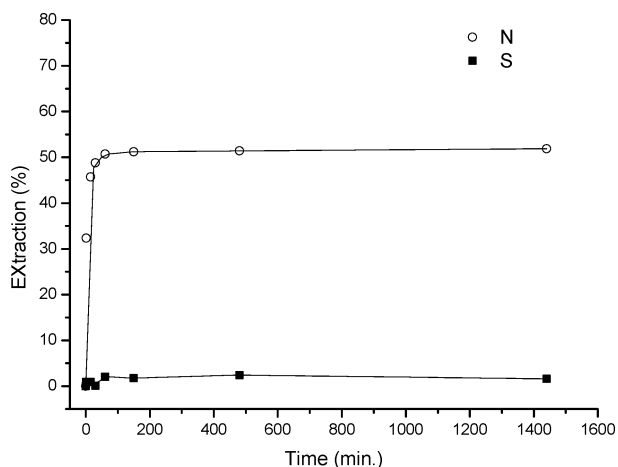


**Fig. 3** Sulfur and nitrogen extraction as the function of time by  $\text{BMIm}^+\text{Cl}^-$ . Straight-run feed containing 13 240 ppm of N and 105 ppm of S. Ratio  $\text{BMIm}^+\text{Cl}^-/\text{feed}$ : 1/10, 24 h at 60 °C.

the distribution of hydrocarbons, two-dimensional GC-MS evidenced the high selectivity towards triaromatic compounds. A few alkenes and monoaromatics remained and some diaromatics were also present but the main contribution of this solution corresponds to triaromatics. Mass spectrometry allowed the identification of some of these compounds and provided evidence of the presence of aromatics (*i.e.* phenanthrene, 2), S-compounds like dibenzothiophene (1) and alkylated dibenzothiophene but also a much higher concentration of N-compounds and especially several alkylated carbazole compounds (3 to 7).

## Conclusion

Chloride based RTILs do represent alternative solvents that can be used for the selective extraction of compounds with a hydrogen-donor group in a hydrocarbon feed. Very low solubility of the  $\text{BMIm}^+\text{Cl}^-$  in the model fuel was observed, lower than 15 ppm. We have shown that the extraction of heterocyclic aromatic compounds decreases on increasing the mass fraction of toluene in the hydrocarbon feed, although the extraction of compounds with a hydrogen-donor group were high and independent of the mass fraction of toluene in the feed.

This extraction procedure was applied to the selective extraction of neutral N-compounds from diesel feed containing 13 240 ppm of S and 105 ppm of N. A nitrogen/sulfur selectivity higher than 60 was reached with this feed. The high selectivity towards heterocyclic triaromatic compounds was further emphasized by two-dimensional GC-MS analysis of the extracted compounds. The highly denitrogenated feed will be used to study the influence of the nitrogen compound concentration on HDS of diesel feed.

## Experimental

### Reagents

$\text{BMIm}^+\text{Cl}^-$  was commercially available (Acros) and before each experiment was dried at 90 °C under reduced pressure. Single component solutions were prepared by dissolving appropriate amounts of analytical grade compound in 100 g of a mixture of toluene/*n*-dodecane mixture (weight/weight). The total nitrogen or sulfur content of the solutions was 100 ppm. Arabian

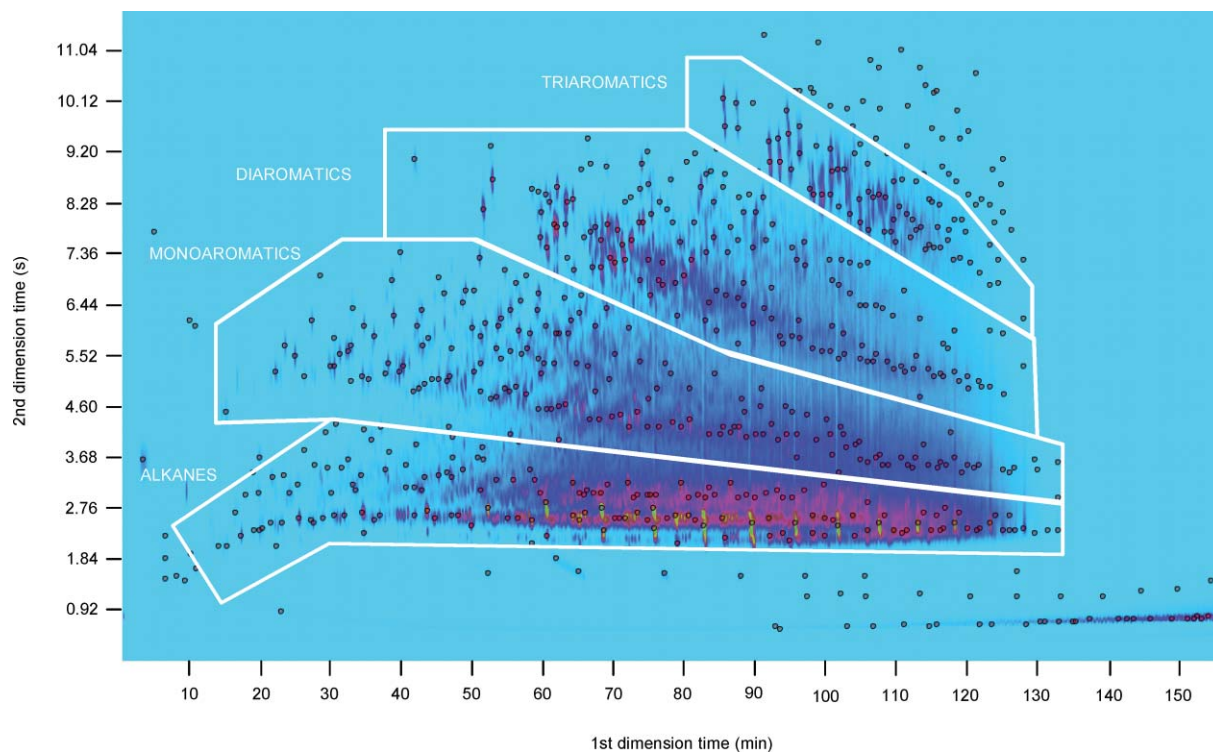


**Fig. 4** Two-dimensional GC-MS chromatogram of Arabian Light Straight Run feed showing group separation.



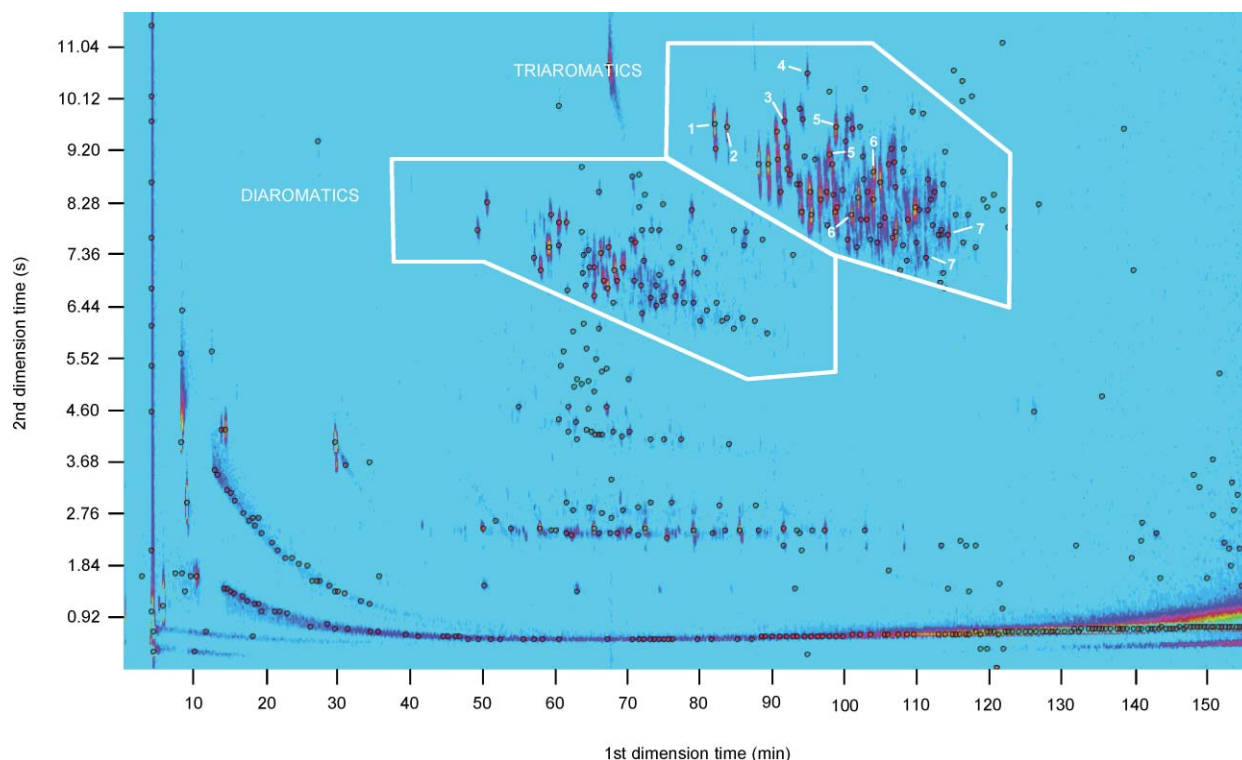


**Fig. 5** Two-dimensional GC-MS chromatogram of the compounds extracted by  $\text{BMIm}^+\text{Cl}^-$  from the Arabian Light Straight Run feed. Peaks identification based on MS: 1 = dibenzothiophene; 2 = phenanthrene; 3 = 3-methylcarbazole; 4 = 9-methylcarbazole; 5 = C2-carbazole; 6 = C3-carbazole; 7 = C5-carbazole.

**Table 3** Composition and physical properties of Arabian Light Straight Run

Density (at 293K)/g L <sup>-1</sup>	852
Sulfur/ppmw	13240
Total nitrogen/ppmw	105
Basic nitrogen/ppmw	<5
Aromatics (wt%)	32.1

Light Straight Run was kindly provided by IFP (Lyon) and was used as feedstock. The relevant properties of this oil are summarized in Table 3.

### Analytical procedures

For sulfur and nitrogen concentrations, the total sulfur and nitrogen concentrations were analyzed by UV fluorescence and by chemiluminescence, respectively, on an Antek 9000 Series nitrogen/sulfur analyser equipped with a robotic liquid autosampler. Measurements were carried out in triplicate and every time each sample was injected three times.

The GCxGC system was installed in a modified 6890 N gas chromatograph (Agilent) equipped with a two stage thermal modulator (Zoex Corporation). A single low temperature valve mounted outside the GC oven controls the cold jet ( $-100\text{ }^\circ\text{C}$ ,  $-120\text{ }^\circ\text{C}$ ) which provides narrow chemical pulses. The modulator accumulates samples eluting from the first column for a period equal to one third to one fifth of the duration of an individual peak. Typically, a modulation period of 12 s was

used. The secondary column effluent was analyzed using a mass selective detector 5975B (Agilent). The carrier gas was high purity helium regulated at a constant flow of  $1.6\text{ ml min}^{-1}$  (initial pressure 36 psi). The temperature of the GC columns was programmed from  $50\text{ }^\circ\text{C}$  (5 mn hold) to  $300\text{ }^\circ\text{C}$  (5 mn hold) at a rate of  $1.5\text{ }^\circ\text{C min}^{-1}$ . Fuel samples were diluted one hundred times in hexane; two microlitres were injected with a split ratio of 250. The first column used was a 30 m, 0.25 mm i.d., 0.2  $\mu\text{m}$  film thickness DB5 MS Agilent, the second was a 0.6 m, 0.1 mm i.d., 0.2  $\mu\text{m}$  film thickness VH 17 MS Varian. The two columns were connected with a standard union, thus the second column worked under Ultra Fast GC conditions. Molecules were separated on the basis of independent chemical properties: volatility for the first column and polarity for the second. The raw signal (total ion count) of a GCxGC experiment is a time ordered series of second dimension chromatograms. The data analysis (GC Image Zoex Corporation) constructs a two dimension chromatogram by placing the second chromatograms side by side. GC Image also constructs a 3D image by placing the detector response on the third axis. In GC, the concentration of a compound is related to the area of the corresponding peak, in 2D GC the concentration is related to a volume or so called "blob". GC Image software package used for the analysis has been designed to perform visualisation of multidimensional data (conversion and plotting of the matrix), data pre-processing (removing artefacts and baseline correction), peak detection and peak quantification (three-dimensional peak volumes are calculated by means of imaging).<sup>61</sup>

### Evaluation of the solubility of BMIm<sup>+</sup>Cl<sup>-</sup> in the toluene/*n*-dodecane solution

In a typical experiment, 1000 mg of toluene/*n*-dodecane mixture was added to 1000 mg of BMIm<sup>+</sup>Cl<sup>-</sup>. A PTFE magnetic stirring bar was added and the screw-capped vial was left for 24 h under stirring at 60 °C with an IKA magnetic stirrer equipped with a thermocouple thermometer. The solubility of BMIm<sup>+</sup>Cl<sup>-</sup> in the toluene/*n*-dodecane mixture could be precisely estimated from the nitrogen concentration in the organic phase determined using an Antek 9000 Series nitrogen/sulfur analyser.

### Extraction using BMIm<sup>+</sup>Cl<sup>-</sup>

In a typical experiment 1000 mg of a toluene/*n*-dodecane mixture containing 100 ppm of nitrogen or 100 ppmw of sulfur was added to 1000 mg of BMIm<sup>+</sup>Cl<sup>-</sup>. A PTFE magnetic stirring bar was added and the screw-capped vials were left for 24 h under magnetic stirring at 60 °C with an IKA magnetic stirrer equipped with a thermocouple thermometer. The resulting hydrocarbon solution was analysed on an Antek 9000 Series nitrogen/sulfur analyser. Extraction efficiency *E*(%), distribution coefficients *D* and selectivity *S*<sub>N/S</sub> were determined according to equation where *C*<sub>i</sub> and *C*<sub>f</sub> are the initial and final concentrations of the studied molecule and *m*<sub>sol</sub> and *m*<sub>IL</sub> are the mass of solution and BMIm<sup>+</sup>Cl<sup>-</sup>, respectively.

$$E(\%) = \frac{C_i - C_f}{C_i} \times 100 \quad (1)$$

$$D = \left( \frac{C_i}{C_f} - 1 \right) \times \frac{m_{\text{sol}}}{m_{\text{IL}}} \quad (2)$$

$$S_{\text{N/S}} = \frac{D_{\text{N}}}{D_{\text{S}}} \quad (3)$$

### Back-extraction and regeneration of BMIm<sup>+</sup>Cl<sup>-</sup>

After 24 h of contact with Arabian Light Straight Run (ratio BMIm<sup>+</sup>Cl<sup>-</sup>/feed: 1/10) aliquot of BMIm<sup>+</sup>Cl<sup>-</sup> (1 g) was collected and first washed with pentane to remove the adsorbed straight run feed. Then 500 mg of water was added and the biphasic solution obtained was extracted with toluene. The organic phase was dry over Na<sub>2</sub>SO<sub>4</sub> and concentrated under vacuum. 65 mg of viscous brown oil was obtained and analysed by two-dimensional GC-MS.

### Acknowledgements

The authors would like to thanks the Ministère des Affaires Etrangères, Ambassade de France en Chine, that partially funded this research through a PhD grant to L.-L. X. and C. Clozen-Fox.

### References

- S. G. Cull, J. D. Holbrey, V. Vargas-Mora, K. R. Seddon and G. J. Lye, *Biotechnol. Bioeng.*, 2000, **69**, 227–233.
- H. Zhao, S. Xia and P. Ma, *J. Chem. Technol. Biotechnol.*, 2005, **80**, 1089–1096.
- R. E. Baltus, R. M. Counce, B. H. Culbertson, H. Luo, D. W. DePaoli, S. Dai and D. C. Duckworth, *Sep. Sci. Technol.*, 2005, **40**, 525–541.
- J. E. Bara, C. J. Gabriel, S. Lessmann, T. K. Carlisle, A. Finotello, D. L. Gin and R. D. Noble, *Ind. Eng. Chem. Res.*, 2007, **46**, 5380–5386.
- J. Zhang, C. Huang, B. Chen, P. Ren and Z. Lei, *Energy Fuels*, 2007, **21**, 1724–1730.
- A. Arce, M. J. Earle, H. Rodriguez and K. R. Seddon, *Green Chem.*, 2007, **9**, 70–74.
- G. Wytze Meindersma, A. Podt, M. B. Klaren and A. B. De Haan, *Chem. Eng. Commun.*, 2006, **193**, 1384–1396.
- G. Wytze Meindersma, A. Podt and A. B. de Haan, *Fuel Proc. Technol.*, 2005, **87**, 59–70.
- S. Zhang, Q. Zhang and Z. C. Zhang, *Ind. Eng. Chem. Res.*, 2004, **43**, 614–622.
- S. Zhang and Z. C. Zhang, *Green Chem.*, 2002, **4**, 376–379.
- C. Huang, B. Chen, J. Zhang, Z. Liu and Y. Li, *Energy Fuels*, 2004, **18**, 1862–1864.
- Y. Nie, C. Li, A. Sun, H. Meng and Z. Wang, *Energy Fuels*, 2006, **20**, 2083–2087.
- J. Eßer, P. Wasserscheid and A. Jess, *Green Chem.*, 2004, **6**, 316–322.
- A. Böesmann, L. Datsevich, A. Jess, A. Lauter, C. Schmitz and P. Wasserscheid, *Chem. Commun.*, 2001, 2494–2495.
- J. D. Holbrey, I. Lopez-Martin, G. Rothenberg, K. R. Seddon, G. Silvero and X. Zheng, *Green Chem.*, 2008, **10**, 87–92.
- T. Kabe, W. Qian and A. Ishihara, *Hydrosulfurization and hydrodenitrogenation: chemistry and engineering*, Wiley-VCH, 1999.
- T. Koltai, M. Macaud, A. Guevara, E. Schulz, M. Lemaire, R. Bacaud and M. Vrinat, *Appl. Catal., A*, 2002, **231**, 253–261.
- M. J. Girgis and B. C. Gates, *Ind. Eng. Chem. Res.*, 1991, **30**, 2021–2058.
- E. Furimsky and F. E. Massoth, *Catal. Today*, 1999, **52**, 381–495.
- G. Laredo, A. De los Reyes, L. Cano and J. Castillo, *Appl. Catal., A*, 2001, **207**, 103–112.
- M. Breyse, G. Djega-Mariadassou, S. Pessayre, C. Geantet, M. Vrinat, G. Perot and M. Lemaire, *Catal. Today*, 2003, **84**, 129–138.
- G. Laredo, E. Altamirano and A. De los Reyes, *Appl. Catal., A*, 2003, **243**, 207–214.
- U. T. Turaga, X. Ma and C. Song, *Catal. Today*, 2003, **86**, 265–275.
- M. E. Prudich, D. C. Cronauer, R. F. Vogel and J. Solash, *Ind. Eng. Chem. Proc. Des. Dev.*, 1986, **25**, 742–746.
- I. Merdrignac, F. Behar, P. Albrecht, P. Briot and M. Vandembroucke, *Energy Fuels*, 1998, **12**, 1342–1355.
- J. Qi, Y. Yan, Y. Su, F. Qu and Y. Dai, *Energy Fuels*, 1998, **12**, 788–791.
- Z.-R. Gao, K.-J. Liao, D.-S. Liu and Y.-L. Dai, *Petrol. Sci. Technol.*, 2005, **23**, 1001–1008.
- P. Gao, Z. Cao, D. Zhao, D. Li and S. Zhang, *Petrol. Sci. Technol.*, 2005, **23**, 1023–1031.
- M. Matsumoto, M. Mikami and K. Kondo, *J. Jpn. Petrol. Inst.*, 2006, **49**, 256–261.
- M. Macaud, E. Schulz, M. Vrinat and M. Lemaire, *Chem. Commun.*, 2002, 2340–2341.
- M. Macaud, M. Sevignon, A. Favre-Reguillon, M. Lemaire, E. Schulz and M. Vrinat, *Ind. Eng. Chem. Res.*, 2004, **43**, 7843–7849.
- S. Arzhantsev, H. Jin, G. A. Baker and M. Maroncelli, *J. Phys. Chem. B*, 2007, **111**, 4978–4989.
- C. Reichardt, *Green Chem.*, 2005, **7**, 339–351.
- L. Crowhurst, P. R. Mawdsley, J. M. Perez-Arlandis, P. A. Salter and T. Welton, *Phys. Chem. Chem. Phys.*, 2003, **5**, 2790–2794.
- S. N. V. K. Aki, J. F. Brennecke and A. Samanta, *Chem. Commun.*, 2001, 413–414.
- B. R. Mellein, S. N. V. K. Aki, R. L. Ladewski and J. F. Brennecke, *J. Phys. Chem. B*, 2007, **111**, 131–138.
- A. J. Carmichael and K. R. Seddon, *J. Phys. Org. Chem.*, 2000, **13**, 591–595.
- K. Iwata, M. Kakita and H.-O. Hamaguchi, *J. Phys. Chem. B*, 2007, **111**, 4914–4919.
- G. Angelini, C. Chiappe, P. De Maria, A. Fontana, F. Gasparri, D. Pieraccini, M. Pierini and G. Siani, *J. Org. Chem.*, 2005, **70**, 8193–8196.
- D. W. Armstrong, L. He and Y.-S. Liu, *Anal. Chem.*, 1999, **71**, 3873–3876.
- J. L. Anderson, J. Ding, T. Welton and D. W. Armstrong, *J. Am. Chem. Soc.*, 2002, **124**, 14247–14254.
- J. G. Huddleston, A. E. Visser, W. M. Reichert, H. D. Willauer, G. A. Broker and R. D. Rogers, *Green Chem.*, 2001, **3**, 156–164.

- 43 S. Carda-Broch, A. Berthod and D. W. Armstrong, *Anal. Bioanal. Chem.*, 2003, **375**, 191–199.
- 44 V. Dichiarante, C. Betti, M. Fagnoni, A. Maia, D. Landini and A. Albini, *Chem.–Eur. J.*, 2007, **13**, 1834–1841.
- 45 P. A. Hunt and I. R. Gould, *J. Phys. Chem. A*, 2006, **110**, 2269–2282.
- 46 S. Kobmann, J. Thar, B. Kirchner, P. A. Hunt and T. Welton, *J. Chem. Phys.*, 2006, **124**, 174506.
- 47 V. Znamenskiy and M. N. Kobra, *J. Phys. Chem. B*, 2004, **108**, 1072–1079.
- 48 C. G. Hanke, A. Johansson, J. B. Harper and R. M. Lynden-Bell, *Chem. Phys. Lett.*, 2003, **374**, 85–90.
- 49 J. D. Holbrey, W. M. Reichert, M. Nieuwenhuyzen, O. Sheppard, C. Hardacre and R. D. Rogers, *Chem. Commun.*, 2003, 476–477.
- 50 M. H. Abraham, J. C. Dearden and G. M. Bresnen, *J. Phys. Org. Chem.*, 2006, **19**, 242–248.
- 51 K. S. Mali, G. B. Dutt and T. Mukherjee, *J. Chem. Phys.*, 2005, **123**, 174504.
- 52 R. P. Swatloski, S. K. Spear, J. D. Holbrey and R. D. Rogers, *J. Am. Chem. Soc.*, 2002, **124**, 4974–4975.
- 53 H. Zhang, J. Wu, J. Zhang and J. He, *Macromolecules*, 2005, **38**, 8272–8277.
- 54 M. H. Abraham and Y. H. Zhao, *J. Org. Chem.*, 2004, **69**, 4677–4685.
- 55 R. C. Remsing, R. P. Swatloski, R. D. Rogers and G. Moyna, *Chem. Commun.*, 2006, 1271–1273.
- 56 W.-H. Lo, H.-Y. Yang and G.-T. Wei, *Green Chem.*, 2003, **5**, 639–642.
- 57 M. Deetlefs, C. Hardacre, M. Nieuwenhuyzen, O. Sheppard and A. K. Soper, *J. Phys. Chem. B*, 2005, **109**, 1593–1598.
- 58 J. Dallüge, J. Beens and U. A. T. Brinkman, *J. Chromatogr., A*, 2003, **1000**, 69–108.
- 59 C. Vendevre, R. Ruiz-Guerrero, F. Bertocini, L. Duval, D. Thiebaut and M.-C. Hennion, *J. Chromatogr., A*, 2005, **1086**, 21–28.
- 60 J. Beens, H. Boelens, R. Tijssen and J. Blomberg, *J. High Resolut. Chromatogr.*, 1998, **21**, 47–54.
- 61 S. E. Reichenbach, M. Ni, V. Kottapalli and A. Visvanathan, *Chemom. Intell. Lab. Syst.*, 2004, **71**, 107–120.

# Isosorbide as a novel polar head derived from renewable resources. Application to the design of short-chain amphiphiles with hydrotropic properties

Ying Zhu, Morgan Durand, Valérie Molinier and Jean-Marie Aubry\*

Received 8th November 2007, Accepted 30th January 2008

First published as an Advance Article on the web 5th March 2008

DOI: 10.1039/b717203f

The potential use of isosorbide, an original diol readily obtained by the double dehydration of sorbitol, has been investigated for the synthesis of novel amphiphilic species. The hydrophilicity of this polar head has been assessed *via* the synthesis and evaluation of three short-chain monoalkyl derivatives. The isosorbide polar head appears to have an unexpectedly low hydrophilicity, comparable to a diethylene oxide unit and it exhibits similar sensitivity to temperature changes. The monobutyl and monopentyl ethers of isosorbide have been found to be very efficient for the solubilisation of a model hydrophobic compound in water, giving promising hints on the use of isosorbide for the design of hydrotropic compounds.

## Introduction

Sugar-based amphiphiles represent a unique class of surface-active compounds due to the wide variety of available polar heads and the different types of chemical links by which they can be attached to the hydrophobic tail.<sup>1–6</sup> Albeit a large number of carbohydrates can be found in nature, or obtained by synthetic means, only a few are available in sufficient quantity and at reasonable prices for industrial applications as raw materials, notably for the synthesis of large-scale products as surfactants. As for now, the main molecules that fulfil these criteria are glucose, derived from starch, sucrose, obtained from beet or sugar cane, and sorbitol, the hydrogenation product of glucose (Fig. 1).

The most popular and widely-used class of sugar-based surfactants is the AlkylPolyGlucosides series—APG—, developed at an industrial scale since the 80s. They are synthesized by Fischer's condensation of glucose with fatty alcohols and are obtained as mixtures of compounds containing one or more glucose moieties linked to an alkyl chain by an ether bond. They are mostly used as non-irritant cleaning agents in liquid soap formulations and are also present in personal care products.<sup>3</sup> Fatty esters of sugar-derived polyols are also an important class of green surfactants, easily biodegradable and of low toxicity and irritancy.<sup>4</sup> Sucrose esters were first synthesized in the 60s and their use was extended in Europe in the early 80s. They are obtained by transesterification of sucrose with vegetal oils methyl esters and are mainly used in cosmetic and food formulations. Sorbitan esters of the Tween and Span series come from monodehydrated sorbitol and find applications as emulsifiers in the pharmaceutical, food and cosmetic industries among others.

Isosorbide (1,4:3,6-dianhydro-D-glucitol) is a V-shaped molecule consisting of two fused tetrahydrofuran rings having two hydroxyl groups with *endo* and *exo* orientations (Fig. 2).<sup>7</sup> It is readily obtained from sorbitol by a double dehydration and is thus an important product of the starch industry (Fig. 1). Isosorbide has already been investigated as a starting material for the synthesis of chiral promoters in organic synthesis and notably asymmetric phase transfer catalysis.<sup>8–12</sup> The monoacetyl derivatives are the precursors of the nitroisosorbide used for its vaso-dilating properties.<sup>13–15</sup> Dimethylisosorbide is a co-solvent used in cosmetic formulations as penetration enhancer.<sup>16</sup> Diethers of isosorbide have also been synthesized in high yields by phase transfer catalysis under microwave.<sup>17</sup>

Finding a way to valorise isosorbide as a starting reagent to synthesize new compounds is thus a challenging and valuable task. However, its use as a polar head for the synthesis of amphiphilic species has never been investigated to date. In the present work, the hydrophilicity of isosorbide has been evaluated, with special emphasis on the comparison with more classical polar heads, as the (poly)ethylene glycols. The hydrotropic properties of short-chain amphiphiles derived from it have also been assessed. Hydrotropes are water-soluble organic molecules that greatly enhance the aqueous solubility of sparingly-soluble compounds.<sup>18</sup> They find applications in a wide variety of industrial fields, such as the detergent industry, where they enhance the solubility and increase the cloud point of nonionic-based systems, also retarding the formation of liquid crystalline structures. They also help solubilising hydrophobic components such as perfumes or colorants in these aqueous-based formulations. Their use is also widely spread in the pharmaceutical industry, where the low water solubility of most active ingredients has to be overcome. A wide-variety of compounds, ranging from alkylbenzene sulfonates or aromatic and aliphatic alcohols to short-chain ethers of ethylene or propylene glycol exhibit hydrotropic properties. APG with short and intermediate alkyl chains have also been found to exhibit hydrotropic properties.<sup>19</sup> When short-chain non-ionic

LCOM, Equipe «Oxydation et Formulation», UMR CNRS 8009, ENSCL BP 108, 59652, Villeneuve d'Ascq Cedex, France.  
E-mail: Jean-Marie.Aubry@univ-lille1.fr; Tel: +33(0)320336364



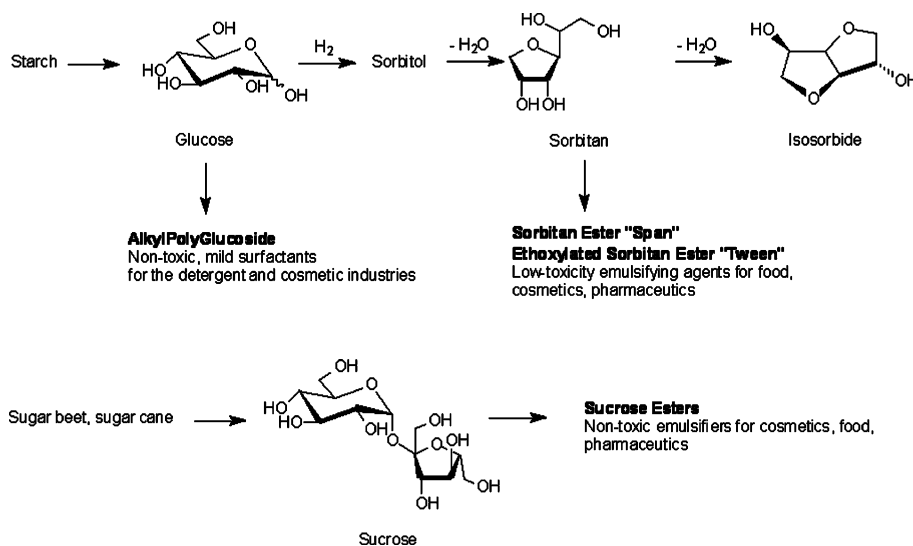


**Fig. 1** Location of isosorbide among the most common sugar or sugar-derived molecules used for the synthesis of amphiphilic species.

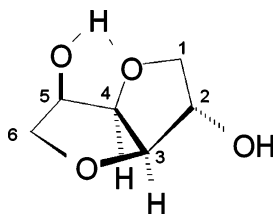


**Fig. 2** 1,4:3,6-dianhydro-D-glucitol; "Isosorbide".

amphiphiles are considered, they can also be called "solvo-surfactants", since they exhibit at the same time properties of solvents (low molecular weight, volatility, solubilising power), and surfactants (amphiphilic structure, self-aggregation in water, surface active properties).<sup>20</sup> Nowadays, the most widely-used solvo-surfactants are the short-chain ethylene or propylene glycol ethers. Their high efficiency has however to be balanced with their petroleum origin, and their use is also a matter of debate since several members of this family are blamed for reprotoxicity.<sup>21</sup> Recently, the efficacy of short-chain glycerol 1-monoethers has been put forward,<sup>22,23</sup> and we are now looking for new classes of potential environmentally-friendly solvo-surfactants, as the monoalkylated derivatives of isosorbide.

In the present work, three monoalkyl ethers of isosorbide, namely monobutyl, monopentyl and monohexylisosorbide, have been synthesized in the pure form and characterized for their surface-active properties and phase diagram in water. Their partition in a cyclohexane/water mixture has been studied and compared to ethylene glycol and glycerol solvo-surfactants. Their hydrotropic behaviour has been looked at by evaluating the efficiency to solubilise a model organic compound in water, 1-methylnaphtalene.

## 1. Experimental

### Chemicals

All chemicals were used as received. 1-Bromobutane (Aldrich, >99%), 1-bromopentane (Aldrich, >99%), 1-bromohexane

(Aldrich, >99%), anhydrous lithium hydroxide (Acros, 98%) and dimethylsulfoxide (Acros, 99.7%) were used for the syntheses. The solvents for extractions and column chromatography were from SDS-Carlo Erba (synthesis grade). Isosorbide was a gift from Roquette (Lestrem). Solubilisation experiments were performed with 1-methylnaphtalene (Acros, 97%). Cyclohexane used for the determination of partition coefficients was of synthesis grade (SDS-Carlo Erba, >99.8%). For the comparison of the amphiphilic and hydrotropic behaviours, ethylene glycol monobutyl ether ( $\text{C}_4\text{E}_1$ ) (Aldrich, >99.5%) and diethyleneglycol monobutyl ether ( $\text{C}_4\text{E}_2$ ) (Acros, >99%) were used, as well as glycerol 1-monopentyl ether ( $\text{C}_5\text{Gly}$ ), whose synthesis is described in ref. 22. For all experiments, ultra-pure water (resistivity 18.2  $\text{M}\Omega\cdot\text{cm}$ ) was used.

### General methods

NMR spectra were recorded on Bruker AC spectrometers at 300.13 MHz for  $^1\text{H}$  and 75.47 MHz for  $^{13}\text{C}$ . LSI-mass spectra were recorded by the Centre de Spectrométrie de Masse of the Université Claude Bernard Lyon I (Villeurbanne). Optical rotations were measured at 20 °C with a Perkin Elmer 343 polarimeter. Gas chromatography analyses were performed on an Agilent 6890 N apparatus, equipped with a HP-1 Crosslinked Methyl Silicone gum column (60 m  $\times$  0.32 mm  $\times$  0.25  $\mu\text{m}$ ), with  $\text{N}_2$  as gas vector and a FID detector. The method used to analyse the reaction media and the isolated products allows separating the two monoethers and the diether. The same method was used for the measurement of cyclohexane–water partition coefficients. A calibration curve for each compound was constructed beforehand.

### Synthesis of the compounds

The synthesis and purification procedures were identical for all compounds and are described below for compound **3**.

Isosorbide (40.2 g, 0.275 mol) was dissolved in DMSO (140 mL) and heated to 90 °C under stirring. LiOH (6.6 g, 0.275 mol) was then added at the same temperature. The medium

was maintained at 90 °C during one hour to allow complete dissolution. Bromohexane (38.6 mL, 0.275 mol) was then added drop wise at the same temperature and at the end of the addition, the medium was left under stirring at 90 °C during 24 hours. After cooling down to room temperature, it was acidified to pH 1 by addition of 2M HCl. DMSO was evaporated under reduced pressure and the residue was extracted with ethyl acetate (3 × 100 mL). The organic phase was dried over magnesium sulfate and the solvent evaporated under reduced pressure to give a dark orange oil. This crude residue contained a mixture of the two monoethers and of the diether. Before purification, it was diluted in dichloromethane and agitated in the presence of charcoal to remove part of the coloured impurities. The medium was then filtrated, concentrated under reduced pressure and then subjected to column chromatography. The eluting system was a gradient from a 50/50 to a 0/100 mixture of petroleum ether/diethyl ether. The diether of isosorbide was eluted first ( $R_f = 0.77$  in a 50/50 mixture) and was not collected. 2-*O*-monoheptyl isosorbide was then isolated ( $R_f = 0.20$  in a 50/50 mixture, 2.9 g, 7.0 mmol, 5%), then 5-*O*-monoheptyl isosorbide 3 ( $R_f = 0.08$  in a 50/50 mixture, 20.5 g, 89.0 mmol, 32%).

The purity of the compounds was ascertained by  $^1\text{H}$  and  $^{13}\text{C}$  NMR spectroscopy and gas chromatography. The NMR spectra of the 5-*O*-monoalkyl ethers, which were studied in this work, are given below. For the numbering of the carbons on the isosorbide cycle, see Fig. 2.

#### 5-*O*-monobutyl isosorbide 1

$[\alpha]_{\text{D}}^{20} +96$  ( $c$  1 in MeOH).  $^1\text{H}$  NMR (300 MHz,  $\text{CDCl}_3$ -1% TMS):  $\delta$  0.91 (3H, t,  $J_{\text{CH}_2\text{-CH}_3} = 7.3$  Hz,  $\text{CH}_3$ ), 1.29–1.47 (2H, m,  $\text{CH}_{2\gamma}$ ), 1.50–1.68 (2H, m,  $\text{CH}_{2\beta}$ ), 2.10–2.40 (1H, m, OH), 3.46 (1H, dt,  $J_{\text{H}_{01}\text{-H}_{02}} = 9.1$  Hz,  $J_{\text{H}_{01}\text{-H}\beta} = 6.8$  Hz,  $\text{CH}_{2\alpha 1}$ ), 3.57 (1H, dd,  $J_{6a-5} = J_{6a-6b} = 8.0$  Hz,  $\text{H}_{6a}$ ), 3.68 (1H, dt,  $J_{\text{H}_{01}\text{-H}_{02}} = 9.1$  Hz,  $J_{\text{H}_{02}\text{-H}\beta} = 6.8$  Hz,  $\text{CH}_{2\alpha 2}$ ), 3.86–4.06 (4H, m,  $\text{H}_{1a/b}$ ,  $\text{H}_5$ ,  $\text{H}_{6b}$ ), 4.30–4.35 (1H, m,  $\text{H}_2$ ), 4.44 (1H, d,  $J_{3-4} = 4.2$  Hz,  $\text{H}_3$ ), 4.69 (1H, dd,  $J_{4-3} = J_{4-5} = 4.3$  Hz,  $\text{H}_4$ ).  $^{13}\text{C}$  NMR (75 MHz,  $\text{CDCl}_3$ -1% TMS):  $\delta$  13.9 ( $\text{CH}_3$ ), 19.2 ( $\text{CH}_{2\gamma}$ ), 31.8 ( $\text{CH}_{2\beta}$ ), 70.1 (C6), 70.7 ( $\text{CH}_{2\alpha}$ ), 75.9 (C1), 76.8 (C2), 80.1 (C4), 80.3 (C5), 88.3 (C3). HRMS: found 203.1283,  $\text{C}_{10}\text{H}_{18}\text{O}_4$  ( $m/z + \text{H}^+$ ) requires 203.1283.

#### 5-*O*-monopentyl isosorbide 2

$[\alpha]_{\text{D}}^{20} +92$  ( $c$  1 in MeOH).  $^1\text{H}$  NMR (300 MHz,  $\text{CDCl}_3$ -1% TMS):  $\delta$  0.84–0.99 (3H, m,  $\text{CH}_3$ ), 1.20–1.47 (4H, m,  $2\text{CH}_2$ ), 1.50–1.70 (2H, m,  $\text{CH}_{2\beta}$ ), 1.90–2.15 (1H, m, OH), 3.45 (1H, dt,  $J_{\text{H}_{01}\text{-H}_{02}} = 9.1$  Hz,  $J_{\text{H}_{01}\text{-H}\beta} = 6.9$  Hz,  $\text{CH}_{2\alpha 1}$ ), 3.57 (1H, dd,  $J_{6a-5} = J_{6a-6b} = 8.0$  Hz,  $\text{H}_{6a}$ ), 3.68 (1H, dt,  $J_{\text{H}_{01}\text{-H}_{02}} = 9.1$  Hz,  $J_{\text{H}_{02}\text{-H}\beta} = 6.9$  Hz,  $\text{CH}_{2\alpha 2}$ ), 3.86–4.06 (4H, m,  $\text{H}_{1a/b}$ ,  $\text{H}_5$ ,  $\text{H}_{6b}$ ), 4.30–4.35 (1H, m,  $\text{H}_2$ ), 4.44 (1H, d,  $J_{3-4} = 4.1$  Hz,  $\text{H}_3$ ), 4.69 (1H, dd,  $J_{4-3} = J_{4-5} = 4.3$  Hz,  $\text{H}_4$ ).  $^{13}\text{C}$  NMR (75 MHz,  $\text{CDCl}_3$ -1% TMS):  $\delta$  14.0 ( $\text{CH}_3$ ), 22.5–29.4 ( $2\text{CH}_2$ ), 28.1 ( $\text{CH}_{2\beta}$ ), 70.0 (C6), 71.0 ( $\text{CH}_{2\alpha}$ ), 75.8 (C1), 76.6 (C2), 80.0 (C4), 80.3 (C5), 88.3 (C3). HRMS: found 217.1447,  $\text{C}_{11}\text{H}_{20}\text{O}_4$  ( $m/z + \text{H}^+$ ) requires 217.1440.

#### 5-*O*-monoheptyl isosorbide 3

$[\alpha]_{\text{D}}^{20} +86$  ( $c$  1 in MeOH).  $^1\text{H}$  NMR (300 MHz,  $\text{CDCl}_3$ -1% TMS):  $\delta$  0.80–0.97 (3H, m,  $\text{CH}_3$ ), 1.15–1.45 (6H, m,  $3\text{CH}_2$ ), 1.50–1.70 (2H, m,  $\text{CH}_{2\beta}$ ), 2.50–2.75 (1H, m, OH),

3.44 (1H, dt,  $J_{\text{H}_{01}\text{-H}_{02}} = 9.2$  Hz,  $J_{\text{H}_{01}\text{-H}\beta} = 6.9$  Hz,  $\text{CH}_{2\alpha 1}$ ), 3.57 (1H, dd,  $J_{6a-5} = J_{6a-6b} = 8.0$  Hz,  $\text{H}_{6a}$ ), 3.67 (1H, dt,  $J_{\text{H}_{01}\text{-H}_{02}} = 9.2$  Hz,  $J_{\text{H}_{02}\text{-H}\beta} = 6.9$  Hz,  $\text{CH}_{2\alpha 2}$ ), 3.85–4.08 (4H, m,  $\text{H}_{1a/b}$ ,  $\text{H}_5$ ,  $\text{H}_{6b}$ ), 4.30–4.35 (1H, m,  $\text{H}_2$ ), 4.43 (1H, d,  $J_{3-4} = 4.4$  Hz,  $\text{H}_3$ ), 4.68 (dd,  $J_{4-3} = J_{4-5} = 4.4$  Hz,  $\text{H}_4$ ).  $^{13}\text{C}$  NMR (75 MHz,  $\text{CDCl}_3$ -1% TMS):  $\delta$  14.0 ( $\text{CH}_3$ ), 22.6–25.7–31.6 ( $3\text{CH}_2$ ), 29.7 ( $\text{CH}_{2\beta}$ ), 70.0 (C6), 71.1 ( $\text{CH}_{2\alpha}$ ), 75.9 (C1), 76.7 (C2), 80.1 (C4), 80.3 (C5), 88.3 (C3). HRMS: found 231.1598,  $\text{C}_{12}\text{H}_{22}\text{O}_4$  ( $m/z + \text{H}^+$ ) requires: 231.1596.

#### Construction of phase diagrams in water

Screwed test tubes containing the sample mixture (3 mL) at different concentrations were immersed in a water bath, the temperature of which was changed gradually. The temperatures at which the solutions became turbid were recorded to build the cloud curve. The temperature was precisely determined on heating and cooling. If a slight discrepancy, smaller than 0.5 °C, was observed, the mean value was taken.

#### Surface tension measurements

Surface tension measurements were performed with the drop shape method using a Tracker-ITConcept tensiometer. A rising air bubble was formed in the solution, the temperature of which was maintained at  $(25.0 \pm 0.1)^\circ\text{C}$  by using a thermostated bath. Equilibrium values were recorded after an interval up to two hours for the  $\text{C}_6$  derivative.

#### Partition coefficient in cyclohexane/water

the determination of partition coefficients of the hydrotropic compounds in a cyclohexane/water mixture was determined according to the shake-flask method, as described in the OECD procedure n° 107 (27.07.95). Both solvents were mutually saturated before the measurement. For the measurements to be valid, the compound should be at a concentration in each phase well below the aggregation concentration. This is achieved by choosing a total concentration inferior to 5 g/L. For each compound, the measurements were carried out at two concentrations ( $C$  and  $C/2$ ), and for two water/oil ratios ranging from 0.5 to 4. The samples were hand-shaken, and left to equilibrate for 48 hours in a water bath thermostated at  $\pm 0.1$  °C. The amount of hydrotrope in each phase was determined by gas chromatography. The partition coefficients are mean values on the different experiments. The deviation on the partition coefficient was usually around 2% and always less than 4%.

#### Solubilisation of 1-methylnaphtalene

2 g-solutions of the hydrotrope in water were prepared at different concentrations and 1-methylnaphtalene was added carefully until reaching saturation (cloudy solution). The solutions were kept under stirring at room temperature during 24 hours. After this period, the solutions were centrifuged to accelerate the phase separation and the aqueous phase was taken out after complete decantation (clear solution). The amount of 1-methylnaphtalene solubilised in the aqueous phase was determined by UV absorption of the solutions at 292 nm. Prior to the measurement, a calibration curve was constructed at this

wavelength. The solutions were diluted in ethanol before the measurement.

## 2. Results and discussion

### 2.1. Synthesis of monobutyl isosorbide 1, monopentyl isosorbide 2 and monohexyl isosorbide 3

The monoalkyl ethers of isosorbide were synthesized by direct selective alkylation of isosorbide by the corresponding bromoalkanes in the presence of lithium hydroxide in dimethylsulfoxide (Scheme 1).<sup>11</sup> In these conditions, selectivity towards the 5-*O*-alkyl isomer is enhanced due to the higher acidity of proton OH-5, which is embedded in a hydrogen bond with the oxygen atom of the adjacent cycle (Fig. 2).

Comparable yields (~35%) in monoalkylated products were obtained for the three chain lengths. The selectivity towards the 5-*O*-alkylation reaches 86% for the butyl chain, and is slightly enhanced to 95% for the two longer chains. In all cases, the diether and the two monoethers can easily be separated during the purification by flash chromatography. This means that these three species have quite different physico-chemical properties, which is particularly interesting to note for the two monoethers. The difference in the polarities of the two monoethers is probably due to the breakdown of the intramolecular hydrogen bond in the case of the 5-*O*-isomers, whereas this bond is maintained in the case of the 2-*O*-isomers. This results in a slightly more hydrophilic head group for the 5-*O*-isomers that contain a more accessible hydroxyl group, as suggested by the order of elution of the two isomers on a silica gel chromatography column. In this work, only the 5-*O*-isomers were studied and characterized.

As the aim of this preliminary study was to get the compounds in a pure form to assess their physico-chemical properties, no effort was made to improve the synthetic route. However, for them to be considered as green alternatives to petroleum-derived glycol ethers, they should be obtained in a more environmentally-friendly manner, for instance by using water as the reaction solvent, as already described for the synthesis of sucrose hydroxyalkyl ethers.<sup>5</sup>

### 2.2. Evaluation of isosorbide as a polar head for amphiphilic species

**2.2.1. First estimation of the isosorbide polarity by LogP calculations.** A first estimation of the polarity of a substance can be performed by looking at its logP value. The octanol-water partition coefficient, *P*, expresses the differential solubility of a substance between these two immiscible solvents. It equals the ratio of the concentration of the substance solubilised in octanol over the concentration of the substance solubilised in water. Therefore, it is often used as a descriptor of the hydrophobicity

of the substance, or conversely, its hydrophilicity. It is usually expressed in its logarithmic form, log*P*, the more negative the log*P*, the more hydrophilic the substance.

In the case of candidate molecules for the design of amphiphilic compounds, the polarity that should be taken into account is the one of the polar moiety remaining after branching the hydrophobic chain. That is why Table 1 gives the calculated log*P* for a series of monomethylated hydrophilic compounds. Monomethylisosorbide is compared to monomethylated ethyleneglycol, glycerol, sorbitan and glucose derivatives. Log*P* were calculated using Advanced Chemistry Development software V10.02 (ACD/Labs).

Table 1 shows, as expected, that the hydrophilicity of the isosorbide moiety is much lower than the one of glucose (G) and, what can be more surprising, also clearly lower than the one of triethyleneglycol (E<sub>3</sub>), which contains the same number of oxygen and carbon atoms. The hydrophilicity of isosorbide seems to be very close to the one of diethyleneglycol (E<sub>2</sub>) and lower than the one of glycerol (Gly).

This information gives hints on the type of amphiphilic compounds that can be obtained by branching a hydrophobic chain to isosorbide. For diethyleneglycol derivatives (C<sub>2</sub>E<sub>2</sub>), a complete miscibility with water is achieved at room temperature when the alkyl chain contains less than six carbons. A similar limitation has been observed for the monoalkylated derivatives of isosorbide, and only mono C<sub>4</sub>, C<sub>5</sub> and C<sub>6</sub> derivatives of isosorbide were synthesized and evaluated, to estimate the contribution of the lipophilic tail/hydrophilic head ratio on the hydrotropic properties. An attempt to work on the C<sub>8</sub> derivative was made, but, as expected by log*P* calculations, its solubility in water revealed to be very poor (comprised between 0.04% and 0.1% w/w).

Isosorbide, due to a fairly limited polarity, could act as a polar head for the design of short-chain amphiphilic species, of the solvo-surfactant type. The strengths of the hydrophilic and the hydrophobic parts in this type of compounds are not sufficient to afford a real surfactant activity.

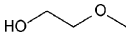
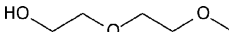
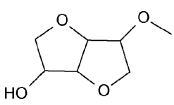
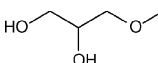
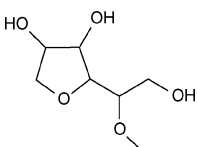
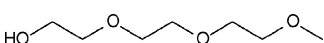
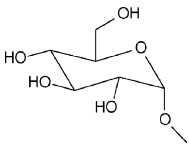
### 2.2.2. Binary phase diagrams of the isosorbide monoethers

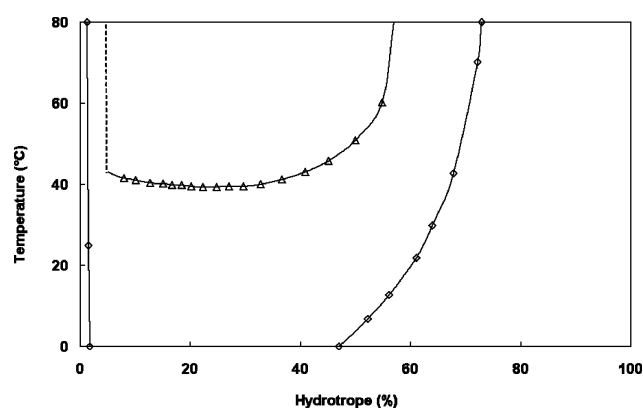
1–3. The binary phase diagrams of short-chain amphiphiles are much less complex than the ones of true surfactants, mainly because of the absence of liquid crystal domains. The binary phase diagrams of the three derivatives in water were constructed and are represented in Fig. 3 for the C<sub>5</sub> and C<sub>6</sub> derivatives. The C<sub>4</sub> derivative exhibited a complete miscibility with water in the whole concentration and temperature ranges (0–90 °C). For all compounds, no liquid crystal domain was observed, which is consistent with the proposed hydrotropic nature of the compounds. However, for the C<sub>5</sub> and especially the C<sub>6</sub> derivatives, a large biphasic domain where two liquids coexist



**Scheme 1** Synthesis of 5-*O*-monobutyl isosorbide 1, 5-*O*-monopentyl isosorbide 2 and 5-*O*-monohexyl isosorbide 3.

**Table 1** LogP calculated for monomethylisorbide, compared to the values for monomethylated ethyleneglycol, sorbitol, glycerol and glucose derivatives

Compound	Polar head denomination	LogP	Predicted polarity
	E <sub>1</sub>	-0.80 ± 0.24	Lower ↓ Higher
	E <sub>2</sub>	-1.16 ± 0.32	
	Iso	-1.17 ± 0.58	
	Gly	-1.30 ± 0.50	
	Sor	-1.49 ± 0.41	
	E <sub>3</sub>	-1.51 ± 0.41	
	G	-2.69 ± 0.24	

**Fig. 3** Binary Phase Diagram of C<sub>5</sub>  $\Delta$  and C<sub>6</sub>  $\diamond$  monoalkyl derivatives of isorbide. The C<sub>4</sub> derivative exhibits a complete miscibility with water in the temperature range studied.

(one surfactant-rich and one surfactant-poor) was observed. Just as oxyethylene-derived amphiphiles, isorbide derivatives are sensitive to temperature changes, with a loss of hydrophilicity when increasing the temperature. The lower temperature above which the phase separation is observed, the so-called Cloud Point, equals 39.3 °C in the case of the C<sub>5</sub> derivative, and is found below 0 °C for the longest homologue.

Table 2 compares the Cloud Points of the isorbide derivatives to the ones of ethyleneglycol and glycerol hydrotropes described in the literature.

**Table 2** Cloud Points for various hydrotropes, from the C<sub>i</sub>E<sub>j</sub>, C<sub>i</sub>Gly and C<sub>i</sub>Iso series

Compound	Cloud Point (°C)	Reference
C <sub>4</sub> E <sub>1</sub>	48.5	24
	45.0	25
C <sub>5</sub> E <sub>2</sub>	34.0	25
C <sub>6</sub> E <sub>2</sub>	0.0	25
	0.1	26
C <sub>6</sub> E <sub>3</sub>	44.0	25
	46.0	27
	40.5	28
C <sub>4</sub> Iso	>100	
C <sub>5</sub> Iso	39.3	
C <sub>6</sub> Iso	<0	
C <sub>4</sub> Gly	>100	22
C <sub>5</sub> Gly	>100	22
C <sub>6</sub> Gly	<0	22

The Cloud Points for the C<sub>5</sub> and C<sub>6</sub> derivatives of isorbide (39.3 °C and <0 °C) are of the same order of magnitude as the ones of the C<sub>5</sub> and C<sub>6</sub> derivatives of E<sub>2</sub> (34.0 °C and 0 °C). This observation is consistent with the close logP values of both polar heads presented in Table 1. The addition of one carbon atom to these derivatives induces the same shift in the Cloud Point value. In the case of glycerol derivatives, this addition has a more dramatic effect on the solubility in water, since the C<sub>5</sub> derivative shows no miscibility gap whereas the C<sub>6</sub> derivative has a Cloud Point below 0 °C. These results confirm that an isorbide polar head can be assimilated, to a first approximation, to a diethylene glycol moiety (E<sub>2</sub>).



Close to the CMC, the C<sub>5</sub>-derivative solutions were slightly turbid, as indicated by a dashed line in the diagram. This behaviour was already observed by Ambrosone *et al.* for C<sub>6</sub>E<sub>3</sub> and was attributed to the “borderline” character of this compound,<sup>29</sup> situated between a completely insoluble C<sub>6</sub>E<sub>2</sub> and a completely soluble and micellizing C<sub>6</sub>E<sub>4</sub>. At low concentrations, the inherent tendency to demixion prevails, until the concentration at which aggregates can be formed is reached.

The position of the miscibility gap for C<sub>5</sub>Iso (39.3 °C) can be interesting for applications in hard-surface cleaning and detergency, since it is located close to the temperature of use (20–40 °C). This means that in this temperature range, the solubility in water is maintained, but the affinity of the hydrotrope is just about to change from water to oil, and it is known that detergency is maximum close to the cloud point. On the contrary, the extended miscibility gap in the case of C<sub>6</sub>Iso could raise problems for applications as hydrotropes, but this could easily be overcome by increasing the cloud point with the addition of salting-in agents.

**2.2.3. Partition of isorbide-, (poly)ethyleneglycol- and glycerol-hydrotropes in a cyclohexane/water mixture.** The partition coefficient of a substance between two immiscible solvents such as oil (o) and water (w) plays an important role in many fields of chemistry, and particularly interfacial chemistry. In the case of surface active species, the partition has to be considered in the monomeric state, that is to say below the critical micellar concentration. In this case, it can be considered as a direct measure of the inner affinity of the amphiphile for both oil and water.<sup>30–34</sup> This measurement is often difficult to carry out for real surfactants, since CMCs are usually very low and the analytical detection limits are reached, but it is more easily achievable for hydrotropes, which start aggregating at higher concentrations (see part 2.3).

The partition coefficients of several short-chain amphiphiles including the isorbide derivatives have been evaluated in the cyclohexane/water system. Cyclohexane was chosen for its relative polarity compared to linear alkanes,<sup>35</sup> in order to get a substantial amount of the compounds in the oil phase, considering their limited hydrophobicity.

The partition coefficients K<sub>ow</sub> have been measured over a 10 °C–60 °C temperature range, in order to access important parameters of the o/w equilibrium by simple thermodynamic considerations. Indeed, considering the following equilibrium:



The partition coefficient is expressed as:

$$K_{\text{ow}} = \frac{a_{\text{Amphiphile,oil}}}{a_{\text{Amphiphile,water}}}$$

Where *a* is the activity of the amphiphile in both phases. In the experimental conditions required for such measurements, concentrations are low and the activity can be replaced by the concentration of the compound in both phases after partition and equilibrium.

Several thermodynamic parameters are related to this equilibrium, namely the standard enthalpy ΔH<sub>w-o</sub><sup>°</sup>, entropy ΔS<sub>w-o</sub><sup>°</sup>

and free energy ΔG<sub>w-o</sub><sup>°</sup> corresponding to the variation of the thermodynamic function during the transfer of one mole of compound from water to cyclohexane.

K<sub>ow</sub> is related to ΔG<sub>w-o</sub><sup>°</sup> by ΔG<sub>w-o</sub><sup>°</sup> = -RT ln K<sub>ow</sub>, where R = 8.31 J.mol<sup>-1</sup>.K<sup>-1</sup> and T is the absolute temperature.

The three thermodynamic constants are related by: ΔG<sub>w-o</sub><sup>°</sup> = ΔH<sub>w-o</sub><sup>°</sup> - TΔS<sub>w-o</sub><sup>°</sup>.

Consequently, it can be written that: ln K<sub>ow</sub> = -ΔH<sub>w-o</sub><sup>°</sup>/RT + ΔS<sub>w-o</sub><sup>°</sup>/R.

If we consider that ΔH<sub>w-o</sub><sup>°</sup> and ΔS<sub>w-o</sub><sup>°</sup> are constant on the considered temperature range, the variation of ln K<sub>ow</sub> with 1/T should be linear and allow accessing these thermodynamic parameters.

Fig. 4 shows the evolution of ln K<sub>ow</sub> with 1/T for two ethylene glycol derivatives (C<sub>4</sub>E<sub>1</sub> and C<sub>4</sub>E<sub>2</sub>), a glycerol derivative (C<sub>5</sub>Gly) and the two shorter isorbide derivatives (C<sub>4</sub>Iso and C<sub>5</sub>Iso).

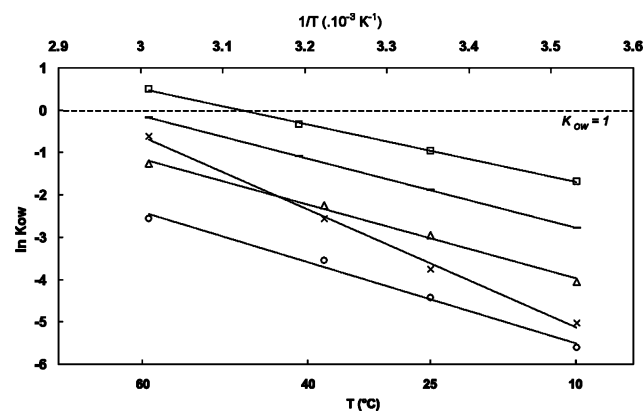


**Fig. 4** Evolution of the logarithm of the partition coefficients in cyclohexane (o)/water (w) in K<sub>ow</sub> with the inverse of temperature for C<sub>4</sub>E<sub>1</sub>, □ C<sub>4</sub>E<sub>2</sub>, C<sub>5</sub>Gly x, C<sub>4</sub>Iso ○ and C<sub>5</sub>Iso △.

For all compounds, the variation of ln K<sub>ow</sub> with 1/T is linear (R<sup>2</sup> > 0.99), which validates the assumption that the standard enthalpy and entropy do not vary significantly in the temperature range studied. These values can be determined from the slope and the y-intercept of the straight lines and are summarized for all compounds in Table 3, together with the standard free energies at 25 °C and 60 °C. These thermodynamic parameters are of the same order of magnitude as the ones obtained for C<sub>i</sub>E<sub>j</sub> surfactants in systems with oils of adapted polarity (ΔH<sub>w-o</sub><sup>°</sup> = 57 kJ/mol for C<sub>10</sub>E<sub>8</sub> in hexane/water,<sup>31</sup> ΔH<sub>w-o</sub><sup>°</sup> = 46 kJ/mol for C<sub>12</sub>E<sub>5</sub> in heptane/water<sup>32</sup>).

The standard free energies ΔG<sub>w-o</sub><sup>°</sup> are all positive at 25 °C, which means that, for all compounds, the transfer from cyclohexane to water is favoured. At this temperature, the affinity for water follows the tendency: C<sub>4</sub>Iso > C<sub>5</sub>Gly > C<sub>5</sub>Iso > C<sub>4</sub>E<sub>2</sub> > C<sub>4</sub>E<sub>1</sub>. At 25 °C, for the same chain length, the isorbide polar head is more hydrophilic than a diethylene glycol, but less than a glyceryl group.

At 60 °C, ΔG<sub>w-o</sub><sup>°</sup> becomes negative for C<sub>4</sub>E<sub>1</sub>, signifying that the loss of hydrophilicity of the E<sub>1</sub> moiety on temperature increase has turned the affinity of the amphiphile to the oil phase. For the other compounds, the greater affinity for water is maintained, and at this temperature, the hydrophilic classification of the compounds is: C<sub>4</sub>Iso > C<sub>5</sub>Iso > C<sub>5</sub>Gly > C<sub>4</sub>E<sub>2</sub> > C<sub>4</sub>E<sub>1</sub>. Thus, at 60 °C, the isorbide derivatives are

**Table 3** Thermodynamic data for the partition of the short-chain amphiphiles in cyclohexane/water obtained from the linear evolution of  $\ln K_{ow}$  with the inverse of temperature presented on Fig. 4

Hydrotrope	$\Delta H_{w-o}^{\circ}$ (kJ/mol)	$\Delta S_{w-o}^{\circ}$ (J/mol/K)	$\Delta G_{w-o}^{\circ}$ (kJ/mol) at 25 °C	$\Delta G_{w-o}^{\circ}$ (kJ/mol) at 60 °C
C <sub>4</sub> E <sub>1</sub>	35	108	2.4	-1.4
C <sub>4</sub> E <sub>2</sub>	42	124	4.7	0.3
C <sub>4</sub> Iso	49	127	11.1	6.7
C <sub>5</sub> Iso	44	124	7.5	3.2
C <sub>5</sub> Gly	71	208	9.2	1.7

still more polar than their ethylene glycol counterparts, and become more polar than their glycerol counterpart. This means that on temperature increase, the isosorbide polar head is less sensitive to a loss of hydrophilicity than glycerol. However, the temperature-dependence seems to be of the same order of magnitude for isosorbide and ethylene glycol derivatives, as indicated by the close slope (*i.e.*  $\Delta H_{w-o}^{\circ}$ ) values. Here again, the isosorbide polar head compares well with the diethylene glycol, as far as the temperature-dependence is concerned. The absolute  $K_{ow}$  values of C<sub>4</sub>E<sub>2</sub> and C<sub>4</sub>Iso, at all temperatures, seem to indicate that the isosorbide moiety brings a slightly higher hydrophilic contribution than diethyleneglycol.

### 2.3. Hydrotropic properties of the isosorbide monoethers

**2.3.1. Surface tension.** The evolution of the surface tension with the concentration is presented in Fig. 5 for the three compounds. The surface tension decreases with increasing concentration in water until reaching a plateau in the case of the C<sub>4</sub> and C<sub>5</sub> derivatives. For the C<sub>6</sub> derivative, the solubility limit is attained before the surface saturation (represented by a dashed line on Fig. 5). As expected for hydrotropic species, the breaks in the curves are not as pronounced as in the case of real surfactants and the minimum surface tension is attained at higher concentrations. However, a change in the slope is usually observed<sup>36-38</sup> at a Minimum Aggregation Concentration (MAC) and coincides with the concentration at which other physico-chemical properties are modified. It is also in accordance with the concentration at which the increase in hydrophobic compound solubilisation becomes significant.

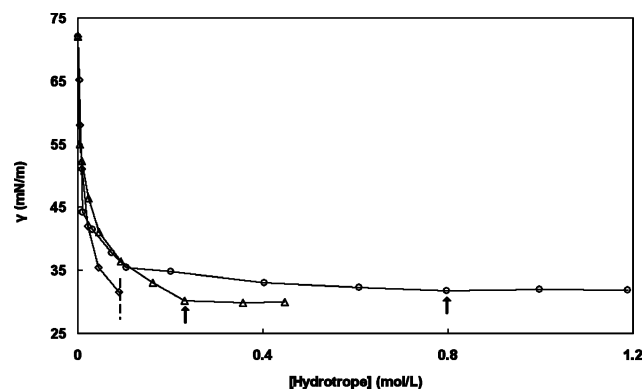


**Fig. 5** Surface tension vs. concentration for the three isosorbide derivatives C<sub>4</sub>Iso, ○ C<sub>5</sub>Iso △ and C<sub>6</sub>Iso ◇.

The minimum aggregation concentrations of the C<sub>4</sub> and C<sub>5</sub> derivatives given in Table 4 are represented by small arrows on the curves. They represent the point from which no more

**Table 4** Air/water surface tension data for the three isosorbide derivatives

Compound	MAC (mol/L)	$\gamma_{min}$ (mN/m)
C <sub>4</sub> Iso	0.80	32.1
C <sub>5</sub> Iso	0.23	29.8
C <sub>6</sub> Iso	—	—

evolution is observed in the measured surface tension. Table 4 also gives the minimum surface tensions, showing a better surface activity of C<sub>5</sub>Iso compared to C<sub>4</sub>Iso, consistent with the longer lipophilic part of the amphiphile.

**2.3.2. Solubilisation.** The main application of hydrotropes is the solubilisation of hydrophobic compounds and ionic surfactants in water. Their solubilising action is not completely understood yet, but it is believed to be linked to their ability to self-associate in water.<sup>39</sup>

The efficiency of the two shorter isosorbide derivatives has been assessed by measuring the amount of 1-methylnaphthalene solubilised in aqueous solutions containing increasing concentrations of hydrotropes. 1-Methylnaphthalene was chosen because it can be considered as a good mimic of organic soil and has the advantage to absorb in the UV region, which makes the quantification easier.

Results are presented in Fig. 6 for C<sub>4</sub>Iso and C<sub>5</sub>Iso compared to C<sub>4</sub>E<sub>1</sub> solutions. From these curves, two characteristic features of the hydrotropic action have been extracted: the efficiency, defined as the slope of the linear part of the solubilisation curves in a log linear representation<sup>20</sup> and the amount of organic compound solubilised for a given concentration of hydrotrope-1 mol/L here. The MHC, Minimum Hydrotropic Concentration, often referred to as the concentration of hydrotrope from which

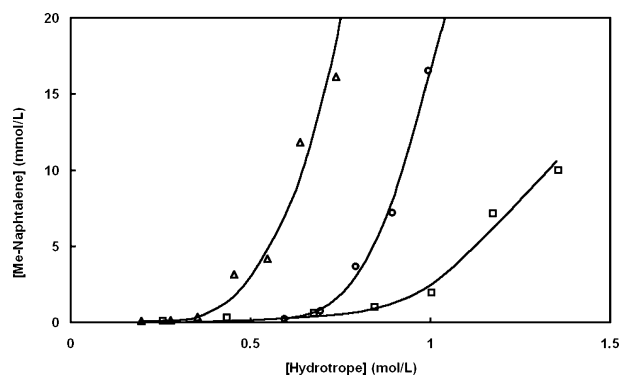


**Fig. 6** Solubilisation of 1-methylnaphthalene by aqueous solutions of the isosorbide derivatives C<sub>4</sub>Iso○ and C<sub>5</sub>Iso△ compared to reference solvo-surfactant C<sub>4</sub>E<sub>1</sub>□.

**Table 5** Solubilising of 1-methylnaphtalene by the isosorbide derivatives C<sub>4</sub>Iso and C<sub>5</sub>Iso compared to reference solvo-surfactant C<sub>4</sub>E<sub>1</sub>. The efficiency is the slope of the linear part of the solubilisation curves in a log linear representation (not presented here)

Hydrotrope	Efficiency [Me-Napht] (mmol/L)/[hydrotrope] (mol/L)	[Me-Napht] (mmol/L) solubilised in a 1M-solution of hydrotrope
C <sub>4</sub> Iso	12.3	17.2
C <sub>5</sub> Iso	13.2	51.8
C <sub>4</sub> E <sub>1</sub>	3.7	1.9

the solubilisation starts to be effective, has not been determined here because of the difficulty to estimate the curve taking-off. It usually corresponds to the MAC given by surface tension measurements, which confirms the supposed solubilisation mechanism of hydrotropes. Table 5 summarizes the values for the three compounds.

It is clear from Fig. 6 and Table 5 that the isosorbide derivatives are more efficient and solubilise 1-methylnaphtalene and at lower concentrations than model hydrotrope C<sub>4</sub>E<sub>1</sub>. C<sub>5</sub>Iso is the most efficient, since it has the right balance between its hydrophilic and hydrophobic parts allowing a good water solubility together with a substantial affinity for organics.

The better efficiency of isosorbide derivatives compared to short-chain ethyleneglycol ether is particularly promising. This result can not be attributed to a particular affinity for the isosorbide derivatives for the model organic compound chosen, since it has been demonstrated that the aqueous solubilisation process by hydrotropes is not dependent on the solute.<sup>20</sup> The higher efficiency could alternatively be attributed to a different molecular organisation of the amphiphiles allowing a better association of the organic compound with the hydrotrope aggregates after the MAC. We can suppose that the molecular structure of the isosorbide polar head, significantly more rigid than an ethylene oxide moiety, dictates the self-association of the compounds and can lead to a better and more efficient structure, compared to the weak aggregates formed by C<sub>4</sub>E<sub>1</sub>.<sup>38</sup> More detailed studies, as for instance the measurement of self-diffusion coefficients in water by PGSE NMR should shed more light on the behaviour and action of such hydrotropes.

## Conclusion

Derived from sorbitol, a leading product of the starch industry, isosorbide can be obtained in large amounts and at reasonable prices. This makes it a good candidate for the valorisation of sugar-derived compounds for the synthesis of new products for large-scale markets as for instance the detergent industry. LogP calculations on different hydrophilic moieties proved to be a good tool to predict the strength of this new polar head, and the type of amphiphiles that can be synthesized from it. The hydrophilicity of isosorbide being somewhat limited, equivalent or slightly higher than a diethylene glycol, monoalkylated derivatives need to have a relatively short alkyl chain to ensure a good water solubility. The amphiphilic species obtained are thus classified as hydrotropes, or solvo-surfactants.

Mono-C<sub>4</sub>, C<sub>5</sub> and C<sub>6</sub> isosorbide have been synthesized, and can be considered as good solvo-surfactants, as regards to their behaviour in water and ability to solubilise model organic compound 1-methylnaphtalene in water. Their sensitivity to temperature changes seems to be lower than glycerol homo-

logues, and of the same order of magnitude as diethyleneglycol counterparts. Additional studies are in progress to evaluate their potential use for degreasing and hard-surface cleaning.

Biodegradability and toxicity studies are still in progress to accurately assess the “green” character of these new derivatives. Preliminary results show that the *in vitro*-cytotoxicity of the isosorbide derivatives is slightly lower than that of glycerol derivatives.<sup>23</sup> These first studies show that the use of isosorbide for the synthesis of new hydrotropes is promising, in fields where it is necessary to enhance the solubility of organic compounds in water, in replacement of petroleum-derived short-chain C<sub>i</sub>E<sub>j</sub>.

## Acknowledgements

Roquette, the world-leader in the production, technology and application of polyols like sorbitol and isosorbide, is gratefully acknowledged for the gift of the isosorbide sample used for the synthesis of short-chain amphiphiles.

## References

- 1 C. Stubenrauch, *Curr. Opin. Colloid Interface Sci.*, 2001, **6**(2), 160–170.
- 2 N. Noiret, Th. Benvegnu and D. Plusquellec, *L'Actualité Chimique*, 2002, **258–259**, 70–75.
- 3 W. von Rybinski and K. Hill, *Angew. Chem., Int. Ed.*, 1998, **37**(10), 1328–1345.
- 4 S. Piccicuto, C. Blecker, J.-C. Brohee, A. Mbampara, G. Lognay, C. Deroanne, M. Paquot and M. Marlier, *Biotechnol. Agron. Soc. Environ.*, 2001, **5**(4), 209–219.
- 5 Y. Queneau, J. Fitremann and S. Trombotto, *C. R. Chim.*, 2004, **7**(2), 177–188.
- 6 M. Roussel, T. Benvegnu, V. Lognone, H. Le Deit, I. Soutrel, I. Laurent and D. Plusquellec, *Eur. J. Org. Chem.*, 2005, **14**, 3085–3094.
- 7 D. J. Claffey, M. F. Casey and P. A. Finan, *Carbohydr. Res.*, 2004, **339**(14), 2433–2440.
- 8 R. Tamion, F. Marsais, P. Ribereau and G. Queguiner, *Tetrahedron: Asymmetry*, 1993, **4**(12), 2415–2418.
- 9 S. Kumar and U. Ramachandran, *Tetrahedron*, 2005, **61**(16), 4141–4148.
- 10 R. Tamion, F. Marsais, P. Ribereau, G. Queguiner, D. Abenhaim, A. Loupy and L. Munnier, *Tetrahedron: Asymmetry*, 1993, **4**(8), 1879–1890.
- 11 D. Abenhaim, A. Loupy, L. Munnier, R. Tamion, F. Marsais and G. Queguiner, *Carbohydr. Res.*, 1994, **261**(2), 255–66.
- 12 P. Stoss and R. Hemmer, *Adv. Carbohydr. Chem. Biochem.*, 1991, **49**, 93–173.
- 13 R. Seemayer, N. Bar and M. P. Schneider, *Tetrahedron: Asymmetry*, 1992, **3**(9), 1123–1126.
- 14 A. Roy and H. P. S. Chawla, *Enzyme Microb. Technol.*, 2001, **29**(8–9), 490–493.
- 15 Z. Cekovic and Z. Tokic, *Synthesis*, 1989, **8**, 610–612.
- 16 P. Rossi, J. W. Wiechers and C. Kelly, *Cosmetics & Toiletries*, 2005, **120**(3), 107–111.
- 17 S. Chatti, M. Bortolussi and A. Loupy, *Tetrahedron Lett.*, 2000, **41**(18), 3367–3370.
- 18 A. Matero, in *Handbook of Applied Surface and Colloid Chemistry*, ed. K. Holmberg, Wiley, Chichester, 2002, vol. 1, ch. 18, pp. 407–420.

- 19 A. Matero, A. Mattsson and M. Svensson, *J. Surf. Det.*, 1998, **1**(4), 485–489.
- 20 P. Bauduin, A. Renoncourt, A. Kopf, D. Touraud and W. Kunz, *Langmuir*, 2005, **21**(15), 6769–6775.
- 21 A. Laudet-Hesbert, *Toxicol. Lett.*, 2005, **156**(1), 51–58.
- 22 S. Queste, P. Bauduin, D. Touraud, W. Kunz and J.-M. Aubry, *Green Chem.*, 2006, **8**(9), 822–830.
- 23 S. Queste, Y. Michina, A. Dewilde, R. Neueder, W. Kunz and J.-M. Aubry, *Green Chem.*, 2007, **9**(5), 491–499.
- 24 K. Y. Kim and K.-H. Lim, *J. Chem. Eng. Data*, 2001, **46**(4), 967–973.
- 25 M. N. Garcia-Lisbona, A. Galindo, G. Jackson and A. N. Burgess, *J. Am. Chem. Soc.*, 1998, **120**(17), 4191–4199.
- 26 H.-S. Lee and H. Lee, *J. Chem. Eng. Data*, 1996, **41**(6), 1358–1360.
- 27 K. V. Schubert, R. Strey and M. Kahlweit, *J. Colloid Interface Sci.*, 1991, **141**(1), 21–29.
- 28 P. D. T. Huibers, D. O. Shah and A. R. Katritzky, *J. Colloid Interface Sci.*, 1997, **193**(1), 132–136.
- 29 L. Ambrosone, L. Costantino, G. D'Errico and V. Vitagliano, *J. Colloid Interface Sci.*, 1997, **190**(2), 286–293.
- 30 F. Ravera, M. Ferrari and L. Liggieri, *Adv Colloid Interface Sci.*, 2000, **88**(1–2), 129–177.
- 31 M. Ferrari, L. Liggieri and F. Ravera, *J. Phys. Chem. B*, 1998, **102**(51), 10521–10527.
- 32 R. Aveyard, B. P. Binks, S. Clark and P. D. I. Fletcher, *J. Chem. Soc. Faraday Trans.*, 1990, **86**(18), 3111–3115.
- 33 F. Ravera, M. Ferrari, L. Liggieri, R. Miller and A. Passerone, *Langmuir*, 1997, **13**(18), 4817–4820.
- 34 I. J. Lin and L. Marszall, *Prog. Colloid Polym. Sci.*, 1978, **63**, 99–104.
- 35 S. Queste, J. L. Salager, R. Strey and J. M. Aubry, *J. Colloid Interface Sci.*, 2007, **312**(1), 98–107.
- 36 G. Onori and A. Santucci, *J. Mol. Liq.*, 1996, **69**, 161–181.
- 37 G. Onori and A. Santucci, *J. Phys. Chem. B*, 1997, **101**(23), 4662–4666.
- 38 P. K. Kilpatrick, H. T. Davis, L. E. Scriven and W. G. Miller, *J. Colloid Interface Sci.*, 1987, **118**(1), 270–285.
- 39 T. K. Hodgdon and E. W. Kaler, *Curr. Opin. Colloid Interface Sci.*, 2007, **12**(3), 121–128.



# Isolute<sup>®</sup> Si-carbonate catalyzes the nitronate addition to both aldehydes and electron-poor alkenes under solvent-free conditions†

Roberto Ballini,<sup>\*a</sup> Giovanna Bosica,<sup>a</sup> Alessandro Palmieri,<sup>a</sup> Ferdinando Pizzo<sup>b</sup> and Luigi Vaccaro<sup>b</sup>

Received 18th December 2007, Accepted 11th February 2008

First published as an Advance Article on the web 5th March 2008

DOI: 10.1039/b719477c

It has been found that commercial ISOLUTE<sup>®</sup> Si-carbonate catalyzes both nitroaldol and Michael reactions, from nitroalkanes and under solvent-free conditions, allowing satisfactory to good yields of nitroalkenols and  $\gamma$ -nitro-functionalized carbonyl and cyano derivatives. In addition, a one-pot Henry–Michael reaction can be performed.

## Introduction

In the 21st century we can expect the drive toward cleaner technologies brought about by public, legislative and corporate pressure to provide new and exciting opportunities for catalysis and catalytic processes.<sup>1</sup> In this context, the heterogeneous catalysis shows great potential for environmental pollution control.

The efficient use of a solid catalyst that stays in a separate phase from the organic compounds can go a long way to achieve important goals. In fact, product isolation is simplified and reactions often run under milder conditions and give higher selectivity. The atom efficiency of the reaction is improved, the process is facilitated, precious raw materials used in the manufacture of the catalyst have increased lifetime (through reuse), and the volume of waste is significantly reduced.<sup>2</sup>

Commercial ISOLUTE<sup>®</sup> Si-carbonate [silica trimethylammonium carbonate; Si-TMS(CO<sub>3</sub><sup>-2</sup>)<sub>0.5</sub>] is a bound equivalent of tetramethylammonium carbonate, which has traditionally been used as a quaternary anion-exchanger for quenching, neutralizing and desalting organic mixtures. Recently more versatile applications have been reported such as organic acid scavenging for fast purification of amide and biaryl libraries.<sup>3</sup>

## Results and discussion

During our studies into the chemistry of nitroalkanes,<sup>4</sup> and particularly to the search for more eco-friendly conditions for their use as stabilized carbanions,<sup>5</sup> we were attracted by ISOLUTE<sup>®</sup> Si-carbonate as a potential supported base to generate the nitronate forms under solvent-free conditions.

Henry<sup>6</sup> and Michael<sup>4c</sup> reactions, involving nitroalkanes, are two of the most used procedures for the generation of new

carbon–carbon bonds and for the preparation of polyfunctionalized structures. As routine procedures, these reactions are performed in the presence of different bases in homogeneous solutions of organic solvents or, alternatively, under heterogeneous catalysis<sup>4c,7</sup> and, for these purposes, even with the help of sonication,<sup>8</sup> high pressure<sup>9,10</sup> or the need for complex catalysts prepared by using toxic solvents<sup>11</sup> have been proposed. In addition, these methodologies very often suffer from different drawbacks such as: (i) (Henry reaction) low yields, retroaldol reaction, formation of side products due to the aldol condensation and/or Cannizzaro reaction of aldehydes or olefin formation, and (ii) (Michael reaction) low yields, multi-addition reactions, the need of a large excess of nitroalkanes that, for valuable nitro derivatives and for the production of waste, is a serious problem from both an economical and ecological point of view.

Thus, considering that over the past few years, a significant amount of research has been directed towards the progress of new technologies for environmentally benign processes, the development of new general, efficient eco-friendly catalytic procedures for both Henry and Michael reactions is desirable.

In this context, we report herein that commercial ISOLUTE<sup>®</sup> Si-carbonate has been found, in our laboratory, to be a new efficient catalyst for both the Henry and Michael reactions under solvent free-conditions.

Firstly, we chose two model reactions for these transformations in order to find the best reaction conditions and, as reported in Table 1 and 2, we examined the nitroaldol reaction of 1-nitrobutane with dihydrocinnamaldehyde (formation of **3a**) and the conjugate addition of 1-nitrobutane to ethyl vinyl

<sup>a</sup>“Green Chemistry Group”, Dipartimento di Scienze Chimiche dell’Università di Camerino, Via S. Agostino 1, 62032, Camerino, Italy. E-mail: roberto.ballini@unicam.it; Fax: +39 07374 02297; Tel: +39 0737 402270

<sup>b</sup>CEMIN-Laboratory of Green Synthetic Organic Chemistry, Dipartimento di Chimica dell’Università di Perugia, Via Elce di Sotto 8, 06123, Perugia, Italy. E-mail: pizzo@unipg.it; Fax: +39 075 5855560; Tel: +39 075 5855546

† Electronic supplementary information (ESI) available: Analytical data for **3a–j**, **5a–k** and **6**. See DOI: 10.1039/b719477c

**Table 1** Best catalyst/substrate ratio for the Henry reaction

Catalyst/substrate	Yield (%) of <b>3a</b>
0.05	10
0.1	87
0.15	80

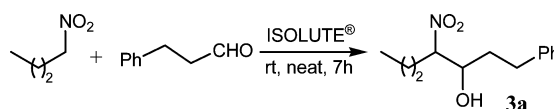


**Table 2** Best catalyst/substrate ratio for the Michael reaction

Catalyst/substrate	Yield (%) of <b>5a</b>
0.05	73
0.1	87
0.15	86
0.2	70

ketone (formation of **5a**). The reactions were carried out at room temperature for 7 h, with different amounts of catalyst, and in both cases the more convenient catalyst/substrate ratio seems to be = 0.1.

In order to verify the efficiency of the method for the nitroaldol reaction, we tested a number of different nitroalkanes and aldehydes (Table 3). All the reactions were carried out at room temperature, mixing a stoichiometric amount of **1** and **2**, with 10 mol% of the catalyst and in the absence of any solvent.

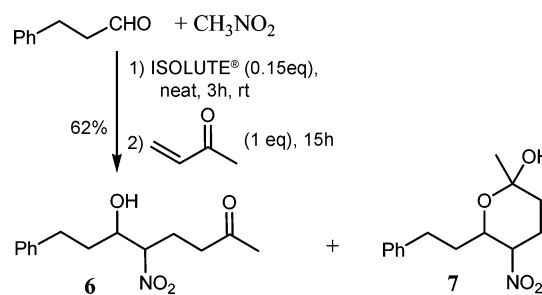
By this method, simple and functionalized primary and secondary nitroalkanes give good results with both aliphatic and aromatic aldehydes. Moreover, 1-bromo-1-nitroalkan-2-ols (entry 9 and 10), an important class of compounds very useful for practical applications in the manufacturing photographic materials,<sup>12</sup> ink-based materials,<sup>13</sup> or for their important properties such as biocide<sup>14</sup> and antimicrobial activity,<sup>15</sup> can be efficiently prepared by our procedure.<sup>16</sup> Although the present method results in a diastereomeric mixture of nitroalcohols, according with most of the reported approaches, this doesn't seem to be a problem since the main uses are the conversion into  $\alpha$ -nitro ketones<sup>17</sup> or conjugated nitroalkenes,<sup>18</sup> in which at least one stereogenic centre is lost.

The generality of our catalytic system has been extended to the Michael reaction, investigating the reactivity of a series of nitroalkanes with an array of electron-poor alkenes (Table 4).

The reaction works well with primary and secondary nitroalkanes and with different electron-poor alkenes, even with poor electrophilic alkenes, such as  $\alpha,\beta$ -unsaturated esters (entry

5 and 11),  $\alpha,\beta$ -unsaturated nitriles (entry 6) or  $\alpha,\beta$ -unsaturated sulfones (entry 10), and with hindered electrophilic alkenes, such as 2-cyclohexen-1-one (72%, entry 3) and 2-cyclopenten-1-one (91%, entry 4) that, usually, give moderate yields.<sup>19</sup> In addition, a further class, 1-bromo-1-nitroderivatives (entry 7), can be efficiently prepared under our conditions.

It is important to point out that the use of the same catalyst for both Henry and Michael reactions, *via* nitroalkanes, offers an important opportunity for a one-pot Henry–Michael solventless process. In fact, as reported in Scheme 1, mixing dihydrocinnamaldehyde with nitromethane (1 equiv.) and catalyst (0.15 equiv.) at room temperature, followed, after 3 h (the reaction was checked by TLC), by the addition of methyl vinyl ketone (1 equiv.) and leaving the mixture for further 15 h, allows the direct preparation of the keto nitroalkanol **6**, in equilibrium with its ketalic form **7**, in 62% overall yield (**6/7**  $\approx$  5:1).

**Scheme 1**

Finally, we faced the problem of catalyst recycling: at the end of the model reaction (formation of **5a**) the catalyst was filtered, washed with EtOAc, dried under vacuum and reused. The catalyst could be utilized with comparable results at least for six further cycles (Table 5).

## Conclusions

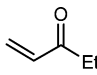
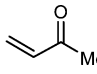
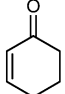
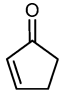
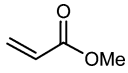
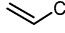
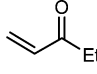
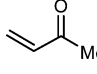
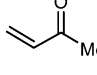
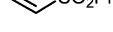
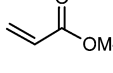
Following our procedures both nitroalkanol **3** (58–87%) and Michael adducts **5** (59–91%) can be efficiently

**Table 3** Nitroalkanol **3** obtained by the Henry reaction

Entry	R	R <sup>1</sup>	R <sup>2</sup>	Reaction time/h	Yield (%) <sup>a</sup> of <b>3</b>
1	<i>n</i> -Pr	H	Ph(CH <sub>2</sub> ) <sub>2</sub>	7	87 ( <b>3a</b> )
2	<i>n</i> -Pr	H	Ph	16	78 ( <b>3b</b> )
3	Ph(CH <sub>2</sub> ) <sub>2</sub>	H	<i>n</i> -C <sub>5</sub> H <sub>11</sub>	5	82 ( <b>3c</b> )
4	MeOCO(CH <sub>2</sub> ) <sub>4</sub>	H	Ph	16	69 ( <b>3d</b> )
5	MeOCO(CH <sub>2</sub> ) <sub>4</sub>	H	<i>n</i> -C <sub>5</sub> H <sub>11</sub>	8	68 ( <b>3e</b> )
6	Me	Me	Et	7	58 ( <b>3f</b> )
7	Me	H	Ph	16	77 ( <b>3g</b> )
8	<i>n</i> -Bu	H	<i>c</i> -C <sub>6</sub> H <sub>11</sub>	8	83 ( <b>3h</b> )
9	Br	H	<i>n</i> -Bu	9	71 ( <b>3i</b> )
10	Br	H	<i>m</i> -NO <sub>2</sub> C <sub>6</sub> H <sub>4</sub>	16	63 ( <b>3j</b> )

<sup>a</sup> Yield of pure isolated product

**Table 4** Michael adducts **5** prepared

$  \begin{array}{c}  \text{NO}_2 \\    \\  \text{R}-\text{C}-\text{R}^1 \\  \mathbf{1}  \end{array}  + \begin{array}{c}  \text{EWG} \\    \\  \text{CH}_2=\text{CH} \\  \mathbf{4}  \end{array}  \xrightarrow[\text{rt, neat}]{\text{ISOLUTE}^\circledast}  \begin{array}{c}  \text{NO}_2 \\    \\  \text{R}-\text{C}-\text{CH}_2-\text{CH}_2-\text{EWG} \\  \mathbf{5a-k}  \end{array}  $						
Entry	R	R <sup>1</sup>	Electron-poor alkene <b>4</b>	Michael Adduct <b>5</b>	Reaction time/h	Yield (%) <sup>a</sup> of <b>5</b>
1	<i>n</i> -Pr	H		<b>5a</b>	7	87
2	<i>n</i> -C <sub>5</sub> H <sub>11</sub>	H		<b>5b</b>	7	86
3	<i>n</i> -C <sub>4</sub> H <sub>9</sub>	H		<b>5c</b>	10	72
4	PhCH <sub>2</sub>	H		<b>5d</b>	16	91
5	<i>n</i> -Pr	H		<b>5e</b>	30	62 <sup>b</sup>
6	PhCH <sub>2</sub>	H		<b>5f</b>	27	59 <sup>b</sup>
7	Br	H		<b>5g</b>	8	71
8	MeCO(CH <sub>2</sub> ) <sub>2</sub>	H		<b>5h</b>	7	75
9	Me	Me		<b>5i</b>	16	85
10	<i>n</i> -C <sub>4</sub> H <sub>9</sub>	H		<b>5j</b>	20	61
11	Me	Me		<b>5k</b>	24	60

<sup>a</sup> Yield of pure isolated product. <sup>b</sup> The reaction performed at 50 °C gave poor yield (45% for **5e** and 40% for **5f**, after 30 and 27 h, respectively), probably due to the partial desorption of the (low boiling) Michael acceptors.

**Table 5** Yield of recycled catalyst in the model Michael reaction

$  \begin{array}{c}  \text{NO}_2 \\    \\  \text{C}_2\text{H}_5 \\  \mathbf{1}  \end{array}  + \begin{array}{c}  \text{O} \\     \\  \text{CH}_2=\text{CH}-\text{C}-\text{CH}_2-\text{CH}_3 \\  \mathbf{4}  \end{array}  \xrightarrow[\text{rt, neat, 7h}]{\text{ISOLUTE}^\circledast}  \begin{array}{c}  \text{NO}_2 \\    \\  \text{C}_2\text{H}_5-\text{C}-\text{CH}_2-\text{CH}_2-\text{C}-\text{CH}_2-\text{CH}_3 \\  \mathbf{5a}  \end{array}  $	
	Yield (%) of <b>5a</b>
Initial reaction	87
1st recycle	80
2nd recycle	78
3th recycle	76
4th recycle	75
5th recycle	73
6th recycle	71
7th recycle	58
8th recycle	50

prepared under moderate reaction times, avoiding the need of any solvent and of expensive use of energy since all the reactions can be carried out at room temperature. Moreover, the very mild conditions needed (room temperature and 10% of the catalyst) favour the observed high chemoselectivity and prevent the typical side reactions of both Henry and Michael processes. Any work up can be avoided since the crude products can be charged, directly, onto a chromatographic column (see Experimental). In addition, the catalyst is easily commercially available and can be reused several times (at least six times, Table 5) with a modest decreasing of the yields. Moreover, under our conditions even a variety of 1-bromo-1-nitro derivatives can be easily obtained, and the one-pot Henry–Michael solvent-free process (Scheme 1) can be efficiently performed, giving rise to the one-flask formation of complex molecules with

evident synthetic advantages. Thus, our procedure represents an important improvement of the Henry and Michael reaction *via* nitroalkanes, especially from an economical and ecological point of view.

## Experimental

### Materials and methods

GLC analyses were performed with an SE-54 fused silica capillary column (25 m, 0.32 mm internal diameter), FID detector and nitrogen as carrier gas. GS-MS analyses were carried out by means of the EI technique (70 eV). All chemicals were purchased and used without further purifications; just some known nitroalkanes, such as 1-nitro-3-phenylpropane, 1-nitro-2-phenylethane, methyl 6-nitrohexanoate and 5-nitro-2-pentanone, were prepared by the standard procedures.<sup>4,6a,7,19</sup> ISOLUTE® Si-carbonate, capacity 0.17 mmol g<sup>-1</sup>, was purchased by StepBio. Analytical data for **3a–j**, **5a–k** and **6** can be found in the ESI.†

### Typical procedure for both nitroaldol and Michael reactions

To a stirred solution of nitroalkane (1 mmol) and the appropriate electrophile (1 mmol of **2** or **4**), 0.588 g (0.1 equiv) of ISOLUTE® Si-carbonate were added at room temperature, then the resulting mixture was mechanically stirred for the appropriate time (TLC and GC, Table 3 and Table 4). After that, the reaction can be treated differently bearing in mind two different goals: avoiding the work up (way a) or recycling the catalyst (way b).

Way a: The mixture was directly charged onto a chromatographic column (EtOAc–cyclohexane) for the immediate purification by flash chromatography, giving the pure product **3** or **5**.

Way b: The mixture was treated with EtOAc (20 mL) and the catalyst was recovered by filtration, then washed with further EtOAc, dried under vacuum and reused, while the organic layer was evaporated and the crude product purified by flash chromatography (EtOAc–cyclohexane), allowing the pure nitroalkanol **3** or **5**.

### Acknowledgements

The authors thanks the University of Camerino, the University of Perugia and MUR-Italy (PRIN 2006, project: Sintesi Organiche Ecosostenibili Mediate da Nuovi Sistemi Catalitici) for financial support.

### Notes and references

- 1 (a) J. H. Clark, C. N. Rhodes, *RSC Clean Technology Monographs*, ed. J. H. Clark, RSC, Cambridge, 2000; (b) J. H. Clark, *Acc. Chem. Res.*, 2002, **35**, 791–797.

- 2 (a) A. McKillop and D. W. Young, *Synthesis*, 1979, 401–422; (b) M. Noritaka and M. Misono, *Chem. Rev.*, 1998, **98**, 199–217; (c) P. M. Maitlis, H. C. Long, R. Quyoum, M. L. Turner and Z.-Q. Wang, *Chem. Commun.*, 1996, 1–8; (d) R. A. Sheldon, *Chem. Ind.*, 1997, 12–15.
- 3 Y. Wang and D. R. Sauer, *Org. Lett.*, 2004, **6**, 2793–2796.
- 4 (a) G. Rosini and R. Ballini, *Synthesis*, 1988, 833–847; (b) R. Ballini and M. Petrini, *Tetrahedron*, 2004, **60**, 1017–1047; (c) R. Ballini, G. Bosica, D. Fiorini, A. Palmieri and M. Petrini, *Chem. Rev.*, 2005, **105**, 933–971.
- 5 (a) G. Sartori, R. Ballini, F. Bigi, G. Bosica, R. Maggi and P. Righi, *Chem. Rev.*, 2004, **104**, 199–250; (b) R. Ballini, L. Barboni, F. Fringuelli, A. Palmieri, F. Pizzo and L. Vaccaro, *Green Chem.*, 2007, **9**, 823–838.
- 6 (a) G. Rosini, in *Comprehensive Organic Synthesis*, ed. B. M. Trost, Pergamon, New York, 1992, 321–340; (b) F. A. Luzzio, *Tetrahedron*, 2001, **57**, 915–945; (c) K. Akutu, H. Kabashima, T. Seki and H. Hattori, *J. Appl. Catal. A*, 2003, **247**, 65–74.
- 7 R. Ballini and A. Palmieri, *Curr. Org. Chem.*, 2006, **10**, 2145–2169.
- 8 B. Jouglot, L. Bianco and G. Rousseau, *Synlett*, 1991, 907–908.
- 9 A. Sera, K. Takagi, H. Katayama and H. Yamada, *J. Org. Chem.*, 1988, **53**, 1157–1161.
- 10 Y. Misuri, R. A. Bulman and W. Matsumoto, *Heterocyclic*, 2002, **56**, 599–606.
- 11 R. Ballini, G. Bosica, D. Livi, A. Palmieri, R. Maggi and G. Sartori, *Tetrahedron Lett.*, 2003, **44**, 2271–2273.
- 12 (a) M. Satake, Y. Maekawa and T. Shishido, (Fuji Photo Film Co., Ltd., Japan), *Japanese Patent Application* JP 01100532 A2, 1989; (b) M. Satake, Y. Maekawa and T. Shishido, *Chem. Abstr.*, 1990, **112**, 108414; (c) S. Hirabayashi, (Konishiroku Photo Industry Co., Ltd., Japan), *Japanese Patent Application* JP 071406206, 1995; (d) S. Hirabayashi, *Chem. Abstr.*, 1995, **123**, 241899; (e) T. Marui, (Konica Co., Japan), *Japanese Patent Application* JP 03120531 A2, 1991; (f) T. Marui, *Chem. Abstr.*, 1991, **115**, 266714; (g) H. Sakata, T. Nagashima, T. Arai, (Konica Co., Japan), *Japanese Patent Application* JP 03038634 A2, 1991; (h) H. Sakata, T. Nagashima and T. Arai, *Chem. Abstr.*, 1991, **115**, 243848.
- 13 (a) K. Mine, Y. Kobayashi, Y. Kawaguchi, S. Aoki, (Konishiroku Photo Industry Co., Ltd., Japan), *Japanese Patent Application* JP 61055173 A2, 1986; (b) K. Mine, Y. Kobayashi, Y. Kawaguchi and S. Aoki, *Chem. Abstr.*, 1986, **105**, 99202.
- 14 (a) R. Elsmore, W. G. Guthrie and J. A. Parr, *Spec. Chem. Mag.*, 1987, **7**, 166–176; (b) T. Yamada, (Konishiroku Photo Industry Co., Ltd., Japan), *Japanese Patent Application* JP 08134371 A2, 1996; (c) T. Yamada, *Chem. Abstr.*, 1996, **125**, 208284; (d) Kanesho Co., Ltd., *Japanese Patent Application* JP 60048903 A2, 1985; (e) W. Shiyunosuke and T. Shigeaki, *Chem. Abstr.*, 1985, **103**, 49761.
- 15 (a) N. G. Clark, B. Croshaw, D. F. Spooner, (Boots Pure Drug Co., Ltd.), *English Patent Application* GB 1057131, 1967; (b) N. G. Clark, B. Croshaw and D. F. Spooner, *Chem. Abstr.*, 1967, **66**, 104675.
- 16 J. M. Cocellón, H. Rodríguez-Solla, C. Concellón, S. Garcia-Granda and R. Diaz, *Org. Lett.*, 2006, **8**, 5979–5982.
- 17 R. Ballini, G. Bosica, D. Fiorini and A. Palmieri, *Tetrahedron*, 2005, **61**, 8971–8993.
- 18 (a) A. G. M. Barret and G. G. Graboski, *Chem. Rev.*, 1986, **86**, 751–762; (b) G. W. Kabalka and R. S. Varma, *Org. Prep. Proc. Int.*, 1987, **19**, 283–328; (c) V. V. Perekalin, E. S. Lipina, V. M. Berestovitskaya, D. A. Efremov, *Nitroalkenes* John Wiley & Sons, Chichester, 1994.
- 19 N. Ono, in *The Nitro Group in Organic Synthesis*, ed. H. Feuer, Wiley, New York, 2001.



# New rhodium catalytic systems with trifluoromethyl phosphite derivatives for the hydroformylation of 1-octene in supercritical carbon dioxide†

Clara Tortosa Estorach, Arantxa Orejón and Anna M. Masdeu-Bultó\*

Received 9th November 2007, Accepted 12th February 2008

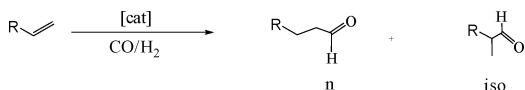
First published as an Advance Article on the web 6th March 2008

DOI: 10.1039/b717346f

Hydroformylation of 1-octene in supercritical carbon dioxide was performed using new soluble rhodium-phosphite catalytic systems. A high conversion and selectivity in the corresponding aldehydes were obtained. The ligands were synthesised and its coordination to Rh(I) complexes was studied. The reactivity of rhodium precursors with these ligands towards CO and H<sub>2</sub> was analyzed by high pressure IR and NMR spectroscopies.

## Introduction

Catalytic hydroformylation is an interesting reaction used to transform alkenes into aldehydes using carbon monoxide and hydrogen (Scheme 1). The linear aldehydes (n) thus obtained are important in industrial applications because they can be converted into plasticizer alcohols and biodegradable detergents. Additionally, the branched aldehydes (iso) are used to promote asymmetric intermediates for the synthesis of arylpropionic acids, which are subsequently used in anti-inflammatory drugs, such as ibuprofen or naproxen.<sup>1</sup>



Scheme 1 Hydroformylation of 1-alkenes.

Supercritical carbon dioxide (scCO<sub>2</sub>) is an environmentally benign solvent that can be used in homogeneous catalysis to replace the organic solvents usually employed. The use of scCO<sub>2</sub> in homogeneous hydroformylation affords control of the phase behaviour, allows dissolution of the catalyst precursors and recovery of the catalyst by precipitation, and has the potential for precise tuning of solvent properties through small changes in temperature and pressure.<sup>2</sup> Water has also been used in hydroformylation as a green solvent, although the low solubility of the organic reactants in this media has restricted its application to the hydroformylation of low alkenes.<sup>3</sup>

P-donor ligands, specifically phosphines and phosphites, with rhodium complexes are the most successful systems in the hydroformylation reactions.<sup>4</sup> The primary advantage for using phosphite ligands rather than phosphines is the higher reactivity of the corresponding rhodium catalysts, which lead to very highly active systems.<sup>5</sup> The first example of the use of phosphite

ligands in rhodium-catalysed hydroformylation of 1-alkenes was reported by Pruett and Smith of Union Carbide Corporation.<sup>6</sup> Generally, using these kinds of ligands results in an increase in the linear aldehyde when the electron withdrawing properties of the ligand increase.<sup>1c</sup> In the 1980s, Trzeciak *et al.* studied the hydroformylation of alkenes using a rhodium catalyst associated with several phosphite ligands.<sup>7</sup> Van Leeuwen *et al.* studied the hydroformylation of alkenes using rhodium complexes with tris(2-tert-butylphenyl)phosphite<sup>8</sup> and bulky ligands as tris(2-tert-butyl-4-methylphenyl)phosphite as catalysts, and obtained high rates in the hydroformylation of 1-octene.<sup>9</sup> Also, van Leeuwen studied ligands with a high electron withdrawing effect such as tris(2,2,2-trifluoroethyl)phosphite.<sup>10</sup>

The rhodium-catalysed hydroformylation of alkenes in scCO<sub>2</sub> has been extensively studied,<sup>2,11</sup> although the majority of the catalytic systems contain phosphine ligands. To increase the solubility in scCO<sub>2</sub> of the low soluble catalysts, CO<sub>2</sub>-philic groups must be introduced in the ligands. The most efficient groups are the perfluorinated long chains, which have been introduced in aryl phosphines and phosphites.<sup>12</sup> Simple low molecular weight trialkylphosphines such as PEt<sub>3</sub> have been used as ligands in phosphine-modified homogeneous rhodium-catalyzed 1-hexene hydroformylation in supercritical carbon dioxide, but as the alkylic chain grows the solubility and catalytic activity decreases.<sup>13</sup> Erkey and Palo demonstrated that simple CF<sub>3</sub>-groups introduced in triphenylphosphine form scCO<sub>2</sub> soluble systems with rhodium, which are active in the hydroformylation of 1-octene in scCO<sub>2</sub>.<sup>14</sup> A cobalt precatalyst with tri(3-fluorophenyl)phosphine has also been reported for the efficient hydroformylation of 1-octene.<sup>15</sup> Very few examples of phosphite-based catalytic systems using scCO<sub>2</sub> can be found in the literature.<sup>16</sup>

Taking into account the above-mentioned considerations, we have prepared new rhodium catalytic systems containing easy-to-prepare aryl phosphite ligands with CF<sub>3</sub>-groups in order to study their catalytic activity in the rhodium-catalysed hydroformylation of 1-octene. The introduction of a trifluoromethyl group increases the π-acceptor ability of the phosphite. To control the electronic properties of these ligands, the fluorine group was also introduced as trifluoromethoxy and a methylene was located between the aryl and the oxygen atom of the

Departament de Química Física i Inorgànica, Universitat Rovira i Virgili, Marcel·li Domingo s/n, 43007, Tarragona, Spain.

E-mail: annamaria.masdeu@urv.net; Fax: +34 977 559563; Tel: +34 977 558779

† Electronic supplementary information (ESI) available: HPNMR and HPIR spectra of [Rh(acac)(CO)<sub>2</sub>]/2-4 under CO/H<sub>2</sub>. See DOI: 10.1039/b717346f

phosphite. Thus, we have prepared a family of phosphites with different donor and steric properties ligands **1–4** (Fig. 1), and we have studied their coordination chemistry to rhodium complexes and the catalytic activity of the  $[\text{Rh}(\text{acac})(\text{CO})_2]/\mathbf{1–4}$  systems in the hydroformylation of 1-octene in  $\text{scCO}_2$ .

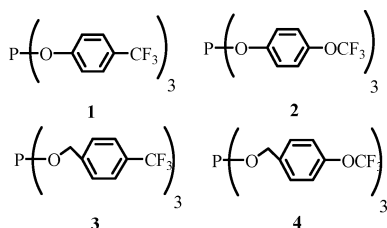
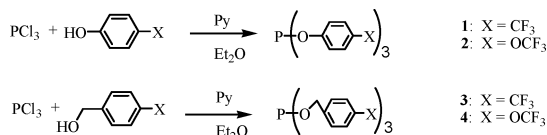


Fig. 1  $\text{CF}_3$ -group phosphite ligands **1–4**.

## Results and discussion

### Synthesis of ligands

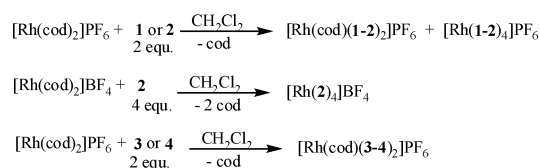
Ligands **1–4** were prepared from the commercially available corresponding alcohol by reaction with phosphorus trichloride in diethyl ether in the presence of pyridine (Scheme 2). The ligands were purified by flash chromatography on basic alumina and eluted with hexane under an inert gas and obtained as air- and moisture-sensitive colourless oils or a white solid in good yields (53–67%). The synthesis of ligand **1** using the lithium phenoxide derivative was previously described by Pringle *et al.*<sup>17</sup> The  $^1\text{H}$  NMR spectra of ligands **1–4** show two doublets in the aromatic region between  $\delta$  7.13 and 7.62 ppm and signals of the  $-\text{CF}_3$  at  $\delta$   $-62.0$  to  $-63.0$  ppm and  $-\text{OCF}_3$  at  $-58.7$  to  $-59.0$  ppm in the  $^{19}\text{F}$  NMR spectra. The  $^1\text{H}$  NMR spectra of the benzylic derivatives **3** and **4** contain a doublet for the methylene resonances at  $\delta$  4.85 and 4.93 ppm, respectively. The singlet signals at the  $^{31}\text{P}\{^1\text{H}\}$  NMR spectra appear at  $\delta$  126.5, 140.1, 140.6 ppm for **2–4**, respectively, which are typical values for these kinds of aryl phosphite compounds.<sup>18</sup>



Scheme 2 Synthesis of **1–4**.

### Synthesis of complexes

In order to study the coordination chemistry of **1–4**, we explored their reactivity with a model cationic rhodium(I) complex  $[\text{Rh}(\text{cod})_2]\text{PF}_6$  (cod = 1,5-cyclooctadiene). When 2 equivalents of the ligands **1–4** were added to a solution of  $[\text{Rh}(\text{cod})_2]\text{PF}_6$  in anhydrous dichloromethane at room temperature, the  $^{31}\text{P}\{^1\text{H}\}$  NMR showed different signals depending on the ligand. For the less  $\pi$ -acceptor and bulkier ligands **3** and **4**, the  $^{31}\text{P}\{^1\text{H}\}$  NMR spectra show only one doublet at  $\delta$  118.5 ppm ( $J_{\text{PRh}} = 246.6$  Hz) and 117.2 ppm ( $J_{\text{PRh}} = 246.1$  Hz), respectively, which correspond to the coordinated phosphite ligand in a rhodium complexes  $[\text{Rh}(\text{cod})(\mathbf{3–4})_2]\text{PF}_6$  (Scheme 3). The  $^1\text{H}$



Scheme 3 Synthesis of rhodium(I) complexes.

NMR signals corresponding to the coordinated ligands are shifted slightly downfield with respect to the free ligand. The presence of coordinated cyclooctadiene was confirmed by  $^1\text{H}$  NMR spectrum with signals at  $\delta$  4.60 ppm ( $\text{CH}=\text{CH}$ ), 2.57 and 2.37 ppm ( $-\text{CH}_2-$ ). The mass spectra confirmed the formation of the complexes that were obtained as orange oils in good yields.

However, in the case of **1** and **2**, the  $^{31}\text{P}\{^1\text{H}\}$  NMR spectra show two doublets in the region of coordinated phosphorous at  $\delta$  108.2 ( $J_{\text{PRh}} = 214$  Hz) and 118.4 ( $J_{\text{PRh}} = 312$  Hz) for phosphite **1** and  $\delta$  104.7 ( $J_{\text{PRh}} = 266.6$  Hz) and 117.8 ppm ( $J_{\text{PRh}} = 320.3$  Hz) for phosphite **2**, indicating that there may be a mixture of the rhodium complexes  $[\text{Rh}(\text{cod})(\mathbf{1–2})_2]\text{PF}_6$  and  $[\text{Rh}(\mathbf{1–2})_4]\text{PF}_6$ . In the case of ligand **2**, when the synthesis was performed with a P/Rh molar ratio of 4 : 1, the  $^{31}\text{P}\{^1\text{H}\}$  NMR spectrum only shows the signal at  $\delta$  108.7 ppm, while there was no evidence of the signals corresponding to coordinated cyclooctadiene in the  $^1\text{H}$  NMR that indicates that  $[\text{Rh}(\mathbf{2})_4]\text{PF}_6$  was formed. The complex was isolated by recrystallisation with  $\text{CH}_2\text{Cl}_2$  and hexane and fully characterised. In the case of the rhodium complex with ligand **1**, when the synthesis was performed at P/Rh molar ratio of 4 : 1, a mixture of two doublets at the  $^{31}\text{P}\{^1\text{H}\}$  NMR persisted. Attempts to separate the complexes by recrystallisation were unsuccessful. The formation of species with more ligands coordinated per rhodium is favoured for the strong  $\pi$ -acceptor and less sterically demanding ligands **1** and **2**. Similar complexes  $[\text{Rh}(\text{ligand})_4]\text{X}$  have been prepared with phosphites.<sup>19,16b</sup>

### Reactivity of $[\text{Rh}(\text{acac})(\text{CO})_2]/\mathbf{1–4}$ with CO and $\text{H}_2$

In order to determine which species are formed in conditions similar to those used in hydroformylation, the reactivity of **1–4** with  $[\text{Rh}(\text{acac})(\text{CO})_2]$  in the presence of CO and  $\text{H}_2$  was analysed by high pressure NMR (HPNMR) and IR (HPIR) spectroscopies.

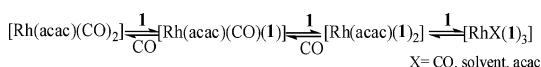
The  $^{31}\text{P}\{^1\text{H}\}$  and  $^1\text{H}$  NMR spectra were recorded for the complex  $[\text{Rh}(\text{acac})(\text{CO})_2]$  in the presence of 6 eq. of ligand **1–4** in toluene- $d_8$  ( $[\text{Rh}] = 2 \times 10^{-2}$  M) after the addition of  $\text{H}_2$  and CO. As the IR technique is more sensitive than NMR, the IR spectra could be recorded at concentrations closer to the catalytic value ( $2.4 \times 10^{-3}$  M) in methyltetrahydrofuran under the same conditions. A list of identified species is given in Table 1.

The  $^{31}\text{P}\{^1\text{H}\}$  NMR spectrum of the solution containing the  $[\text{Rh}(\text{acac})(\text{CO})_2]/\mathbf{1}$  system at room temperature consists of a major doublet of doublets at  $\delta$  108.4 ppm ( $J_{\text{PP}} = 54$ ;  $J_{\text{PRh}} = 222$  Hz) and a doublet of triplets at  $\delta$  116.9 ppm ( $J_{\text{PP}} = 53$ ;  $J_{\text{PRh}} = 280$  Hz) attributed to  $[\text{RhX}(\mathbf{1})_3]^+$  ( $\text{X} = \text{CO}$ , solvent, acac) in comparison with reported data.<sup>20</sup> A small broad signal also appeared at  $\delta$  114.7 that can be related to species  $[\text{Rh}(\text{acac})(\text{CO})_n(\mathbf{1})_{2-n}]$  formed by substitution of the CO by **1** at the starting material (Scheme 4).<sup>18c,21</sup> The signal corresponding

**Table 1** Identified species for  $[\text{Rh}(\text{acac})(\text{CO})_2]/1-4$  with  $\text{CO}/\text{H}_2$  after 1 h at  $70^\circ\text{C}^a$ 

Complex	$\delta(^{31}\text{P})$ (ppm) $J_{\text{Rh,P}}/\text{Hz}$	$\delta(^1\text{H})$ (hydride) (ppm) $J_{\text{P,H}}, J_{\text{Rh,H}}/\text{Hz}$	$\nu(\text{CO})/\text{cm}^{-1}$
$[\text{RhH}(\text{CO})(1)_3]$	135.9 d (239.8)	-10.7 quint n.d.	2078
$[\text{RhH}(\text{CO})(2)_3]$	138.2 d (238)	-10.7 d (3.6)	2072
$[\text{RhH}(2)_4]$	143.9 d (237)	-10.9 dq (1.6, 4.7)	—
$[\text{RhH}(\text{CO})(3)_3]$	156.8 d (214.5)	-10.5 dq (7.5, 14.5)	2040
$[\text{RhH}(3)_4]$	154.6 d (210)	-11.4 dq (10.5, 36.6)	—
$[\text{RhH}(\text{CO})(4)_3]$	156.5 d (213.5)	-10.5 dq (7.3, 14.5)	2052
$[\text{RhH}(4)_4]$	154.6 d (206.1)	-11.4 dq (10.0, 35.5)	—

<sup>a</sup> Reaction conditions:  $1-4/[\text{Rh}(\text{acac})(\text{CO})_2]=6$ , after 1 h at  $70^\circ\text{C}$  with  $\text{CO}:\text{H}_2(1:1) = 20$  atm; n.d. = non determined; d = doublet, t = triplet, dq = double quadruplet, quint = quintuplet, dq = double quintuplet.

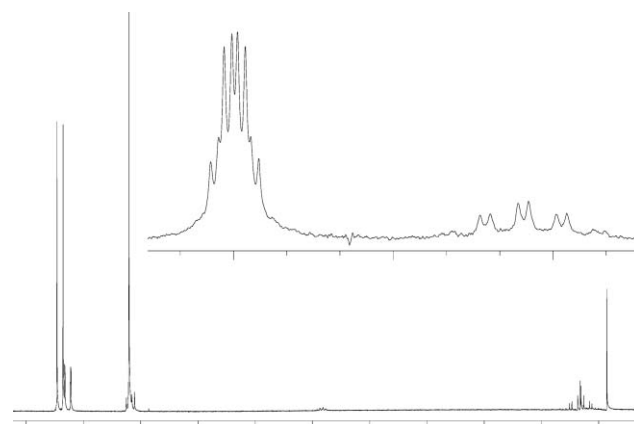
**Scheme 4** Species formed by reaction of  $[\text{Rh}(\text{acac})(\text{CO})_2] + 1$ .

to free phosphite **1** was also observed. Decomposition of the ligand was detected (signals at  $\delta 0$  ppm).

After addition of 20 atm of  $\text{H}_2 : \text{CO}$  (1 : 1) and heating the solution at  $70^\circ\text{C}$  for 1 h, the  $^{31}\text{P}\{^1\text{H}\}$ NMR showed a major doublet at  $\delta 135.9$  ppm and in the  $^1\text{H}$  NMR spectrum showed a quintuplet signal at the hydride region ( $\delta -10.7$  ppm), which were assigned to the species  $[\text{Rh}(\text{CO})\text{H}(1)_3]$  in comparison with published data for the analogous species  $[\text{Rh}(\text{CO})\text{H}\{\text{P}(\text{O}Ph)_3\}_3]$ .<sup>7d</sup> A minor doublet of doublets at  $\delta 123.9$  ( $J = 292.6, J = 180.0$  Hz) related with a double triplet at  $\delta 63.0$  ( $J = 295.6, J = 101.0$  Hz) was attributed to rhodium species with mixed phosphite–phosphonate ligands. Similar species were observed with alkyl phosphites.<sup>16</sup> Resonances corresponding to the free and decomposed ligand **1** were also observed.

The HPIR of the system  $[\text{Rh}(\text{acac})(\text{CO})_2]/1$  at 20 atm  $\text{CO}/\text{H}_2$  (1 : 1) after 1 h stirring at  $70^\circ\text{C}$  showed signals at 2078, 1994, 1968 and  $1945\text{ cm}^{-1}$  in the  $\nu(\text{CO})$  region. In comparison with reported data for  $[\text{Rh}(\text{CO})\text{H}\{\text{P}(\text{O}Ph)_3\}_3]$ ,<sup>22</sup> we assigned the band at  $2078\text{ cm}^{-1}$  to  $[\text{RhH}(\text{CO})(1)_3]$ . The other signals are in the range of those reported in the literature for dicarbonyl species  $[\text{Rh}(\text{CO})_2\text{H}\{\text{P}(\text{O}Ph)_3\}_2]$ ,<sup>18c,23</sup> and could therefore be attributed to the isomers of  $[\text{Rh}(\text{CO})_2\text{H}(1)_2]$ . This species was not detected in the HPNMR, but the lower concentration used for the HPIR solution may favour their formation. Nevertheless, they may also correspond to carbonyl species with the phosphonate ligands formed by decomposition of **1** observed at the HPNMR.

The  $^{31}\text{P}\{^1\text{H}\}$ NMR and  $^1\text{H}$  NMR spectra of the systems  $[\text{Rh}(\text{acac})(\text{CO})_2]/2-4$  indicated that the major species formed by the reaction with  $\text{CO}/\text{H}_2$  were also the species  $[\text{Rh}(\text{CO})\text{H}(2-4)_3]$ . In all these cases, a slight amount of  $[\text{RhH}(2-4)_4]$  was detected by the characteristic signal at the  $^1\text{H}$  hydride region *ca.*  $-11$  ppm (Fig. 2).

**Fig. 2** NMR spectra at  $20^\circ\text{C}$  of  $[\text{Rh}(\text{acac})(\text{CO})_2]/3$  ( $\text{P}/\text{Rh} = 6$ ) in toluene- $d_8$ .

In summary, for all these phosphites, the major rhodium species formed under  $\text{CO}/\text{H}_2$  pressure were the expected carbonyls  $[\text{Rh}(\text{CO})\text{H}(1-4)_3]$ , which are the precursors for the active hydroformylation catalysts. The values of the stretching  $\nu(\text{CO})$  bands confirm that the ligands **1** and **2** are stronger  $\pi$ -acceptors than ligands **3** and **4**. The species lacking the carbonyl  $[\text{RhH}(2-4)_4]$  were also detected at lower concentrations. The analogous species  $[\text{Rh}(\text{CO})\text{H}\{\text{P}(\text{O}Ph)_3\}_3]$  and  $[\text{RhH}\{\text{P}(\text{O}Ph)_3\}_4]$  also exist in equilibrium when  $[\text{Rh}(\text{acac})\{\text{P}(\text{O}Ph)_3\}_2]$  reacts with  $\text{CO}$  and  $\text{H}_2$  in the presence of free phosphite.<sup>7d</sup> To determine which type of species are formed, it is important to understand the catalytic behaviour, since it has been shown that  $[\text{Rh}(\text{CO})\text{H}\{\text{P}(\text{O}Ph)_3\}_3]$  is active in hydroformylation while  $[\text{RhH}\{\text{P}(\text{O}Ph)_3\}_4]$  produces isomerisation by-products.<sup>7d,24</sup> In the case of phenol-derived phosphites (**1** and **2**), mixed phosphite/phosphonate carbonyl rhodium species were formed during the experiment. It is likely that dicarbonyl species such as  $[\text{RhH}(\text{CO})_2(1-4)_2]$  were formed in the HPIR solution conditions, due to its low concentration.

### Hydroformylation of 1-octene

We studied the hydroformylation of 1-octene with the catalytic precursors system  $[\text{Rh}(\text{acac})(\text{CO})_2]/1-4$ , in  $\text{scCO}_2$  and in toluene as a model solvent.

Initially, the solubility in  $\text{scCO}_2$  of the catalysts precursors at catalytic concentration in the presence of  $\text{CO}$  and  $\text{H}_2$  was evaluated. To do this, a 100 mL Thar autoclave equipped with sapphire windows was used. The purged autoclave was charged with 0.06 mmol of  $[\text{Rh}(\text{acac})(\text{CO})_2]$  and the corresponding ligand **1-4** ( $\text{P}/\text{Rh} = 6$ ), filled with  $\text{CO}/\text{H}_2$  at 20 atm ( $\text{CO}/\text{H}_2 = 1/1$ ), and pressurized with  $\text{CO}_2$  up to 250 atm at  $70^\circ\text{C}$ . The solubility was determined by visual inspection through the windows which showed the coloured supercritical phase at different conditions depending on the ligand used. Catalytic systems with phenol-derived phosphites **1** and **2** were soluble at milder conditions (175 atm) compared to the benzyl derivatives **3** and **4**, which were soluble at 210 atm. There were no apparent differences between the solubility in  $\text{scCO}_2$  of the systems containing the ligands with trifluoromethyl or trifluoromethoxy groups.

For comparative purposes and as a reference organic medium, we performed the hydroformylation of 1-octene in toluene at

100 °C, 20 atm of total pressure and at a phosphite/rhodium ratio of 6. The results are shown in Fig. 3.

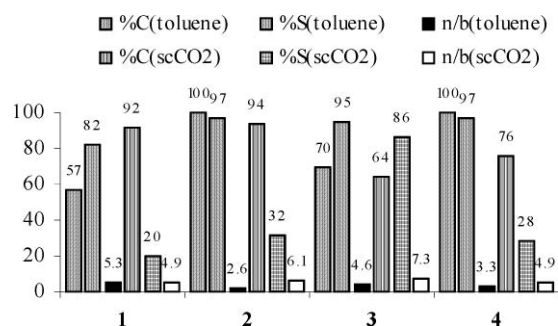


**Fig. 3** Hydroformylation of 1-octene in scCO<sub>2</sub> and in toluene. [Rh(acac)(CO)<sub>2</sub>] = 2.4 × 10<sup>-3</sup> M, 1-octene/Rh = 200, P<sub>CO</sub> = P<sub>H<sub>2</sub></sub> = 10 atm, T(°C) = 100, t = 3 h; for toluene: V = 10 mL; for scCO<sub>2</sub>: V = 25 mL, P<sub>TOT</sub> = 250 atm. %C = total conversion measured by GC. %S = selectivity in aldehydes.

Catalytic systems with ligands containing the -OCF<sub>3</sub> groups **2** and **4** show total conversion and very high selectivity in the aldehydes. Lower conversions and chemoselectivities were obtained with the catalytic systems with the ligands **1** and **3**. The by-products were 2-octenes, which can be formed through isomerisation due to the presence of [RhH(**1-4**)<sub>4</sub>]. The n/iso ratio for all the systems was high (2.5–5.2), as was similarly observed for other rhodium–phosphite systems.<sup>7a,24</sup> Nevertheless, the cases with the higher values of n/iso can be related with high isomerisation, which transforms the branched Rh–alkyl intermediate in the product of isomerisation.

The catalytic experiments using scCO<sub>2</sub> as solvent with the catalytic systems [Rh(acac)(CO)<sub>2</sub>]/**1-4** are summarized in Fig. 3 and Table 2. The hydroformylation of 1-octene was performed at 250 atm of total pressure and 100 °C to ensure the solubility of the catalytic systems. The catalytic systems with phosphites **1**, **2** and **4** resulted in very high conversions. In the case of [Rh(acac)(CO)<sub>2</sub>]/**1**, the conversion was higher than that obtained in toluene. Nevertheless, the selectivities in aldehydes for scCO<sub>2</sub> systems were lower than the ones obtained in toluene. However, the catalytic systems with ligand **3** in scCO<sub>2</sub> resulted in high selectivity in aldehydes, which was only slightly lower than the one obtained in toluene (Fig. 3). Comparing with analogous Rh–trifluoromethyl-phosphine catalysts reported in the literature, these systems provide similar conversions and higher regioselectivity although the chemoselectivity in aldehydes is, in

general, lower, as expected for Rh–phosphite systems.<sup>14a,b</sup> To improve the selectivity of the Rh/**1-2** catalytic systems, the reaction conditions were optimised with the catalytic system [Rh(acac)(CO)<sub>2</sub>]/**1** (Table 2).

Decreasing the concentration of rhodium leads to less conversion of products, although the selectivity in aldehydes increased from 20% to 40% (entry 1, Table 2). In this case the internal aldehyde, 3-ethyl-heptanal, was also detected.

Since the isomerisation process involves β-hydride elimination which requires the creation of a vacant site,<sup>25,26</sup> it can be suppressed by low temperatures. Decreasing the temperature from 100 °C to 70 °C leads to an increase in the selectivity in aldehydes from 20 to 40%, as well as a higher regioselectivity to the linear product (entry 2, Table 2).

Decreasing the total pressure to the limit conditions of solubility (180 atm, 70 °C) increased the selectivity to 60% and the conversion remained high (entry 3, Table 2). When the partial pressure of carbon monoxide and hydrogen was decreased to 10 atm (CO/H<sub>2</sub> = 5/5) at 70 °C, the selectivity in aldehydes dropped to 20% and the conversion decreased to 86% (entry 4, Table 2). To avoid the effect of a possible decomposition of the ligand, the ligand/rhodium ratio was increased to 10, although no improvement of the results was obtained (entry 5, Table 2), indicating that this decomposition is not produced to a large extent in catalytic conditions.

These experiments lead us to conclude that the best conditions for hydroformylation of 1-octene is 70 °C, 20 atm of partial pressure, a phosphite/rhodium ratio of 6 and a total pressure close to the solubility conditions. After this experiment we attempted to extract the products formed in the reaction by flushing scCO<sub>2</sub> at conditions in which the catalyst showed no solubility (ca. 50 °C, 100 atm) and collecting the extracted fraction in a cold trap. Although the conditions of the extraction were not optimised, analysis of the extracted residue by GC showed the presence of the aldehydes and isomerisation products. No signal of ligand **1** was detected in the <sup>31</sup>P{<sup>1</sup>H} NMR spectra.

At the best conditions found, we performed the hydroformylation of 1-octene with the other phosphite ligands (Table 3). For the [Rh(acac)(CO)<sub>2</sub>]/**2** catalytic system, the conversion and the selectivity increased up to 99% and 37%, respectively, although the regioselectivity to the linear aldehyde decreased to 61% (entries 1 vs. 4, Table 3). For [Rh(acac)(CO)<sub>2</sub>]/**3**, the reaction was performed at 210 atm and we observed an increase in the selectivity to 94%, although the conversion dropped to 50% (entries 2 vs. 5, Table 3). Finally, for the catalytic system [Rh(acac)(CO)<sub>2</sub>]/**4** at 210 atm, the conversion increased from

**Table 2** Hydroformylation of 1-octene using Rh(acac)(CO)<sub>2</sub>/**1** catalytic system in scCO<sub>2</sub><sup>a</sup>

Entry	T/°C	P <sub>CO</sub> : P <sub>H<sub>2</sub></sub> / atm	P <sub>TOT</sub> <sup>b</sup> / atm	%C <sup>c</sup>	%S <sub>a</sub> <sup>d</sup>	n/iso/int <sup>e</sup>	%S <sub>f</sub> <sup>f</sup>
1 <sup>g</sup>	100	10/10	250	53	40	70/20/10	60
2	70	10/10	250	99	40	86/11/3	60
3	70	10/10	180	99	60	87/12/1	40
4	70	5/5	180	86	20	90/10/-	80
5 <sup>h</sup>	70	10/10	180	71	49	86/14/-	51

<sup>a</sup> Reaction conditions: [Rh(acac)(CO)<sub>2</sub>] = 0.06 mmol, [Rh] = 2.4 × 10<sup>-3</sup> M, 1-octene = 12 mmol, 1-octene/Rh = 200, L/Rh = 6, V = 25 mL, t = 3 h.

<sup>b</sup> Total pressure. <sup>c</sup> Total conversion measured by GC. <sup>d</sup> Selectivity for aldehydes. <sup>e</sup> int = internal aldehydes: 2-ethylheptanal. <sup>f</sup> Selectivity in isomerised products (internal octenes). <sup>g</sup> [Rh(acac)(CO)<sub>2</sub>] = 0.03 mmol, [Rh] = 1 × 10<sup>-3</sup> M. <sup>h</sup> L/Rh = 10.



**Table 3** Hydroformylation of 1-octene with system [Rh(acac)(CO)<sub>2</sub>]/**2–4** at soluble and non soluble conditions<sup>a</sup>

Entry	Ligand	<i>T</i> /°C	<i>P</i> <sub>TOT</sub> /atm <sup>b</sup>	%Conv <sup>c</sup>	%S <sub>a</sub> <sup>d</sup>	n/iso/int <sup>e</sup>	%S <sub>f</sub> <sup>f</sup>
1	<b>2</b>	100	250	94	32	86/14/-	68
2	<b>3</b>	100	250	64	86	88/12/-	14
3	<b>4</b>	100	250	76	28	83/17/-	72
4	<b>2</b>	70	180	99	37	61/21/11	63
5	<b>3</b>	70	210	50	94	80/20/-	6
6	<b>4</b>	70	210	93	62	77/22/1	38

<sup>a</sup> Reaction conditions: [Rh(acac)(CO)<sub>2</sub>] = 0.06 mmol, [Rh] = 2.4 × 10<sup>-3</sup> M, 1-octene = 12 mmol, 1-octene/Rh = 200, *V* = 25 mL, *P*<sub>CO</sub> = *P*<sub>H<sub>2</sub></sub> = 10 atm, *t* = 3 h. <sup>b</sup> Total pressure. <sup>c</sup> Total conversion measured by GC. <sup>d</sup> Selectivity for aldehydes. <sup>e</sup> int = internal aldehydes: 2-ethylheptanal. <sup>f</sup> Selectivity in isomerised products (internal octenes).

76% to 93% and the selectivity from 28 to 62%, respectively (entries 3 vs. 6, Table 3).

In summary, the catalyst precursors [Rh(acac)(CO)<sub>2</sub>]/**1–4** were active in the hydroformylation of 1-octene in scCO<sub>2</sub>. Changing the solvent from toluene to a more environmentally friendly scCO<sub>2</sub> resulted in higher or similar conversions and regioselectivities for systems [Rh(acac)(CO)<sub>2</sub>]/**1,2,4** although the selectivity was lower. With catalytic system [Rh(acac)(CO)<sub>2</sub>]/**3** the selectivity obtained in scCO<sub>2</sub> was similar to the one in toluene and the conversion was 20% lower.

## Conclusions

Here, we have synthesized new P-donor ligands **2–4** with CF<sub>3</sub> and –OCF<sub>3</sub> groups and studied their coordination with rhodium(I). The reactivity of [Rh(acac)(CO)<sub>2</sub>]/**1–4** with CO/H<sub>2</sub> at 20 atm and 70 °C, studied by HPNMR and HPIR, showed [RhH(CO)(**1–4**)] as the main species formed in solution. The solubility conditions of the systems were similar for phenol derivative phosphites (180 atm) and for benzyl derivative phosphites (210 atm). All of them were active in the hydroformylation of 1-octene in scCO<sub>2</sub>, affording conversions of up to 93–99% for the systems [Rh(acac)(CO)<sub>2</sub>]/**1,2,4** and selectivities up to 94% for the system [Rh(acac)(CO)<sub>2</sub>]/**3**.

## Experimental

All reactions were performed under nitrogen using standard Schlenk techniques. Solvents were distilled and degassed prior to use. <sup>1</sup>H, <sup>13</sup>C{<sup>1</sup>H}, <sup>19</sup>F and <sup>31</sup>P{<sup>1</sup>H} NMR spectra were recorded with Varian Gemini spectrometers operating at 300 or 400 MHz (<sup>1</sup>H), 75.43 or 100.57 MHz (<sup>13</sup>C), 376.3 MHz (<sup>19</sup>F) or 121.4 or 161.9 MHz (<sup>31</sup>P). Chemical shifts are reported relative to tetramethylsilane for <sup>1</sup>H and <sup>13</sup>C{<sup>1</sup>H} as internal reference, 85% H<sub>3</sub>PO<sub>4</sub> for <sup>31</sup>P{<sup>1</sup>H}. Mass spectrometry was performed with a Voyager-DE-STR (Applied Biosystems, MDS SCIEX) instrument equipped with a 337 nm nitrogen laser. All spectra were acquired in the positive ion reflector mode 2,5-dihydroxybenzoic acid (DHB) was used as the matrix. The matrix was dissolved in MeOH at a concentration of 10 mg mL<sup>-1</sup>. The sample was dissolved in CH<sub>2</sub>Cl<sub>2</sub> (5 mg mL<sup>-1</sup>) and was deposited (0.5 mL) prior to the matrix on the target. For each spectrum, 100 laser shots were accumulated. In a typical MALDI experiment, the matrix and the salt solutions were premixed in the ratio 1 mL matrix : 0.5 mL sample. Approximately 1 μL of the obtained mixture was hand spotted on the target plate. High-

pressure NMR experiments (HPNMR) were carried out in a 10 mm-diameter sapphire tube with a titanium cap equipped with a Teflon/polycarbonate protection.<sup>27</sup> High-pressure IR experiments were performed *in situ* with an infrared autoclave.<sup>28</sup> Gas chromatography analyses were performed with a Hewlett-Packard 5890A apparatus in an HP-5 (5% diphenylsilicone/95% dimethylsilicone) column (25 m × 0.2 mm) for the separation of the products and undecane as internal standard.

### Preparation of tris(4-trifluoromethylphenyl)phosphite (**1**)

To a solution of 4-(trifluoromethyl)phenol (1 g, 5.98 mmol) and pyridine (0.58 mL, 7.18 mmol, 1.2 eq) in 15 mL diethylether at 0 °C, a solution of PCl<sub>3</sub> (0.21 mL, 2.39 mmol, 1.2 eq) in 3 mL of diethyl ether was added drop wise. The solution was stirred at room temperature under inert atmosphere for 2 h. The formation of a salt was observed immediately. After 2 h, the solvent was removed under reduced pressure. The resulting colourless solid was redissolved in hexane and purified by flash chromatography on basic alumina eluting with hexane to give **1** (0.619 g, 60%) as a white solid. <sup>1</sup>H NMR (400 MHz, CDCl<sub>3</sub>) δ (ppm) 7.23 (d, 6H, CH, *J*<sub>HH</sub> = 8.4 Hz), 7.62 (d, 6H, CH, *J*<sub>HH</sub> = 8.4 Hz). <sup>13</sup>C{<sup>1</sup>H} NMR (100.57 MHz, CDCl<sub>3</sub>) δ (ppm) 121.2 (d, CH, *J*<sub>CF</sub> = 6.8 Hz), 124.4 (q, CF<sub>3</sub>, *J*<sub>CF</sub> = 271.5 Hz), 127.4 (s, C), 127.9 (q, CH, *J*<sub>CF</sub> = 3.8 Hz), 154.1 (s, C). <sup>31</sup>P{<sup>1</sup>H} NMR (161.9 MHz, CDCl<sub>3</sub>) δ (ppm) 126.1 (in accordance with ref. 17). <sup>19</sup>F NMR (376.3 MHz, CDCl<sub>3</sub>) δ (ppm) –62.5. EIMS *m/z*: 515.2 (M + H)<sup>+</sup>.

### Preparation of tris(4-trifluoromethoxyphenyl)phosphite (**2**)

To a solution of 4-(trifluoromethoxy)phenol (1 mL, 7.56 mmol) and pyridine (0.73 mL, 9.08 mmol, 1.2 eq) in 10 mL diethyl ether at 0 °C, a solution of PCl<sub>3</sub> (0.27 mL, 3.03 mmol, 1.2 eq) in 3 mL of diethyl ether was added drop wise. The solution was stirred at room temperature under inert atmosphere for 2 h. The formation of a salt was observed immediately. After 2 h, the solvent was removed under reduced pressure. The resulting colourless solid was redissolved in hexane and purified by flash chromatography on basic alumina eluting with hexane to give **2** (0.543 g, 53%) as a colourless oil. <sup>1</sup>H NMR (400 MHz, CDCl<sub>3</sub>) δ (ppm) 7.13 (d, 6H, CH, *J*<sub>HH</sub> = 9 Hz); 7.19 (d, 6H, CH, *J*<sub>HH</sub> = 9 Hz). <sup>13</sup>C{<sup>1</sup>H} NMR (75.43 MHz, CDCl<sub>3</sub>) δ (ppm) 120.7 (q, CF<sub>3</sub>, *J*<sub>CF</sub> = 257.2 Hz), 121.9 (d, CH, *J*<sub>CP</sub> = 6.7 Hz), 122.8 (s, CH), 145.9 (s, C), 149.8 (s, C). <sup>31</sup>P{<sup>1</sup>H} NMR (161.9 MHz, CDCl<sub>3</sub>)

$\delta$  (ppm) 126.5.  $^{19}\text{F}$  NMR (376.3 MHz,  $\text{CDCl}_3$ )  $\delta$  (ppm)  $-58.7$ . EIMS  $m/z$ : 563.2 (MH) $^+$ .

#### Preparation of tris(4-trifluoromethylbenzyl)phosphite (3)

To a solution of 4-(trifluoromethyl)benzylalcohol (1 mL, 7.06 mmol) and pyridine (0.7 mL, 8.59 mmol, 1.2 eq) in 15 mL diethyl ether at 0 °C, a solution of  $\text{PCl}_3$  (0.25 mL, 2.86 mmol, 1.2 eq) in 3 mL of diethyl ether was added drop wise. The solution was stirred at room temperature under inert atmosphere for 2 h. The formation of a salt was observed immediately. After 2 h, the solvent was removed under reduced pressure. The resulting colourless solid was redissolved in hexane and purified by flash chromatography on basic alumina eluting with hexane to give **3** (0.896 g, 67%) as a white solid.  $^1\text{H}$  NMR (400 MHz,  $\text{CDCl}_3$ )  $\delta$  (ppm) 4.93 (d, 6H,  $\text{CH}_2$ ,  $J_{\text{HP}} = 8$  Hz), 7.38 (d, 6H, CH,  $J_{\text{HH}} = 8$  Hz), 7.56 (d, 6H, CH,  $J_{\text{HH}} = 8$  Hz).  $^{13}\text{C}\{^1\text{H}\}$  NMR (100.57 MHz,  $\text{CDCl}_3$ )  $\delta$  (ppm) 64.0 (d,  $\text{CH}_2$ ,  $J_{\text{CP}} = 11.4$  Hz), 125.6 (q, CH,  $J_{\text{CF}} = 3.7$  Hz), 127.6 (s, CH), 130.5 (q, C,  $J_{\text{CF}} = 32$  Hz), 124.3 (q,  $\text{CF}_3$ ,  $J_{\text{CF}} = 277.6$  Hz), 142.0 (d, C,  $J_{\text{CP}} = 4.5$  Hz).  $^{31}\text{P}\{^1\text{H}\}$  NMR (161.9 MHz,  $\text{CDCl}_3$ )  $\delta$  (ppm) 140.1.  $^{19}\text{F}$  NMR (376.3 MHz,  $\text{CDCl}_3$ )  $\delta$  (ppm)  $-63.0$ . EIMS  $m/z$ : 553.2 (M-3H) $^+$ ; 175.0 ( $\text{C}_8\text{H}_6\text{F}_3\text{O}$ ) $^+$ .

#### Preparation of tris(4-trifluoromethoxybenzyl)phosphite (4)

To a solution of 4-(trifluoromethoxy)benzylalcohol (1 mL, 6.70 mmol) and pyridine (0.6 mL, 8.03 mmol, 1.2 eq) in 15 mL diethyl ether at 0 °C, a solution of  $\text{PCl}_3$  (0.2 mL, 2.68 mmol, 1.2 eq) in 3 mL of diethyl ether was added drop wise. The solution was stirred at room temperature under inert atmosphere for 2 h. The formation of a salt was observed immediately. After 2 h, the solvent was removed under reduced pressure. The resulting colourless solid was redissolved in hexane and purified by flash chromatography on basic alumina eluting with hexane to produce **4** (0.780 g, 58%) as a colourless oil.  $^1\text{H}$  NMR (400 MHz,  $\text{CDCl}_3$ )  $\delta$  (ppm) 4.86 (d, 6H,  $\text{CH}_2$ ,  $J_{\text{HP}} = 8$  Hz), 7.17 (d, 6H, CH,  $J_{\text{HH}} = 8.4$  Hz), 7.31 (d, 6H, CH,  $J_{\text{HH}} = 8.4$  Hz).  $^{13}\text{C}\{^1\text{H}\}$  NMR (100.57 MHz,  $\text{CDCl}_3$ )  $\delta$  (ppm) 63.9 (d,  $\text{CH}_2$ ,  $J_{\text{CP}} = 11.3$  Hz), 121.2 (s, CH), 129.0 (s, CH), 136.9 (d, C,  $J_{\text{CP}} = 4.5$  Hz), 149.0 (s, C), 120.7 (q, C,  $J_{\text{CF}} = 256.3$  Hz).  $^{31}\text{P}\{^1\text{H}\}$  NMR (161.9 MHz,  $\text{CDCl}_3$ )  $\delta$  (ppm) 140.6.  $^{19}\text{F}$  NMR (376.3 MHz,  $\text{CDCl}_3$ )  $\delta$  (ppm)  $-58.4$ . EIMS  $m/z$ : 605.2 (MH) $^+$ .

#### Reaction of $[\text{Rh}(\text{cod})_2]\text{BF}_4$ with **1**

Ligand **1** (154 mg, 0.30 mmol or 308 mg, 0.60 mmol) was added to a solution of  $[\text{Rh}(\text{cod})_2]\text{BF}_4$  (30.4 mg, 0.07 mmol) in 2 mL of anhydrous dichloromethane. The solution turned yellow immediately and was stirred for 1 h. The solvent was then evaporated in a vacuum to obtain a yellow solid containing a mixture of  $[\text{Rh}(\text{I})_4]\text{BF}_4$  and  $[\text{Rh}(\text{cod})(\text{I})_2]\text{BF}_4$ .  $^{31}\text{P}\{^1\text{H}\}$  NMR (161.9 MHz,  $\text{CDCl}_3$ )  $\delta$  (ppm) 108.2 (d,  $J = 216.9$  Hz) corresponding to  $[\text{Rh}(\text{I})_4]\text{BF}_4$ ; 118.4 (d,  $J = 316.9$  Hz) corresponding to  $[\text{Rh}(\text{cod})(\text{I})_2]\text{BF}_4$ .

#### Preparation of $[\text{Rh}(\text{2})_4]\text{BF}_4$

Ligand **2** (168 mg, 0.32 mmol) was added to a solution of  $[\text{Rh}(\text{cod})_2]\text{BF}_4$  (30.4 mg, 0.08 mmol) in 2 mL of anhydrous dichloromethane. The solution turned yellow immediately and

was stirred for 1 h. The solvent was then evaporated in a vacuum and was dried under vacuum overnight. The product was obtained as a yellow solid. (125.6 mg, 69%).

$^1\text{H}$  NMR (300 MHz,  $(\text{CD}_3)_2\text{CO}$ )  $\delta$  (ppm) 6.9 (d, 24H, CH,  $J_{\text{HH}} = 9$  Hz), 7.15 (d, 24H, CH,  $J_{\text{HH}} = 9$  Hz).  $^{13}\text{C}\{^1\text{H}\}$  NMR (75.43 MHz,  $(\text{CD}_3)_2\text{CO}$ )  $\delta$  (ppm) 117.4 (br q), 123.8 (d, CH), 123.5 (q, CH,  $J = 25$  Hz), 147.5 (s, C), 150.7 (s, C).  $^{31}\text{P}\{^1\text{H}\}$  NMR (121.4 MHz,  $(\text{CD}_3)_2\text{CO}$ )  $\delta$  (ppm) 108.7 (d,  $J_{\text{PRh}} = 216$  Hz).  $^{19}\text{F}$  NMR (376.3 MHz,  $(\text{CD}_3)_2\text{CO}$ )  $\delta$  (ppm)  $-63.4$ . MALDI-TOF  $m/z$ : 2442 (M) $^+$ , 2354 (M $^+$ -BF $_4$ ).

#### Preparation of $[\text{Rh}(\text{C}_8\text{H}_{12})(\text{3})_2]\text{BF}_4$

Ligand **3** (63 mg, 0.11 mmol) was added to a solution of  $[\text{Rh}(\text{cod})_2]\text{BF}_4$  (19 mg, 0.05 mmol) in 2 mL of anhydrous dichloromethane. The solution turned yellow immediately and was stirred for 1 h. The solvent was then evaporated in a vacuum and was dried under vacuum overnight. The product was obtained as an orange solid. (20 mg, 30%).

$^1\text{H}$  NMR (300 MHz,  $\text{CDCl}_3$ )  $\delta$  (ppm) 2.37 (m, 4H,  $\text{CH}_2$  cod), 2.58 (m, 4H,  $\text{CH}_2$  cod), 4.67 (m, 4H, CH cod), 5.15 (d, 12H,  $\text{CH}_2$ ,  $J_{\text{HP}} = 9$  Hz), 7.31 (d, 12H, CH,  $J_{\text{HH}} = 8.7$  Hz), 7.54 (d, 12H, CH,  $J_{\text{HH}} = 8$  Hz).  $^{13}\text{C}\{^1\text{H}\}$  NMR (100.57 MHz,  $\text{CDCl}_3$ )  $\delta$  (ppm) 29.7 (s,  $\text{CH}_2$  cod), 68.5 (d,  $\text{CH}_2$ ,  $J_{\text{CP}} = 5.3$  Hz), 113.8 (s, CH cod), 126.4 (q,  $\text{CF}_3$ ,  $J_{\text{CF}} = 271.6$  Hz), 125.6 (q, CH,  $J = 3.8$  Hz), 127.8 (s, CH), 131.0 (s, C), 139.3 (s, C).  $^{31}\text{P}\{^1\text{H}\}$  NMR (121.4 MHz,  $\text{CDCl}_3$ )  $\delta$  (ppm) 118.5 (d,  $J_{\text{PRh}} = 246.6$  Hz).  $^{19}\text{F}$  NMR (376.3 MHz,  $\text{CDCl}_3$ )  $\delta$  (ppm)  $-63.1$ . MALDI-TOF  $m/z$ : 1351 (M $^+$ -BF $_4$ ).

#### Preparation of $[\text{Rh}(\text{C}_8\text{H}_{12})(\text{4})_2]\text{PF}_6$

Ligand **4** (109 mg, 0.18 mmol) was added to a solution of  $[\text{Rh}(\text{cod})_2]\text{PF}_6$  (35 mg, 0.08 mmol) in 2 mL of anhydrous dichloromethane. The solution turned yellow immediately and was stirred for 1 h. The solvent was then evaporated in a vacuum and was dried under vacuum overnight. The product  $[\text{Rh}(\text{C}_8\text{H}_{12})(\text{4})_2]\text{PF}_6$  was obtained as an orange oil (105 mg, 90%).  $^1\text{H}$  NMR (300 MHz,  $\text{CDCl}_3$ )  $\delta$  (ppm) 2.54 (m, 8H,  $\text{CH}_2$  cod), 4.56 (b, 4H, CH cod), 5.02 (d, 12H,  $\text{CH}_2$ ), 7.14 (d, 12H, CH,  $J_{\text{HH}} = 8.4$  Hz), 7.22 (d, 12H, CH,  $J_{\text{HH}} = 8.4$  Hz).  $^{13}\text{C}\{^1\text{H}\}$  NMR (100.57 MHz,  $\text{CDCl}_3$ )  $\delta$  (ppm) 29.7 (s,  $\text{CH}_2$  cod), 68.5 (d,  $\text{CH}_2$ ,  $J_{\text{CP}} = 5.5$  Hz), 127.7 (q, C,  $J_{\text{CF}} = 237$  Hz), 121.1 (s, CH), 129.4 (s, CH), 134.1 (s, C), 142.5 (s, C).  $^{31}\text{P}\{^1\text{H}\}$  NMR (161.9 MHz,  $\text{CDCl}_3$ )  $\delta$  (ppm) 117.2 (d,  $J_{\text{PRh}} = 246.1$  Hz).  $^{19}\text{F}$  NMR (376.3 MHz,  $\text{CDCl}_3$ )  $\delta$  (ppm)  $-58.3$ . MALDI-TOF  $m/z$ : 1419.7 (M-PF $_6$ ) $^+$  required for 1419.14.

#### Catalysis

Hydroformylation experiments were carried out in a Parr autoclave (25 mL) with magnetic stirring. The autoclave was equipped with a liquid inlet, a gas inlet, a  $\text{CO}_2$  inlet and a thermocouple. An electric heating mantle kept the temperature constant.

#### Standard hydroformylation experiment in toluene

The reactions in toluene were performed in the same Parr autoclave as above. The complex  $[\text{Rh}(\text{acac})(\text{CO})_2]$  (0.02 mmol) and the ligand (0.10 mmol) in toluene (10 mL) were stirred at room

temperature for 1 h. The substrate (4.80 mmol) and undecane as GC internal standard were then added and the resulting solution was introduced into the evacuated autoclave. The system was pressurised and heated. When thermal equilibrium was reached, additional gas mixture was introduced until the desired pressure was attained. After the required reaction time, the autoclave was cooled to room temperature and depressurised. The products were identified by GC-MS.

### Standard hydroformylation experiment in scCO<sub>2</sub>

The complex [Rh(acac)(CO)<sub>2</sub>] (0.06 mmol) was introduced into the evacuated autoclave, after which the autoclave was purged with nitrogen/vacuum cycles. Next, 1-octene (12 mmol), the ligand (0.36 mmol) and undecane (1.11 g) as the GC internal standard, were added. The system was pressurised with 20 atm of CO/H<sub>2</sub> (1 : 1), and liquid CO<sub>2</sub> was introduced until a total pressure of 60 bar was reached. The autoclave was heated to the desired temperature. When thermal equilibrium was reached, the total pressure was adjusted with a Thar syringe pump. After the reaction time, the autoclave was cooled down to 0 °C and depressurised. The final mixture was analysed by GC. The products were identified by GC-MS. The extraction was performed by flushing CO<sub>2</sub> through the reactor at a flow rate of approximately 6 mL min<sup>-1</sup>. The reactor was maintained at 50 °C and a pressure between 80 and 100 atm. Then the CO<sub>2</sub> stream was vented to ambient pressure through a series of two cold traps (−80 °C). The contents were analyzed by NMR and GC.

### Solubility studies

The solubility studies were carried out in a Thar reactor (100 mL) equipped with sapphire windows and magnetic stirring. The autoclave was charged with a solution of the ligand (0.22 mmol) and [Rh(acac)(CO)<sub>2</sub>] (0.06 mmol) in diethyl ether. The solvent was removed in vacuum, the reactor was pressurised with syngas and CO<sub>2</sub>, the system was heated to 80 °C, and the total pressure was adjusted to 250 atm. Solubility was monitored by visual inspection through the sapphire windows with a mirror due to safety requirements.

### HPNMR

In a typical experiment, the NMR tube was filled under N<sub>2</sub> with a solution of [Rh(acac)(CO)<sub>2</sub>] (0.04 mmol), the ligand **1-4** (0.24 mmol) and toluene-d<sub>8</sub> (2 mL). The tube was pressurised to 20 atm of CO/H<sub>2</sub> (1 : 1) and left at 70 °C for 1 h. The NMR spectra were then recorded.

### HPIR

In a typical experiment, the HPIR cell was filled under N<sub>2</sub> with a solution of [Rh(acac)(CO)<sub>2</sub>] (0.04 mmol), the ligand **1-4** (0.22 mmol) and methyltetrahydrofuran (15 mL). The cell was pressurised to 20 atm of CO/H<sub>2</sub> (1 : 1) and left at 70 °C for 1 h. The IR spectra were then recorded.

## Acknowledgements

We gratefully acknowledge the Generalitat de Catalunya (DURSI and Fons Social Europeu) for a Fellowship (FI) to C. T. and 2005SGR00777 and the Ministerio de Educacion y Ciencia (CTQ2004-03831/PPQ, CSD2006-0003).

## Notes and references

- (a) *Applied Homogeneous Catalysis with Organometallic Compounds*, ed. B. Cornils and W. A. Herrmann, VCH, Weinheim, 1996; (b) A. M. Trzeciak and J. J. Ziolkowski, *Coord. Chem. Rev.*, 1999, **190–192**, 883; (c) *Rhodium Catalyzed Hydroformylation*, ed. P. W. N. M. van Leeuwen and C. Claver, Kluwer Academic Publishers, Dordrecht, 2000.
- S. Bektsev, A. M. Kleman, A. E. Marteel-Parrish and M. A. Abraham, *J. Supercrit. Fluids*, 2006, **38**, 232.
- E. Wiebus and B. Cornils, *Chem. Eng. Technol.*, 1994, **66**, 916.
- M. Beller, B. Cornils, C. D. Frohning and C. W. Kohlpainter, *J. Mol. Catal. A: Chem.*, 1995, **104**, 17.
- A. Van Rooy, J. N. H. De Bruijn, K. F. Roobeek, P. C. J. Kamer and P. W. N. M. Van Leeuwen, *J. Organomet. Chem.*, 1996, **507**, 69.
- R. L. Pruett and J. A. Smith, *J. Org. Chem.*, 1969, **34**, 327.
- (a) A. M. Trzeciak and J. J. Ziolkowski, *J. Mol. Catal.*, 1986, **34**, 213; (b) H. Jancko, A. M. Trzeciak and J. J. Ziolkowski, *J. Mol. Catal.*, 1984, **26**, 355; (c) A. M. Trzeciak and J. J. Ziolkowski, *J. Mol. Catal.*, 1987, **43**, 15; (d) A. M. Trzeciak, J. J. Ziolkowski, S. Aygen and R. Van Eldik, *J. Mol. Catal.*, 1986, **34**, 337.
- P. W. N. M. van Leeuwen and C. F. Roobeek, *J. Organomet. Chem.*, 1983, **258**, 343.
- (a) A. Van Rooy, E. N. Orij, P. C. J. Kamer, F. Van den Aardweg and P. W. N. M. van Leeuwen, *J. Chem. Soc. Chem. Commun.*, 1991, 1096; (b) A. Van Rooy, E. N. Orij, P. C. J. Kamer and P. W. N. M. van Leeuwen, *Organometallics*, 1995, **14**, 34.
- P. W. N. M. van Leeuwen, C. F. Roobeek, *Brit. Pat.* 2068377, 1980 (to Shell); *Chem. Abstr.*, 1984, 101, 191142.
- (a) D. J. Cole-Hamilton, *Science*, 2003, **299**, 1702; (b) P. G. Jessop, *J. Supercrit. Fluids*, 2006, **38**, 211; (c) P. G. Jessop, T. Ikariya and R. Noyori, *Chem. Rev.*, 1999, **99**, 475; (d) W. Leitner, *Acc. Chem. Res.*, 2002, **35**, 746.
- (a) S. Kainz, D. Koch, W. Baumann and W. Leitner, *Angew. Chem., Int. Ed Engl.*, 1997, **36**, 1628; (b) D. Koch and W. Leitner, *J. Am. Chem. Soc.*, 1998, **120**, 13398; (c) D. R. Palo and C. Erkey, *Organometallics*, 2000, **19**, 81; (d) A. M. Banet Osuna, W. Chen, E. G. Hope, R. D. W. Kemmitt, D. R. Paige, A. M. Stuart, J. Xiao and L. Xu, *J. Chem. Soc., Dalton Trans.*, 2000, 4052; (e) G. Franciò and W. Leitner, *Chem. Commun.*, 1999, 1663; (f) G. Franciò, K. Wittmann and W. Leitner, *J. Organomet. Chem.*, 2001, **621**, 130; (g) Y. Hu, W. Chen, A. M. Banet Osuna, A. M. Stuart, E. G. Hope and J. Xiao, *Chem. Commun.*, 2001, 725.
- (a) I. Bach and D. J. Cole-Hamilton, *Chem. Commun.*, 1998, 1463; (b) M. F. Sellin, I. Bach, J. M. Webster, F. Montilla, V. Rosa, T. Avilés, M. Poliakov and D. J. Cole-Hamilton, *J. Chem. Soc., Dalton Trans.*, 2002, 4569.
- (a) D. R. Palo and C. Erkey, *Ind. Eng. Chem. Res.*, 1998, **37**, 4203; (b) D. R. Palo and C. Erkey, *Ind. Eng. Chem. Res.*, 1999, **38**, 3786; (c) A. C. J. Koeken, M. C. A. van Vliet, L. J. P. van de Broeke, B. J. Deelman and J. T. F. Keurentjes, *Adv. Synth. Catal.*, 2006, **348**, 1553.
- F. Patcas, C. Maniut, C. Ionescu, S. Pitter and E. Dinjus, *Appl. Catal., B*, 2007, **70**, 630.
- (a) M. F. Sellin and D. J. K. Cole-Hamilton, *J. Chem. Soc., Dalton Trans.*, 2000, 1681; (b) M. Gimenez-Pedros, A. Aghmiz, N. Ruiz and A. M. Masdeu-Bultó, *Eur. J. Inorg. Chem.*, 2006, 1067.
- C. J. Copley and P. G. Pringle, *Inorg. Chim. Acta*, 1997, **265**, 107.
- (a) *Handbook of Phosphorus-31 Nuclear Magnetic Resonance Data*, ed. J. C. Tebb, CRC Press Inc., Boca Raton, 1991, p. 65; (b) A. W. Verstuyft, D. A. Redfield, L. W. Cary and J. H. Nelson, *Inorg. Chem.*, 1977, **16**, 2776; (c) A. M. Trzeciak and J. J. Ziolkowski, *J. Mol. Catal.*, 1983, **19**, 41.
- (a) R. R. Schrock and J. A. Osborn, *J. Am. Chem. Soc.*, 1971, **93**, 2397; (b) M. A. Garralda and L. A. Oro, *Trans. Met. Chem.*, 1980, **5**, 65.

- 
- 20 A. M. Trzeciak and J. J. Ziolkowski, *Transition Met. Chem.*, 1989, **14**, 135.
- 21 A. M. Trzeciak and J. J. Ziolkowski, *Inorg. Chim. Acta*, 1982, **64**, L267.
- 22 A. M. Trzeciak, *J. Organomet. Chem.*, 1990, **390**, 105.
- 23 P. W. N. M. Van Leeuwen and G. C. Schoemaker, *Organometallics*, 1999, **18**, 2107.
- 24 A. M. Trzeciak, J. J. Ziolkowski and R. Choukroun, *J. Organomet. Chem.*, 1996, **525**, 145.
- 25 B. E. Hanson and N. E. Davis, *J. Chem. Educ.*, 1987, **64**, 928.
- 26 J. P. Collman, L. S. Hegedus, J. R. Norton, R. G. Finke, *Principles and Applications of Organotransition Metal Chemistry*, University Science Books, Mill Valley, CA, 2<sup>nd</sup> edn, 1987.
- 27 A. Cusanelli, U. Frey, D. T. Richens and A. Merbach, *J. Am. Chem. Soc.*, 1996, **118**, 5265.
- 28 P. C. J. Kamer, A. Van Rooy, G. C. Schoemaker and P. W. N. M. Van Leeuwen, *Coord. Chem. Rev.*, 2004, **248**, 2409.



# Hydrous ruthenium oxide supported on $\text{Co}_3\text{O}_4$ as efficient catalyst for aerobic oxidation of amines

Feng Li, Jing Chen, Qinghong Zhang and Ye Wang\*

Received 10th October 2007, Accepted 30th January 2008

First published as an Advance Article on the web 6th March 2008

DOI: 10.1039/b715627h

Ruthenium catalysts supported on various metal oxides and  $\text{Co}_3\text{O}_4$ -supported various transition metal catalysts prepared by an adsorption-precipitation method were examined for the aerobic oxidation of benzyl amine. We found that the  $\text{Co}_3\text{O}_4$ -supported ruthenium catalyst exhibited the best catalytic performance. The  $\text{Co}_3\text{O}_4$ -supported ruthenium catalyst was also effective for the aerobic oxidation of several other amines. The present catalyst could be used recyclably and be operated under solvent-free conditions. The activity of the present catalyst for the aerobic oxidation of benzyl amine depended less on the oxygen pressure, and the catalyst was also efficient even when air was used as an oxidant. The content of ruthenium and the size of  $\text{Co}_3\text{O}_4$  particles played crucial roles in determining the catalytic performance. We have clarified that the supported hydrous ruthenium oxide ( $\text{RuO}_2 \cdot x\text{H}_2\text{O}$ ) is the active species for the aerobic oxidation of benzyl amine, whereas the supported metallic ruthenium ( $\text{Ru}^0$ ) and supported ruthenium chloride ( $\text{RuCl}_3$ ) are inactive, and the supported anhydrous ruthenium oxide ( $\text{RuO}_2$ ) only exhibits a lower activity.

## Introduction

Many oxidative transformations of organic compounds are currently still carried out using stoichiometric amounts of metal-based oxidants such as dichromate, permanganate and silver oxide, and large amounts of heavy metal salts are produced.<sup>1</sup> Selective oxidation of organic compounds by a catalytic method using  $\text{O}_2$  or air as a sole oxidant has become urgent from the viewpoints of green chemistry.<sup>2</sup> Nitriles are important and versatile synthetic intermediates. As compared with the current production methods such as the nucleophilic substitution of halides with cyanide ions, the ammoxidation and the oxidation of amines with stoichiometric reagents, the catalytic oxidation of primary amines by  $\text{O}_2$  or air is a more desirable route for the synthesis of nitriles. However, only limited catalytic systems have been reported for the selective oxidation of amines by  $\text{O}_2$ .<sup>3–11</sup>

We have focused on the development of efficient heterogeneous catalysts for the selective oxidation of amines by  $\text{O}_2$  or air because heterogeneous catalysts possess obvious advantages in product isolation and catalyst recycling uses than homogeneous catalysts. Although a large number of heterogeneous catalysts have been reported for the selective oxidation of alcohols, only very few studies have been contributed to the oxidation of amines over a heterogeneous catalyst.<sup>7,8,11</sup> A Ru/hydroxyapatite could catalyze the aerobic oxidation of several primary amines to the corresponding nitriles with good efficiencies.<sup>7</sup> For example, the conversion and selectivity for the oxidation of benzyl amine to

benzonitrile were 100% and 90%, respectively, after a reaction at 383 K for 12 h over this catalyst, giving a turnover frequency (TOF) of  $\sim 0.5 \text{ h}^{-1}$ .<sup>7</sup> Yamaguchi and Mizuno<sup>8</sup> reported that  $\text{Ru}/\text{Al}_2\text{O}_3$  was more active for the aerobic oxidation of amines; the conversion of benzyl amine was >99% after 1 h of reaction at 373 K, providing a TOF of  $\sim 29 \text{ h}^{-1}$ , but the selectivity of benzonitrile was lower (82%). Recently, a  $\text{Ru}/\text{Fe}_3\text{O}_4$  was also reported to show good activity for the aerobic oxidation of amines, and the conversion and selectivity for the oxidation of benzyl amine to benzonitrile were 96% and 82%, respectively, after a 7 h reaction at 378 K, showing a TOF of  $\sim 3 \text{ h}^{-1}$ .<sup>11</sup>

Recently, we examined the catalytic performances of ruthenium catalysts loaded on various metal oxide supports and various transition metal catalysts supported on  $\text{Co}_3\text{O}_4$  for the aerobic oxidation of benzyl amine. We found that the  $\text{Co}_3\text{O}_4$ -supported ruthenium catalyst prepared by an adsorption-precipitation method exhibited outstanding catalytic performances. The present paper reports the catalytic behaviour of the  $\text{Co}_3\text{O}_4$ -supported ruthenium catalyst for the aerobic oxidation of amines. Catalyst requirements for this green oxidation and the nature of the active ruthenium species are also discussed *via* investigations of structure-reactivity relationships.

## Experimental

### Catalyst preparation

The catalysts used in the present work were mainly prepared by an adsorption-precipitation method. As an example, the procedure for the preparation of the  $\text{Co}_3\text{O}_4$ -supported ruthenium catalyst was described as follows. Powdery  $\text{Co}_3\text{O}_4$  (1 g), purchased from the Sinopharm Group Chemical Reagent Co., was added into an aqueous solution of  $\text{RuCl}_3$  (30  $\text{cm}^3$ ), and the

State Key Laboratory of Physical Chemistry of Solid Surfaces and Department of Chemistry, College of Chemistry and Chemical Engineering, Xiamen University, Xiamen, 361005, P. R. China.  
E-mail: wangye@xmu.edu.cn; Fax: +86-592-2183047;  
Tel: +86-592-2186156

**Table 1** Preparation procedures for Co<sub>3</sub>O<sub>4</sub>-supported ruthenium catalysts possibly with ruthenium in different states

Catalyst denotation	Preparation procedure	Surf. area (m <sup>2</sup> g <sup>-1</sup> )
2.5 wt% Ru/Co <sub>3</sub> O <sub>4</sub>	Adsorption-precipitation method	32
2.5 wt% Ru/Co <sub>3</sub> O <sub>4</sub> -C573	Calcination of the 2.5 wt% Ru/Co <sub>3</sub> O <sub>4</sub> in air at 573 K for 6 h	29
2.5 wt% Ru/Co <sub>3</sub> O <sub>4</sub> -C573-R623	Reduction of the 2.5 wt% Ru/Co <sub>3</sub> O <sub>4</sub> -C573 in H <sub>2</sub> at 623 K for 2 h	13
3 wt% Ru/Co <sub>3</sub> O <sub>4</sub> ( <i>imp</i> )	Impregnation of Co <sub>3</sub> O <sub>4</sub> with a RuCl <sub>3</sub> aqueous solution, followed by drying at 373 K	26
3 wt% Ru/Co <sub>3</sub> O <sub>4</sub> ( <i>imp</i> )-C573	Calcination of the 3 wt% Ru/Co <sub>3</sub> O <sub>4</sub> ( <i>imp</i> ) in air at 573 K for 6 h	30

concentration of RuCl<sub>3</sub> was used to regulate the Ru content. After the suspension was stirred at room temperature for 1 h, the pH was adjusted to 13.0 using 1 M NaOH aqueous solution. The solid powder obtained was recovered by filtration after the suspension was further stirred for 1 h. Subsequently, the solid powder was washed thoroughly with deionised water until Cl<sup>-</sup> was removed. The sample was washed further with ethanol, and was finally dried at room temperature (~298 K) in vacuum. The catalyst prepared by this adsorption-precipitation method was denoted as *m* wt% Ru/Co<sub>3</sub>O<sub>4</sub>, where *m* was the weight percentage of ruthenium. It should be noted that this denotation does not mean that ruthenium is in metallic (Ru<sup>0</sup>) state. For comparison, Co<sub>3</sub>O<sub>4</sub> purchased from Alfa Aesar Co. (denoted as Co<sub>3</sub>O<sub>4</sub>-A) was also used for the preparation of a 2.5 wt% Ru/Co<sub>3</sub>O<sub>4</sub>-A catalyst by the same procedure. We clarified that the mean size of the Co<sub>3</sub>O<sub>4</sub>-A particles was larger than that of the Co<sub>3</sub>O<sub>4</sub> particles purchased from the Sinopharm Group Chemical Reagent Co.

To gain information about the state of ruthenium in active catalysts, we also prepared Co<sub>3</sub>O<sub>4</sub>-supported ruthenium catalysts possibly with ruthenium in different states by different procedures as summarized in Table 1. The catalyst denoted as 2.5 wt% Ru/Co<sub>3</sub>O<sub>4</sub>-C573 was obtained by calcination of the 2.5 wt% Ru/Co<sub>3</sub>O<sub>4</sub> catalyst prepared above with the adsorption-precipitation method at 573 K in air for 6 h. The 2.5 wt% Ru/Co<sub>3</sub>O<sub>4</sub>-C573-R623 denotes the catalyst obtained by further reduction of the 2.5 wt% Ru/Co<sub>3</sub>O<sub>4</sub>-C573 sample at 623 K in a H<sub>2</sub> gas flow for 2 h. The catalyst denoted as 3 wt% Ru/Co<sub>3</sub>O<sub>4</sub> (*imp*) was prepared by an impregnation method as follows. Powdery Co<sub>3</sub>O<sub>4</sub> (1 g) was added into the aqueous solution of RuCl<sub>3</sub> (30 cm<sup>3</sup>) with a fixed concentration. The suspension was stirred for 4 h and was then allowed to rest overnight at ambient temperature. Subsequently, the mixture was evaporated to dryness at 343 K with continuous stirring, followed by further drying in air at 373 K to obtain the 3 wt% Ru/Co<sub>3</sub>O<sub>4</sub> (*imp*). The 3 wt% Ru/Co<sub>3</sub>O<sub>4</sub> (*imp*) was calcined in air at 573 K for 6 h, giving the sample denoted as 3 wt% Ru/Co<sub>3</sub>O<sub>4</sub> (*imp*)-C573.

### Catalyst characterization

The content of ruthenium in each sample was determined by inductively coupled plasma (ICP) optical emission spectrometry using an Agilent ICP-MS 4500–300. The BET surface areas were measured with a high-speed automated area and pore size analyzer (Quantachrome NOVA 4000e). X-ray diffraction (XRD) patterns of the catalysts were measured with a Panalytical X'Pert Pro Super X-ray diffractometer equipped with X'Celerator detection systems. Cu K<sub>α</sub> radiation (40 kV and 30 mA) was used as the X-ray source. Scanning electron microscopy (SEM) was carried out using a LEO1530 scanning electron

microscope with 20 kV accelerating voltage. X-ray photoelectron spectroscopy (XPS) was measured with a PHI Quantum 2000 Scanning ESCA Microprobe equipment using monochromatic Al K<sub>α</sub> radiation. H<sub>2</sub> temperature-programmed reduction (H<sub>2</sub>-TPR) was performed using a Micromeritics AutoChem 2920 II instrument. Typically, the temperature of the sample loaded in a quartz reactor was raised to 1200 K in a H<sub>2</sub>-Ar gas mixture (10 vol% H<sub>2</sub>) at a rate of 10 K min<sup>-1</sup>. The consumption of H<sub>2</sub> was monitored by a thermal conductivity detector, and the detector response was calibrated using the reduction of CuO powder.

### Catalytic reaction

The selective oxidation of amines with O<sub>2</sub> or air was carried out using a round-bottomed glass flask reactor equipped with a reflux condenser. In a typical run, a measured amount of catalyst (typically, 0.1 g) was added to the reactor pre-charged with desired amounts of reactant and solvent at a fixed temperature (typically, 373 K). Trifluorotoluene (PhCF<sub>3</sub>), a stable and versatile solvent with relatively higher boiling point (375K) and lower toxicity as compared with many other organic solvents such as benzene and dichloromethane,<sup>12</sup> was used as the solvent in most of our experiments. The inhalation and direct contacts of PhCF<sub>3</sub> with the skin or eyes should be avoided because its toxicological properties have not been thoroughly investigated. The reaction was started by bubbling O<sub>2</sub> or O<sub>2</sub> diluted with N<sub>2</sub> or air into the liquid. The reactant mixture was stirred vigorously during the reaction. After the reaction, the catalyst was filtered off *via* centrifugation, and the liquid organic products were quantified by a gas chromatograph (Shimadzu 14B) equipped with a capillary column (DB-5, 30 M × 0.25 mm × 0.25 μm) and a FID detector using hexane as an internal standard. The turnover frequency (TOF) was calculated by the moles of amines converted per mole of ruthenium contained in the catalyst per hour.

## Results and discussion

### Superior catalytic performance of Ru/Co<sub>3</sub>O<sub>4</sub> catalyst for the aerobic oxidation of benzyl amine

Only very limited heterogeneous catalysts have been reported for the aerobic oxidation of amines, and ruthenium has been exploited as the active component in all of these catalysts.<sup>7,8,11</sup> However, different supports were employed in different studies. Thus, we first examined the most suitable catalyst support. Table 2 shows the catalytic performances of ruthenium catalysts supported on various inorganic supports prepared by the adsorption-precipitation method. Under the

**Table 2** Catalytic behaviours of various metal oxide-supported Ru catalysts for aerobic oxidation of benzyl amine to benzonitrile<sup>a</sup>

Entry	Catalyst	Surf. area (m <sup>2</sup> g <sup>-1</sup> )	Conv. (%)	Select. (%)
1	None	—	<0.1	—
2	Ru/SiO <sub>2</sub>	6.3	21	>99
3	Ru/Al <sub>2</sub> O <sub>3</sub>	245	54	>99
4	Ru/ZrO <sub>2</sub>	17	36	>99
5	Ru/SBA-15	324	29	>99
6	Ru/CeO <sub>2</sub>	8.7	34	>99
7	Ru/Pb <sub>3</sub> O <sub>4</sub>	8.5	11	>99
8	Ru/MnO <sub>2</sub>	3.7	26	>99
9	Ru/Fe <sub>2</sub> O <sub>3</sub>	10	35	>99
10	Ru/Fe <sub>3</sub> O <sub>4</sub>	47	30	>99
11	Ru/CoO	7.2	43	>99
12	Ru/Co <sub>3</sub> O <sub>4</sub>	32	95	>99
13	Ru/ZnO	12	15	>99
14	Ru/hydroxalcite	41	35	>99
15	Ru/hydroxyapatite	78	83	70

<sup>a</sup> Reaction conditions: Ru content, 3.0 wt% for all of the catalysts except for the Ru/Co<sub>3</sub>O<sub>4</sub>, which has a Ru content of 2.5 wt%; catalyst amount, 0.1 g; benzyl amine, 1 mmol; solvent (PhCF<sub>3</sub>), 5 mL; O<sub>2</sub> flow rate, 3 mL min<sup>-1</sup>; temperature, 373 K; time, 1 h.

reaction conditions shown in Table 2, all of these catalysts except for the Ru/hydroxyapatite exhibited good selectivity for the formation of benzonitrile from benzyl amine. Although the Ru/hydroxyapatite showed a relatively higher conversion of benzyl amine (entry 15), this catalyst produced *N*-benzylidenebenzylamine as a main by-product with a considerable selectivity. This is different from the result reported for the hydroxyapatite-immobilized monomeric Ru<sup>III</sup> catalyst prepared by an ion-exchange method, where a higher selectivity could be obtained.<sup>7</sup> This may imply that different states of ruthenium exhibit different catalytic properties. The BET surface area of each sample is also shown in Table 2. It can be seen that there is no definite correlation between the activity and the BET surface area for the catalysts with different kinds of supports. Thus, the chemical nature of the support may play a key role in determining the catalytic performance. Among various supported ruthenium catalysts we examined, the Ru/Co<sub>3</sub>O<sub>4</sub> showed the best catalytic performance for the aerobic oxidation of benzyl amine to benzonitrile (entry 12). Benzyl amine conversion and benzonitrile selectivity were 95 and >99%, respectively. The present Ru/Co<sub>3</sub>O<sub>4</sub> catalyst provided a TOF of 38 h<sup>-1</sup> at 373 K for the conversion of benzyl amine based on Ru, which was significantly higher than those reported for the Ru/hydroxyapatite and the Ru/Fe<sub>3</sub>O<sub>4</sub> catalysts.<sup>7,11</sup> This TOF value was slightly higher than that reported for the Ru/Al<sub>2</sub>O<sub>3</sub> catalyst.<sup>8</sup> We also examined the catalytic performance of Ru/Al<sub>2</sub>O<sub>3</sub> (entry 3), and it showed a relatively higher activity than other supported Ru catalysts except for the Ru/Co<sub>3</sub>O<sub>4</sub> and the Ru/hydroxyapatite in our case.

Subsequently, we tested Co<sub>3</sub>O<sub>4</sub>-supported various transition metal catalysts for the aerobic oxidation of benzyl amine. The catalytic performances over these catalysts prepared by the adsorption-precipitation method are summarized in Table 3. Over these catalysts, the selectivity to benzonitrile was always >99%. However, only the Ru/Co<sub>3</sub>O<sub>4</sub> catalyst exhibited a considerable benzyl amine conversion. Other catalysts could not provide benzyl amine conversions significantly higher than Co<sub>3</sub>O<sub>4</sub> alone. Thus, ruthenium was a very unique active component and Co<sub>3</sub>O<sub>4</sub> was a superior catalyst support for the aerobic oxidation of benzyl amine to benzonitrile.

**Table 3** Catalytic behaviours of Co<sub>3</sub>O<sub>4</sub>-supported various transition metal catalysts for aerobic oxidation of benzyl amine to benzonitrile<sup>a</sup>

Entry	Catalyst <sup>b</sup>	Conversion (%)	Selectivity (%)
1	Co <sub>3</sub> O <sub>4</sub>	2.0	>99
2	Au/Co <sub>3</sub> O <sub>4</sub>	1.0	>99
3	Pd/Co <sub>3</sub> O <sub>4</sub>	1.4	>99
4	Rh/Co <sub>3</sub> O <sub>4</sub>	0.8	>99
5	Pt/Co <sub>3</sub> O <sub>4</sub>	1.0	>99
6	Ru/Co <sub>3</sub> O <sub>4</sub>	95	>99
7	Cu/Co <sub>3</sub> O <sub>4</sub>	1.5	>99
8	Co/Co <sub>3</sub> O <sub>4</sub>	0.6	>99
9	Fe/Co <sub>3</sub> O <sub>4</sub>	0.2	>99
10	Ni/Co <sub>3</sub> O <sub>4</sub>	0.7	>99
11	Ir/Co <sub>3</sub> O <sub>4</sub>	0.9	>99

<sup>a</sup> Reaction conditions: metal content, 3.0 wt% for all of the catalysts except for the Ru/Co<sub>3</sub>O<sub>4</sub>, which has a Ru content of 2.5 wt%; catalyst amount, 0.1 g; benzyl amine, 1 mmol; solvent (PhCF<sub>3</sub>), 5 mL; O<sub>2</sub> flow rate, 3 mL min<sup>-1</sup>; temperature, 373 K; time, 1 h. <sup>b</sup> All of the supported catalysts were prepared by the adsorption-precipitation method, and the metal precursors were AuCl<sub>3</sub>, PdCl<sub>2</sub>, RhCl<sub>3</sub>, PtCl<sub>2</sub>, RuCl<sub>3</sub>, Cu(NO<sub>3</sub>)<sub>2</sub>, Co(NO<sub>3</sub>)<sub>2</sub>, Fe(NO<sub>3</sub>)<sub>3</sub>, Ni(NO<sub>3</sub>)<sub>2</sub> and IrCl<sub>3</sub> for the catalysts used for entries 2–11, respectively.

#### Effects of Ru content and Co<sub>3</sub>O<sub>4</sub> size of Ru/Co<sub>3</sub>O<sub>4</sub> catalysts on their catalytic performances for aerobic oxidation of benzyl amine

Table 4 shows the effect of Ru loadings on catalytic properties of the Ru/Co<sub>3</sub>O<sub>4</sub> catalysts prepared by the adsorption-precipitation method. At a fixed amount of catalyst (0.1 g, entries 1–6), benzyl amine conversion increased with increasing Ru content up to 2.5 wt%, and a further increase in Ru content from 2.5 to 3.5 wt% decreased benzyl amine conversion. Comparisons at a fixed amount of Ru (9.8 μmol, entries 7–11) by regulating the catalyst amount showed that the conversion of benzyl amine decreased monotonically with a rise in Ru content. Especially, a sharp decrease was observed as Ru content was raised from 2.5 to 3.5 wt%. This significant drop in catalytic activity at higher Ru contents may imply that only the ruthenium species highly dispersed on Co<sub>3</sub>O<sub>4</sub> or intimately contacted with Co<sub>3</sub>O<sub>4</sub> particles are active for the aerobic oxidation of benzyl amine.

**Table 4** Catalytic behaviours of Ru/Co<sub>3</sub>O<sub>4</sub> catalysts with different Ru contents or different sizes of Co<sub>3</sub>O<sub>4</sub> for aerobic oxidation of benzyl amine to benzonitrile<sup>a</sup>

Entry	Catalyst	Ru amount ( $\mu\text{mol}$ )	Conv. (%)	Select. (%)
1 <sup>b</sup>	Co <sub>3</sub> O <sub>4</sub>	—	2.0	>99
2 <sup>b</sup>	1.0 wt% Ru/Co <sub>3</sub> O <sub>4</sub>	9.8	61	>99
3 <sup>b</sup>	1.7 wt% Ru/Co <sub>3</sub> O <sub>4</sub>	16.8	83	>99
4 <sup>b</sup>	2.5 wt% Ru/Co <sub>3</sub> O <sub>4</sub>	24.7	95	>99
5 <sup>b</sup>	3.5 wt% Ru/Co <sub>3</sub> O <sub>4</sub>	34.6	75	>99
6 <sup>b</sup>	10 wt% Ru/Co <sub>3</sub> O <sub>4</sub>	98.9	70	>99
7 <sup>c</sup>	1.0 wt% Ru/Co <sub>3</sub> O <sub>4</sub>	9.8	61	>99
8 <sup>c</sup>	1.7 wt% Ru/Co <sub>3</sub> O <sub>4</sub>	9.8	43	>99
9 <sup>c</sup>	2.5 wt% Ru/Co <sub>3</sub> O <sub>4</sub>	9.8	34	>99
10 <sup>c</sup>	3.5 wt% Ru/Co <sub>3</sub> O <sub>4</sub>	9.8	7.7	>99
11 <sup>c</sup>	10 wt% Ru/Co <sub>3</sub> O <sub>4</sub>	9.8	4.1	>99
12 <sup>b</sup>	2.5 wt% Ru/Co <sub>3</sub> O <sub>4</sub> -A	24.7	54	>99

<sup>a</sup> Reaction conditions: benzyl amine, 1 mmol; solvent (PhCF<sub>3</sub>), 5 mL; O<sub>2</sub> flow rate, 3 mL min<sup>-1</sup>; temperature, 373 K; time, 1 h. <sup>b</sup> Catalyst amount was fixed at 0.10 g. <sup>c</sup> Ru amount was fixed at 9.8  $\mu\text{mol}$  by regulating the catalyst weight.

If the contact boundary between Ru species and Co<sub>3</sub>O<sub>4</sub> particles plays a role in determining the catalytic activity, it can be expected that the size of Co<sub>3</sub>O<sub>4</sub> will also affect the catalytic performances. The effect of size of oxide support on catalytic performances of supported catalysts has attracted much attention in recent years.<sup>13,14</sup> We exploited two Co<sub>3</sub>O<sub>4</sub> samples (Co<sub>3</sub>O<sub>4</sub> and Co<sub>3</sub>O<sub>4</sub>-A with surface areas of 26 and 5.6 m<sup>2</sup> g<sup>-1</sup>, respectively) with different sizes for the preparation of supported ruthenium catalysts by the same adsorption-precipitation method. The BET surface areas of the 2.5 wt% Ru/Co<sub>3</sub>O<sub>4</sub> and 2.5 wt% Ru/Co<sub>3</sub>O<sub>4</sub>-A were 32 and 13 m<sup>2</sup> g<sup>-1</sup>, respectively. XRD patterns of the two Co<sub>3</sub>O<sub>4</sub> samples and the two supported ruthenium catalysts are shown in Fig. 1. Only the diffraction peaks of crystalline Co<sub>3</sub>O<sub>4</sub> with spinel structure were observed for these samples. No information about ruthenium species could be obtained possibly because the ruthenium species were in amorphous state or the Ru content was too low. Actually, any diffraction peaks assignable to Ru species could not be detected even for the Ru/Co<sub>3</sub>O<sub>4</sub> catalyst with a Ru content of 10 wt%, indicating the amorphous state of ruthenium species

in these catalysts. The diffraction peaks for the Co<sub>3</sub>O<sub>4</sub> and the 2.5 wt% Ru/Co<sub>3</sub>O<sub>4</sub> were significantly broader than those for the Co<sub>3</sub>O<sub>4</sub>-A and the 2.5 wt% Ru/Co<sub>3</sub>O<sub>4</sub>-A. Calculations using the Scherrer equation revealed that the sizes of Co<sub>3</sub>O<sub>4</sub> and Co<sub>3</sub>O<sub>4</sub>-A were  $\sim 30$  and  $\sim 100$  nm, respectively, either before or after the loading of ruthenium species. SEM images shown in Fig. 2 for the 2.5 wt% Ru/Co<sub>3</sub>O<sub>4</sub> and the 2.5 wt% Ru/Co<sub>3</sub>O<sub>4</sub>-A clearly revealed that the particle sizes of Co<sub>3</sub>O<sub>4</sub> in the former catalyst were significantly smaller than those in the latter catalyst. We observed a significant difference in catalytic performance between these two catalysts (Table 4, entries 4 and 12). The Ru/Co<sub>3</sub>O<sub>4</sub>-A catalyst with larger Co<sub>3</sub>O<sub>4</sub> particles exhibited a significantly lower conversion of benzyl amine (entry 12). It is reasonable to think that the smaller Co<sub>3</sub>O<sub>4</sub> particles can lead to larger interfaces between the supported ruthenium species and the Co<sub>3</sub>O<sub>4</sub> particles, and thus result in the higher catalytic performance of the Ru/Co<sub>3</sub>O<sub>4</sub> catalyst. Thus, the present result further suggests that the interface between the Ru species and the Co<sub>3</sub>O<sub>4</sub> particles plays a key role in determining the catalytic activity.

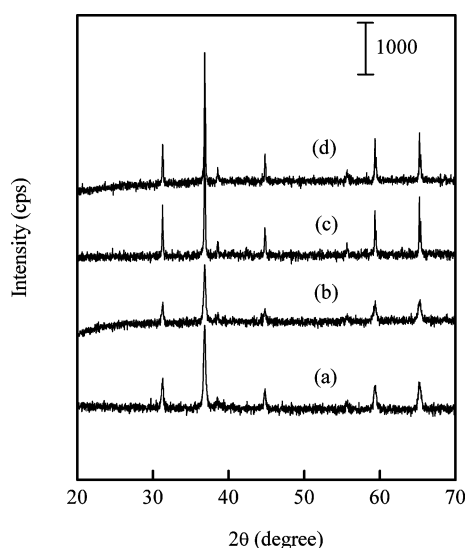


**Fig. 1** XRD patterns. (a) Co<sub>3</sub>O<sub>4</sub>, (b) 2.5 wt% Ru/Co<sub>3</sub>O<sub>4</sub>, (c) Co<sub>3</sub>O<sub>4</sub>-A and (d) 2.5 wt% Ru/Co<sub>3</sub>O<sub>4</sub>-A.

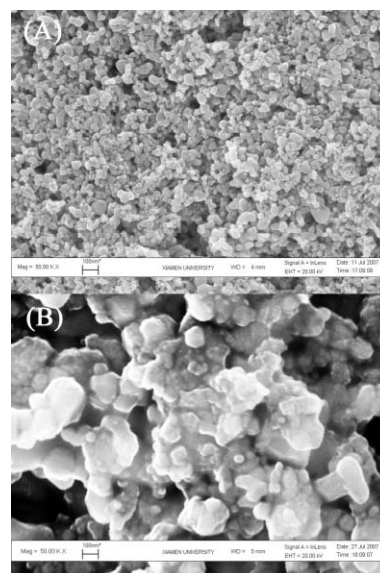
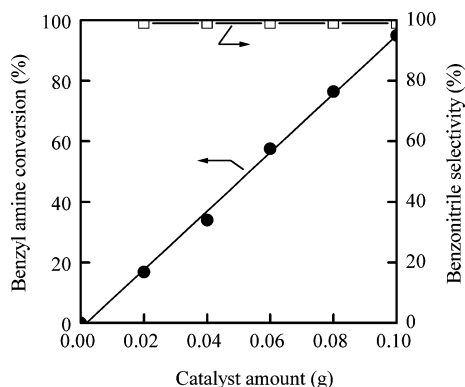


**Fig. 2** SEM images. (A) 2.5 wt% Ru/Co<sub>3</sub>O<sub>4</sub>, (B) 2.5 wt% Ru/Co<sub>3</sub>O<sub>4</sub>-A.



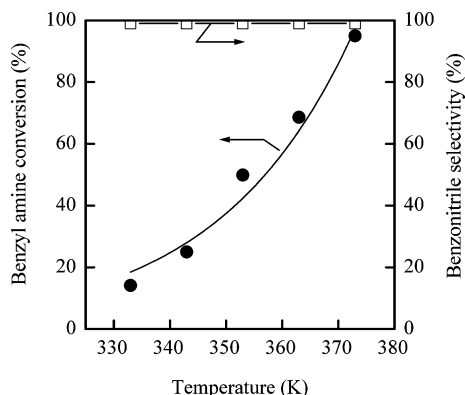
### Effects of kinetic factors on catalytic performances of Ru/Co<sub>3</sub>O<sub>4</sub> catalyst for aerobic oxidation of benzyl amine

Fig. 3 shows the influence of the amount of catalyst on catalytic performances for the 2.5 wt% Ru/Co<sub>3</sub>O<sub>4</sub> catalyst. Without a catalyst, benzyl amine conversion was almost zero. The conversion increased proportionally to the catalyst amount in the whole range investigated (0–0.10 g). These observations confirm that the catalyst plays essential roles in the aerobic oxidation of benzyl amine and the reaction proceeds steadily over the catalyst. The linear increase in benzyl amine conversion even at a higher conversion level may imply that the reaction rate is not strongly dependent on the concentration of the substrate.



**Fig. 3** Effect of catalyst amount on catalytic performance of the 2.5 wt% Ru/Co<sub>3</sub>O<sub>4</sub> for the aerobic oxidation of benzyl amine. Symbols: (●) benzyl amine conversion, (□) benzonitrile selectivity. Reaction conditions: benzyl amine, 1 mmol; solvent (PhCF<sub>3</sub>), 5 mL; O<sub>2</sub> flow rate, 3 mL min<sup>-1</sup>; temperature, 373 K; time, 1 h.

The effect of reaction temperature on catalytic performance of the 2.5 wt% Ru/Co<sub>3</sub>O<sub>4</sub> catalyst is shown in Fig. 4. Benzyl amine conversion increased exponentially with temperature. The activation energy calculated using the Arrhenius equation was 62 kJ mol<sup>-1</sup>, further suggesting that the reaction was not rate-limited by the diffusion.



**Fig. 4** Effect of reaction temperature on catalytic performance of the 2.5 wt% Ru/Co<sub>3</sub>O<sub>4</sub> for the aerobic oxidation of benzyl amine. Symbols: (●) benzyl amine conversion, (□) benzonitrile selectivity. Reaction conditions: catalyst, 0.1 g; benzyl amine, 1 mmol; solvent (PhCF<sub>3</sub>), 5 mL; O<sub>2</sub> flow rate, 3 mL min<sup>-1</sup>; time, 1 h.

The time course plotted in Fig. 5 for the aerobic oxidation of benzyl amine over the 2.5 wt% Ru/Co<sub>3</sub>O<sub>4</sub> catalyst at 353 K

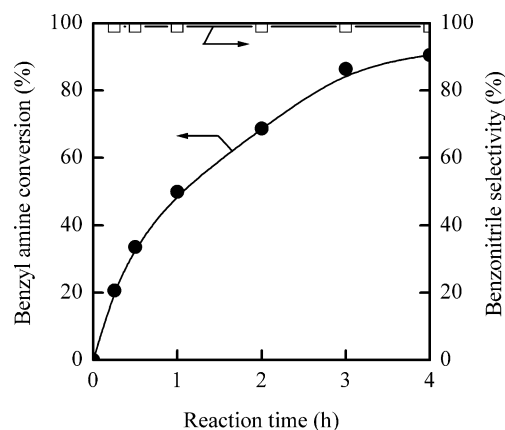


**Fig. 5** Time course for the aerobic oxidation of benzyl amine over the 2.5 wt% Ru/Co<sub>3</sub>O<sub>4</sub> catalyst. Symbols: (●) benzyl amine conversion, (□) benzonitrile selectivity. Reaction conditions: catalyst, 0.1 g; benzyl amine, 1 mmol; solvent (PhCF<sub>3</sub>), 5 mL; O<sub>2</sub> flow rate, 3 mL min<sup>-1</sup>; temperature, 353 K.

showed that the conversion increased linearly with time in the initial 0.5 h, and then the rate became slow. The initial conversion rate at 353 K was calculated to be 32 mol h<sup>-1</sup> mol-Ru<sup>-1</sup>.

The effect of oxygen pressure on catalytic performances at 353 K was investigated using (O<sub>2</sub>+N<sub>2</sub>) gas mixture instead of pure O<sub>2</sub> for the oxidation of benzyl amine over the 2.5 wt% Ru/Co<sub>3</sub>O<sub>4</sub> catalyst. The result in Fig. 6 revealed that benzyl amine conversion did not change significantly with changing the partial pressure of oxygen in the range we investigated (0.2–1.0 atm). In other words, the reaction order with respect to oxygen was zero in this range. Thus, it is expected that air can also be used as an oxidant over our catalyst. Actually, using air (3 mL min<sup>-1</sup>) instead of pure oxygen, the conversion of benzyl amine was 92% and the selectivity to benzonitrile was >99% over the 2.5 wt% Ru/Co<sub>3</sub>O<sub>4</sub> catalyst under the reaction conditions shown in Table 2 (373 K).

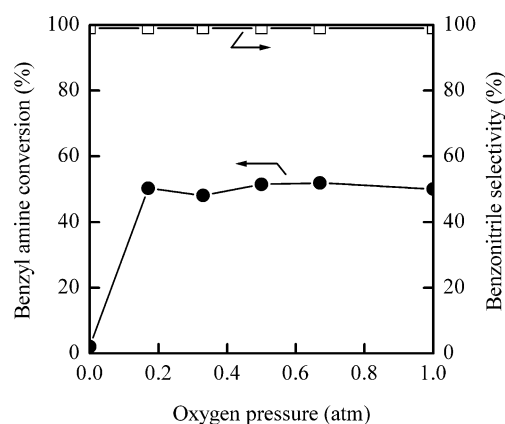


**Fig. 6** Effect of oxygen pressure on catalytic performance of the 2.5 wt% Ru/Co<sub>3</sub>O<sub>4</sub> for the aerobic oxidation of benzyl amine. Symbols: (●) benzyl amine conversion, (□) benzonitrile selectivity. Reaction conditions: catalyst, 0.1 g; benzyl amine, 1 mmol; solvent (PhCF<sub>3</sub>), 5 mL; (O<sub>2</sub> + N<sub>2</sub>) flow rate, 6 mL min<sup>-1</sup>; temperature, 353 K; time, 1 h.

Recycling uses of the 2.5 wt% Ru/Co<sub>3</sub>O<sub>4</sub> catalyst for the aerobic oxidation of benzyl amine were investigated. The recovered catalyst after each run was washed with ethanol for

several times and then was reused in the next run after drying at ambient temperature. The result (Fig. 7) shows that the conversion of benzyl amine and the selectivity to benzonitrile are almost unchanged after repeated uses for 5 times. Therefore, the present Ru/Co<sub>3</sub>O<sub>4</sub> catalyst is recyclable.

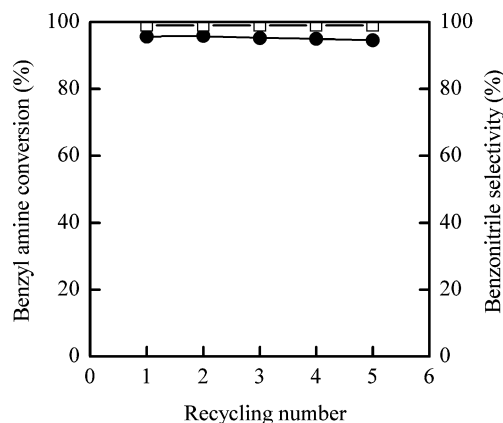


**Fig. 7** Recycling uses of the 2.5 wt% Ru/Co<sub>3</sub>O<sub>4</sub> for the aerobic oxidation of benzyl amine. Symbols: (●) benzyl amine conversion, (□) benzonitrile selectivity. Reaction conditions: catalyst, 0.1 g; benzyl amine, 1 mmol; solvent (PhCF<sub>3</sub>), 5 mL; O<sub>2</sub> flow rate, 3 mL min<sup>-1</sup>; temperature, 373 K; time, 1 h.

#### Ru/Co<sub>3</sub>O<sub>4</sub> catalyst for the aerobic oxidation of other amines and for the solvent-free aerobic oxidation of amines

We applied the 2.5 wt% Ru/Co<sub>3</sub>O<sub>4</sub> catalyst to the aerobic oxidation of several other amines. As summarized in Table 5, the substituted benzyl amines could also be selectively oxidized

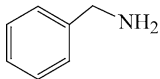
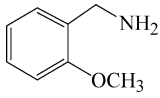
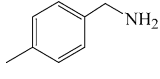
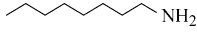
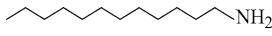
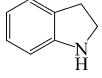
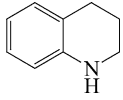
into the corresponding nitriles although the activity was slightly lower than benzyl amine. The oxidation of non-activated aliphatic amines also proceeded efficiently over the present catalyst (entries 4 and 5). Not only the primary amines, but also the heterocyclic amines were selectively oxidized in the presence of the Ru/Co<sub>3</sub>O<sub>4</sub> catalyst. For example, indoline and 1,2,3,4-tetrahydroquinoline were oxidized selectively to indole and quinoline in good yields (≥ 90%) after 2 and 6 h of reactions, respectively (entries 6 and 7).

It is highly desirable to perform solvent-free aerobic oxidation of amines from the viewpoint of green chemistry. We found that the 2.5 wt% Ru/Co<sub>3</sub>O<sub>4</sub> catalyst was useful for the solvent-free aerobic oxidation of several kinds of amines (Table 6). Benzyl amine conversion and benzonitrile selectivity reached 91 and 98% after 24 h reaction at 423 K over our catalyst, giving a TON of 1829 h<sup>-1</sup> and a TOF of 76 h<sup>-1</sup>. Other amines shown in Table 6 could also be selectively oxidized under solvent-free conditions. To the best of our knowledge, this is the first report on the solvent-free catalytic aerobic oxidation of amines. We have carried out recycling uses of the 2.5 wt% Ru/Co<sub>3</sub>O<sub>4</sub> catalyst for the solvent-free aerobic oxidation of 1,2,3,4-tetrahydroquinoline. The catalyst could be recovered easily through centrifugation, and the conversion of 1,2,3,4-tetrahydroquinoline only decreased slightly after 4 reaction cycles (Table 6, entry 8).

#### Insights into the state of ruthenium species active for aerobic oxidation of amines

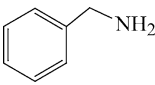
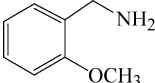
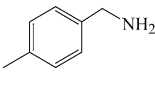


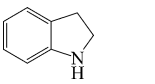
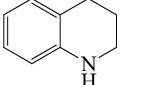
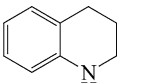
To gain insights into the state of ruthenium species active for aerobic oxidation of amines, we have investigated the state-activity relationships using the catalysts deliberately prepared

**Table 5** Aerobic oxidation of various amines catalyzed by the 2.5 wt% Ru/Co<sub>3</sub>O<sub>4</sub> catalyst<sup>a</sup>

Entry	Substrate	Time (h)	Conv. (%)	Select. (%)
1		1	95	>99
2		2	89	>99
3		2	98	>99
4		2	88	>99
5		1	77	>99
6		2	>99	>99
7		6	90	>99

<sup>a</sup> Reaction conditions: amine, 1 mmol; catalyst, 0.10 g; solvent (PhCF<sub>3</sub>), 5 mL; O<sub>2</sub> flow rate, 3 mL min<sup>-1</sup>; temperature, 373 K.

**Table 6** Solvent-free aerobic oxidation of various amines catalyzed by the 2.5 wt% Ru/Co<sub>3</sub>O<sub>4</sub> catalyst<sup>a</sup>

Entry	Substrate	Temp. (K)	Time (h)	Conv. (%)	Select. (%)
1		423	24	91	98
2		373	48	51	>99
3		383	30	41	>99
4		373	48	98	>99
5		373	48	99	>99
6		423	24	77	>99
7		423	24	76	>99
8 <sup>b</sup>		423	24	69	>99

<sup>a</sup> Reaction conditions: amine, 50 mmol; catalyst, 0.10 g; O<sub>2</sub> flow rate, 3 mL min<sup>-1</sup>. <sup>b</sup> Result after 4 recycles.

with different procedures as listed in Table 1. The catalysts were characterized by XRD, XPS and H<sub>2</sub>-TPR techniques. From XRD measurements, we could not see significant differences among these catalysts. We only observed the diffraction peaks ascribed to Co<sub>3</sub>O<sub>4</sub> (similar to those in Fig. 1), and no information about Ru species could be obtained possibly because of the lower content of Ru or the amorphous feature of the Ru species. Ru 3d XPS spectra of these catalysts are shown in Fig. 8. Generally, the

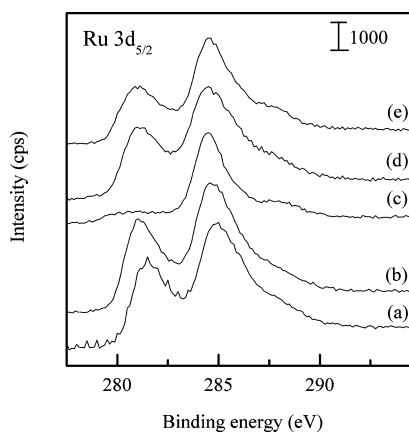


**Fig. 8** Ru 3d XPS spectra for the Co<sub>3</sub>O<sub>4</sub>-supported ruthenium catalysts prepared with different procedures. (a) 2.5 wt% Ru/Co<sub>3</sub>O<sub>4</sub>, (b) 2.5 wt% Ru/Co<sub>3</sub>O<sub>4</sub>-C573, (c) 2.5 wt% Ru/Co<sub>3</sub>O<sub>4</sub>-C573-R623, (d) 3 wt% Ru/Co<sub>3</sub>O<sub>4</sub> (*imp*), (e) 3 wt% Ru/Co<sub>3</sub>O<sub>4</sub> (*imp*)-C573.

C 1 s peak for carbon contamination at 284.6 eV was used as a reference for the correction of binding energy (BE). However, because of the overlapping of the peaks of Ru 3d<sub>3/2</sub> and C 1 s, the Co 2p<sub>3/2</sub> peak (BE, 779.5 eV) was used as a reference for our samples except for the 2.5 wt% Ru/Co<sub>3</sub>O<sub>4</sub>-C573-R623, for which the intensity of Ru 3d<sub>3/2</sub> was very low and the peak position of C 1 s could be clearly discerned. The obtained BE of Ru 3d<sub>5/2</sub> and the possible state of ruthenium species for each catalyst are summarized in Table 7. The BE of Ru 3d<sub>5/2</sub> for the 2.5 wt% Ru/Co<sub>3</sub>O<sub>4</sub> catalyst prepared by the adsorption-precipitation method was at 281.5 eV. The hydrous ruthenium oxide (RuO<sub>2</sub>·xH<sub>2</sub>O or RuO<sub>x</sub>H<sub>y</sub>) was reported to exhibit a BE of Ru 3d<sub>5/2</sub> at 281.4–281.8 eV,<sup>15–17</sup> which was higher than that for RuO<sub>2</sub> (280.7–281.0 eV)<sup>18</sup> owing to the presence of OH functional groups.<sup>16</sup> Thus, the XPS result suggests that the ruthenium species in the 2.5 wt% Ru/Co<sub>3</sub>O<sub>4</sub> catalyst is in the hydrous RuO<sub>2</sub> state. The 2.5 wt% Ru/Co<sub>3</sub>O<sub>4</sub>-C573 possessed a lower BE of Ru 3d<sub>5/2</sub> at 281.0 eV, indicating the transformation of RuO<sub>2</sub>·xH<sub>2</sub>O to anhydrous RuO<sub>2</sub> species. The 2.5 wt% Ru/Co<sub>3</sub>O<sub>4</sub>-C573-R623 showed a much lower BE of Ru 3d<sub>5/2</sub> at 280.0 eV, which could be assigned to metallic Ru.<sup>18</sup> For the 3 wt% Ru/Co<sub>3</sub>O<sub>4</sub> (*imp*) and the 3 wt% Ru/Co<sub>3</sub>O<sub>4</sub> (*imp*)-C573, the BE values of Ru 3d<sub>5/2</sub> were both 280.9 eV. However, the surface molar ratio of Cl/Co estimated from XPS for the 3 wt% Ru/Co<sub>3</sub>O<sub>4</sub> (*imp*) was significantly larger. The surface molar ratio of Cl/Ru for this sample was ~1.3. Thus, this sample might contain a mixture of RuCl<sub>3</sub> and RuO<sub>2</sub>. This is consistent with some reported

**Table 7** XPS results for Co<sub>3</sub>O<sub>4</sub>-supported ruthenium catalysts prepared by different procedures

Catalyst	BE of Ru3d <sub>5/2</sub> (eV)	Main state of Ru	Ru/Co <sup>a</sup>	Cl/Co <sup>a</sup>
2.5 wt% Ru/Co <sub>3</sub> O <sub>4</sub>	281.5	RuO <sub>2</sub> ·xH <sub>2</sub> O	0.12	0.025
2.5 wt% Ru/Co <sub>3</sub> O <sub>4</sub> -C573	281.0	RuO <sub>2</sub>	0.11	0.022
2.5 wt% Ru/Co <sub>3</sub> O <sub>4</sub> -C573-R623	280.0	Ru <sup>o</sup>	0.02	0.020
3 wt% Ru/Co <sub>3</sub> O <sub>4</sub> ( <i>imp</i> )	280.9	RuCl <sub>3</sub> and RuO <sub>2</sub>	0.13	0.17
3 wt% Ru/Co <sub>3</sub> O <sub>4</sub> ( <i>imp</i> )-C573	280.9	RuO <sub>2</sub>	0.09	0.014

<sup>a</sup> Molar ratio calculated from XPS analysis.

results that RuCl<sub>3</sub> is not stable and may easily be converted to RuO<sub>2</sub> by heating in air, and that even some commercial RuCl<sub>3</sub> comprises ruthenium species with higher valence states.<sup>15,19,20</sup> After calcination, the 3 wt% Ru/Co<sub>3</sub>O<sub>4</sub> (*imp*)-C573 sample exhibited a lower ratio of Cl/Co, indicating that RuO<sub>2</sub> became the main ruthenium species. The surface Cl/Co molar ratios for the series of samples prepared by the adsorption-precipitation method were also quite low, confirming that only a small amount of Cl remained in these samples. Table 7 also shows that the surface molar ratios of Ru/Co for these samples (except for the 2.5 wt% Ru/Co<sub>3</sub>O<sub>4</sub>-C573-R623) are similar (0.09–0.13). These values of Ru/Co molar ratio are larger than that expected from the bulk composition (~0.02). Thus, the ruthenium species are probably located on the surface of Co<sub>3</sub>O<sub>4</sub> in these samples except for the 2.5 wt% Ru/Co<sub>3</sub>O<sub>4</sub>-C573-R623.

Fig. 9 shows H<sub>2</sub>-TPR profiles for the Co<sub>3</sub>O<sub>4</sub>-supported ruthenium catalysts prepared by different procedures. Co<sub>3</sub>O<sub>4</sub> alone showed two reduction peaks at 588 and 696 K, and the quantitative calculations suggested that these two peaks likely corresponded to the reductions of Co<sup>III</sup> to Co<sup>II</sup> and Co<sup>II</sup> to Co<sup>o</sup>, respectively. The hydrous ruthenium oxide (RuO<sub>2</sub>·xH<sub>2</sub>O) exhibited a single reduction peak at 430 K, corresponding to the reduction of Ru<sup>IV</sup> to Ru<sup>o</sup>. The 2.5 wt% Ru/Co<sub>3</sub>O<sub>4</sub> catalyst exhibited two reduction peaks at 403 and 564 K (curve b). The quantification suggested that the lower-temperature peak could not be assigned only to the reduction of Ru species from +IV to 0, and it must also comprise the reduction of Co<sub>3</sub>O<sub>4</sub>. The calculation implied that the lower-temperature peak comprised the reduction of Co<sup>III</sup> to Co<sup>II</sup> in addition to Ru<sup>IV</sup> to Ru<sup>o</sup>, and the higher-temperature peak corresponded to the reduction of Co<sup>II</sup> to Co<sup>o</sup>. Thus, the loading of Ru species on Co<sub>3</sub>O<sub>4</sub> significantly enhanced the reduction of Co<sub>3</sub>O<sub>4</sub>. The same phenomenon was also observed for the Ru-Co binary oxides prepared by a co-precipitation method.<sup>21</sup> As compared with the 2.5 wt% Ru/Co<sub>3</sub>O<sub>4</sub>, the reduction peaks for the 2.5 wt% Ru/Co<sub>3</sub>O<sub>4</sub>-

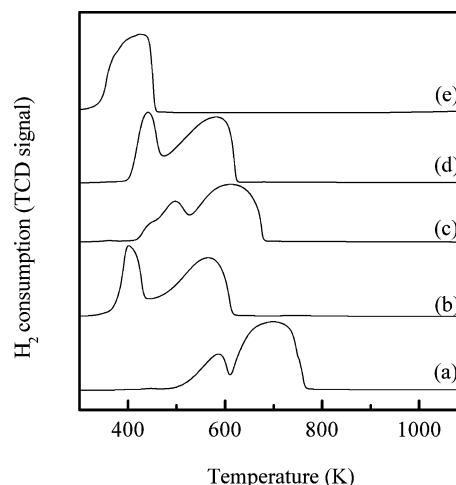


**Fig. 9** H<sub>2</sub>-TPR profiles for the Co<sub>3</sub>O<sub>4</sub>-supported ruthenium catalysts prepared with different procedures together with Co<sub>3</sub>O<sub>4</sub> and hydrous RuO<sub>2</sub>. (a) Co<sub>3</sub>O<sub>4</sub>, (b) 2.5 wt% Ru/Co<sub>3</sub>O<sub>4</sub>, (c) 2.5 wt% Ru/Co<sub>3</sub>O<sub>4</sub>-C573, (d) 3 wt% Ru/Co<sub>3</sub>O<sub>4</sub> (*imp*)-C573, (e) RuO<sub>2</sub>·xH<sub>2</sub>O.

C573 (curve c) and the 3.0 wt% Ru/Co<sub>3</sub>O<sub>4</sub> (*imp*)-C573 (curve d) shifted significantly to higher temperatures. Combined with the information from XPS measurements described above, this result suggests that the Co<sub>3</sub>O<sub>4</sub>-supported hydrous RuO<sub>2</sub> possesses higher reducibility than the supported anhydrous RuO<sub>2</sub>.

The catalytic performances of these catalysts as well as the single Co<sub>3</sub>O<sub>4</sub> and RuO<sub>2</sub>·xH<sub>2</sub>O for the aerobic oxidation of benzyl amine are summarized in Table 8. The single RuO<sub>2</sub>·xH<sub>2</sub>O showed a very low conversion under the reaction conditions of Table 8, indicating that the dispersion of RuO<sub>2</sub>·xH<sub>2</sub>O on a support played a key role in enhancing its catalytic performance. The Ru/Co<sub>3</sub>O<sub>4</sub> (*imp*) without calcination showed a conversion comparable to that of Co<sub>3</sub>O<sub>4</sub> alone (entry 3). Moreover, we

**Table 8** Catalytic behaviours of Co<sub>3</sub>O<sub>4</sub>-supported ruthenium catalysts with ruthenium in different states for aerobic oxidation of benzyl amine to benzonitrile<sup>a</sup>

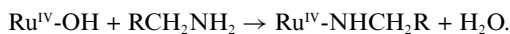
Entry	Catalyst	Ru amount (μmol)	Conv. (%)	Select. (%)
1	Co <sub>3</sub> O <sub>4</sub>	—	2.0	>99
2	RuO <sub>2</sub> ·xH <sub>2</sub> O	29.7	1.2	>99
3	3 wt% Ru/Co <sub>3</sub> O <sub>4</sub> ( <i>imp</i> )	29.7	1.8	>99
4	3 wt% Ru/Co <sub>3</sub> O <sub>4</sub> ( <i>imp</i> )-C573	29.7	14	>99
5	2.5 wt% Ru/Co <sub>3</sub> O <sub>4</sub>	24.7	95	>99
6	2.5 wt% Ru/Co <sub>3</sub> O <sub>4</sub> -C573	24.7	19	>99
7	2.5 wt% Ru/Co <sub>3</sub> O <sub>4</sub> -C573-R623	24.7	0.9	>99

<sup>a</sup> Reaction conditions: benzyl amine, 1 mmol; solvent (PhCF<sub>3</sub>), 5 mL; O<sub>2</sub> flow rate, 3 mL min<sup>-1</sup>; temperature, 373 K; time, 1 h.



confirmed that the homogeneous oxidation of benzyl amine by O<sub>2</sub> using RuCl<sub>3</sub> catalyst could not occur under our reaction conditions. Thus, the supported RuCl<sub>3</sub> species should not be the active species. On the other hand, the catalyst prepared by the adsorption-precipitation method without calcination exhibited a significantly higher activity (entry 5). Thus, the supported hydrous RuO<sub>2</sub> was a highly efficient species for the aerobic oxidation of amines. The conversion of benzyl amine over the calcined 2.5 wt% Ru/Co<sub>3</sub>O<sub>4</sub>-C573 became remarkably lower (entry 6). The 3 wt% RuO<sub>x</sub>/Co<sub>3</sub>O<sub>4</sub> (*imp*)-C573 exhibited a similar activity (entry 4) to the 2.5 wt% Ru/Co<sub>3</sub>O<sub>4</sub>-C573. These observations further confirm that the ruthenium species in these two catalysts are the same (i.e., anhydrous RuO<sub>2</sub>). Thus, the supported anhydrous RuO<sub>2</sub> possesses a lower activity in the aerobic oxidation of benzyl amine. The result in Table 8 also suggests that the metallic Ru species cannot catalyse the aerobic oxidation of amines because the 2.5 wt% Ru/Co<sub>3</sub>O<sub>4</sub>-C573-R623 is almost inactive (entry 7).

Because the heterogeneous catalysts reported for the aerobic oxidation of amines are still scarce,<sup>7,8,11</sup> the insights into the active sites are very limited. Kaneda and co-workers suggested that a monomeric Ru<sup>III</sup> with Cl ligands attached on hydroxyapatite was responsible for the selective oxidation of amines.<sup>7,22</sup> Yamaguchi and Mizuno proposed Ru(OH)<sub>3</sub> as the active species for their Ru/Al<sub>2</sub>O<sub>3</sub> catalyst.<sup>8</sup> Our results described above have revealed that the Co<sub>3</sub>O<sub>4</sub>-supported hydrous RuO<sub>2</sub> is the active species for the aerobic oxidation of amines. The supported anhydrous RuO<sub>2</sub> only showed a lower activity. The metallic Ru (Ru<sup>0</sup>) or the RuCl<sub>3</sub> species were inactive for the aerobic oxidation of amines. It is of interest to note that the hydrous RuO<sub>2</sub> with or without a support has been reported to be an active phase for the aerobic oxidation of alcohols by a few groups.<sup>21,23–25</sup> EXAFS studies showed that the hydrous RuO<sub>2</sub> possesses a two-dimensional structure of independent chains, in which RuO<sub>6</sub> octahedra are connected by two shared oxygen atoms, and the RuO<sub>6</sub> octahedra contain Ru-OH or Ru-OH<sub>2</sub> bonds of ~2.5 Å.<sup>25,26</sup> With reference to the reaction mechanism proposed for the aerobic oxidation of alcohols over the hydrous RuO<sub>2</sub> species,<sup>21</sup> we consider that the Ru-OH or Ru-OH<sub>2</sub> bond may be transformed into Ru-NHCH<sub>2</sub>R *via* the interaction with RNH<sub>2</sub> as follows,



The Ru<sup>IV</sup>-NHCH<sub>2</sub>R may undergo β-hydrogen elimination to give imine, which would be further oxidized and transformed into nitrile.<sup>8</sup> Whether the redox of Ru<sup>IV</sup>/Ru<sup>III</sup> occurs during the reaction or the Ru<sup>IV</sup> only acts as a Lewis acid still remains unclear. Our H<sub>2</sub>-TPR result (Fig. 9) showed that the supported hydrous RuO<sub>2</sub> could be reduced at a significantly lower temperature than the supported anhydrous RuO<sub>2</sub>. The higher reducibility of the hydrous RuO<sub>2</sub> species might contribute to its higher catalytic activity. It is well known that hydrous RuO<sub>2</sub> is a mixed electron-proton conductor.<sup>26</sup> We speculate that the proton-conducting property of the hydrous RuO<sub>2</sub> may be beneficial to the β-hydrogen elimination, which might be the rate-determining step.

Because RuO<sub>2</sub>·xH<sub>2</sub>O alone only exhibits a lower activity in the aerobic oxidation of benzyl amine, the synergistic effect between RuO<sub>2</sub>·xH<sub>2</sub>O and Co<sub>3</sub>O<sub>4</sub> is very significant. The results of effects of Ru loadings and Co<sub>3</sub>O<sub>4</sub> sizes on catalytic performances

(Table 4) suggest that the contact boundary between the amorphous RuO<sub>2</sub>·xH<sub>2</sub>O and the Co<sub>3</sub>O<sub>4</sub> particles really plays a key role in enhancing the catalytic activity. The synergistic effect between Ru<sup>IV</sup> and Co<sup>III</sup> or Co<sup>II</sup> has also been observed for a few catalysts effective for the aerobic oxidation of alcohols such as the Ru-Co binary oxide catalyst prepared by the co-precipitation method,<sup>21,24</sup> and the Ru-Co-Al hydrotalcite catalyst.<sup>27</sup> The role of Co was proposed to facilitate the catalyst regeneration by removing the hydrogen (hydride species) attached on Ru sites over the Ru-Co binary oxide for alcohol oxidation.<sup>21</sup> We speculate that, in our case, the Co sites may play a similar role. In our case, Co<sup>II</sup> may participate in the activation of O<sub>2</sub> to reoxidise the reduced Ru<sup>III</sup> species if the redox of Ru<sup>IV</sup>/Ru<sup>III</sup> exists or to remove the hydride species to regenerate the Ru sites.

## Conclusions

The Co<sub>3</sub>O<sub>4</sub>-supported ruthenium catalyst was found to exhibit the best catalytic performance for the aerobic oxidation of benzyl amine among various metal oxide-supported ruthenium catalysts and Co<sub>3</sub>O<sub>4</sub>-supported various transition metal catalysts prepared by an adsorption-precipitation method. The increase in ruthenium loadings to ≥ 3.5 wt% significantly decreased the catalytic activity. The size of Co<sub>3</sub>O<sub>4</sub> particles affected the performance of the supported ruthenium catalyst, and the smaller size of Co<sub>3</sub>O<sub>4</sub> led to the higher catalytic activity. The catalytic activity was strongly dominated by the state of ruthenium species. While the supported anhydrous ruthenium oxide only exhibited a lower activity, the hydrous ruthenium oxide dispersed on Co<sub>3</sub>O<sub>4</sub> showed remarkably higher efficiency for the aerobic oxidation of benzyl amine. The supported metallic ruthenium and ruthenium chloride species were inactive. The present Co<sub>3</sub>O<sub>4</sub>-supported hydrous ruthenium oxide catalyst was also effective for the aerobic oxidation of several other amines and could be used recyclably. The catalyst could be operated under solvent-free conditions or using air instead of oxygen as an oxidant.

## Acknowledgements

This work was supported by the National Natural Science Foundation of China (Nos. 20625310, 20773099 and 20433030), the National Basic Research Program of China (grants 2003CB615803 and 2005CB221408), the Key Scientific Project of Fujian Province of China (No. 2005HZ01-3), and the Programs for New Century Excellent Talents in University of China (No. NCET-04-0602). We thank Mr. Wenming Zhu for assistance in XPS measurements.

## References

- 1 R. A. Sheldon and J. K. Kochi, *Metal Catalyzed Oxidations of Organic Compounds*, Academic Press, New York, 1981.
- 2 (a) B. M. Trost, *Science*, 1991, **254**, 1471; (b) R. A. Sheldon, *Pure Appl. Chem.*, 2000, **72**, 1233; (c) R. A. Sheldon, *Green. Chem.*, 2000, **2**, G1; (d) P. T. Anastas, L. B. Bartlett, M. M. Kirchoff and T. C. Williamson, *Catal. Today*, 2000, **55**, 11; (e) M. Beller, *Adv. Synth. Catal.*, 2004, **346**, 107.
- 3 R. Tang, S. E. Diamond, N. Neary and F. Mares, *J. Chem. Soc. Chem. Commun.*, 1978, 562.
- 4 S. Cenini, F. Porta and M. Pizzotio, *J. Mol. Catal.*, 1982, **15**, 297.
- 5 S. Yamazaki and Y. Yamazaki, *Bull. Chem. Soc. Jpn.*, 1990, **63**, 301.
- 6 A. J. Bailey and B. R. James, *Chem. Commun.*, 1996, 2343.

- 7 K. Mori, K. Yamaguchi, T. Mizugaki, K. Ebitani and K. Kaneda, *Chem Commun.*, 2001, 461.
- 8 (a) K. Yamaguchi and N. Mizuno, *Angew. Chem. Int. Ed.*, 2003, **42**, 1480; (b) K. Yamaguchi and N. Mizuno, *Chem. Eur. J.*, 2003, **9**, 4353.
- 9 J. S. M. Samec, A. H. Éll and J. E. Bäckvall, *Chem. Eur. J.*, 2005, **11**, 2327.
- 10 J. R. Wang, Y. Fu, B. B. Zhang, X. Cui, L. Liu and Q. X. Guo, *Tetrahedron Lett.*, 2006, **47**, 8293.
- 11 M. Kotani, T. Koike, K. Yamaguchi and N. Mizuno, *Green. Chem.*, 2006, **8**, 735.
- 12 J. J. Maul, P. J. Ostrowski, G. A. Ublacker, B. Linclau and D. P. Curran, Benzotrifluoride and Derivatives: Useful Solvents for Organic Synthesis and Fluorous Synthesis, in *Modern Solvents in Organic Synthesis (Topics in Current Chemistry vol. 206)*, ed. P. Knochel, Springer-Verlag, Berlin/Heidelberg, 1999, p.79.
- 13 A. T. Bell, *Science*, 2003, **299**, 1688.
- 14 (a) B. Q. Xu, J. M. Wei, Y. T. Yu, Y. Li, J. L. Li and Q. M. Zhu, *J. Phys. Chem. B*, 2003, **107**, 5203; (b) X. Zhang, H. Wang and B. Q. Xu, *J. Phys. Chem. B*, 2005, **109**, 9678.
- 15 J. Walker, R. B. King and R. Tannenbaum, *J. Solid State Chem.*, 2007, **180**, 2290.
- 16 D. R. Rolison, P. L. Hagans, K. E. Swider and J. W. Long, *Langmuir*, 1999, **15**, 774.
- 17 L. Ji, J. Lin and H. C. Zeng, *Chem. Mater.*, 2001, **13**, 2403.
- 18 J. F. Moulder, W. F. Stickle, P. E. Sobol and K. D. Bomben, *Handbook of X-ray Photoelectron Spectroscopy*, Physical Electronics, Inc., Eden Prairie, 1995.
- 19 P. Froment, M. J. Genet and M. Devillers, *J. Electron Spectrosc. Relat. Phenom.*, 1999, **104**, 119.
- 20 D. H. Kerridge and A. Zellipour, *Thermochim. Acta*, 1990, **159**, 163.
- 21 T. L. Stuchinskaya, M. Musawir, E. F. Kozhevnikova and I. V. Kozhevnikov, *J. Catal.*, 2005, **231**, 41.
- 22 K. Yamaguchi, K. Mori, T. Mizugaki, K. Ebitani and K. Kaneda, *J. Am. Chem. Soc.*, 2000, **122**, 7144.
- 23 M. Matsumoto and N. Watanabe, *J. Org. Chem.*, 1984, **49**, 3436.
- 24 M. Musawir, P. N. Davey, G. Kelly and I. V. Kozhevnikov, *Chem. Commun.*, 2003, 1414.
- 25 B. Z. Zhan, M. A. White, T. K. Sham, J. A. Pincock, R. J. Doucet, K. V. R. Rao, K. N. Robertson and T. S. Cameron, *J. Am. Chem. Soc.*, 2003, **125**, 2195.
- 26 D. A. Mckeown, P. L. Hagans, L. P. L. Carette, A. E. Russell, K. E. Swider and D. R. Rolison, *J. Phys. Chem. B*, 1999, **103**, 4825.
- 27 T. Matsushita, K. Ebitani and K. Kaneda, *Chem. Commun.*, 1996, 265.

# Aqueous/organic cross coupling: Sustainable protocol for Sonogashira reactions of heterocycles†

Christoph A. Fleckenstein and Herbert Plenio\*

Received 7th January 2008, Accepted 13th February 2008

First published as an Advance Article on the web 11th March 2008

DOI: 10.1039/b800154e

The water soluble Pd complex of dicyclohexyl(2-sulfo-9-(3-(4-sulfophenyl)propyl)-9H-fluoren-9-yl)phosphine was used for an efficient copper free and sustainable reaction protocol for Sonogashira cross couplings. Using a water/*i*propanol mixture as the solvent and  $K_2CO_3$  as base, numerous heterocyclic and aryl bromides and chlorides were reacted with various acetylenes in near quantitative yield at 1 mol% catalyst loading and 90 °C.

## Introduction

Compounds bearing carbon–carbon triple bonds are ubiquitous in pharmaceuticals and fine chemicals;<sup>1,2</sup> examples are tazarotene,<sup>3</sup> terbinafin<sup>4,5</sup> or the oncology candidate CP-724,714.<sup>6</sup>

The Sonogashira reaction is a powerful tool to effect  $C(sp^2)$ – $C(sp^2)$ - and  $C(sp^2)$ – $C(sp^3)$  coupling reactions.<sup>1,7–17</sup> However, typical solvents utilized in such reactions, like DMF/DMAc,<sup>8,12,18</sup> DMSO,<sup>19,20</sup> toluene,<sup>14,21</sup> dioxane<sup>9,22</sup> or amine-bases<sup>17</sup> are less favourable from an ecological and economical point of view<sup>23–27</sup> than water.<sup>28</sup> Furthermore, the use of CuI, which is often used as the co-catalyst, can be problematic in large scale reactions due to the formation of insoluble copper-acetylides.<sup>29</sup>

Considering these limitations, it was our intention to develop a Sonogashira protocol for the synthesis of heterocyclic compounds which is more sustainable, safe and useful. This approach is motivated by the fact that the vast majority of biologically active compounds and APIs (active pharmaceutical ingredients) contains heterocyclic structures—often combined with problematic functional groups like free amine moieties.<sup>30–37</sup> Notable, in this respect is recent work from Beller *et al.* who reported on the Sonogashira coupling of various heterocyclic substrates.<sup>38</sup> With Beller the use of TMEDA (tetramethylethylenediamine) as solvent and CuI as the co-catalyst were the key to the efficient transformation of some *N*- and *S*-heterocyclic substrates.

While efforts have been made in designing highly active catalytic systems for Pd cross coupling,<sup>39</sup> the catalyst loading is not the determining factor making a process more benign.<sup>40,41</sup> In (Sonogashira) cross coupling reactions, solvents as well as various additives have by far the largest economical and environmental impact. Hence, it follows that critical organic solvents and additives should be avoided.<sup>42</sup> Water appears to be an obvious alternative,<sup>23,24</sup> but for organic transformations of

lipophilic substrates the poor solubility of some organic reactants in water in the absence of other solvents creates problems. Due to several favourable properties, *i*propanol was chosen as the co-solvent: besides decreasing the polarity of the reaction medium and consequently increasing the solubility of organic substrates, it is inexpensive, safe and easily biodegradable *via* the acetone pathway and thus a particularly favourable organic co-solvent.<sup>23,25,42</sup>

For our work, we have tested a broad range of heterocyclic substrates with a view to a sustainable protocol, while on the other hand preserving high catalytic activities.

## Results and discussion

We recently reported the synthesis of fluorenyldialkylphosphines<sup>43</sup> whose Pd-complexes are excellent catalysts for various cross coupling reactions.<sup>32,44</sup> The disulfonated derivative **1**·3H<sup>+</sup> (Fig. 1) forms highly water soluble Pd-complexes. In combination with aqueous reaction media these complexes showed unprecedented catalytic activity in Suzuki cross coupling of *N*- and *S*- heterocyclic substrates, thus facilitating the synthesis of important heterocyclic building blocks.<sup>31,45</sup> We found out then, that the use of water as a (co-)solvent is essential for good catalytic activity, as hydrogen bonding with the nitrogen donor moieties appears to prevent inhibition of the catalyst.

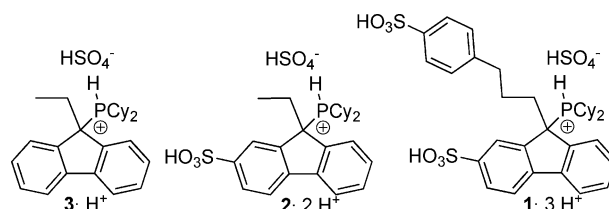


Fig. 1 Fluorenyldicyclohexylphosphine and mono- and disulfonated relative ( $H_2SO_4$  adducts).

In order to extend the scope of Pd complexes with phosphine **1** to other cross coupling reactions, we tested those complexes in Sonogashira cross coupling reactions of heteroaryl chlorides and bromides in a benign aqueous solvent mixture of water/*i*propanol (1 : 1) in combination with unproblematic  $K_2CO_3$

Anorganische Chemie im Zintl-Institut, TU Darmstadt, Petersenstr. 18, 64287, Darmstadt, Germany. E-mail: plenio@tu-darmstadt.de

† Electronic supplementary information (ESI) available: Supporting information for this article contains the NMR spectra of all Sonogashira coupling products as well as cyclic voltammograms of the synthesized ferrocenyl derivatives. See DOI: 10.1039/b800154e

**Table 1** Sonogashira reactions involving *N*-heterocyclic or *N*-containing substrates<sup>a</sup>

Entry	Aryl halide	Acetylene	Product	<i>t</i> /h	Conversion <sup>b</sup>	Yield <sup>c</sup>
1				3	≥99%	94%
2				4	≥99%	91%
				10	90% <sup>d</sup>	
				10	72% <sup>e</sup>	
				10	0% <sup>f</sup>	
				20	0% <sup>g</sup>	
3				10	≥99%	93%
4				10	≥99%	89%
5				10	≥99%	94%
6				8	≥99%	91%
7				5	≥99%	94%
8				10	89%	85%
9				10	96%	91%

<sup>a</sup> 1.5 mmol aryl chloride, 1.7 mmol acetylene, 2.0 mmol K<sub>2</sub>CO<sub>3</sub>, 6 mL water/*i*propanol (1 : 1), catalyst 1 mol% (1 mL stock solution : Na<sub>2</sub>PdCl<sub>4</sub>/ligand (1 : 2)), 90 °C. <sup>b</sup> Determined *via* gas chromatography (heptadecane, internal standard). <sup>c</sup> Average of two runs, column chromatography (silica (15 × 3 cm)). <sup>d</sup> 0.5 mol% Pd-catalyst. <sup>e</sup> 0.1 mol% Pd-catalyst. <sup>f</sup> No Pd-catalyst. <sup>g</sup> 2 mol% Na<sub>2</sub>PdCl<sub>4</sub>, no ligand.

as base. The catalyst is formed *in situ* from Na<sub>2</sub>PdCl<sub>4</sub>, and two equivalents of the triply protonated ligand 1·3H<sup>+</sup> in the presence of five equivalents of base.

In a preliminary test the activity of the catalyst was studied in the reaction of 2-chloropyridine with phenylacetylene (Table 1, entry 2). The respective Sonogashira coupling affords the desired coupling product in quantitative yield (4 h, 100 °C, 1 mol% catalyst). Applying 0.1 mol% catalyst 72% conversion is found after 10 h. Tests using 2 mol% Pd salt in absence of phosphine **1** or in complete absence of catalyst gave no conversion in the same reaction.

Interestingly, the Sonogashira cross coupling reactions reported here proceed smoothly without the use of a copper(I) salt as co-catalyst.<sup>46</sup> Others performing this kind of coupling reaction under copper free conditions are either restricted to aryl iodides and non-deactivated aryl bromides,<sup>47–52</sup> or require severe reaction conditions, like high reaction temperatures,<sup>18,53</sup> microwave activation,<sup>54</sup> or high Pd-catalyst concentrations.<sup>10,37,55,56</sup>

The cross coupling of additional *N*-heteroarylchlorides and other nitrogen-containing substrates with aryl acetylenes in Sonogashira reactions is found in Table 1. The generality of our reaction protocol was demonstrated by reacting a sterically



demanding, deactivated arylhalide with a *N*-heterocyclic acetylene. Utilizing 1 mol% of the Pd-catalyst 2,6-dimethylbromobenzene (**2a**) was quantitatively coupled with 2-pyridylacetylene (**3a**) at 90 °C in 3 h (Table 1, entry 1) in water/*i*propanol (1 : 1) as solvent.

2-Chloropyridine and 2-chloropyrimidine were successfully coupled with phenyl-, octyl- or 2-pyridylacetylene (Table 1, entries 3–5). 5-Bromo-2-amino-pyridine with a free amino group is a challenging substrate for Pd catalyzed cross coupling reactions. Applying the given conditions, 5-bromo-2-amino-pyridine can be directly coupled with phenylacetylene in near quantitative yield without the need for *N*-protection (Table 1, entry 8).

Next, Sonogashira reactions of *S*- and *O*-heterocyclic substrates were investigated (Table 2). Electron rich and thus deactivated 2-bromothiophene and 3-bromothiophene were coupled in excellent yields with both aliphatic acetylenes (Table 2, entries 1, 8) and arylacetylenes (Table 2, entries 2, 13). The efficient coupling of sulfur containing substrates with nitrogen heterocycles under the same conditions is demonstrated (Table 2, entries 3, 4).

Interesting is the effective coupling of the labile 3-bromofurane with acetylenes. Similar structures have received interest due to their biological activity, but with the exception of the recent Beller publication<sup>38</sup> 3-bromofurane was rarely used in Sonogashira reactions and known to cause problems resulting in poor product yields.<sup>57</sup> With phenylacetylene as the coupling partner, the desired product was obtained in quantitative yield (Table 2, entry 6). Substituted ferrocenes receive interest in medicinal and life science chemistry because of their biological activity in cancer-,<sup>58–63</sup> malaria-<sup>58,64–66</sup> and HIV-treatment<sup>67,68</sup> or as auxiliary in DNA detection.<sup>69–71</sup> To facilitate this chemistry, we investigated some coupling reactions of ferrocenylacetylene with heterocyclic aryl halides. 3-Ferrocenylethynyl-thiophene and 3-ferrocenylethynyl-furan were obtained in yields of around 95% and excellent purity (Table 2, entries 5, 7).

The coupling of the unprotected and deactivated 2-bromoaniline with 2-ethynylthiophene selectively yielded the Sonogashira coupling product (Table 2, entry 12). In the same manner, unprotected 5-bromo-2-amino-pyridine is coupled with 2-ethynylthiophene in 93% yield (table 2, entry 14). When propargylic alcohols were used as coupling partners (table 2, entry 11), no coupling product was observed. This was not entirely unexpected as we had learnt earlier, that propargylic alcohols can be reacted in Sonogashira reactions only under strict exclusion of water.<sup>17</sup>

Due to the significant amount of salts, the reaction mixture consisting of water, *i*propanol and the reactants form two phases. Hence, in a larger scale synthesis of heterocycles using the Sonogashira coupling, we were able to simply separate the product containing the organic layer from the water solution containing the salts without adding additional non-polar solvent such as ether. Therefore, the whole process can be run as a truly green process utilizing exclusively environmentally neutral water and sustainable, biodegradable *i*propanol as solvents.

## Summary

We have developed a sustainable copper free protocol for Sonogashira cross coupling reactions utilizing a benign and

easily biodegradable mixture of water and *i*propanol as the solvent. In the presence of 1 mol% of the *in situ* formed Pd/1 complex, deactivated and sterically hindered arylbromides as well as various *N*-, *S*- or *O*- heterocyclic arylchlorides and bromides are effectively reacted with a variety of hetero and non-hetero acetylenes, including ferrocenylacetylene.

## Experimental

All chemicals were purchased as reagent grade from commercial suppliers and used without further purification, unless otherwise noted. Used solvents (water, *i*propanol (technical grade)) were deaerated *via* freeze and thaw technique. Ligand **1·3H<sup>+</sup>** is commercially available under the trade name cataCXium F from Degussa GmbH. All experiments were carried out under an argon atmosphere, unless otherwise noted. Proton (<sup>1</sup>H NMR), carbon (<sup>13</sup>C NMR) and nitrogen (<sup>15</sup>N NMR) nuclear magnetic resonance spectra were recorded on a Bruker DRX 500 at 500 MHz, 125.75 MHz, 202.46 MHz and 50.69 MHz, respectively at 293 K. The chemical shifts are given in parts per million (ppm) on the delta scale ( $\delta$ ) and are referenced to tetramethylsilane (<sup>1</sup>H and <sup>13</sup>C NMR:  $\delta$  = 0 ppm), nitromethane (<sup>15</sup>N NMR:  $\delta$  = 0 ppm). Abbreviations for NMR data: s = singlet; d = doublet; t = triplet; q = quartet; qi = quintet; dd = doublet of doublets; dt = doublet of triplets; dq = doublet of quartets; tt = triplet of triplets; m = multiplet. Mass spectra were recorded on a Finnigan MAT 95 magnetic sector spectrometer. Thin layer chromatography (TLC) was performed using Fluka silica gel 60 F 254 (0.2 mm) on Al-plates. Silica gel columns for chromatography were prepared with E. Merck silica gel 60 (0.063–0.20 mesh ASTM). GC experiments were run on a Clarus 500 GC with autosampler and FID detector. Column: Varian CP-Sil 8 CB (*l* = 15 m, *d<sub>i</sub>* = 0.25 mm, *d<sub>F</sub>* = 1.0  $\mu$ m), N<sub>2</sub> (flow: 17 cm s<sup>-1</sup>; split 1 : 50); Injector-temperature: 270 °C, detector temperature: 350 °C. Temperature program: isotherm 150 °C for 5 min, heating to 300 °C with 25 °C min<sup>-1</sup>, isotherm for 15 min. Cyclic voltammetry: EG & G 263A-2 potentiostat. Cyclic voltammograms were recorded in dry CH<sub>2</sub>Cl<sub>2</sub> under an argon atmosphere at ambient temperature. A three-electrode configuration was employed. The working electrode was a Pt disk (diameter 1 mm) sealed in soft glass with a Pt wire as the counter electrode. The pseudo reference electrode was an Ag wire. Potentials were calibrated internally against the formal potential of octamethylferrocene (–0.010 mV (CH<sub>2</sub>Cl<sub>2</sub>) vs. Ag/AgCl). NBu<sub>4</sub>PF<sub>6</sub> (0.1 mol L<sup>-1</sup>) was used as supporting electrolyte.

### Preparation of the catalyst stock solution

Na<sub>2</sub>PdCl<sub>4</sub> (14.7 mg, 0.05 mmol), **1·3H<sup>+</sup>** (80 mg, 0.1 mmol) and K<sub>2</sub>CO<sub>3</sub> (56 mg, 0.4 mmol) were placed in a Schlenk tube under argon. Degassed water (5.0 mL) was added and the mixture was stirred at 55 °C for 3 h until the clear solution turned nearly colourless (very slightly yellow). This stock solution had a Pd-concentration of 0.01 mol L<sup>-1</sup>.

### Typical screening procedure of cross coupling reactions

K<sub>2</sub>CO<sub>3</sub> (2 mmol) was placed in a 25 mL Schlenk tube under an argon atmosphere. Degassed water (1.5 mL) and degassed

**Table 2** Sonogashira reactions involving *S/O*-heterocyclic or *S/O*-containing substrates<sup>a</sup>

Y = CH, S, O

Entry	Aryl halide	Acetylene	Product	<i>t</i> /h	Conversion <sup>b</sup>	Yield <sup>c</sup>
1				10	≥99%	91%
2				10	≥99%	94%
3				10	≥99%	90%
4				10	≥99%	92%
5				10	≥99%	95%
6				10	≥99%	91%
7				10	≥99%	94%
8				10	98%	91%
9				5	≥99%	95%
10				5	≥99%	95%
11				10	<5%	0
12				5	≥99%	94%
13				5	≥99%	96%
14				5	98%	93%

<sup>a</sup> 1.5 mmol aryl chloride, 1.7 mmol acetylene, 2.0 mmol K<sub>2</sub>CO<sub>3</sub>, 6 mL water/isopropanol (1 : 1), catalyst 1 mol% (1 mL stock solution : Na<sub>2</sub>PdCl<sub>4</sub>/ligand (1 : 2)), 90 °C. <sup>b</sup> Determined *via* gas chromatography (heptadecane internal standard). <sup>c</sup> Average of two runs, column chromatography (silica (15 × 3cm)).

ipropanol (3 mL) were added as well as the respective aryl halide (1.5 mmol) and acetylene (1.7 mmol). After addition of 1.5 mL catalyst stock solution (1.5 mL = 1 mol% Pd) the reaction mixture was stirred at 90 °C for the given time. After cooling to room temperature the reaction mixture was diluted with ether (10 mL), washed with water (10 mL), the organic phase dried over MgSO<sub>4</sub>, filtered and concentrated *in vacuo*. The product was isolated by column chromatography (silica, cyclohexane : EtOAc : NEt<sub>3</sub> = 9 : 1 : 1). Alternatively the yield was determined *via* gas chromatography with heptadecane as an internal standard.

#### Typical “g-scale” procedure of cross coupling reactions

K<sub>2</sub>CO<sub>3</sub> (2.76 g, 20 mmol) was placed in a 50 mL Schlenk flask under an argon atmosphere. Degassed water (7.5 mL) and degassed ipropanol (15 mL) were added, as well as 2-chloropyridine (1.14 g, 939 μL, 10 mmol) and acetylene (1.22 g, 1.32 mL, 12 mmol). After addition of 7.5 mL of the aqueous catalyst stock solution (7.5 mL = 1 mol% Pd-loading) the reaction mixture was stirred at 90 °C for 7 h. After cooling to room temperature, the reaction mixture was transferred into a separation funnel. The upper (organic) layer was isolated, dried over MgSO<sub>4</sub> for 10 min, filtered and concentrated *in vacuo*. The product was purified by column chromatography (silica, cyclohexane : EtOAc : NEt<sub>3</sub> = 9 : 1 : 1). Yield: 1.63 g (91%).

#### 2-(2,6-Dimethyl-phenylethynyl)-pyridine (4a)

The crude product was purified *via* column chromatography on silica (cyclohexane : EtOAc : NEt<sub>3</sub> = 9 : 1 : 1). <sup>1</sup>H NMR (500 MHz, CDCl<sub>3</sub>) δ = 8.64 (ddd, <sup>5</sup>J = 1.0 Hz, <sup>4</sup>J = 1.5 Hz, <sup>3</sup>J = 4.5 Hz, 1 H, CH, ar), 7.66 (dt, <sup>4</sup>J = 1.8 Hz, <sup>3</sup>J = 7.3 Hz, 1 H, CH, ar), 7.52 (td, <sup>4</sup>J = 1.5 Hz, <sup>3</sup>J = 7.5 Hz, 1 H, CH, ar), 7.21 (ddd, <sup>4</sup>J = 1.5 Hz, <sup>3</sup>J = 7.5 Hz, <sup>3</sup>J = 5.0 Hz, 1 H, CH, ar), 7.15 (t, <sup>3</sup>J = 8.0 Hz, 1 H, CH, ar), 7.07 (d, <sup>3</sup>J = 7.5 Hz, 2 H, CH, ar), 2.55 (s, 6 H, CH<sub>3</sub>); <sup>13</sup>C{<sup>1</sup>H} NMR (125.77 MHz, CDCl<sub>3</sub>) δ = 149.1, 142.9, 139.9, 135.0, 127.5, 126.2, 125.7, 121.5, 121.0, 96.0, 86.0, 20.1; HRMS calcd. for C<sub>15</sub>H<sub>13</sub>N: 207.1048, found 207.10290.

#### 2-Phenylethynyl-pyridine (4b)

The crude product was purified *via* column chromatography on silica (cyclohexane : EtOAc : NEt<sub>3</sub> = 9 : 1 : 1). <sup>1</sup>H- and <sup>13</sup>C NMR-spectra are consistent with those in the literature.<sup>72</sup>

#### 2-Oct-1-ynyl-pyridine (4c)

The crude product was purified *via* column chromatography on silica (cyclohexane : EtOAc : NEt<sub>3</sub> = 9 : 1 : 1). <sup>1</sup>H NMR (500 MHz, CDCl<sub>3</sub>) δ = 8.64 (ddd, <sup>5</sup>J = 1.0 Hz, <sup>4</sup>J = 1.5 Hz, <sup>3</sup>J = 5.0 Hz, 1 H, CH, ar), 7.60 (dt, <sup>4</sup>J = 2.0 Hz, <sup>3</sup>J = 8.5 Hz, 1 H, CH, ar), 7.36 (td, <sup>4</sup>J = 1.0 Hz, <sup>3</sup>J = 8.0 Hz, 1 H, CH, ar), 7.17 (ddd, <sup>4</sup>J = 1.0 Hz, <sup>3</sup>J = 7.5 Hz, <sup>3</sup>J = 5.0 Hz, 1 H, CH, ar), 2.43 (t, <sup>3</sup>J = 7.0 Hz, 2 H, C-CH<sub>2</sub>), 1.63 (qui, <sup>3</sup>J = 7.0 Hz, 2 H, CH<sub>2</sub>), 1.49–1.42 (m, 2 H, CH<sub>2</sub>), 1.37–1.27 (m, 4 H, CH<sub>2</sub>), 0.90 (t, <sup>3</sup>J = 7.0 Hz, 3 H, CH<sub>3</sub>); <sup>13</sup>C{<sup>1</sup>H} NMR (125.77 MHz, CDCl<sub>3</sub>) δ = 149.8, 144.1, 136.0, 126.8, 122.2, 91.2, 80.4, 31.4, 28.7, 28.4, 22.5, 19.4, 14.1; HRMS calcd. for C<sub>13</sub>H<sub>17</sub>N: 187.1361, found 187.13295. <sup>1</sup>H- and <sup>13</sup>C NMR-spectra are literature consistent.<sup>73</sup>

#### 1,2-Di-(2,2'-pyridyl)-ethyne (4d)

The crude product was purified *via* column chromatography on silica (cyclohexane : EtOAc : NEt<sub>3</sub> = 9 : 1 : 1). <sup>1</sup>H NMR (300 MHz, CDCl<sub>3</sub>) δ = 8.54 (ddd, <sup>5</sup>J = 0.9 Hz, <sup>4</sup>J = 1.8 Hz, <sup>3</sup>J = 4.8 Hz, 2 H, CH, ar), 7.63 (dt, <sup>4</sup>J = 1.8 Hz, <sup>3</sup>J = 7.8 Hz, 2 H, CH, ar), 7.55 (td, <sup>4</sup>J = 1.5 Hz, <sup>3</sup>J = 7.5 Hz, 2 H, CH, ar), 7.21 (ddd, <sup>4</sup>J = 1.2 Hz, <sup>3</sup>J = 5.0 Hz, <sup>3</sup>J = 8.3 Hz, 2 H, CH, ar); <sup>13</sup>C{<sup>1</sup>H} NMR (75 MHz, CDCl<sub>3</sub>) δ = 149.2, 141.7, 135.2, 126.8, 122.4, 86.9; HRMS calcd. for C<sub>12</sub>H<sub>8</sub>N<sub>2</sub>: 180.0688, found 180.06814.

#### 2-Oct-1-ynyl-pyrimidine (4e)

The crude product was purified *via* column chromatography on silica (cyclohexane : EtOAc : NEt<sub>3</sub> = 9 : 2 : 1). <sup>1</sup>H NMR (500 MHz, CDCl<sub>3</sub>) δ = 8.68 (d, <sup>3</sup>J = 5.0 Hz, 2 H, CH, ar), 7.19 (dt, <sup>3</sup>J = 5.0 Hz, 1 H, CH, ar), 2.47 (t, <sup>3</sup>J = 7.5 Hz, 2 H, C-CH<sub>2</sub>), 1.66 (qui, <sup>3</sup>J = 7.0 Hz, 2 H, CH<sub>2</sub>), 1.51–1.42 (m, 2 H, CH<sub>2</sub>), 1.36–1.25 (m, 4 H, CH<sub>2</sub>), 0.89 (t, <sup>3</sup>J = 6.5 Hz, 3 H, CH<sub>3</sub>); <sup>13</sup>C{<sup>1</sup>H} NMR (125.77 MHz, CDCl<sub>3</sub>) δ = 157.6, 153.8, 119.7, 91.2, 80.3, 31.7, 29.0, 28.4, 22.9, 19.6, 14.4; HRMS calcd. for C<sub>12</sub>H<sub>16</sub>N<sub>2</sub>: 188.1314, found 188.13016.

#### 5-Pyridin-2-ylethynyl-indan-1-one (4f)

The crude product was purified *via* column chromatography on silica (cyclohexane : EtOAc : NEt<sub>3</sub> = 9 : 2 : 1). <sup>1</sup>H NMR (500 MHz, CDCl<sub>3</sub>) δ = 8.57–8.53 (m, 1 H, CH<sub>ar</sub>), 7.65–7.57 (m, 3 H, CH<sub>ar</sub>), 7.49–7.43 (m, 2 H, CH<sub>ar</sub>), 7.21–7.16 (m, 1 H, CH<sub>ar</sub>), 3.04 (t, <sup>3</sup>J = 5.1 Hz, 2 H, CH<sub>2</sub>), 2.63–2.58 (m, 2 H, CH<sub>2</sub>); <sup>13</sup>C{<sup>1</sup>H} NMR (125.77 MHz, CDCl<sub>3</sub>) δ = 204.9, 153.8, 149.2, 141.8, 136.0, 135.2, 130.1, 129.1, 127.4, 126.4, 122.6, 122.2, 90.5, 87.3, 35.3, 24.6; <sup>15</sup>N NMR (50.69 MHz, CDCl<sub>3</sub>) δ = -64.6; HRMS calcd. for C<sub>16</sub>H<sub>11</sub>NO: 233.0841, found 233.08329.

#### 4-Phenylethynyl-pyridine (4g)

The crude product was purified *via* column chromatography on silica (cyclohexane : EtOAc : NEt<sub>3</sub> = 9 : 2 : 1). <sup>1</sup>H NMR (500 MHz, CDCl<sub>3</sub>) δ = 8.60 (dd, <sup>3</sup>J = 4.5 Hz, <sup>2</sup>J = 1.6 Hz, 2 H, CH, ar), 7.56–7.54 (m, 2 H, CH, ar), 7.39–7.36 (m, 5 H, CH, ar); <sup>13</sup>C{<sup>1</sup>H} NMR (125.77 MHz, CDCl<sub>3</sub>) δ = 149.9, 132.0, 131.6, 129.3, 128.6, 125.7, 122.3, 94.1, 86.8; <sup>15</sup>N NMR (50.69 MHz, CDCl<sub>3</sub>) δ = -68.9; HRMS calcd. for C<sub>13</sub>H<sub>9</sub>N: 179.0735, found 179.07323.

#### 5-Phenylethynyl-pyridin-2-ylamine (4h)

The crude product was purified *via* column chromatography on silica (cyclohexane : EtOAc : NEt<sub>3</sub> = 5 : 5 : 1). <sup>1</sup>H NMR (500 MHz, CDCl<sub>3</sub>) δ = 8.28 (dd, <sup>2</sup>J = 2.2 Hz, <sup>2</sup>J = 0.7 Hz, 1 H, CH<sub>ar</sub>), 7.56 (dd, <sup>3</sup>J = 8.5 Hz, <sup>2</sup>J = 2.2 Hz, 1 H, CH<sub>ar</sub>), 7.51–7.48 (m, 2 H, CH<sub>ar</sub>), 7.36–7.29 (m, 3 H, CH<sub>ar</sub>), 6.46 (dd, <sup>3</sup>J = 8.5 Hz, <sup>2</sup>J = 0.7 Hz, 1 H, CH<sub>ar</sub>), 4.66 (s(br), 2 H, NH<sub>2</sub>); <sup>13</sup>C{<sup>1</sup>H} NMR (125.77 MHz, CDCl<sub>3</sub>) δ = 156.5, 150.5, 139.4, 130.4, 127.3, 127.0, 122.4, 108.9, 106.9, 88.8, 86.0; <sup>15</sup>N-NMR (50.7 MHz, CDCl<sub>3</sub>) δ = -114.7 (Pyr-N), (NH<sub>2</sub>): signal not observed; HRMS calcd. for C<sub>13</sub>H<sub>10</sub>N<sub>2</sub>: 194.0844, found 194.08527.

### 5-(3-Diisopropylamino-prop-1-ynyl)-pyridin-2-ylamine (4i)

The crude product was purified *via* column chromatography on silica (cyclohexane : EtOAc : NEt<sub>3</sub> = 5 : 5 : 1). <sup>1</sup>H NMR (500 MHz, CDCl<sub>3</sub>) δ = 8.12 (d, *J* = 2.2 Hz, 1 H, CH<sub>ar</sub>), 7.41 (dd, <sup>3</sup>*J* = 8.5 Hz, *J* = 2.2 Hz, 1 H, CH<sub>ar</sub>), 6.40 (dd, <sup>3</sup>*J* = 8.5 Hz, *J* = 0.7 Hz, 1 H, CH<sub>ar</sub>), 4.71 (s(br), 2 H, NH<sub>2</sub>), 3.61 (s, 2 H, CH<sub>2</sub>), 3.42 (sept, <sup>3</sup>*J* = 6.7 Hz, 2 H, CH<sub>ipr</sub>), 1.13 (d, <sup>3</sup>*J* = 6.7 Hz, 12 H, CH<sub>3</sub>); <sup>13</sup>C{<sup>1</sup>H} NMR (125.77 MHz, CDCl<sub>3</sub>) δ = 157.7, 151.5, 140.7, 110.7, 108.2, 89.7, 81.1, 48.9, 35.3, 21.0; <sup>15</sup>N-NMR (50.7 MHz, CDCl<sub>3</sub>) δ = -114.6 (Pyr-N), -309.0 (NH<sub>2</sub>), -323.9 (N<sup>i</sup>Pr<sub>2</sub>); HRMS calcd. for C<sub>14</sub>H<sub>21</sub>N<sub>3</sub>: 231.1736, found 231.17283.

### 2-Oct-1-ynyl-thiophene (4j)

The crude product was purified *via* column chromatography on silica (cyclohexane : EtOAc = 9 : 1). <sup>1</sup>H NMR (500 MHz, CDCl<sub>3</sub>) δ = 7.15 (dd, <sup>3</sup>*J* = 5.0 Hz, *J* = 1.0 Hz, 1 H, CH<sub>thiophene</sub>), 7.10 (dd, <sup>3</sup>*J* = 3.6 Hz, *J* = 1.0 Hz, 1 H, CH<sub>thiophene</sub>), 6.92 (dd, <sup>3</sup>*J* = 5.0 Hz, *J* = 3.6 Hz, 1 H, CH<sub>thiophene</sub>), 2.41 (t, <sup>3</sup>*J* = 7.2 Hz, 2 H, CCCH<sub>2</sub>), 1.62–1.56 (m, 2 H, CH<sub>2</sub>), 1.47–1.39 (m, 2 H, CH<sub>2</sub>), 1.35–1.24 (m, 4 H, CH<sub>2</sub>), 0.90 (t, <sup>3</sup>*J* = 7.0 Hz, 3 H, CH<sub>3</sub>); <sup>13</sup>C{<sup>1</sup>H} NMR (125.77 MHz, CDCl<sub>3</sub>) δ = 130.9, 126.7, 125.8, 124.3, 94.6, 73.7, 31.4, 28.6, 22.6, 22.5, 19.7, 14.0; HRMS calcd. for C<sub>12</sub>H<sub>16</sub>S: 192.0973, found 192.09713. <sup>1</sup>H- and <sup>13</sup>C NMR-spectra are literature consistent.<sup>74</sup>

### 3-Phenylethynyl-thiophene (4k)

The crude product was purified *via* column chromatography on silica (cyclohexane : EtOAc = 9 : 1). <sup>1</sup>H NMR (500 MHz, CDCl<sub>3</sub>) δ = 7.52–7.49 (m, 3 H, CH<sub>thiophene</sub> + CH<sub>ar</sub>), 7.34–7.29 (m, 3 H, CH<sub>ar</sub>), 7.27 (dd, <sup>3</sup>*J* = 5.0 Hz, *J* = 3.0 Hz, 1 H, CH<sub>thiophene</sub>), 7.19 (dd, <sup>3</sup>*J* = 5.0 Hz, *J* = 1.2 Hz, 1 H, CH<sub>thiophene</sub>); <sup>13</sup>C{<sup>1</sup>H} NMR (125.77 MHz, CDCl<sub>3</sub>) δ = 131.5, 129.9, 128.6, 128.3, 128.2, 125.3, 123.2, 122.3, 88.9, 84.5; HRMS calcd. for C<sub>12</sub>H<sub>8</sub>S: 184.0347, found 184.03444. <sup>1</sup>H- and <sup>13</sup>C NMR-spectra are literature consistent.<sup>52</sup>

### 2-Thiophen-2-ylethynyl-pyrimidine (4l)

The crude product was purified *via* column chromatography on silica (cyclohexane : EtOAc : NEt<sub>3</sub> = 9 : 2 : 1). <sup>1</sup>H NMR (500 MHz, CDCl<sub>3</sub>) δ = 8.75 (d, <sup>3</sup>*J* = 5.0 Hz, 2 H, CH<sub>ar</sub>), 7.50 (dd, <sup>3</sup>*J* = 3.7 Hz, *J* = 1.1 Hz, 1 H, CH<sub>thiophene</sub>), 7.41 (dd, <sup>3</sup>*J* = 5.1 Hz, *J* = 1.1 Hz, 1 H, CH<sub>thiophene</sub>), 7.23 (t, <sup>3</sup>*J* = 5.0 Hz, 1 H, CH<sub>ar</sub>), 7.05 (dd, <sup>3</sup>*J* = 5.1 Hz, <sup>3</sup>*J* = 3.7 Hz, 1 H, CH<sub>thiophene</sub>); <sup>13</sup>C{<sup>1</sup>H} NMR (125.77 MHz, CDCl<sub>3</sub>) δ = 157.4, 153.3, 134.9, 129.7, 127.4, 121.3, 119.6, 91.9, 81.8; <sup>15</sup>N-NMR (50.7 MHz, CDCl<sub>3</sub>) δ = -85.2; HRMS calcd. for C<sub>10</sub>H<sub>6</sub>N<sub>2</sub>S: 186.0253, found 186.02351.

### 2-Thiophen-2-ylethynyl-pyridine (4m)

The crude product was purified *via* column chromatography on silica (cyclohexane : EtOAc : NEt<sub>3</sub> = 9 : 1 : 1). <sup>1</sup>H NMR (500 MHz, CDCl<sub>3</sub>) δ = 8.62 (ddd, <sup>3</sup>*J* = 5.0 Hz, *J* = 1.8 Hz, *J* = 1.0 Hz, 1 H, CH<sub>pyr</sub>), 7.67 (dt, <sup>3</sup>*J* = 7.8 Hz, *J* = 1.8 Hz, 1 H, CH<sub>pyr</sub>), 7.50 (dt, <sup>3</sup>*J* = 7.8 Hz, *J* = 1.0 Hz, 1 H, CH<sub>pyr</sub>), 7.38 (dd, <sup>3</sup>*J* = 3.7 Hz, *J* = 1.2 Hz, 1 H, CH<sub>thiophene</sub>), 7.34 (dd, <sup>3</sup>*J* = 5.3 Hz, *J* = 1.2 Hz, 1 H, CH<sub>thiophene</sub>), 7.23 (ddd, <sup>3</sup>*J* = 7.7 Hz, <sup>3</sup>*J* = 5.0 Hz,

*J* = 1.2 Hz, 1 H, CH<sub>pyr</sub>), 7.03 (dd, <sup>3</sup>*J* = 5.2 Hz, <sup>3</sup>*J* = 3.7 Hz, 1 H, CH<sub>thiophene</sub>); <sup>13</sup>C{<sup>1</sup>H} NMR (125.77 MHz, CDCl<sub>3</sub>) δ = 150.2, 143.3, 136.2, 133.4, 128.4, 127.3, 127.0, 122.9, 122.3, 92.4, 82.8; <sup>15</sup>N-NMR (50.7 MHz, CDCl<sub>3</sub>) δ = -67.5; HRMS calcd. for C<sub>11</sub>H<sub>7</sub>NS: 185.0300, found 185.02890. The <sup>1</sup>H NMR-spectrum is literature consistent.<sup>75</sup>

### 3-Ferrocenylethynyl-thiophene (4n)

The crude product was purified *via* column chromatography on silica (*n*heptane). <sup>1</sup>H NMR (500 MHz, CDCl<sub>3</sub>) δ = 7.44 (dd, <sup>3</sup>*J* = 3.0 Hz, *J* = 1.1 Hz, 1 H, CH<sub>thiophene</sub>), 7.27 (dd, <sup>3</sup>*J* = 5.0 Hz, <sup>3</sup>*J* = 3.0 Hz, 1 H, CH<sub>thiophene</sub>), 7.15 (dd, <sup>3</sup>*J* = 5.0 Hz, *J* = 1.1 Hz, 1 H, CH<sub>thiophene</sub>), 4.48 (t, <sup>3</sup>*J* = 1.9 Hz, 2 H, CH<sub>Fc</sub>), 4.24 (s, 5 H, CH<sub>Fc</sub>), 4.22 (t, <sup>3</sup>*J* = 1.9 Hz, 2 H, CH<sub>Fc</sub>); <sup>13</sup>C{<sup>1</sup>H} NMR (125.77 MHz, CDCl<sub>3</sub>) δ = 129.9, 127.7, 125.1, 122.9, 87.7, 80.7, 71.3, 70.0, 68.8, 65.2; CV: (*E*<sub>1/2</sub> = 0.550 V; Δ*E* = 92 mV); HRMS calcd. for C<sub>16</sub>H<sub>12</sub>SFe: 292.0009, found 292.00108.

### 3-Phenylethynyl-furan (4o)

The crude product was purified *via* column chromatography on silica (cyclohexane : EtOAc = 200 : 1). <sup>1</sup>H NMR (500 MHz, CDCl<sub>3</sub>) δ = 7.68 (dd, *J* = 1.6 Hz, *J* = 0.9 Hz, 1 H, CH<sub>furyl</sub>), 7.50–7.47 (m, 2 H, CH<sub>ar</sub>), 7.39 (dd, *J* = 1.9 Hz, *J* = 1.6 Hz, 1 H, CH<sub>furyl</sub>), 7.33–7.30 (m, 3 H, CH<sub>ar</sub>), 6.52 (dd, *J* = 1.9 Hz, *J* = 0.6 Hz, 1 H, CH<sub>furyl</sub>); <sup>13</sup>C{<sup>1</sup>H} NMR (125.77 MHz, CDCl<sub>3</sub>) δ = 145.6, 142.9, 132.5, 131.4, 128.4, 128.2, 123.2, 112.6, 91.0, 80.5; HRMS calcd. for C<sub>12</sub>H<sub>8</sub>O: 168.0575, found 168.06009.

### 3-Ferrocenylethynyl-furan (4p)

The crude product was purified *via* column chromatography on silica (*n*heptane). <sup>1</sup>H NMR (500 MHz, CDCl<sub>3</sub>) δ = 7.65–7.63 (m, 1H, CH<sub>furyl</sub>), 7.38–7.36 (m, 1H, CH<sub>furyl</sub>), 7.48 (d, *J* = 1.3 Hz, 1 H, CH<sub>furyl</sub>), 4.47 (t, <sup>3</sup>*J* = 1.8 Hz, 2 H, CH<sub>Fc</sub>), 4.23 (s, 5 H, CH<sub>Fc</sub>), 4.22 (t, <sup>3</sup>*J* = 1.8 Hz, 2 H, CH<sub>Fc</sub>); <sup>13</sup>C{<sup>1</sup>H} NMR (125.77 MHz, CDCl<sub>3</sub>) δ = 144.07, 141.67, 111.62, 107.13, 88.63, 75.46, 70.27, 68.96, 67.72, 64.30; CV: (*E*<sub>1/2</sub> = 0.546 V; Δ*E* = 82 mV); HRMS calcd. for C<sub>16</sub>H<sub>12</sub>OFe: 276.0237, found 276.0223.

### 2-Cyclohexylethynyl-thiophene (4q)

The crude product was purified *via* column chromatography on silica (*n*pentane : EtOAc = 200 : 1). <sup>1</sup>H NMR (500 MHz, CDCl<sub>3</sub>) δ = 7.15 (dd, <sup>3</sup>*J* = 5.2 Hz, *J* = 1.2 Hz, 1 H, CH<sub>thiophene</sub>), 7.10 (dd, <sup>3</sup>*J* = 3.7 Hz, *J* = 1.2 Hz, 1 H, CH<sub>thiophene</sub>), 6.92 (dd, <sup>3</sup>*J* = 5.2 Hz, *J* = 3.7 Hz, 1 H, CH<sub>thiophene</sub>), 2.62–2.56 (m, 1 H, CH), 1.90–1.84 (m, 2 H, CH<sub>2</sub>), 1.79–1.68 (m, 2 H, CH<sub>2</sub>), 1.57–1.48 (m, 4 H, CH<sub>2</sub>), 1.37–1.30 (m, 4 H, CH<sub>2</sub>); <sup>13</sup>C{<sup>1</sup>H} NMR (125.77 MHz, CDCl<sub>3</sub>) δ = 130.8, 126.7, 125.8, 124.3, 98.4, 73.6, 32.4, 29.9, 25.9, 24.9; HRMS calcd. for C<sub>12</sub>H<sub>14</sub>S: 190.0817, found 190.07977.

### 1-Methylsulfanyl-4-(4'-methoxy-phenylethynyl)-benzene (4r)

The crude product was purified *via* column chromatography on silica (cyclohexane : EtOAc = 100 : 1). <sup>1</sup>H NMR (500 MHz, CDCl<sub>3</sub>) δ = 7.45 (d, <sup>3</sup>*J* = 9.0 Hz, 2 H, CH<sub>ar</sub>), 7.42 (d, <sup>3</sup>*J* = 8.5 Hz, 2 H, CH<sub>ar</sub>), 7.20 (d, <sup>3</sup>*J* = 8.5 Hz, 2 H, CH<sub>ar</sub>), 6.87 (d, <sup>3</sup>*J* = 9.0 Hz, 2 H, CH<sub>ar</sub>), 3.82 (s, 3 H, OCH<sub>3</sub>), 2.49 (s, 3 H, SCH<sub>3</sub>); <sup>13</sup>C{<sup>1</sup>H} NMR (125.77 MHz, CDCl<sub>3</sub>) δ = 158.6, 137.8,



132.0, 130.7, 125.0, 119.0, 114.4, 113.0, 88.5, 86.8, 54.3, 14.5; HRMS calcd. for  $C_{16}H_{14}OS$ : 254.0766, found 254.07671.

### 2-(4-Methylsulfanyl-phenylethynyl)-thiophene (4s)

The crude product was purified *via* column chromatography on silica (cyclohexane : EtOAc = 100 : 1).  $^1H$  NMR (500 MHz,  $CDCl_3$ )  $\delta$  = 7.41 (d,  $^3J$  = 8.4 Hz, 2 H,  $CH_{ar}$ ), 7.27 (dd,  $^3J$  = 5.1 Hz,  $J$  = 1.2 Hz, 1 H,  $CH_{thiophene}$ ), 7.26 (dd,  $^3J$  = 3.8 Hz,  $J$  = 1.3 Hz, 1 H,  $CH_{thiophene}$ ), 7.19 (d,  $^3J$  = 8.4 Hz, 2 H,  $CH_{ar}$ ), 7.00 (dd,  $^3J$  = 5.1 Hz,  $^3J$  = 3.8 Hz, 1 H,  $CH_{thiophene}$ ), 2.48 (s, 3 H,  $SCH_3$ );  $^{13}C\{^1H\}$  NMR (125.77 MHz,  $CDCl_3$ )  $\delta$  = 140.0, 132.2, 132.0, 127.6, 127.5, 126.3, 123.8, 119.6, 93.3, 83.1, 15.7; HRMS calcd. for  $C_{13}H_{10}S_2$ : 230.0225, found 230.02168.

### 2-Thiophen-2-ylethynyl-phenylamine (4u)

The crude product was purified *via* column chromatography on silica (cyclohexane : EtOAc :  $NEt_3$  = 9 : 1 : 1).  $^1H$  NMR (500 MHz,  $CDCl_3$ )  $\delta$  = 7.33 (dd,  $^3J$  = 8.0 Hz,  $J$  = 1.5 Hz, 1 H,  $CH_{ar}$ ), 7.27 (dd,  $^3J$  = 5.1 Hz,  $J$  = 1.2 Hz, 1 H,  $CH_{thiophene}$ ), 7.25 (dd,  $^3J$  = 3.8 Hz,  $J$  = 1.2 Hz, 1 H,  $CH_{thiophene}$ ), 7.15–7.11 (m, 1 H,  $CH_{ar}$ ), 7.00 (dd,  $^3J$  = 5.1 Hz,  $^3J$  = 3.8 Hz, 1 H,  $CH_{thiophene}$ ), 6.72–6.68 (m, 2 H,  $CH_{ar}$ ), 4.23 (s(br), 2 H,  $NH_2$ );  $^{13}C\{^1H\}$  NMR (125.77 MHz,  $CDCl_3$ )  $\delta$  = 148.0, 132.3, 131.8, 130.1, 127.3, 127.2, 123.5, 118.1, 114.5, 107.7, 89.7, 87.8;  $^{15}N$ -NMR (50.7 MHz,  $CDCl_3$ )  $\delta$  = –321.9; HRMS calcd. for  $C_{12}H_9NS$ : 199.0456, found 199.04614.  $^1H$ - and  $^{13}C$  NMR-spectra are literature consistent.<sup>76</sup>

### 1-(4-Thiophen-3-ylethynyl-phenyl)-ethanone (4v)

The crude product was purified *via* column chromatography on silica (cyclohexane : EtOAc = 10 : 1).  $^1H$  NMR (500 MHz,  $CDCl_3$ )  $\delta$  = 7.92 (d,  $^3J$  = 8.5 Hz, 2 H,  $CH_{ar}$ ), 7.58 (d,  $^3J$  = 8.5 Hz, 2 H,  $CH_{ar}$ ), 7.57 (dd,  $J$  = 2.8 Hz,  $J$  = 1.1 Hz, 1 H,  $CH_{thiophene}$ ), 7.32 (dd,  $^3J$  = 5.0 Hz,  $J$  = 3.1 Hz, 1 H,  $CH_{thiophene}$ ), 7.21 (dd,  $^3J$  = 5.0 Hz,  $J$  = 1.1 Hz, 1 H,  $CH_{thiophene}$ ), 2.60 (s, 3 H,  $CH_3$ );  $^{13}C\{^1H\}$  NMR (125.77 MHz,  $CDCl_3$ )  $\delta$  = 197.6, 136.6, 132.0, 130.2, 129.9, 128.7, 128.6, 126.0, 122.2, 88.6, 88.3, 27.0; HRMS calcd. for  $C_{14}H_{10}OS$ : 226.0453, found 226.04413.

### 5-Thiophen-2-ylethynyl-pyridin-2-ylamine (4w)

The crude product was purified *via* column chromatography on silica (cyclohexane : EtOAc :  $NEt_3$  = 5 : 5 : 1).  $^1H$  NMR (500 MHz,  $DMSO-d_6$ )  $\delta$  = 8.11 (dd,  $J$  = 2.4 Hz,  $J$  = 0.8 Hz, 1 H,  $CH_{ar}$ ), 7.58 (dd,  $^3J$  = 5.4 Hz,  $J$  = 1.2 Hz, 1 H,  $CH_{thiophene}$ ), 7.49 (dd,  $^3J$  = 8.6 Hz,  $J$  = 2.3 Hz, 1 H,  $CH_{ar}$ ), 7.31 (dd,  $^3J$  = 3.6 Hz,  $J$  = 1.2 Hz, 1 H,  $CH_{thiophene}$ ), 7.08 (dd,  $^3J$  = 5.4 Hz,  $^3J$  = 3.6 Hz, 1 H,  $CH_{thiophene}$ ), 6.46 (dd,  $^3J$  = 8.6 Hz,  $J$  = 0.8 Hz, 1 H,  $CH_{ar}$ ), 6.45 (s(br), 2 H,  $NH_2$ );  $^{13}C\{^1H\}$  NMR (125.77 MHz,  $CDCl_3$ )  $\delta$  = 159.7, 151.5, 139.6, 132.0, 128.4, 128.0, 123.0, 108.0, 106.0, 92.1, 82.5;  $^{15}N$ -NMR (50.7 MHz,  $CDCl_3$ )  $\delta$  = –113.6 (Pyr-N), –299.7 ( $NH_2$ ); HRMS calcd. for  $C_{11}H_8N_2S$ : 200.0409, found 200.03900.

### Acknowledgements

This work was supported by the DFG and the Evonik Degussa GmbH, Provadis Partner für Bildung und Beratung GmbH,

and to C. A. F. by the Fonds der Chemischen Industrie and the Studienstiftung des Deutschen Volkes with a fellowship.

### Notes and references

- H.-U. Blaser, A. Indolese and A. Schnyder, *Curr. Sci.*, 2000, **78**, 1336–1344.
- A. Zapf and M. Beller, *Top. Catal.*, 2002, **19**, 101–109.
- S. Frigoli, C. Fuganti, L. Malpezzi and S. Serra, *Org. Process Res. Dev.*, 2005, **9**, 646–650.
- A. Stütz, *Angew. Chem., Int. Ed.*, 1987, **26**, 320–328.
- P. Nussbaumer, I. Leitner, K. Mraz and A. Stuetz, *J. Med. Chem.*, 1995, **38**, 1831–1836.
- D. H. B. Ripin, D. E. Bourassa, T. Brandt, M. J. Castaldi, H. N. Frost, J. Hawkins, P. J. Johnson, S. S. Massett, K. Neumann, J. Phillips, J. W. Raggan, P. R. Rose, J. L. Rutherford, B. Sitter, A. M. Stewart, M. G. Vetelino and L. Wei, *Org. Process Res. Dev.*, 2005, **9**, 440–450.
- J. W. B. Cooke, R. Bright, M. J. Coleman and K. P. Jenkins, *Org. Process Res. Dev.*, 2001, **5**, 383–386.
- M. Eckhardt and G. C. Fu, *J. Am. Chem. Soc.*, 2003, **125**, 13642–13643.
- T. Hundertmark, A. F. Littke, S. L. Buchwald and G. C. Fu, *Org. Lett.*, 2000, **2**, 1729–1731.
- K. W. Anderson and S. L. Buchwald, *Angew. Chem., Int. Ed.*, 2005, **44**, 6173–6177.
- E. A. B. Kantchev, C. J. O'Brien and M. G. Organ, *Aldrichchimica Acta*, 2006, **39**, 97–111.
- C. Yang and S. P. Nolan, *Organometallics*, 2002, **21**, 1020–1022.
- Z. Novák, P. Nemes and A. Kotschy, *Org. Lett.*, 2004, **6**, 4917–4920.
- A. Köllhofer, T. Pullmann and H. Plenio, *Angew. Chem., Int. Ed.*, 2003, **42**, 1056–1058.
- R. Chinchilla and C. Najera, *Chem. Rev.*, 2007, **107**, 874–922.
- H. Doucet and J.-C. Hierso, *Angew. Chem., Int. Ed.*, 2007, **46**, 834–871.
- A. Köllhofer and H. Plenio, *Adv. Synth. Catal.*, 2005, **347**, 1295–1300.
- J.-C. Hierso, A. Fihri, R. Amardeil, P. Meunier, H. Doucet, M. Santelli and V. V. Ivanov, *Org. Lett.*, 2004, **6**, 3473–3476.
- J. Hillerich and H. Plenio, *Chem. Commun.*, 2003, 3024–3025.
- A. Datta and H. Plenio, *Chem. Commun.*, 2003, 1504–1505.
- A. Datta, K. Ebert and H. Plenio, *Organometallics*, 2003, **22**, 4685–4691.
- A. C. Hillier, G. A. Grasa, M. S. Viciu, H. M. Lee, C. Yang and S. P. Nolan, *J. Organomet. Chem.*, 2002, **653**, 69.
- C. Capello, U. Fischer and K. Hungerbühler, *Green Chem.*, 2007, **9**, 927–934.
- R. A. Sheldon, *Green Chem.*, 2005, **7**, 267–278.
- D. J. C. Constable, C. Jimenez-Gonzalez and R. K. Henderson, *Org. Process Res. Dev.*, 2007, **11**, 133–137.
- C.-J. Li and L. Chen, *Chem. Soc. Rev.*, 2006, **35**, 68–82.
- D. J. C. Constable, A. D. Curzons and V. L. Cunningham, *Green Chem.*, 2002, **4**, 521–527.
- J. T. Guan, T. Q. Weng, G.-A. Yu and S. H. Liu, *Tetrahedron Lett.*, 2007, **48**, 7129–7133.
- P. Bertus, F. Fecourt, C. Bauder and P. Pale, *New J. Chem.*, 2004, **28**, 12–14.
- K. L. Billingsley, K. W. Anderson and S. L. Buchwald, *Angew. Chem., Int. Ed.*, 2006, **45**, 3484–3488.
- C. A. Fleckenstein and H. Plenio, *Green Chem.*, 2007, **9**, 1287–1291.
- C. A. Fleckenstein and H. Plenio, *Chem.–Eur. J.*, 2007, **13**, 2701–2716.
- C. A. Fleckenstein, S. Roy, S. Leuthäuber and H. Plenio, *Chem. Commun.*, 2007, 2870–2872.
- K. Billingsley and S. L. Buchwald, *J. Am. Chem. Soc.*, 2007, **129**, 3358–3366.
- N. Kudo, M. Perseghini and G. C. Fu, *Angew. Chem., Int. Ed.*, 2006, **45**, 1282–1284.
- A. S. Guram, X. Wang, E. E. Bunel, M. M. Faul, R. D. Larsen and M. J. Martinelli, *J. Org. Chem.*, 2007, **72**, 5104–5112.
- A. Soheili, J. Albaneze-Walker, J. A. Murry, P. G. Dormer and D. L. Hughes, *Org. Lett.*, 2003, **5**, 4191–4194.
- C. Torborg, A. Zapf and M. Beller, *Chem. Sus. Chem.*, 2008, **1**, 91–96.
- J.-C. Hierso, M. Beauperin and P. Meunier, *Eur. J. Inorg. Chem.*, 2007, **24**, 3767–3780.

- 40 P. T. Anastas and M. M. Kirchhoff, *Acc. Chem. Res.*, 2002, **35**, 686–694.
- 41 R. A. Sheldon, *Green Chem.*, 2007, **9**, 1273–1283.
- 42 K. Alfonsi, J. Colberg, P. J. Dunn, T. Fevig, S. Jennings, T. A. Johnson, H. P. Kleine, C. Knight, M. A. Nagy, D. A. Perry and M. Stefaniak, *Green Chem.*, 2008, **10**, 31–36.
- 43 C. A. Fleckenstein, R. Kadyrov and H. Plenio, *Org. Process Res. Dev.*, 2008, **12**, DOI: 10.1021/op7001479.
- 44 C. A. Fleckenstein and H. Plenio, *Organometallics*, 2007, **26**, 2758–2767.
- 45 C. A. Fleckenstein and H. Plenio, *Chem.–Eur. J.*, 2008, **14**, DOI: 10.1002/chem.200701877.
- 46 The authors are aware that the here mentioned cross coupling reaction effected by Pd without use of Cu(I)-cocatalyst is more accurately named as “Cassar-reaction”. However, the term “Sonogashira-reaction” is established as an umbrella term for couplings of aryl halides with terminal acetylenes.
- 47 S. Park, M. Kim, D. H. Koo and S. Chang, *Adv. Synth. Cat.*, 2004, **346**, 1638–1640.
- 48 B. Liang, M. Dai, J. Chen and Z. Yang, *J. Org. Chem.*, 2005, **70**, 391–393.
- 49 K. Heuzé, D. Meré, D. Gauss, J.-C. Blais and D. Astruc, *Chem.–Eur. J.*, 2004, **10**, 3936–3944.
- 50 T. Fukuyama, M. Shinmen, S. Nishitani, M. Sato and I. Ryu, *Org. Lett.*, 2002, **4**, 1691–1694.
- 51 T. Ljungdahl, K. Pettersson, B. Albinsson and J. Martensson, *J. Org. Chem.*, 2006, **71**, 1677–1687.
- 52 F. Yang, X. Cui, Y.-N. Li, J. Zhang, G.-R. Rena and Y. Wu, *Tetrahedron*, 2007, **63**, 1963–1969.
- 53 C. S. Consorti, F. R. Flores, F. Rominger and J. Dupont, *Adv. Synth. Catal.*, 2006, **348**, 133–141.
- 54 P. Appukkuttan, W. Dehaen and E. V. d. Eycken, *Eur. J. Org. Chem.*, 2003, 4713–4716.
- 55 Y. Ma, C. Song, W. Jiang, Q. Wu, Y. Wang, X. Liu and M. B. Andrus, *Org. Lett.*, 2003, **5**, 3317.
- 56 C. Yi and R. Hua, *J. Org. Chem.*, 2006, **71**, 2535–2537.
- 57 P. A. Wender, T. J. Paxton and T. J. Williams, *J. Am. Chem. Soc.*, 2006, **128**, 14814–14815.
- 58 M. F. R. Fouda, M. M. Abd-Elzaher, R. A. Abdelsamaia and A. A. Labib, *Appl. Organomet. Chem.*, 2007, **21**, 613–625.
- 59 R. F. Shago, J. C. Swarts, E. Kreft and C. E. J. Van Rensburg, *Anticancer Res.*, 2007, **27**, 3431–3434.
- 60 E. Hillard, A. Vessieres, L. Thouin, G. Jaouen and C. Amatore, *Angew. Chem., Int. Ed.*, 2006, **45**, 285–290.
- 61 W. C. M. Duivendoorn, Y.-N. Liu, G. Schatte and H.-B. Kraatz, *Inorg. Chim. Acta*, 2005, **358**, 3183–3189.
- 62 E. W. Neuse, *J. Inorg. Organomet. Polym. Mater.*, 2005, **15**, 3–32.
- 63 B. Weber, A. Serafin, J. Michie, C. Van Rensburg, J. C. Swarts and L. Bohm, *Anticancer Res.*, 2004, **24**, 763–770.
- 64 C. Biot, W. Daher, C. M. Ndiaye, P. Melnyk, B. Pradines, N. Chavain, A. Pellet, L. Fraisse, L. Pelinski, C. Jarry, J. Brocard, J. Khalife, I. Forfar-Bares and D. Dive, *J. Med. Chem.*, 2006, **49**, 4707–4714.
- 65 C. Biot, D. Taramelli, I. Forfar-Bares, L. A. Maciejewski, M. Boyce, G. Nowogrocki, J. S. Brocard, N. Basilio, P. Olliaro and T. J. Egan, *Mol. Pharm.*, 2005, **2**, 185–193.
- 66 B. Pradines, T. Fusai, W. Daries, V. Laloge, C. Rogier, P. Millet, E. Panconi, M. Kombila and D. Parzy, *J. Antimicrob. Chemother.*, 2001, **48**, 179–184.
- 67 A. K. Kondapi, N. Satyanarayana and A. D. Saikrishna, *Arch. Biochem. Biophys.*, 2006, **450**, 123–132.
- 68 C. H. T. P. da Silva, G. Del Ponte, A. F. Neto and C. A. Taft, *Bioorg. Chem.*, 2005, **33**, 274–284.
- 69 P. Brázdilová, M. Vrabel, R. Pohl, H. Pivonková, L. Havran, M. Hocek and M. Fojta, *Chem.–Eur. J.*, 2007, **13**, 9527–9533.
- 70 H. Aoki and H. Tao, *Analyst*, 2007, **132**, 784–791.
- 71 F. Le Floch, H. A. Ho and M. Leclerc, *Anal. Chem.*, 2006, **78**, 4727–4731.
- 72 P. Li, L. Wang and H. Li, *Tetrahedron*, 2005, **61**, 8633–8640.
- 73 G. H. Torres, S. Choppin and F. Colobert, *Eur. J. Org. Chem.*, 2006, **6**, 1450–1454.
- 74 D. A. Alonso, C. Najera and M. C. Pacheco, *Adv. Synth. Catal.*, 2003, **345**, 1146–1158.
- 75 I. Novak, S.-C. Ng, C.-Y. Mok, H.-H. Huang, J. Fang and K. K.-T. Wang, *J. Chem. Soc., Perkin Trans. 2*, 1994, 1771–1776.
- 76 C. Koradin, W. Dohle, A. L. Rodriguez, B. Schmid and P. Knochel, *Tetrahedron*, 2003, **59**, 1571–1588.

# Purification of chemical feedstocks by the removal of aerial carbonyl sulfide by hydrolysis using rare earth promoted alumina catalysts†

Hongmei Huang,<sup>a</sup> Nicola Young,<sup>b</sup> B. Peter Williams,<sup>b</sup> Stuart H. Taylor<sup>a</sup> and Graham Hutchings<sup>\*a</sup>

Received 2nd November 2007, Accepted 12th February 2008

First published as an Advance Article on the web 11th March 2008

DOI: 10.1039/b717031a

The effect of rare earth doping of alumina catalysts is investigated for the carbonyl sulfide (COS) hydrolysis reaction ( $\text{COS} + \text{H}_2\text{O} = \text{CO}_2 + \text{H}_2\text{S}$ ). The effect of the catalyst preparation method is described and discussed, and three methods are compared, namely: impregnation by incipient wetness, coprecipitation and deposition precipitation. The most effective catalysts are prepared using the incipient wetness impregnation method. The addition of rare earth oxides, namely  $\text{Y}_2\text{O}_3$ ,  $\text{Gd}_2\text{O}_3$ ,  $\text{Nd}_2\text{O}_3$ ,  $\text{La}_2\text{O}_3$ , increases the basicity of the material as shown by pulsed  $\text{CO}_2$  chemisorption and the basicity increases with the amount of rare earth oxide added.  $\text{CO}_2$  TPD shows that the  $\text{La}_2\text{O}_3$ -doped alumina has the strongest basic sites. The promoted catalysts are all effective for the COS hydrolysis reaction and the best results are obtained with  $\text{Y}_2\text{O}_3$ -doped materials, as these have the most pronounced promotion of activity over the reaction timescale we have examined. The combination of the results for COS conversion with the  $\text{H}_2\text{S}$  selectivity data and the effects of  $\text{H}_2\text{S}$  pre-treatment shows that a highly active catalyst also has a high  $\text{H}_2\text{S}$  selectivity. The  $\text{La}_2\text{O}_3$ -doped materials deactivate rapidly and have poor  $\text{H}_2\text{S}$  selectivities, and we propose that the higher basicity of this material leads to reaction with the acidic COS and  $\text{H}_2\text{S}$  leading to the formation of the less basic lanthanum sulfide. This study has presented results for the first time showing that an alumina catalyst for COS hydrolysis can be promoted by the addition of rare earth oxides, and this is related to the enhanced basicity of the promoted catalyst.

## Introduction

In recent years the emission of chemicals into the environment has come under increasing scrutiny. Whilst a large part of the focus has been on greenhouse gas emissions there is still widespread concern over sulfur compounds as they are potent precursors of acid rain. In this sense there are strict limits on the amounts of sulfur in fuels such as diesel, and there is a current emphasis on the search for cleaner fuels, and this has seen a renaissance in Fischer Tropsch technology.<sup>1</sup> Catalysis plays a major role in decreasing emissions to the environment, but it should also be noted that sulfur often has a detrimental effect on the performance of many catalysts, as well as leading to increased corrosion in reactors.<sup>2</sup> Hence, it is crucial that sulfur is removed from hydrocarbon feedstocks that are used within the petrochemical industry for the manufacture of fuels. Most sulfur present in hydrocarbon feedstocks is removed by hydrodesulfurisation to form  $\text{H}_2\text{S}$  that is subsequently absorbed onto  $\text{ZnO}$ .<sup>3</sup> Whilst this process is highly efficient it does not affect carbonyl sulfide (COS), which is a potent catalyst poison. Unless the residual low levels of COS are efficiently removed

the residual sulfur can have deleterious effects on downstream processes. Hence, removal of COS is not simply a process of waste abatement as it provides a means to clean-up important chemical feedstocks that can subsequently be used for the production of chemicals and fuels by green processes.

COS is treated by hydrolysis to form  $\text{H}_2\text{S}$ , which is then removed in the standard way by absorption. This process has been well studied and to date alumina and titania have been found to be promising catalysts and alumina is used commercially.<sup>4-15</sup> There has been interest in improving the activity of catalysts by the addition of promoters and to date most of these studies have been concerned with the modification of alumina to affect its acid/base properties. George<sup>16</sup> and Fiedorow *et al.*<sup>17</sup> demonstrated that the rate of COS hydrolysis could be increased by the presence of a base and that basic sites were essential for the reaction. To date, a wide range of alkali metals (Li, Na, K, Cs), alkaline earth metals (Mg, Ca, Sr, Ba), first row transition metals (Fe, Co, Ni, Cu, Zn) and Sn have been considered as promoters for alumina.<sup>18-22</sup> However, the effect of rare earth metal cations as promoters for the alumina catalysed COS hydrolysis reaction has received, as yet, no attention, and this is the scope of the study we report here.

The effect of rare earth metal oxides on the properties of alumina has been studied extensively although none of these studies has focused on using rare earth metal modified alumina as a catalyst for COS hydrolysis. Church *et al.*<sup>23</sup> concluded that  $\text{La}^{3+}$  and  $\text{Ce}^{4+}$  were effective surface area stabilisers for alumina at temperatures up to 1100 °C, and  $\text{La}^{3+}$  was much

<sup>a</sup>School of Chemistry, Cardiff University, Main Building, Park Place, Cardiff, UK CF10 3AT. E-mail: hutch@cardiff.ac.uk

<sup>b</sup>Johnson Matthey Catalysts, PO Box 1, Billingham, Teeside, UK TS23 1LB

† Electronic supplementary information (ESI) available: TGA profiles for catalyst precursors (Fig. S1) and SEM analysis of catalysts prepared by the incipient wetness method (Fig. S2). See DOI: 10.1039/b717031a

more effective than  $\text{Ce}^{4+}$ . Zhao *et al.*,<sup>24</sup> using TPD-MS, found that there were mainly strong basic sites and relatively few acidic sites on rare earth oxide surfaces. The strength of the strong basic sites decreased in the order:  $\text{La}_2\text{O}_3 > \text{Nd}_2\text{O}_3 > \text{Y}_2\text{O}_3 > \text{Ce}_2\text{O}_3$ . Microcalorimetric and infrared spectroscopic studies of ammonia and carbon dioxide adsorption were carried out by Shen *et al.*<sup>25</sup> to investigate the surface acid/base properties of  $\gamma\text{-Al}_2\text{O}_3$  following the addition of  $\text{K}_2\text{O}$ ,  $\text{MgO}$  and  $\text{La}_2\text{O}_3$ . They found that even a low loading of these oxides was effective for the elimination of strong acid sites on alumina. With higher loadings, the effectiveness of generation of basicity followed the order of  $\text{K}_2\text{O} > \text{La}_2\text{O}_3 > \text{MgO}$ . The acid/base properties of alumina supported rare earth metal oxides ( $\text{Ln}/\text{Al}_2\text{O}_3$ ;  $\text{Ln} = \text{La}$ ,  $\text{Ce}$ ,  $\text{Eu}$ ,  $\text{Tb}$ , and  $\text{Yb}$ ) were also investigated by Yamamoto *et al.*<sup>26</sup> using  $\alpha$ -pinene isomerization and 2-butanol decomposition as probe reactions, together with TPD and FTIR techniques. They found that new Lewis acid sites were formed on  $\gamma\text{-Al}_2\text{O}_3$  by the addition of rare earth elements but the maximum base strength of  $\text{Ln}/\text{Al}_2\text{O}_3$  never exceeded the corresponding rare earth metal oxide itself.

We have selected yttrium, lanthanum, neodymium and gadolinium oxides as representative rare earth promoters for alumina. These were selected as they all show 3+ as the most stable oxidation state, demonstrate a decrease of basicity due to the lanthanide contraction and span a suitable range across the period. In this paper we present our results for the use of these rare earth-promoted catalysts for the hydrolysis of COS.

## Results and discussion

### Catalyst preparation and characterisation

A series of catalysts were prepared using incipient wetness, coprecipitation and deposition precipitation techniques. TGA of the uncalcined precursors (see ESI Fig. S1†) shows very similar weight loss profiles with maxima at *ca.* 90, 300 and 450 °C. Consequently catalysts were calcined at 500 °C to ensure the nitrate was decomposed to the oxide. The catalysts after calcination at 500 °C were analysed by the BET surface area method and XRF and the results are given in Table 1. Samples prepared using the incipient wetness method containing <10 wt% of the rare earth oxide showed a decrease of surface area when compared with the non-impregnated alumina. At higher loadings the surface area decreased further. The coprecipitation and deposition precipitation methods lead to high surface areas even at higher loading. XRF analysis shows that the metal loading for the coprecipitation and impregnation methods is close to that expected, but the deposition method leads to much lower loadings than expected. TPR analysis of the calcined catalysts showed that the materials were stable with respect to reduction up to 1000 °C.

The catalysts were characterised by XRD. For the 3 and 10%  $\text{La}_2\text{O}_3/\text{Al}_2\text{O}_3$ , 3 and 10%  $\text{Nd}_2\text{O}_3/\text{Al}_2\text{O}_3$ , 3 and 10%  $\text{Gd}_2\text{O}_3/\text{Al}_2\text{O}_3$ , and 10 and 30%  $\text{Y}_2\text{O}_3/\text{Al}_2\text{O}_3$  catalysts, prepared by coprecipitation and deposition precipitation methods, no rare earth metal oxide phase was observed and only diffraction reflections attributable to  $\gamma\text{-Al}_2\text{O}_3$  were observed. For the incipient wetness method reflections associated with the rare earth oxide can be observed above 20 wt% loading

**Table 1** Catalyst samples and results of surface area and elemental analysis

Catalyst	BET surface area/ $\text{m}^2 \text{g}^{-1}$	Metal loading (wt%)	
		Theoretical	XRF analysis
3% $\text{Y}_2\text{O}_3/\text{Al}_2\text{O}_3^a$	280	2.2	2.9
3% $\text{La}_2\text{O}_3/\text{Al}_2\text{O}_3^a$	280	2.3	2.2
3% $\text{Nd}_2\text{O}_3/\text{Al}_2\text{O}_3^a$	290	2.3	2.9
3% $\text{Gd}_2\text{O}_3/\text{Al}_2\text{O}_3^a$	300	2.4	3.7
10% $\text{Y}_2\text{O}_3/\text{Al}_2\text{O}_3^a$	230	7.2	7.1
10% $\text{La}_2\text{O}_3/\text{Al}_2\text{O}_3^a$	220	7.7	8.4
10% $\text{Nd}_2\text{O}_3/\text{Al}_2\text{O}_3^a$	240	7.8	7.8
10% $\text{Gd}_2\text{O}_3/\text{Al}_2\text{O}_3^a$	250	7.9	9.2
20% $\text{Y}_2\text{O}_3/\text{Al}_2\text{O}_3^a$	200	14.4	15.0
30% $\text{Y}_2\text{O}_3/\text{Al}_2\text{O}_3^a$	100	21.6	20.6
50% $\text{Y}_2\text{O}_3/\text{Al}_2\text{O}_3^a$	80	36.0	27.0
10% $\text{Y}_2\text{O}_3/\text{Al}_2\text{O}_3^b$	280	7.2	6.9
30% $\text{Y}_2\text{O}_3/\text{Al}_2\text{O}_3^b$	210	21.6	17.9
10% $\text{Y}_2\text{O}_3/\text{Al}_2\text{O}_3^c$	250	7.2	4.2
30% $\text{Y}_2\text{O}_3/\text{Al}_2\text{O}_3^c$	230	21.6	9.4
$\text{Y}_2\text{O}_3^d$	9	—	—
$\text{Al}_2\text{O}_3^b$	200	—	—
$\text{Al}_2\text{O}_3^e$	300	—	—

<sup>a</sup> Incipient wetness impregnation. <sup>b</sup> Coprecipitation. <sup>c</sup> Deposition precipitation. <sup>d</sup> Calcination of  $\text{Y}(\text{NO}_3)_3 \cdot 6\text{H}_2\text{O}$  at 500 °C. <sup>e</sup> Support for incipient wetness impregnation.

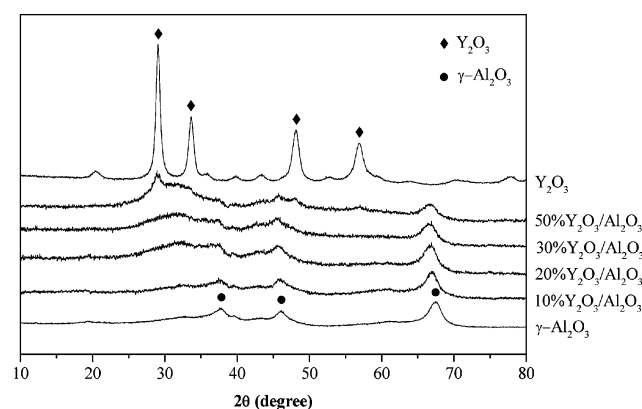


**Fig. 1** Powder X-ray diffraction patterns for  $\text{Y}_2\text{O}_3/\text{Al}_2\text{O}_3$  catalysts prepared by incipient wetness impregnation.

and representative data for the  $\text{Y}_2\text{O}_3/\text{Al}_2\text{O}_3$  catalysts are shown in Fig. 1. These data suggest that at low loadings the rare earth oxide is well dispersed and SEM analysis confirmed this to be the case, as the morphology was very similar to the parent alumina (see ESI Fig. S2†). SEM-EDX was used to analyse 10% and 30%  $\text{Y}_2\text{O}_3/\text{Al}_2\text{O}_3$  catalysts and the results are given in Table 2 and although the analysis of the catalyst composition is only semi-quantitative, the Y/Al ratios are very similar to those expected for the incipient wetness and coprecipitation methods. For the deposition precipitation method the Y/Al ratios are lower than expected and this is in agreement with the XRF analysis.

The  $\text{CO}_2$  pulse chemisorption technique was used to quantify the number of basic sites on alumina and promoted alumina catalysts. Assuming that one  $\text{CO}_2$  molecule interacts with one basic site, the total amount of basic sites on the catalyst can be calculated. However, we present the results using  $\mu\text{mol CO}_2 \text{ m}^{-2}$  sample as this permits facile comparison of different samples (Table 3). For the catalysts prepared using the incipient



**Table 2** EDX analysis of  $\text{Y}_2\text{O}_3/\text{Al}_2\text{O}_3$  catalysts

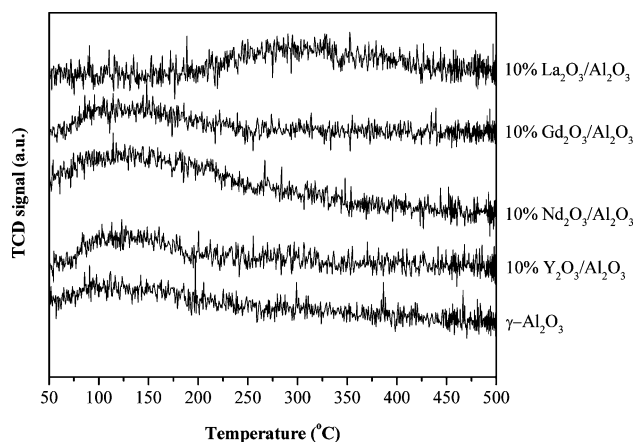
Catalyst	Preparation method	Y/Al (wt%)	
		Theoretical	EDX analysis
10% $\text{Y}_2\text{O}_3/\text{Al}_2\text{O}_3$	Incipient wetness	15	20
30% $\text{Y}_2\text{O}_3/\text{Al}_2\text{O}_3$		45	56
10% $\text{Y}_2\text{O}_3/\text{Al}_2\text{O}_3$	Coprecipitation	15	14
30% $\text{Y}_2\text{O}_3/\text{Al}_2\text{O}_3$		45	54
10% $\text{Y}_2\text{O}_3/\text{Al}_2\text{O}_3$	Deposition precipitation	15	8
30% $\text{Y}_2\text{O}_3/\text{Al}_2\text{O}_3$		45	10

**Table 3** Comparison of the concentration of basic sites determined by  $\text{CO}_2$  chemisorption

Catalyst	Preparation method	$\text{CO}_2$ adsorbed/ $\mu\text{mol m}^{-2}$
$\text{Al}_2\text{O}_3$	Incipient wetness	0.22
3% $\text{Y}_2\text{O}_3/\text{Al}_2\text{O}_3$		0.38
10% $\text{Y}_2\text{O}_3/\text{Al}_2\text{O}_3$		0.78
20% $\text{Y}_2\text{O}_3/\text{Al}_2\text{O}_3$		1.32
30% $\text{Y}_2\text{O}_3/\text{Al}_2\text{O}_3$		2.55
10% $\text{La}_2\text{O}_3/\text{Al}_2\text{O}_3$		0.57
10% $\text{Nd}_2\text{O}_3/\text{Al}_2\text{O}_3$		0.55
10% $\text{Gd}_2\text{O}_3/\text{Al}_2\text{O}_3$		0.43
10% $\text{Y}_2\text{O}_3/\text{Al}_2\text{O}_3$	Precipitation deposition	0.38
30% $\text{Y}_2\text{O}_3/\text{Al}_2\text{O}_3$		0.75
$\text{Al}_2\text{O}_3$	Co-precipitation	0.27
10% $\text{Y}_2\text{O}_3/\text{Al}_2\text{O}_3$		0.38
30% $\text{Y}_2\text{O}_3/\text{Al}_2\text{O}_3$		0.62

wetness method, the amount of adsorbed  $\text{CO}_2$  and hence basicity follows the decreasing order of 10% $\text{Y}_2\text{O}_3/\text{Al}_2\text{O}_3 > 10\%\text{Nd}_2\text{O}_3/\text{Al}_2\text{O}_3 \approx 10\%\text{La}_2\text{O}_3/\text{Al}_2\text{O}_3 > 10\%\text{Gd}_2\text{O}_3/\text{Al}_2\text{O}_3 > \gamma\text{-Al}_2\text{O}_3$ . All the promoted catalysts have more basic sites than the alumina support. For a series of  $\text{Y}_2\text{O}_3/\text{Al}_2\text{O}_3$  catalysts prepared using the incipient wetness method, the number of basic sites increases with increasing  $\text{Y}_2\text{O}_3$  loading. All the  $\text{Y}_2\text{O}_3$  promoted alumina catalysts have more basic sites than alumina. The amount of  $\text{CO}_2$  adsorbed for the 10% $\text{Y}_2\text{O}_3/\text{Al}_2\text{O}_3$  catalyst after being tested for COS hydrolysis at 150 °C for 29 h was 0.39  $\mu\text{mol m}^{-2}$ . It is clear that the used catalyst has a lower number of basic sites than the fresh sample and this is consistent with the deactivation that is observed during use. For the catalysts prepared using coprecipitation and deposition precipitation methods, the number of basic sites follows the order of 30% $\text{Y}_2\text{O}_3/\text{Al}_2\text{O}_3 > 10\%\text{Y}_2\text{O}_3/\text{Al}_2\text{O}_3 > \gamma\text{-Al}_2\text{O}_3$ . For 10% $\text{Y}_2\text{O}_3/\text{Al}_2\text{O}_3$  catalysts, the number of basic sites depends on the preparation method and follows the decreasing order of incipient wetness > coprecipitation  $\approx$  deposition precipitation, *i.e.* the catalyst prepared using incipient wetness has the largest number of basic sites, whilst the other preparation methods had a similar number.

$\text{CO}_2$  desorption experiments were carried out following the pulsed  $\text{CO}_2$  uptake experiments to identify the strength of basic sites for alumina and rare earth metal oxide promoted alumina catalysts (Fig. 2). The results show that the  $\text{CO}_2$  desorption peak appears at *ca.* 100 °C for  $\gamma\text{-Al}_2\text{O}_3$  and slightly higher than 100 °C for 10% $\text{Y}_2\text{O}_3/\text{Al}_2\text{O}_3$ , 10% $\text{Nd}_2\text{O}_3/\text{Al}_2\text{O}_3$  and 10% $\text{Gd}_2\text{O}_3/\text{Al}_2\text{O}_3$ . For the 10% $\text{La}_2\text{O}_3/\text{Al}_2\text{O}_3$  catalyst the  $\text{CO}_2$  desorption peak appears at *ca.* 275 °C. This confirms that the rare earth doped alumina catalysts have stronger surface basic sites than the undoped alumina.

**Fig. 2**  $\text{CO}_2$  desorption profiles for alumina and rare earth metal oxide promoted alumina catalysts.

### COS hydrolysis

Initial studies compared catalysts prepared by incipient wetness impregnation. 3% and 10% rare earth doped catalysts prepared using incipient wetness were evaluated for the hydrolysis of COS at 150 °C and the results for the effect of time on line on conversion are shown in Fig. 3. All the catalysts show deactivation towards COS hydrolysis under these conditions. However, the undoped alumina shows an initial rapid deactivation, which is not so apparent in the doped samples. The rare earth doped materials demonstrate higher catalyst activity but sustained effects are only observed with the 10% $\text{Y}_2\text{O}_3/\text{Al}_2\text{O}_3$  and 10% $\text{Gd}_2\text{O}_3/\text{Al}_2\text{O}_3$  catalysts (Table 4).

After 10 h time-on-line, the activity is in the order: 10% $\text{Y}_2\text{O}_3/\text{Al}_2\text{O}_3 > 10\%\text{Gd}_2\text{O}_3/\text{Al}_2\text{O}_3 > \gamma\text{-Al}_2\text{O}_3 \approx 10\%\text{Nd}_2\text{O}_3/\text{Al}_2\text{O}_3 > 10\%\text{La}_2\text{O}_3/\text{Al}_2\text{O}_3$ . Comparing the activities after 5 min and 10 h on line, shows that the 10% $\text{Y}_2\text{O}_3/\text{Al}_2\text{O}_3$  catalyst has the least deactivation combined with the highest promotion of activity. The 10% $\text{La}_2\text{O}_3/\text{Al}_2\text{O}_3$  catalyst has the greatest deactivation rate and after 10 h exhibits a lower catalyst activity compared with the undoped parent alumina.

The selectivity to  $\text{H}_2\text{S}$  for the alumina and the 10% rare earth doped alumina catalysts is shown in Fig. 4. For  $\gamma\text{-Al}_2\text{O}_3$  and 10% $\text{Y}_2\text{O}_3/\text{Al}_2\text{O}_3$  catalysts, relatively stable  $\text{H}_2\text{S}$  selectivities are observed in the range of 0–10 h. For the 10% $\text{Gd}_2\text{O}_3/\text{Al}_2\text{O}_3$  catalyst  $\text{H}_2\text{S}$  selectivity decreases gradually with increasing time on line. However, for 10% $\text{La}_2\text{O}_3/\text{Al}_2\text{O}_3$  and 10% $\text{Nd}_2\text{O}_3/\text{Al}_2\text{O}_3$  catalysts, the  $\text{H}_2\text{S}$  selectivity decreases markedly with increasing time on line. After 10 h on line,  $\text{H}_2\text{S}$  selectivity follows the decreasing

**Table 4** Activity comparison of COS hydrolysis over 10% rare earth metal oxide promoted alumina catalysts. Conditions: catalyst: 10 mg diluted by 500 mg silicon carbide; 0.5% $\text{COS}/\text{N}_2$ : 58  $\text{ml min}^{-1}$ ;  $\text{N}_2$ : 180  $\text{ml min}^{-1}$ ;  $\text{H}_2\text{O}$ : 4559 ppm; reaction temperature: 150 °C

Catalyst	Conversion (%)	
	5 min time-on-line	10 h time-on-line
$\text{Al}_2\text{O}_3$	68	26
10% $\text{Y}_2\text{O}_3/\text{Al}_2\text{O}_3$	76	52
10% $\text{La}_2\text{O}_3/\text{Al}_2\text{O}_3$	71	15
10% $\text{Nd}_2\text{O}_3/\text{Al}_2\text{O}_3$	75	24
10% $\text{Gd}_2\text{O}_3/\text{Al}_2\text{O}_3$	76	35

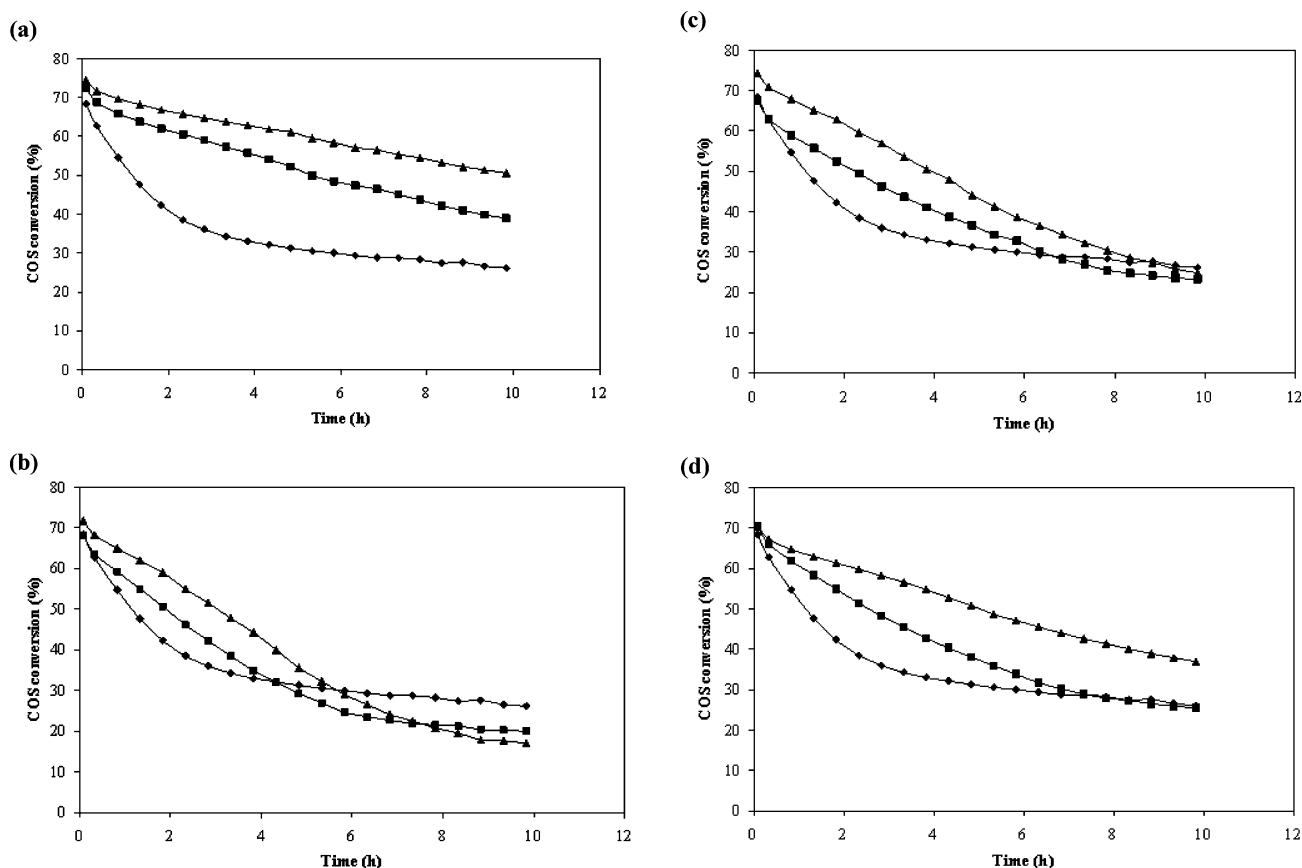


**Fig. 3** Comparison of the activity of COS hydrolysis over (a)  $\gamma$ -Al<sub>2</sub>O<sub>3</sub>, 3 and 10%Y<sub>2</sub>O<sub>3</sub>/Al<sub>2</sub>O<sub>3</sub> catalysts, (b)  $\gamma$ -Al<sub>2</sub>O<sub>3</sub>, 3 and 10%La<sub>2</sub>O<sub>3</sub>/Al<sub>2</sub>O<sub>3</sub> catalysts, (c)  $\gamma$ -Al<sub>2</sub>O<sub>3</sub>, 3 and 10%Nd<sub>2</sub>O<sub>3</sub>/Al<sub>2</sub>O<sub>3</sub> catalysts, (d)  $\gamma$ -Al<sub>2</sub>O<sub>3</sub>, 3 and 10%Gd<sub>2</sub>O<sub>3</sub>/Al<sub>2</sub>O<sub>3</sub> catalysts: Key (◆) Al<sub>2</sub>O<sub>3</sub>, (■) 3% loading, (▲) 10% loading; Conditions: catalyst: 10 mg diluted by 500 mg silicon carbide; 0.5%COS/N<sub>2</sub>: 58 ml min<sup>-1</sup>; N<sub>2</sub>: 180 ml min<sup>-1</sup>; H<sub>2</sub>O: 4559 ppm; reaction temperature: 150 °C.

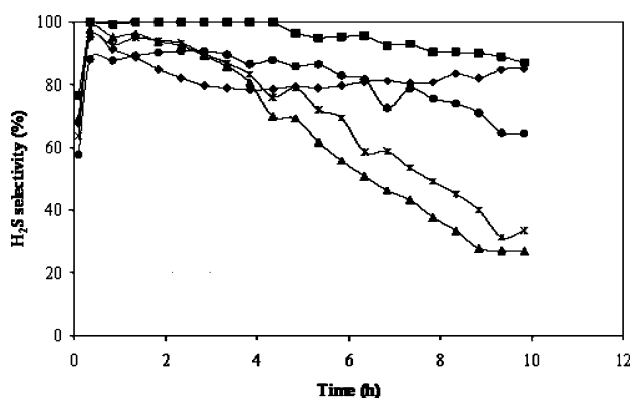


**Fig. 4** Comparison of H<sub>2</sub>S selectivities for the COS hydrolysis reaction: Key (◆) Al<sub>2</sub>O<sub>3</sub>, (■) 10%Y<sub>2</sub>O<sub>3</sub>/Al<sub>2</sub>O<sub>3</sub>, (▲) 10%La<sub>2</sub>O<sub>3</sub>/Al<sub>2</sub>O<sub>3</sub>, (×) 10%Nd<sub>2</sub>O<sub>3</sub>/Al<sub>2</sub>O<sub>3</sub>, (●) 10%Gd<sub>2</sub>O<sub>3</sub>/Al<sub>2</sub>O<sub>3</sub>; Conditions: catalyst: 10 mg diluted by 500 mg silicon carbide; 0.5%COS/N<sub>2</sub>: 58 ml min<sup>-1</sup>; N<sub>2</sub>: 180 ml min<sup>-1</sup>; H<sub>2</sub>O: 4559 ppm; reaction temperature: 150 °C.

order of 10%Y<sub>2</sub>O<sub>3</sub>/Al<sub>2</sub>O<sub>3</sub>  $\approx$   $\gamma$ -Al<sub>2</sub>O<sub>3</sub> > 10%Gd<sub>2</sub>O<sub>3</sub>/Al<sub>2</sub>O<sub>3</sub> > 10%Nd<sub>2</sub>O<sub>3</sub>/Al<sub>2</sub>O<sub>3</sub> > 10%La<sub>2</sub>O<sub>3</sub>/Al<sub>2</sub>O<sub>3</sub>.

To understand the deactivation mechanism in COS hydrolysis, the rare earth metal oxide promoted alumina catalysts were pre-treated *in situ* using H<sub>2</sub>S/H<sub>2</sub>O/N<sub>2</sub> at 150 °C for 1 h (41 ml min<sup>-1</sup>, 0.28%/H<sub>2</sub>S/0.26%/H<sub>2</sub>O/N<sub>2</sub>) and the pretreated

catalysts were evaluated for COS hydrolysis (Table 5). The initial activities (5 min on line) of the catalysts pre-treated by H<sub>2</sub>S/H<sub>2</sub>O/N<sub>2</sub> were lower than those of untreated catalysts. After pre-treatment with H<sub>2</sub>S/H<sub>2</sub>O/N<sub>2</sub>, the 10%Y<sub>2</sub>O<sub>3</sub>/Al<sub>2</sub>O<sub>3</sub> catalyst shows the highest activities both in the initial reaction stage (5 min on line) and after 7.5 h on line. After 7.5 h on line, the activity follows the trend 10%Y<sub>2</sub>O<sub>3</sub>/Al<sub>2</sub>O<sub>3</sub> >  $\gamma$ -Al<sub>2</sub>O<sub>3</sub> > 10%Gd<sub>2</sub>O<sub>3</sub>/Al<sub>2</sub>O<sub>3</sub> > 10%Nd<sub>2</sub>O<sub>3</sub>/Al<sub>2</sub>O<sub>3</sub> > 10%La<sub>2</sub>O<sub>3</sub>/Al<sub>2</sub>O<sub>3</sub> while the initial activity (5 min on line) decreases in the order 10%Y<sub>2</sub>O<sub>3</sub>/Al<sub>2</sub>O<sub>3</sub> > 10%Gd<sub>2</sub>O<sub>3</sub>/Al<sub>2</sub>O<sub>3</sub> >  $\gamma$ -Al<sub>2</sub>O<sub>3</sub> > 10%Nd<sub>2</sub>O<sub>3</sub>/Al<sub>2</sub>O<sub>3</sub>  $\approx$  10%La<sub>2</sub>O<sub>3</sub>/Al<sub>2</sub>O<sub>3</sub>. These studies show that the deactivation observed with these catalysts is due to

**Table 5** Comparison of catalytic activity of COS hydrolysis over  $\gamma$ -Al<sub>2</sub>O<sub>3</sub> and 10% rare earth metal oxide promoted alumina catalysts pre-treated by H<sub>2</sub>S/H<sub>2</sub>O/N<sub>2</sub>. Conditions: catalyst: 10 mg diluted by 500 mg silicon carbide; 0.5%COS/N<sub>2</sub>: 58 ml min<sup>-1</sup>; N<sub>2</sub>: 180 ml min<sup>-1</sup>; H<sub>2</sub>O: 4559 ppm; reaction temperature: 150 °C

Catalyst	Conversion (%)	
	5 min time-on-line	7.5 h time-on-line
Al <sub>2</sub> O <sub>3</sub>	36	30
10%Y <sub>2</sub> O <sub>3</sub> /Al <sub>2</sub> O <sub>3</sub>	61	32
10%La <sub>2</sub> O <sub>3</sub> /Al <sub>2</sub> O <sub>3</sub>	26	13
10%Nd <sub>2</sub> O <sub>3</sub> /Al <sub>2</sub> O <sub>3</sub>	29	16
10%Gd <sub>2</sub> O <sub>3</sub> /Al <sub>2</sub> O <sub>3</sub>	49	23

exposure to H<sub>2</sub>S, and possibly due to H<sub>2</sub>O to a lesser extent. The experimental approach has used a pre-treatment stream containing both H<sub>2</sub>S and H<sub>2</sub>O so that it is representative of the conditions that the catalyst is exposed to during COS hydrolysis. Water is always present under conditions when the COS hydrolysis reaction is employed, and the simultaneous presence of H<sub>2</sub>S and H<sub>2</sub>O results in competitive adsorption leading to a more representatively treated surface compared to treatment with H<sub>2</sub>S and H<sub>2</sub>O alone.

In COS hydrolysis, both alumina and promoted alumina catalysts deactivated with increasing time on line, particularly in the initial stage of the reaction. The investigation of 10%Y<sub>2</sub>O<sub>3</sub>/Al<sub>2</sub>O<sub>3</sub> catalyst shows that after *ca.* 29 h on line the number of basic sites on the used catalyst dropped by *ca.* 40% compared to the fresh catalyst. This result strongly suggests that the deactivation is related to the decrease in the number of basic sites. In the COS hydrolysis reaction both COS (reactant) and H<sub>2</sub>S (product) are acidic compounds and consequently a strong interaction between these acidic molecules and the surface basic sites on the catalysts can be expected. Sulfide formation is readily feasible under the reaction conditions, for example Y<sub>2</sub>O<sub>3</sub> + H<sub>2</sub>S → Y<sub>2</sub>S<sub>3</sub> + H<sub>2</sub>O. The formation of rare earth metal sulfide reduces the number of basic sites, therefore reducing the catalyst activity. It is also possible that H<sub>2</sub>O and CO<sub>2</sub> are potential species to deactivate the catalysts. Indeed, the CO<sub>2</sub> chemisorption studies indicate that adsorption to the catalyst surface is readily possible. However, the TPD studies are carried out using CO<sub>2</sub> alone and there is no competitive adsorption, which would be prevalent under reaction conditions. In previous studies of alumina catalysts kinetic investigations changing the partial pressures of H<sub>2</sub>O and CO<sub>2</sub> have shown that whilst both species inhibit the rate of COS hydrolysis, at higher temperatures they did not significantly affect deactivation.<sup>15</sup> Hence, we consider that H<sub>2</sub>S is the component in the reaction mixture that is mainly responsible for catalyst deactivation.

The La<sub>2</sub>O<sub>3</sub>/Al<sub>2</sub>O<sub>3</sub> catalyst, having the strongest basic sites on the basis of the CO<sub>2</sub> TPD experiments (Fig. 2), has the strongest affinity for the formation of La<sub>2</sub>S<sub>3</sub>. This explains why the La<sub>2</sub>O<sub>3</sub>/Al<sub>2</sub>O<sub>3</sub> catalyst deactivates rapidly, although it is possible that only a surface sulfide is formed rather than a bulk sulfide. The combination of COS conversion with the H<sub>2</sub>S selectivity data and the effects of H<sub>2</sub>S pre-treatment shows that a highly active catalyst also has a high H<sub>2</sub>S selectivity and *vice versa*. The high activity catalysts are also more resistant to pre-treatment with H<sub>2</sub>S. These results suggest that the lower activity may be due to more S species deposited on or even reacted with the catalyst resulting in the blocking of the active sites and/or the formation of an inactive phase. Therefore, it is apparent that the preparation of an improved catalyst by the incorporation of rare earth metal oxides to introduce more basic sites is a balance between the promotion of basic sites to enhance activity, whilst the introduction of too many strong basic sites enhances deactivation.

Amongst the 10% rare earth metal oxide promoted alumina catalysts, Y<sub>2</sub>O<sub>3</sub> showed the most promising promotion effect (Fig. 3 and Table 3). Hence in our subsequent experiments we have concentrated on the study of Y<sub>2</sub>O<sub>3</sub> promoted alumina catalysts using different preparation procedures. A series of Y<sub>2</sub>O<sub>3</sub>/Al<sub>2</sub>O<sub>3</sub> (0, 10, 20 and 30%Y<sub>2</sub>O<sub>3</sub>) catalysts were prepared by

using the incipient wetness technique and tested for COS hydrolysis at 150 °C (Fig. 5). Initially the 10 and 20%Y<sub>2</sub>O<sub>3</sub>/Al<sub>2</sub>O<sub>3</sub> catalysts have similar activity to  $\gamma$ -Al<sub>2</sub>O<sub>3</sub> whilst the 30%Y<sub>2</sub>O<sub>3</sub>/Al<sub>2</sub>O<sub>3</sub> catalyst has lower activity than  $\gamma$ -Al<sub>2</sub>O<sub>3</sub>. However, the 10, 20%Y<sub>2</sub>O<sub>3</sub>/Al<sub>2</sub>O<sub>3</sub> and  $\gamma$ -Al<sub>2</sub>O<sub>3</sub> catalysts deactivated rapidly with increasing time on line, particularly in the initial stage of the reaction, whilst 30%Y<sub>2</sub>O<sub>3</sub>/Al<sub>2</sub>O<sub>3</sub> deactivated slowly. Time-on-line studies up to 40 h showed that the rate of deactivation after 30 h was not significant, and relatively stable activity was observed. After *ca.* 35 h on line, the activity follows the decreasing order of 30%Y<sub>2</sub>O<sub>3</sub>/Al<sub>2</sub>O<sub>3</sub> > 20%Y<sub>2</sub>O<sub>3</sub>/Al<sub>2</sub>O<sub>3</sub> >  $\gamma$ -Al<sub>2</sub>O<sub>3</sub> > 10%Y<sub>2</sub>O<sub>3</sub>/Al<sub>2</sub>O<sub>3</sub>.

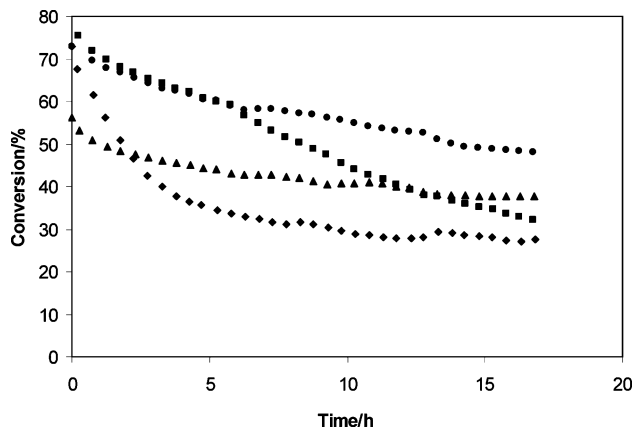


**Fig. 5** COS hydrolysis over Y<sub>2</sub>O<sub>3</sub>/Al<sub>2</sub>O<sub>3</sub> catalysts prepared by incipient wetness method: Key (■) Al<sub>2</sub>O<sub>3</sub>, (◆) 10%Y<sub>2</sub>O<sub>3</sub>/Al<sub>2</sub>O<sub>3</sub>, (▲) 20%Y<sub>2</sub>O<sub>3</sub>/Al<sub>2</sub>O<sub>3</sub>, (●) 30%Y<sub>2</sub>O<sub>3</sub>/Al<sub>2</sub>O<sub>3</sub>; Conditions: catalyst: 10 mg diluted by 500 mg silicon carbide; 0.5%COS/N<sub>2</sub>: 58 ml min<sup>-1</sup>; N<sub>2</sub>: 180 ml min<sup>-1</sup>; H<sub>2</sub>O: 4559 ppm; reaction temperature: 150 °C.

The coprecipitation method was used to prepare 10 and 30%Y<sub>2</sub>O<sub>3</sub>/Al<sub>2</sub>O<sub>3</sub> catalysts. The catalytic testing results for COS hydrolysis at 150 °C are shown in Fig. 6. The results show that the coprecipitated catalysts deactivate more slowly than the catalysts prepared by the incipient wetness method, and after *ca.* 6 h on line, the activity follows 30%Y<sub>2</sub>O<sub>3</sub>/Al<sub>2</sub>O<sub>3</sub> > 10%Y<sub>2</sub>O<sub>3</sub>/Al<sub>2</sub>O<sub>3</sub> >  $\gamma$ -Al<sub>2</sub>O<sub>3</sub>. However, these catalysts were less

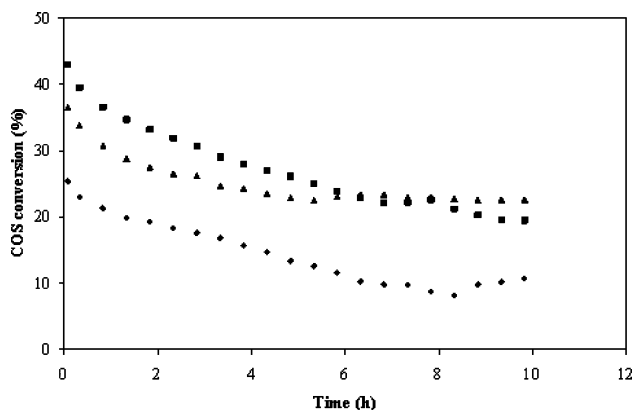


**Fig. 6** COS hydrolysis over Y<sub>2</sub>O<sub>3</sub>/Al<sub>2</sub>O<sub>3</sub> catalysts prepared by coprecipitation method: Key (◆) Al<sub>2</sub>O<sub>3</sub>, (■) 10%Y<sub>2</sub>O<sub>3</sub>/Al<sub>2</sub>O<sub>3</sub>, (▲) 20%Y<sub>2</sub>O<sub>3</sub>/Al<sub>2</sub>O<sub>3</sub>, (●) 30%Y<sub>2</sub>O<sub>3</sub>/Al<sub>2</sub>O<sub>3</sub>; Conditions: catalyst: 10 mg diluted by 500 mg silicon carbide; 0.5%COS/N<sub>2</sub>: 58 ml min<sup>-1</sup>; N<sub>2</sub>: 180 ml min<sup>-1</sup>; H<sub>2</sub>O: 4559 ppm; reaction temperature: 150 °C.

active than the catalysts prepared using the incipient wetness method (Fig. 5).

The 10 and 30%Y<sub>2</sub>O<sub>3</sub>/Al<sub>2</sub>O<sub>3</sub> catalysts were also prepared using deposition precipitation and the results for COS hydrolysis at 150 °C are shown in Fig. 7. The results show that during the initial stage of reaction the activity of the catalysts decreases rapidly and after *ca.* 28 h on line the activities of these three catalysts were very similar. As observed for the catalysts prepared by impregnation, the catalysts prepared by co-precipitation and precipitation deposition showed relatively stable time-on-line activity once 30 h was attained.

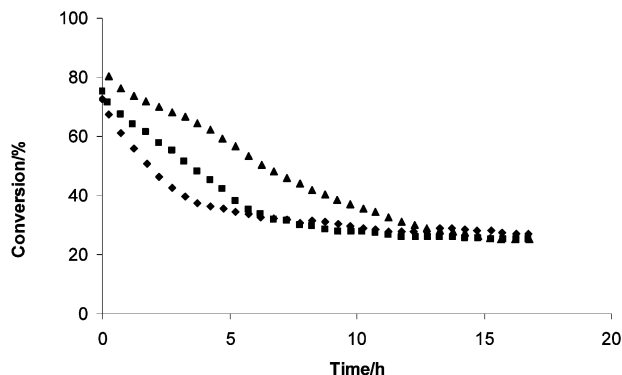


**Fig. 7** COS hydrolysis over Y<sub>2</sub>O<sub>3</sub>/Al<sub>2</sub>O<sub>3</sub> catalysts prepared by deposition precipitation method: Key (◆) Al<sub>2</sub>O<sub>3</sub>, (■) 10%Y<sub>2</sub>O<sub>3</sub>/Al<sub>2</sub>O<sub>3</sub>, (▲) 30% Y<sub>2</sub>O<sub>3</sub>/Al<sub>2</sub>O<sub>3</sub>; Conditions: catalyst: 10 mg diluted by 500 mg silicon carbide; 0.5% COS/N<sub>2</sub>: 58 ml min<sup>-1</sup>; N<sub>2</sub>: 180 ml min<sup>-1</sup>; H<sub>2</sub>O: 4559 ppm; reaction temperature: 150 °C.

Comparison of the different preparation methods indicates that the most active catalysts for COS hydrolysis are prepared using the relatively simple impregnation method by incipient wetness. Catalysts prepared using coprecipitation have lower activities but still demonstrate a promotional effect for the Y<sub>2</sub>O<sub>3</sub> dopant. Deposition precipitation leads to catalysts that deactivate rapidly and consequently it is not a preferred method of preparation. For the 30%Y<sub>2</sub>O<sub>3</sub>/Al<sub>2</sub>O<sub>3</sub> catalysts the materials prepared by the two precipitation methods have significantly higher surface areas compared with the material prepared by incipient wetness. When the effect of the surface area is taken into account the promotional effect of the addition of Y<sub>2</sub>O<sub>3</sub> using incipient wetness is very marked indeed.

## Conclusions

The hydrolysis of COS over an efficient catalyst is an important industrial process. It is not simply waste abatement as it provides a means to clean-up important chemical feedstocks that can subsequently be used for the production of chemicals and fuels by green processes. We have shown for the first time that an alumina catalyst for the COS hydrolysis reaction can be promoted by the addition of rare earth oxides and this is related to the enhanced basicity of the promoted catalyst. The addition of rare earth oxides, namely Y<sub>2</sub>O<sub>3</sub>, Gd<sub>2</sub>O<sub>3</sub>, Nd<sub>2</sub>O<sub>3</sub> and La<sub>2</sub>O<sub>3</sub>, increases the basicity of the material as shown by pulsed CO<sub>2</sub> chemisorption. CO<sub>2</sub> TPD shows that the La<sub>2</sub>O<sub>3</sub>-doped alumina has the strongest basic sites. The promoted catalysts are all effective for COS hydrolysis and the best results are

obtained with Y<sub>2</sub>O<sub>3</sub>-doped materials as these have the most pronounced promotion of activity that is sustained over the reaction timescale we have examined. The combination of the results for COS conversion with the H<sub>2</sub>S selectivity data and the effects of H<sub>2</sub>S pre-treatment shows that a highly active catalyst also has a high H<sub>2</sub>S selectivity and *vice versa*. The high activity catalysts are also more resistant to being pretreated with H<sub>2</sub>S. The La<sub>2</sub>O<sub>3</sub>-doped materials deactivate rapidly and have poor H<sub>2</sub>S selectivities and we propose that the higher basicity of this material leads to reaction with the acidic COS and H<sub>2</sub>S leading to the formation of the less basic surface sulfide. The most effective catalysts are prepared using the incipient wetness impregnation method. A balance between the increased basicity of the catalyst leading to promotion of COS hydrolysis, whilst not increasing the basicity to an extent that enhances deactivation is required for optimal catalyst performance.

## Experimental

### Catalyst preparation

Catalysts were prepared using impregnation with incipient wetness, coprecipitation and deposition precipitation methods. For incipient wetness impregnation,  $\gamma$ -Al<sub>2</sub>O<sub>3</sub> (Johnson Matthey, No. 55-1, BET surface area 300 m<sup>2</sup> g<sup>-1</sup>) was ground to 150–250  $\mu$ m particles and used as a catalyst support. The appropriate amount of metal nitrate was dissolved in distilled water (0.9 ml) to form an aqueous solution. The solution was added dropwise to  $\gamma$ -Al<sub>2</sub>O<sub>3</sub> particles (1 g) and the solid was shaken for 10 min to ensure uniform distribution of the solution. The wet solid was dried in air (90 °C, 16 h). TGA results showed that metal nitrate on alumina decomposed at around 450 °C. Consequently, the catalyst precursors were calcined at 500 °C for 3 h in static air, at the temperature ramp rate of 10 °C min<sup>-1</sup>, to obtain the final catalysts.

For catalysts prepared by coprecipitation the appropriate metal nitrate and Al(NO<sub>3</sub>)<sub>3</sub>·9H<sub>2</sub>O (20.9 g) were dissolved in distilled water (30 ml) at room temperature and the solution was stirred continuously. Aqueous ammonia (17.5%) was added dropwise to the solution until a pH of 7.0–8.0 was attained. The solution was kept stirring at room temperature for 2 h. The precipitate was recovered by filtration and dried in air (90 °C, 16 h). Calcination at 500 °C for 3 h in static air was used to obtain the final catalyst. The catalyst was crushed and sieved to a particle size of 150–250  $\mu$ m and used for catalytic tests.

A deposition–precipitation method was used to prepare 10 and 30%Y<sub>2</sub>O<sub>3</sub>/Al<sub>2</sub>O<sub>3</sub>. The procedure, using 10%Y<sub>2</sub>O<sub>3</sub>/Al<sub>2</sub>O<sub>3</sub> as an example, is as follows:  $\gamma$ -Al<sub>2</sub>O<sub>3</sub> (2 g, 150–250  $\mu$ m) was added to distilled water (100 ml) at room temperature and the solution was stirred continuously. Y(NO<sub>3</sub>)<sub>3</sub>·6H<sub>2</sub>O (0.6778 g) was dissolved in distilled water (10 ml). The Y(NO<sub>3</sub>)<sub>3</sub> solution was added to the  $\gamma$ -Al<sub>2</sub>O<sub>3</sub> solution and the temperature was controlled at 70 °C. Aqueous ammonia (17.5%) was added dropwise to the solution until a pH of 8.0 was attained. The suspension/solution was stirred at 70 °C for 1 h. The solid product was recovered by filtration and then dried in air (90 °C, 16 h). Calcination at 500 °C for 3 h in static air was used to obtain the final 10%Y<sub>2</sub>O<sub>3</sub>/Al<sub>2</sub>O<sub>3</sub> catalyst. The catalyst was crushed and sieved to a particle size



of 150–250  $\mu\text{m}$  and used for catalytic testing. A sample of  $\text{Y}_2\text{O}_3$  was also prepared by calcination of the nitrate (500  $^\circ\text{C}$ , 16 h).

### Catalyst characterisation

The catalysts were characterised using a number of techniques. The specific surface area was measured according to the BET method from the  $\text{N}_2$  isotherm adsorption at 77 K using a Gemini 2360 Surface Analyser (Micromeritics). Before measurement, the samples were treated in  $\text{N}_2$  (150  $^\circ\text{C}$ , 2 h). XRD patterns were obtained using an Enraf Nonius FR590 X-ray generator employing a  $\text{Cu K}\alpha$  source ( $\lambda = 1.5418 \text{ \AA}$ ), fitted with an Inel CPS 120 $^\circ$  position sensitive detector. The tube voltage was set to 40 kV and the current was set to 30 mA. Each sample was scanned for 30 min. Thermogravimetric analysis was obtained using a Perkin Elmer TGA 7 Thermo gravimetric Analyser.

Elemental analysis was carried out by X-ray fluorescence spectroscopy using a Philips MagiX PRO, a 4 kw Rh anode wavelength dispersive spectrometer. SEM images and EDX analysis were obtained by a FEI XL30 ESEM FEG scanning electron microscope. The temperature programmed reduction (TPR) profiles of promoted catalysts were obtained using an Autochem 2910 (Micromeritics) instrument fitted with a thermal conductivity detector. The catalyst sample (150 mg) was placed in the quartz reactor tube and heated from room temperature to 120  $^\circ\text{C}$  for 0.5 h under argon flow (20  $\text{ml min}^{-1}$ ) to remove adsorbed water from the catalyst, and then cooled to room temperature. The analysis was carried out from room temperature to 1050  $^\circ\text{C}$  (10  $^\circ\text{C min}^{-1}$ ) using 10% $\text{H}_2/\text{Ar}$  (50  $\text{ml min}^{-1}$ ) as reducing gas. The same instrument was used for pulsed  $\text{CO}_2$  chemisorption and temperature programmed desorption (TPD). In this case the sample (100 mg) was degassed at the calcination temperature prior to analysis. A fixed amount of carbon dioxide was injected to the sample using a pulse technique at ambient temperature. After the sample was fully saturated with  $\text{CO}_2$ , the sample was purged using argon to remove any physisorbed  $\text{CO}_2$ . Then, a TPD analysis was performed from ambient temperature to 500  $^\circ\text{C}$  using a temperature ramp rate of 40  $^\circ\text{C min}^{-1}$ .

### Determination of COS hydrolysis activity

COS hydrolysis was carried out using a standard laboratory microreactor with on line analysis of the products using gas chromatography fitted with a flame photometric detector, as described previously.<sup>15,21</sup> Conversion was calculated from the difference of COS concentration at reaction conditions with

that determined under conditions where there was no reaction of COS.  $\text{H}_2\text{S}$  selectivity was expressed as a percentage of the sulfur converted, and hence a selectivity  $<100\%$  denotes a sulfur balance of  $<100\%$ , indicating sulfur deposition on the catalyst.

### Acknowledgements

We thank Johnson Matthey for financial support.

### References

- 1 M. V. Twigg, *Catalyst Handbook*, Wolfe Publishers, Frome, 1989.
- 2 C. N. Satterfield, *Heterogeneous Catalysis in Industrial Practice*, McGraw-Hill, New York, 1991, p. 379.
- 3 R. Shafi and G. J. Hutchings, *Catal. Today*, 2000, **59**, 423.
- 4 E. Laperdix, I. Justin, G. Constatin, O. Saur, J. C. Lavalley, A. Aboulayt, J. L. Ray and C. Nèdez, *Appl. Catal. B*, 1998, **17**, 167.
- 5 E. S. Martin and M. L. Weaver, *Am. Ceram. Soc. Bull.*, 1993, **72**, 71.
- 6 J. L. Zotin and A. C. Faro, *Appl. Catal.*, 1991, **75**, 57.
- 7 A. Maglio and P. F. Schubert, *Oil Gas J.*, 1988, **12**, 85.
- 8 B. Nèdez and J.-L. Ray, *Catal. Today*, 1996, **27**, 49.
- 9 W. Przystajko, R. Fiedorowand and I. G. Dalla Lana, *Appl. Catal.*, 1985, **15**, 265.
- 10 J. Bachelier, A. Aboulyat, J. C. Lavalley, O. Legendre and F. Luck, *Catal. Today*, 1993, **17**, 55.
- 11 O. Saur, M. Bensitel, A. B. M. Saad, J. C. Lavalley, C. P. Tripp and B. A. Morrow, *J. Catal.*, 1986, **99**, 104.
- 12 T. T. Chuang, I. G. Dalla Lana and C. L. Lui, *J. Chem. Soc., Faraday Trans.*, 1973, **69**, 643.
- 13 B. P. Williams, N. C. Young, J. West, C. Rhodes and G. J. Hutchings, *Catal. Today*, 1999, **49**, 99.
- 14 C. Rhodes, S. A. Riddel, J. West, B. P. Williams and G. J. Hutchings, *Catal. Today*, 2000, **59**, 443.
- 15 J. West, B. P. Williams, N. C. Young, C. Rhodes and G. J. Hutchings, *Catal. Lett.*, 2001, **74**, 111.
- 16 Z. M. George, *J. Catal.*, 1974, **35**, 218.
- 17 R. Fiedorow, R. Léauté and I. G. Dalla Lana, *J. Catal.*, 1984, **85**, 339.
- 18 V. A. Ivanov, A. Piéplu, J. C. Lavalley and P. Nortier, *Appl. Catal. A*, 1995, **131**, 323.
- 19 S. Tan, C. Li, S. Liang and H. Guo, *Catal. Lett.*, 1991, **8**, 155.
- 20 J. Shangguan, C. H. Li and H. X. Guo, *J. Natural Gas Chem.*, 1998, **7**, 16.
- 21 J. West, B. P. Williams, N. Young, C. Rhodes and G. J. Hutchings, *Catal. Commun.*, 2001, **2**, 135.
- 22 B. Thomas, B. P. Williams, N. Young, C. Rhodes and G. J. Hutchings, *Catal. Lett.*, 2003, **86**, 201.
- 23 J. S. Church, N. W. Cant and D. L. Trimm, *App. Catal. A*, 1993, **101**, 105.
- 24 L. Zhao, X. Zheng and J. Fei, *Cuihua Xuebao*, 1996, **17**, 227.
- 25 J. Shen, R. D. Cortright, Y. Chen and J. A. Dumesic, *J. Phys. Chem.*, 1994, **98**, 8067.
- 26 T. Yamamoto, T. Tanaka, T. Matsuyama, T. Funabiki and S. Yoshida, *J. Phys. Chem. B*, 2001, **105**, 1908.

# A new separation method: combination of CO<sub>2</sub> and surfactant aqueous solutions

Xiaoying Feng, Jianling Zhang, Siqing Cheng, Chaoxing Zhang, Wei Li and Buxing Han\*

Received 13th September 2007, Accepted 22nd February 2008

First published as an Advance Article on the web 14th March 2008

DOI: 10.1039/b714164e

In this work, the effect of CO<sub>2</sub> on the cloud point temperature (*CPT*) of an aqueous solution of *p*-tert-octylphenoxy polyethylene (Triton X-100) was studied at different temperatures, pressures and surfactant concentrations. It was demonstrated that CO<sub>2</sub> could reduce the *CPT* of the micellar solutions considerably. On the basis of this finding, we proposed a new route to separate different substances from water by combination of Triton X-100 and CO<sub>2</sub>. It was discovered that phenol or vanadium ion in aqueous solutions could be separated efficiently from water by combination of CO<sub>2</sub> and Triton X-100. Our study also showed that the gold nanoparticles synthesized in Triton X-100 micellar solutions could be recovered using CO<sub>2</sub> while the surfactant remained in the solution. This is attractive because recovery of gold nanoparticles is very convenient. This separation method has some unusual advantages, such as high separation efficiency, simple post-treatment process, and lower separation temperature, which is especially advantageous when temperature-sensitive substances are involved.

## 1. Introduction

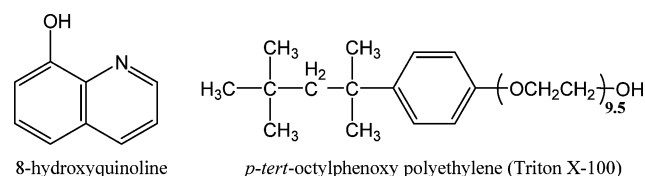
Micellar systems have been very attractive for many years due to their importance in both fundamental research and practical applications. Controlling the properties of micellar systems conveniently is of great importance.

It is well known that phase separation of nonionic surfactant aqueous solutions occurs when heated over the cloud point temperature (*CPT*). Additives, such as electrolytes, organics, can also be used to induce phase separation of micellar solutions. However, some undesired post-treatments are usually required to separate the additives from the micellar solutions or products, which make it difficult to reuse the micellar systems.<sup>1</sup>

CO<sub>2</sub> is widely used as an environmentally benign solvent. Recently, surfactant solutions related with CO<sub>2</sub> have been studied extensively. For example, many researchers have investigated microemulsions with CO<sub>2</sub> as continuous phase.<sup>2</sup> Zielinski *et al.*<sup>3</sup> studied properties of D<sub>2</sub>O/*n*-hexaethylene glycol monododecyl ether (C<sub>12</sub>E<sub>6</sub>)/CO<sub>2</sub> system, and found that CO<sub>2</sub> could reduce the *CPT* of the C<sub>12</sub>E<sub>6</sub>/D<sub>2</sub>O system considerably. Johnston and coworkers reported that addition of dense CO<sub>2</sub> to perfluoropolyether micelles in water could swell the micelles to form CO<sub>2</sub>-in-water microemulsions.<sup>4</sup> Jessop *et al.*<sup>5</sup> reported that long-chain alkyl amidine compounds could be transformed into charged surfactants by exposure to an atmosphere of CO<sub>2</sub>, thereby stabilizing water/organics emulsions. The emulsions could be broken after removing CO<sub>2</sub>. In our previous work, we studied the effect of CO<sub>2</sub> on the stability of reverse micelles in

organic solvents, and found that CO<sub>2</sub> could tune the properties of reverse micelles, which had potential applications in material processing, chemical reactions and protein extractions.<sup>6</sup>

Separation is crucial for many chemical processes, and development of new separation methods has been an interesting topic for many years.<sup>7</sup> In this work, we studied the effect of CO<sub>2</sub> on the *CPT* of the aqueous solution of *p*-tert-octylphenoxy polyethylene (Triton X-100, Scheme 1), which is a typical nonionic surfactant and widely used in industry and research.<sup>8</sup> It was demonstrated that CO<sub>2</sub> could reduce the *CPT* of the micellar solutions significantly. On the basis of this result, we proposed a new separation method by combination of CO<sub>2</sub> and the surfactant solution. It was discovered that phenol or vanadium-8-hydroxyquinoline (Scheme 1) complexes in water could be separated efficiently from the solutions by this method at suitable conditions; and gold nanoparticles synthesized in Triton X-100 micellar solutions could be recovered by adding CO<sub>2</sub> while the surfactant still remained in the solution. To the best of our knowledge, this is the first demonstration of application of CO<sub>2</sub> and surfactant aqueous solutions in separation. We believe that this new, simple, high efficient and clean separation method has wide potential applications.



**Scheme 1** Molecular structure of 8-hydroxyquinoline and Triton X-100.

Beijing National Laboratory for Molecular Sciences, Institute of Chemistry, Chinese Academy of Sciences, Beijing, 100080, China.  
E-mail: hanbx@iccas.ac.cn; Fax: +86-10-62562821;  
Tel: +86-10-62562821

## 2. Experimental

### Materials

Triton X-100 (AR grade), phenol (AR grade), aurichlorohydric acid (AR grade), potassium borohydride (AR grade) were provided by Beijing Chemical Reagent Factory. 8-Hydroxyquinoline (AR grade) was produced by Shantou Xilong Chemical Factory. CO<sub>2</sub> (99.995% purity) was supplied by Beijing Analytical Instrument Factory. The standard vanadium ion solution (100 µg mL<sup>-1</sup>) was purchased from National Research Center for Standard Reference Materials. It was prepared by adding 0.2296 g ammonium metavanadate (NH<sub>4</sub>VO<sub>3</sub>) and 15 mL nitric acid (1.42 g mL<sup>-1</sup>) into 500 mL pure water. The solution was then diluted to 100 mg L<sup>-1</sup>. All the reagents were used without further purification. Double distilled water was used throughout the experiments.

### Detection of the cloud point of Triton X-100 aqueous solution

The *CPT* of Triton X-100 aqueous solutions under compressed CO<sub>2</sub> was measured by visual observation. The high pressure view cell (45 mL) used was similar to that used in our previous work.<sup>6a</sup> In a typical experiment, the air in the view cell was replaced by CO<sub>2</sub>. 20 mL aqueous solution of Triton X-100 was loaded into the high-pressure view cell. The cell was placed into the constant temperature water bath. After thermal equilibrium had been reached, CO<sub>2</sub> was charged into the cell slowly by a syringe pump (DB-80) until the clear and transparent liquid solution became turbid and milky, and the pressure was recorded. It was estimated that the uncertainty of cloud point pressure (*CPP*) was ±0.03 MPa.

### Separation of vanadium ion in water

The high-pressure view cell used above was also utilized to study separation of V ion. In the experiment, 8-hydroxyquinoline (8-HQ) as the chelating agent was first loaded into the Triton X-100 aqueous solution of vanadium (V) ion to form vanadium–8-hydroxyquinoline (V–8-HQ) complexes. The initial concentrations of Triton X-100, V ion and 8-HQ in the solution were 5 wt%,  $2.00 \times 10^{-5}$  mol L<sup>-1</sup> and  $10^{-3}$  mol L<sup>-1</sup>, respectively. 20 mL of the solution was loaded into the high-pressure view cell, which was placed in a constant temperature water bath of 318.15 K. CO<sub>2</sub> was charged into the system to desired pressure, and the stirrer was started. After stirring for 30 min, the stirrer was stopped and the system was kept still for 12 h for phase separation. The micellar solution was separated into two phases and V–8-HQ complexes were precipitated together with Triton X-100. The volumes of the upper aqueous phase and the lower surfactant-rich phase were known from the graduation on the view cell, which was pre-calibrated with water. The sample of the upper aqueous phase was taken through the sample valve, and the pressure remained constant during sampling by charging CO<sub>2</sub> into the view cell continuously. The concentration of V ions in the upper aqueous phase was determined by inductively coupled plasma atomic emission spectrometer (ICP-AES, VISTA-MPX, VARIAN Corp., USA), which is the one of the most commonly utilized methods for analysis of V and some other metals. The procedure of separating V ions from the

micellar solutions by heating was similar to that using CO<sub>2</sub>. The main difference was that no CO<sub>2</sub> was loaded and the temperature of the water bath was much higher.

### Separation of phenol from Triton X-100 aqueous solutions

Separation of phenol from the Triton X-100 micellar solutions using CO<sub>2</sub> was also studied with the high-pressure view cell utilized to study the separation of V ion. 20 mL Triton X-100 aqueous solution of known phenol concentration was loaded into the view cell, which was placed in a constant temperature water bath (313.15 K, 318.15 K, 323.15 K and 328.15 K). CO<sub>2</sub> was charged into the system to desired pressure, and the stirrer was started. After 30 min the stirrer was stopped and the system was kept still for 12 h for phase separation. The volumes of the aqueous phase and Triton X-100-rich phase were known from the graduation on the view cell. Samples of the upper aqueous phase were taken through the sample valve, and the pressure remained constant during sampling by charging CO<sub>2</sub> continuously. The samples were analyzed by UV-vis spectrometer (TU 190, Beijing Instrument Company). The concentration of the samples was calculated with the absorption at 276 nm. The procedure of separating phenol from the micellar solutions by heating was similar to that using CO<sub>2</sub>. The main difference was that no CO<sub>2</sub> was loaded and the temperature of the water bath was much higher (333.15 K, 338.15 K, 343.15 K, 348.15 K, 353.15 K).

### Separation of gold nanoparticles from Triton X-100 micellar solution

The high pressure view cell used above was also used to study the recovery of gold nanoparticles from the Triton X-100 aqueous solutions. In the experiment, 10 mL 1 wt% Triton X-100 solution with  $10^{-4}$  mol L<sup>-1</sup> HAuCl<sub>4</sub> and 10 mL 1 wt% Triton X-100 solutions with  $10^{-4}$  mol L<sup>-1</sup> KBH<sub>4</sub> were mixed in the view cell, and gold nanoparticles were therein formed. The view cell was placed in a water bath of 313.15 K. After 30 min, CO<sub>2</sub> was charged into the cell to suitable pressure and the solution was stirred for 1 h. The stirrer was stopped to precipitate the gold nanoparticles. The CO<sub>2</sub> in the surfactant solution was released after 40 min. The nanoparticles were collected and washed with water and alcohol, and were then characterized by transmission electron microscopy (TEM, JEOL JEM-2010) operating at 200 kV. X-ray photoelectron spectroscopy (XPS) spectrum of the nanoparticles was collected by means of an ESCALab220i-XL spectrometer at a pressure of about  $3 \times 10^{-9}$  mbar using Al K $\alpha$  as the exciting source ( $h\nu = 1486.6$  eV) and operating at 15 kV and 20 mA.

The UV-vis spectrometer (TU 1901) and the high pressure UV-Vis sample cell used previously<sup>6b</sup> were utilized to determine the surface plasmon absorption of gold nanoparticles in Triton X-100 aqueous solutions. In the experiment, the Triton X-100 aqueous solution with gold nanoparticles was first prepared at the same condition described above. Desired amount of solution was charged into sample cell which was maintained at 313.15 K. CO<sub>2</sub> was then charged into the sample cell to the desired pressure. The solution was stirred for 1 h, and was kept unstirred for 40 min to allow gold nanoparticles to precipitate. The UV-vis absorbance was then recorded.

### 3. Results and discussion

#### Cloud point of Triton X-100 aqueous solution

Fig. 1 displays the relationship between the *CPT* of Triton X-100 aqueous solutions and  $\text{CO}_2$  pressure. The concentrations of the surfactant were 0.20 wt%, 1.0 wt%, 2.0 wt% and 8.0 wt%, respectively, which were all above critical micelle concentration (*cmc*) of Triton X-100.<sup>9</sup> It can be seen that the *CPT* decreases with increasing pressure at all concentrations. In other words,  $\text{CO}_2$  can induce phase separation of the surfactant solution. However, our experiments showed that as the temperature was lower than 310 K, the surfactant could not be precipitated up to 17 MPa. In this work, we define the minimum pressure required to induce the phase separation as cloud point pressure (*CPP*). The surfactant solution is separated into aqueous phase and surfactant-rich phase as the pressure is above the *CPP*. At the *CPP*, the solution became clear again as the pressure was reduced slightly. In other words,  $\text{CO}_2$  could be used to switch the phase separation of the solution repeatedly by controlling the pressure of  $\text{CO}_2$  at a fixed temperature.

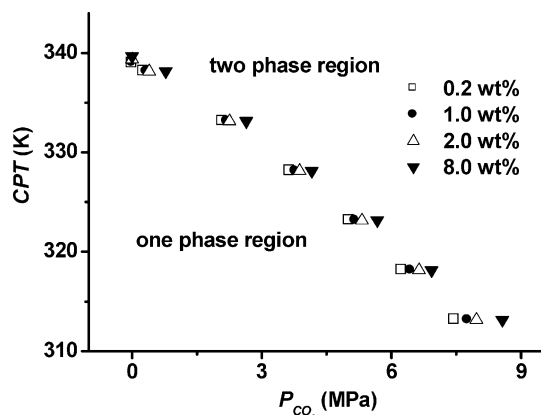


Fig. 1 The effect of  $\text{CO}_2$  pressure on the *CPT* of Triton X-100 aqueous solutions of different concentrations.

#### Separation of vanadium ion in water

Removal or pre-concentration of heavy metal ions in water are often required in industry and analytical processes,<sup>10</sup> and extraction based on phase separation of micellar solutions is one of the effective methods with many advantages, such as high extraction and pre-concentration factors, operational safety, lower toxicity for analysts.<sup>11</sup> The methodology used is based on the principle that metal complexes in nonionic surfactant solutions can be extracted into the surfactant-rich phase above *CPT*. This method has been utilized to extract vanadium ion in aqueous solutions, and 8-hydroxyquinoline has been used as the chelating agent.<sup>12</sup> To induce the phase separation of the surfactant solution is a crucial step in this method. As an example, we studied the separation of V ion in water by  $\text{CO}_2$  using 8-hydroxyquinoline as the chelating agent. The micellar solution was separated into two phases and the V–8-hydroxyquinoline complexes were precipitated together with Triton X-100. Here, extraction efficiency (*E*) is defined as the ratio of the amount of V ion extracted into the surfactant-rich phase to the total amount of V ion. The concentration of V ions

in aqueous phase was determined by ICP-AES method, which is the one of the most commonly used methods for analysis of V and some other metals. The *E* can be easily calculated from the volume of the upper aqueous phase, the concentration of V in the upper phase, and total amount of V loaded in the system. Fig. 2a illustrates the effect of  $\text{CO}_2$  pressure on the separation efficiency *E* of V ion at 318.15 K. It is estimated that the uncertainty of data is 1.0%. It can be seen from Fig. 2a that over an extraction efficiency of 0.99 for V ions extracted into the surfactant-rich phase could be obtained at 11.0 MPa. In addition, Figs. 2b and 2c show the photographs of the surfactant solution with 8-hydroxyquinoline complexes before and after addition of  $\text{CO}_2$ . It is evident that the micellar system was separated into two phases. The aqueous phase was almost colorless while the Triton X-100-rich phase was much darker than the original solution, demonstrating that 8-hydroxyquinoline complexes were extracted into the surfactant-rich phase by addition of  $\text{CO}_2$ .

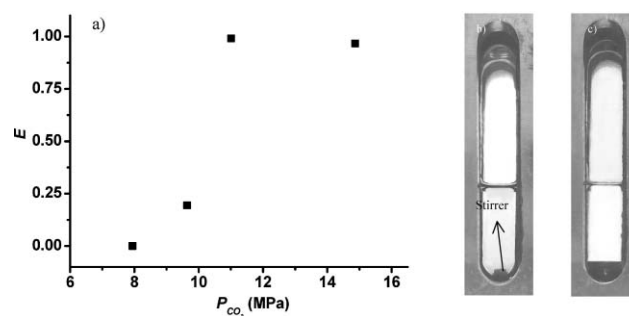


Fig. 2 (a) Dependence of separation efficiency of V ion on  $\text{CO}_2$  pressure at 318.15 K ([Triton X-100] = 5 wt%); (b) Photograph of V–8-HQ complexes in Triton X-100 aqueous solution without  $\text{CO}_2$ ; (c) Photograph of V–8-HQ complexes in Triton X-100 aqueous system after phase separation at 11.01 MPa (upper,  $\text{CO}_2$ ; middle, aqueous phase; bottom, surfactant-rich phase with V–8-HQ complexes).

For comparison, we also studied the separation of V ion by conventional method, *i.e.* the phase separation of the V–8-HQ micellar solution was induced by heating the solution to higher temperature. At 343.15 K and 353.15 K, the *E* determined in this work was 0.78 and 0.83, respectively, which is in agreement with the results reported by other authors determined using the same method.<sup>12b</sup> This indicates that the  $\text{CO}_2$ -induced separation method proposed in this work is more efficient than conventional method.

#### Separation of phenol from water

Phenol is widely used in different fields, such as agriculture, food industry and biology.<sup>13</sup> Due to its high toxicity and corrosiveness, severe environmental problems are often caused during its utilization processes.<sup>14</sup> Conversion or removal of this compound from water as well as the determination of its concentration are required in many processes.<sup>15</sup> It has been shown that phenol in the micellar solution can be precipitated together with surfactants at suitable conditions, which has been utilized to separate phenol from aqueous solutions or to pre-concentrate phenol.<sup>16</sup> Precipitating the surfactants from the solution is also one of the key steps in this method, and this



is usually achieved by altering the temperature and/or with the assistance of additives. To verify the versatility of the method of this work, separation of phenol from water using Triton X-100 and CO<sub>2</sub> was also studied. The initial concentration of phenol was 0.01 wt% and that of Triton X-100 was 1 wt% and 5 wt%, respectively. The experiments were performed at different temperatures and CO<sub>2</sub> pressures. As CO<sub>2</sub> was added into the system to suitable pressure, the solution was separated into two phases and most of the phenol in the solution was precipitated together with Triton X-100. Fig. 3a to 3d show the dependence

of the extraction efficiency ( $E$ ) on CO<sub>2</sub> pressure at 313.15 K, 318.15 K, 323.15 K and 328.15 K, respectively. It is estimated that the uncertainty of  $E$  data is 1%.  $E$  increased sharply at lower pressure region and increased slightly at higher pressure range. The concentration of Triton X-100 also affected  $E$  obviously. Generally,  $E$  with 1 wt% Triton X-100 was larger than that with 5 wt% of the surfactant in the lower pressure range. While at higher pressures, the  $E$  with 5 wt% Triton X-100 became larger. At all the temperatures studied  $E$  could exceed 0.96 at suitable conditions.

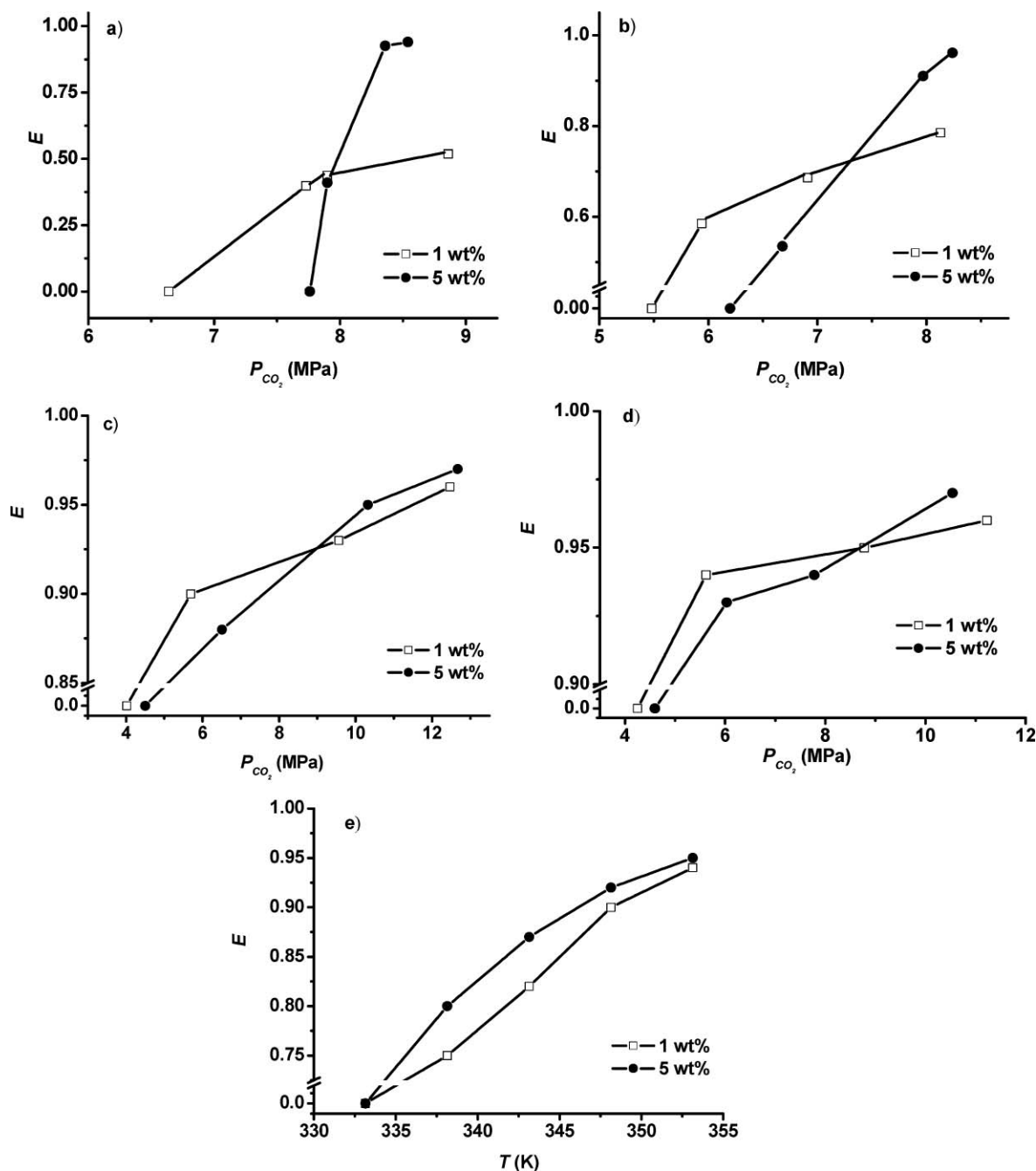


**Fig. 3** The effect of CO<sub>2</sub> pressure on the separation efficiency of phenol with 1 wt% and 5 wt% Triton X-100 aqueous solutions at (a) 313.15 K, (b) 318.15 K, (c) 323.15 K and (d) 328.15 K. (e) is the separation efficiency of phenol with 1 wt% and 5 wt% Triton X-100 aqueous solutions at different temperatures without CO<sub>2</sub>.

We also determined  $E$  by conventional heating-induced separation method at 333.15 K, 338.15 K, 343.15 K, 348.15 K and 353.15 K and the results are shown in Fig. 3e. As expected,  $E$  increased with increasing temperature and reached 0.95 at 358.15 K, while 0.96 could be achieved by our method in this work even when the temperature was as low as 313.15 K. Haddou *et al.*<sup>16a</sup> also separated phenol from 10 wt% oxo- $C_{13}E_9$  aqueous solutions by adding sodium chloride, and  $E$  reached 0.95. Moreover, in our method,  $CO_2$  pressure was the only factor to be optimized, and  $CO_2$  was the only additive to control the phase separation, which simplified the post-treatment processes effectively.

### Separation of gold nanoparticles from Triton X-100 micellar solution

Triton X-100 micelles can act as template and stabilizer for the synthesis of gold nanoparticles.<sup>17</sup> In this work, we investigated the possibility of recovering gold nanoparticles from Triton X-100 micellar solution by  $CO_2$ . The gold nanoparticles were first synthesized in Triton X-100 micellar solution using  $HAuCl_4$  and  $KBH_4$ . The concentration of Triton X-100 was 0.2 wt%, and those of  $HAuCl_4$  and  $KBH_4$  were both  $10^{-4}$  mol  $L^{-1}$ . Fig. 4a illustrates the surface plasmon absorption of gold nanoparticles in the solution before and after the addition of  $CO_2$  of various pressures for 40 min. The maximum absorbance was at 527 nm,

indicating that the size of the nanoparticles prepared was around 10 nm.<sup>17</sup> The absorbance could keep constant for at least 7 days in the absence of  $CO_2$ . The absorbance of gold nanoparticles decreased with the increase of  $CO_2$  pressure, indicating the precipitation of the gold nanoparticles in the solution. As the pressure reached 4.10 MPa, most of the gold nanoparticles were precipitated (Fig. 4a).

Precipitation of the gold nanoparticles can also be observed clearly from the change of color of gold-containing Triton X-100 aqueous solution with and without  $CO_2$ . The purple color of the solution originated from the gold nanoparticles disappeared after their precipitation at 4.10 MPa, which showed that the gold nanoparticles began to precipitate at the pressure below the  $CPP$  of Triton X-100 at this temperature (7.46 MPa, shown in Fig. 1). And this also indicated that the gold nanoparticles could be precipitated completely, while the surfactant still remained in the aqueous solution. This is very attractive because both recovery of gold nanoparticles is convenient and little surfactant is lost. The collected gold nanoparticles were characterized by TEM. As shown in Fig. 4b, spherical nanoparticles with diameter of  $10 \pm 2$  nm were obtained. In addition, the gold nanoparticles recovered at 1.20 MPa were also characterized by TEM (Fig. 4c), which demonstrated that the size and shape were similar to those recovered at the higher pressure. The XPS spectrum of the products is given in Fig. 4d. The two peaks are

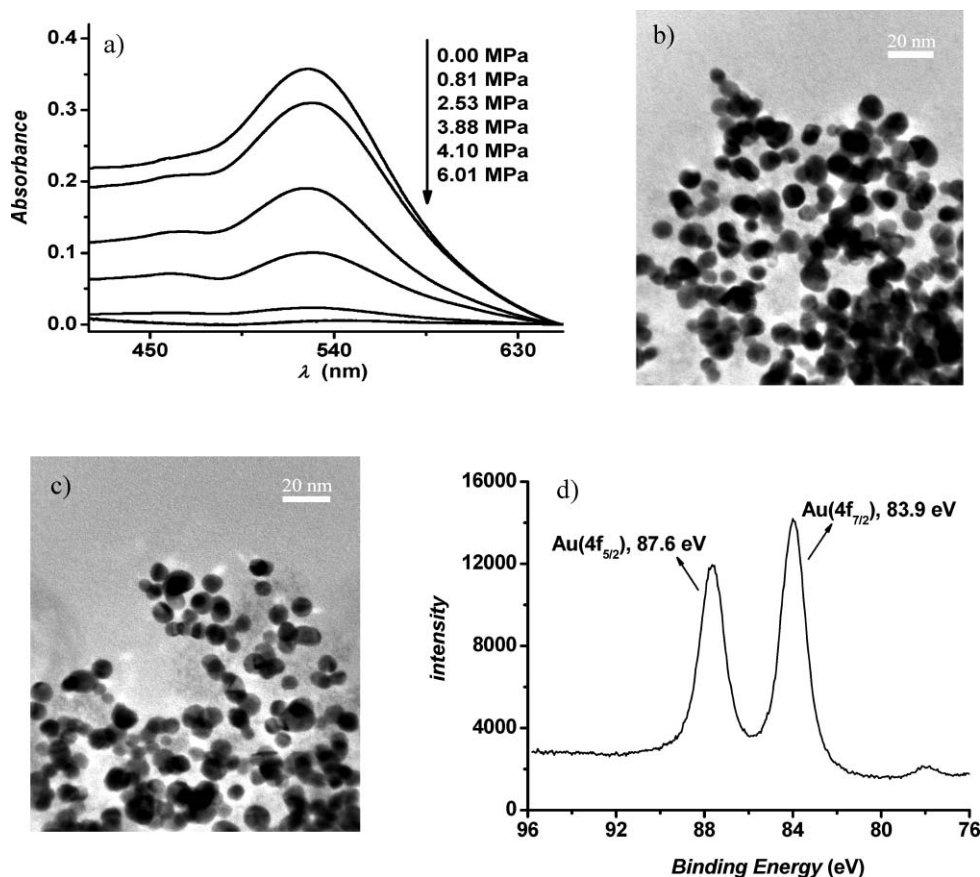


**Fig. 4** (a) UV-vis absorption spectra of gold nanoparticles in Triton X-100 micellar solution at different  $CO_2$  pressures; (b, c) TEM images of gold nanoparticles recovered from Triton X-100 micellar solution at 4.10 and 1.20 MPa, respectively. ([Triton X-100] = 0.2 wt%,  $T = 313.15$  K, precipitation time = 40 min); (d) XPS spectrum of gold nanoparticles recovered from Triton X-100 micellar solution at 313.15 K and 4.10 MPa.

at 83.9 eV (Au 4f<sub>7/2</sub>) and 87.6 eV (Au 4f<sub>5/2</sub>), respectively, which is consistent with standard XPS spectrum of pure gold (Au<sub>0</sub>).<sup>18</sup>

#### 4. Conclusion

The effect of CO<sub>2</sub> on the CPT of the aqueous solution of Triton X-100 as well as the separation of different substances from water by combination of the surfactant and CO<sub>2</sub> have been investigated. It is shown that CO<sub>2</sub> can reduce the CPT of the micellar solutions considerably. Phenol or vanadium ion in aqueous solutions can be separated efficiently from water by this method. Furthermore, gold nanoparticles synthesized in Triton X-100 micellar solutions can be recovered using CO<sub>2</sub> while the surfactant remains in the solution, which simplifies the recycling process of surfactant solutions. This separation method has some unusual advantages including: (1) the separation efficiency is very high and can be optimized by CO<sub>2</sub> pressure; (2) other additives are not required, which simplifies the post-treatment significantly; (3) the separation can be conducted at lower temperature, which is especially advantageous when temperature-sensitive substances are involved. This new, highly efficient and clean separation method has potential applications in a range of separation processes.

#### Acknowledgements

The authors are grateful to the National Natural Science Foundation of China (20633080).

#### References

- (a) M. de A. Bezerra, M. A. Z. Arruda and S. L. C. Ferreira, *Appl. Spectrosc. Rev.*, 2005, **40**, 269; (b) F. J. Ruiz, S. Rubio and D. Perez-Bendito, *Anal. Chem.*, 2006, **78**, 7229; (c) M. S. Alam, S. Kumar, A. Z. Naqvi and Kabir-ud-Din, *Colloid Surf. A*, 2006, **287**, 197; (d) W. L. Hinze and E. Pramauro, *Crit. Rev. Anal. Chem.*, 1993, **24**, 133.
- (a) T. A. Hoefling, R. M. Enick and E. J. Beckman, *J. Phys. Chem.*, 1991, **95**, 7127; (b) E. J. Beckman, *Science*, 1996, **271**, 613; (c) K. P. Johnston, K. L. Harrison, M. J. Clarke, S. M. Howdle, M. P. Heitz, F. V. Bright, C. Carlier and T. W. Randolph, *Science*, 1996, **271**, 624; (d) X. Fan, V. K. Potluri, M. C. McLeod, Y. Wang, J. Lui, R. M. Enick, A. D. Hamilton, C. B. Roberts, J. K. Johnston and E. J. Beckman, *J. Am. Chem. Soc.*, 2005, **127**, 11754; (e) J. Eastoe, S. Gold, S. Rogers, P. Wyatt, D. C. Steytler, A. Gurgel, R. K. Heenan, X. Fan, E. J. Beckman and R. M. Enick, *Angew. Chem., Int. Ed.*, 2006, **45**, 3675; (f) M. Ji, X. Y. Chen, C. M. Wai and J. L. Fulton, *J. Am. Chem. Soc.*, 1999, **121**, 2631.
- R. G. Zielinski, E. W. Kaler and M. E. Paulaitis, *J. Phys. Chem.*, 1995, **99**, 10354.
- C. T. Lee, Jr., W. Ryoo, P. G. Smith, Jr., J. Arellano, D. R. Mitchell, R. J. Lagow, S. E. Webber and K. P. Johnston, *J. Am. Chem. Soc.*, 2003, **125**, 3181.
- Y. X. Liu, P. G. Jessop, M. Cuningham, C. A. Eckert and C. L. Liotta, *Science*, 2006, **313**, 958.
- (a) D. Shen, R. Zhang, B. Han, Y. Dong, W. Wu, J. Zhang, J. Li, T. Jiang and Z. Liu, *Chem.–Eur. J.*, 2004, **10**, 5123; (b) X. Y. Feng, J. L. Zhang, J. Chen, B. X. Han and D. Shen, *Chem.–Eur. J.*, 2006, **12**, 2087.
- A. M. Scurto, S. N. V. K. Aki and J. F. Brennecke, *J. Am. Chem. Soc.*, 2002, **124**, 10276.
- T. F. Tadros, in *Applied Surfactants: Principles and Applications*, Wiley-VCH, Weinheim, 2005, pp. 115–116.
- L. Hsiao, H. N. Dunning and P. B. Lorenz, *J. Phys. Chem.*, 1956, **60**, 657.
- (a) X. Long, M. Miro and E. H. Hansen, *Anal. Chem.*, 2005, **77**, 6032; (b) V. A. Lemos, P. X. Baliza, J. S. Santos, L. S. Nunes, A. A. de Jesus and M. E. Rocha, *Talanta*, 2005, **66**, 174; (c) R. S. Praveen, S. Daniel and T. P. Rao, *Talanta*, 2005, **66**, 513.
- M. A. Korn, J. B. de Andrade, D. S. de Jesus, V. A. Lemos, M. L. S. F. Bandeira, W. N. L. dos Santos, M. A. Bezerra, F. A. C. Amorim, A. S. Souza and S. L. C. Ferreira, *Talanta*, 2006, **69**, 16.
- (a) E. K. Paleologos, M. A. Koupparis, M. I. Karayannis and P. G. Veltsistas, *Anal. Chem.*, 2001, **73**, 4428; (b) A. Ohashi, H. Ito, C. Kanai, H. Imura and K. Ohashi, *Talanta*, 2005, **65**, 525.
- (a) P. Chomeczynski and N. Sacchi, *Nat. Protoc.*, 2006, **1**, 581; (b) P. J. Tsai and C. H. She, *J. Agric. Food Chem.*, 2006, **54**, 8491.
- S. Molloy, *Nat. Rev. Microbiol.*, 2006, **4**, 880.
- S. Niwa, M. Eswaramoorthy, J. Nair, A. Raj, N. Itoh, H. Shoji, T. Namba and F. Mizukami, *Science*, 2002, **295**, 105.
- (a) B. Haddou, J. P. Canselier and C. Gourdon, *Sep. Purif. Technol.*, 2006, **50**, 114; (b) K. Materna, E. Goralska, A. Sobczynska and J. Szymanowski, *Green Chem.*, 2004, **6**, 176; (c) R. P. Frankewich and W. L. Hinze, *Anal. Chem.*, 1994, **66**, 944.
- M. Antonietti, E. Wenz, L. Bronstein and M. Seregina, *Adv. Mater.*, 1995, **7**, 1000.
- B. V. Crist in *Handbooks of Monochromatic XPS Spectra*, XPS International, LLC, Mountain View, California, USA, Demo Version, 1999, vol. 1, pp. 17.

# Imidazolium based ionic liquids in soils: effects of the side chain length on wheat (*Triticum aestivum*) and cress (*Lepidium sativum*) as affected by different clays and organic matter†

Marianne Matzke,<sup>\*a</sup> Stefan Stolte,<sup>b</sup> Jürgen Arning,<sup>b</sup> Ute Uebers<sup>a</sup> and Juliane Filser<sup>a</sup>

Received 19th November 2007, Accepted 30th January 2008

First published as an Advance Article on the web 19th March 2008

DOI: 10.1039/b717811e

This study provides data on the behaviour and toxicity of selected imidazolium based ionic liquids in the terrestrial environment with the aim to contribute to a prospective hazard assessment. Using the plant growth inhibition assay with wheat (*Triticum aestivum*) and cress (*Lepidium sativum*) we investigated the influence of two different clay minerals (kaolinite and smectite) in varying concentrations and clay mineral mixtures as well as the influence of organic matter in varying concentrations on the toxicity of three imidazolium based ionic liquids differing in the alkyl side chain length. The obtained results were compared to the German standard soil Lufa 2.2. Overall the influence of the 2:1 layer mineral smectite on toxicity was stronger than for the 1:1 layer mineral kaolinite resulting in lower toxicities when smectite was present. Comparable results were achieved in the tests with different clay mineral mixtures. The influence of the clay minerals was substance concentration dependent and the side chain effect could not consistently be confirmed for the different soil mixtures. The 1:1 clay mineral kaolinite caused in some cases an increase in toxicity. The obtained results for the influence of organic matter on the toxicity proved to be much more consistent than for the clay minerals: here an increase in organic matter concentration always resulted in a decrease of the toxicity. Differences in plant species sensitivity could be shown, but not in a consistent manner. A site specific hazard assessment of ionic liquids should therefore take into account organic matter content, quantity and especially quality of clay minerals.

## Introduction

Ionic liquids are a fast-growing substance class and discussed mainly as substitutes for conventional solvents. They are low melting salts (melting point below 100 °C, mostly below room temperature) with no measurable vapour pressure, typically consisting of nitrogen-containing organic cations such as 1-alkyl-3-methylimidazolium and inorganic or organic anions, commonly containing fluorine *e.g.* tetrafluoroborate (BF<sub>4</sub><sup>-</sup>). Because of their missing vapour pressure they are very attractive for users in terms of their reduced air emission and their non-flammability resulting in an improved operational safety for man compared to conventional solvents. Ionic liquids are discussed for manifold applications *e.g.* in the fields of synthesis,<sup>1,2</sup> electrochemistry<sup>3</sup> and (bio)catalysis.<sup>4,5</sup>

The heterogeneity within the pool of ionic liquids provides an almost unlimited number of compounds complicating a hazard assessment. To reduce this elusive number of possible ionic

liquids the substances are systematically subdivided into the structural elements head group, side chain and anion and are analysed according to the “testkit concept”.<sup>6–8</sup>

Previous studies mainly focused on ecotoxicity of ionic liquids in the aquatic environment,<sup>9–20</sup> but data sets which are needed for a profound and prospective hazard assessment for the terrestrial environment, *e.g.* effects on plants and soil animals<sup>14,17,21–23</sup> or studies dealing with biodegradability,<sup>13,20,24–28</sup> are very limited or still missing so far. For the aquatic as well as the terrestrial environment a side chain effect was found in previous studies:<sup>12,13,15,17–20,29</sup> an increase of the alkyl side chain length results in an increase in toxicity. A previous study from our group<sup>17</sup> found also a side chain effect of two ionic liquids (1-butyl-3-methyl-1-imidazolium tetrafluoroborate and 1-methyl-3-octyl-imidazolium tetrafluoroborate) for wheat and cress tested in the German standard soil Lufa 2.2. So part of the present study was to verify if this side chain effect can be found independently of the investigated soil composition with the three ionic liquids 1-ethyl-3-methyl-imidazolium tetrafluoroborate (IM12 BF<sub>4</sub>), 1-butyl-3-methyl-1-imidazolium tetrafluoroborate (IM14 BF<sub>4</sub>) and 1-methyl-3-octyl-imidazolium tetrafluoroborate (IM18 BF<sub>4</sub>). The structures of the selected test compounds, only varying in their alkyl side chain length, are given in Fig. 1. The ionic liquids names are abbreviated with acronyms according to Stolte *et al.* (2006).<sup>8</sup>

A release of ionic liquids to the environment is still most likely for the aquatic environment through waste water processes, but in cases of accidental spills, waste disposal or a leakage of landfill

<sup>a</sup>UFT - Centre for Environmental Research and Technology, Department 10: Ecology, University of Bremen, Leobener Straße, D-28359, Bremen, Germany. E-mail: matzke@uni-bremen.de

<sup>b</sup>UFT - Centre for Environmental Research and Technology, Department 3: Bioorganic Chemistry, University of Bremen, Leobener Straße, D-28359, Bremen, Germany

† Electronic supplementary information (ESI) available: Overview on the ANOVA—results performed for the factors mineral type and mineral concentrations as well as possible interactions of mineral type and concentration. See DOI: 10.1039/b717811e



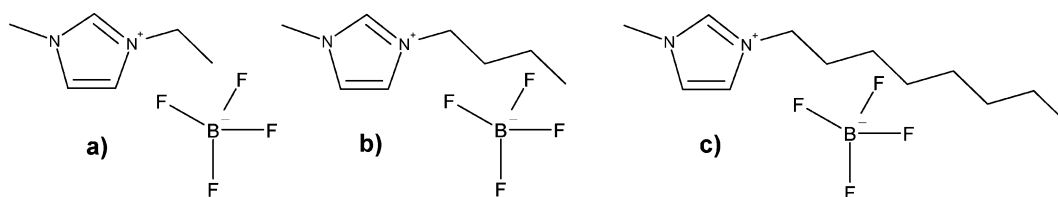


**Fig. 1** The selected test compounds a) 1-ethyl-3-methyl-imidazolium tetrafluoroborate (IM12 BF<sub>4</sub>), b) 1-butyl-3-methyl-imidazolium tetrafluoroborate (IM14 BF<sub>4</sub>), c) 1-octyl-3-methyl-imidazolium tetrafluoroborate (IM18 BF<sub>4</sub>).

sites an exposure for the terrestrial environment is also possible. Soils are sinks for contaminants and some soil properties are of essential influence to the bioavailability of xenobiotics<sup>30,31</sup> and therefore also on the bioavailability of ionic liquids. Previous studies proved that the here investigated compounds represent a hazard for terrestrial plants<sup>14,17</sup> or higher aquatic plants<sup>14,17,32</sup> and so a closer analysis of the influence of soil properties on the ionic liquids behaviour, bioavailability and toxicity is necessary. The bioavailability of ionic liquids on the terrestrial environment is strongly determined by sorption processes of the compounds and varies in dependence on different soil types. The sorption of imidazolium based ionic liquids was investigated so far by few studies including the sorption on bacterial and mineral surfaces<sup>33</sup> as well as natural soils<sup>34,35</sup> or aquatic sediments.<sup>36</sup> All publications stated that probably ionic interactions are the dominating sorption mechanism and hydrophobic interactions are of minor importance even though for ionic liquids both is likely due to the positive charge and the hydrophobic component (*e.g.* the alkyl side chain). This would imply that the influence of organic matter as well as increasing alkyl side chains on the sorption behaviour of ionic liquids is of minor importance in comparison to *e.g.* clay minerals with high cation exchange capacities and the positive charge. The results concerning the influence of hydrophobic interactions on ionic liquids sorption from Stepnowski *et al.* (2007)<sup>35</sup> and Beaulieu *et al.* (2007)<sup>36</sup> are somewhat contradictory. Whereas Stepnowski and co-workers proved an influence of hydrophobic interactions on the sorption behaviour of imidazolium based ionic liquids for concentrations up to 1 mM Beaulieu *et al.* could not confirm this. Gorman-Lewis and Fein (2004)<sup>33</sup> stated that clays have probably the highest influence to affect the sorption of ionic liquids in soils and proposed an interlayer cation exchange and/or a fixed negative surface charge to be the responsible mechanism. In general it is likely that the observed sorption strengths are a mixture of varying sorption mechanisms.

We focused our study on the influence of organic matter on ionic liquids toxicity to investigate the hydrophobic interactions as well as two types of clay minerals with differing cation exchange capacities to investigate the strength of ionic interactions. Additionally the concentrations of the added organic matter and clay minerals were varied and mixtures of clay minerals in different ratios were tested. The clay mineral mixtures were chosen to analyse if there are interactions between the different clay minerals influencing the bioavailability of ionic liquids because clays are often present in the environment in mixtures.

Clays consist of silicon tetrahedrons and aluminium octahedron layers and depending on the formation of the layers they are divided into different clay mineral classes.<sup>37,38</sup> Kaolinite as a 1:1 or two layer mineral and smectite as a 2:1 or three

layer mineral were chosen. Kaolinite has almost no swelling ability and a low sorption potential. Here the layers are kept together *via* hydrogen bonds.<sup>38</sup> In contrast the smectite layers are linked by exchangeable cations. Therefore 2:1 minerals possess the ability to shrink and swell, and a (reversible) incorporation of cations, organic molecules or water can occur.<sup>37,38</sup> These different structures of the clay mineral classes are responsible for a differing bioavailability of imidazolium based ionic liquids. In general smectites show a much higher sorption capacity for ionic liquids than kaolinites due to the high negative surface charge.<sup>38</sup>

The second important factor influencing the bioavailability of substances in soils is the organic matter content. Organic matter ( $C_{org}$ ) is by definition the whole of dead organic substance in soils originating from plant and animal detritus. It is a highly diverse mix of molecules in terms of its chemical structure and represents several interaction potentials for ionic liquids, *e.g.* hydrogen bonding, hydrophobic sorption or electrostatic interactions.<sup>36,39</sup> Therefore we investigated the influence of varying organic matter concentrations on the toxicity of 1-butyl-3-methyl-1-imidazolium tetrafluoroborate and 1-methyl-3-octyl-imidazolium tetrafluoroborate which clearly differ in their hydrophobicity and will probably be affected in a different manner by organic matter.

Finally we studied if the ionic liquids effect on growth inhibition is comparable for wheat and cress or if there are differences in sensitivity between monocotyledonous and dicotyledonous plants. Monocotyledonous and dicotyledonous plant species strongly differ in their morphology, *e.g.* the roots of monocotyledonous plants are adventitious and they do not perform secondary growth (in the stem the vascular bundles are arranged in a ring and not scattered and they do not possess a meristem between the phloem and xylem).<sup>40</sup> Those morphological differences could lead to differing sensitivities (toxicities) when being exposed to chemicals and therefore we selected in this study one common representative from each group.

We especially analysed the following hypotheses:

1. Toxic effects of ionic liquids on plants are reduced with higher clay contents because clays show sorption capacities for ionic liquids owing to their high specific surface, surface charge and ionic exchange capacity.

2. Smectite has a stronger reducing effect on the ionic liquid bioavailability than kaolinite because of the higher ability to absorb and adsorb ionic liquids.

3. The toxicity of ionic liquids in soils with varying clay mineral mixtures can hardly be predicted based on their effects in soils with additions of single clay minerals because they are able to interact with each other and therefore influence the bioavailability of chemicals in a different manner compared to singly applied clay minerals.

4. The effects of soil properties on ionic liquid bioavailability depend on substance properties: ionic liquids with longer alkyl side chains (e.g. -octyl) show a lower bioavailability than ionic liquids with short alkyl side chains (e.g. -butyl) in the tested concentration ranges.

5. A higher content of organic matter reduces the toxicity of the ionic liquids.

6. Monocotyledonous (wheat) and dicotyledonous (cress) plant species react different to the ionic liquids exposure.

## Results

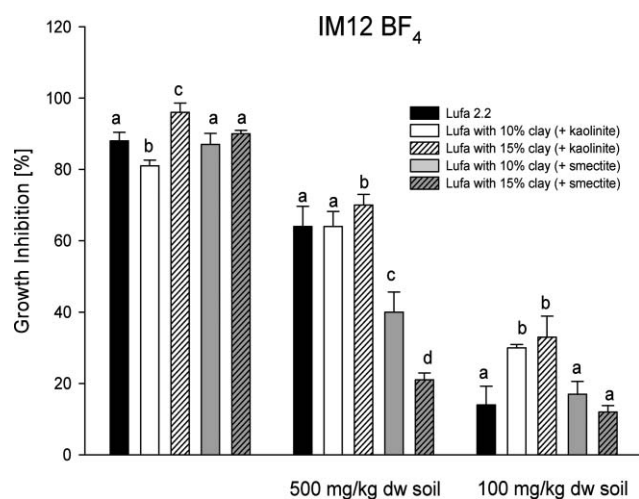
### Effects of different clay minerals on toxicity

Table 1 gives an overview on all obtained growth inhibition data for wheat (*Triticum aestivum*). The major results are shown in figures and discussed at the particular place.

The effect of the clay minerals on the toxicity of IM12 BF<sub>4</sub> (Fig. 2) depended on the substance concentration: at 1000 mg/kg dw soil kaolinite significantly influenced the toxicity-10% kaolinite resulted in a decrease in toxicity whereas

15% kaolinite increased the toxic effect in comparison to the reference soil. This increasing effect on toxicity became more pronounced with decreasing IM12 BF<sub>4</sub> concentrations. Smectite on the other hand had no effect at 1000 mg/kg dw soil and at 100 mg/kg dw soil but strongly decreased toxicity at the intermediate substance concentration of 500 mg/kg dw soil.

For IM14 BF<sub>4</sub> (Fig. 3) a heterogeneous pattern became obvious, the influence of the clay minerals proved to be substance concentration dependent. With a substance concentration of 1000 mg/kg dw only kaolinite decreased the toxicity in comparison to the reference soil Lufa and to the soils with smectite. An increase of the kaolinite concentration had no influence on the toxicity. For 500 mg IM14 BF<sub>4</sub>/kg dw soil only 10% kaolinite and 15% smectite significantly reduced the toxicity in comparison to the other tested soil compositions. In contrast for the tested IM14 BF<sub>4</sub> concentration of 100 mg/kg dw soil the addition of smectite clearly reduced the toxicity in comparison to the reference soil and 15% kaolinite. Also the addition of kaolinite (10%) resulted in a reduction of toxicity on the level of the soils with smectite.



**Fig. 2** Toxicities of three different concentrations of IM12 BF<sub>4</sub> for wheat (*Triticum aestivum*) expressed as growth inhibition [%] compared to untreated controls ( $\pm$  SD, n = 3) for the reference soil Lufa 2.2 and the soils with varying concentrations of kaolinite and smectite. Columns sharing the same letters do not differ significantly within each substance concentration, otherwise  $P \leq 0.05$  (Post-Hoc, Bonferroni).

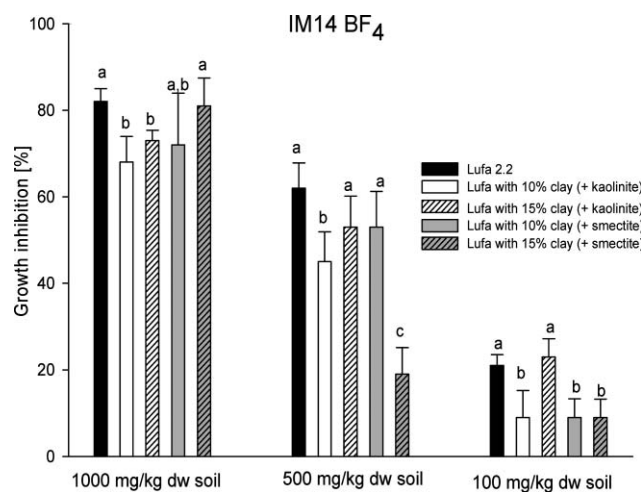


**Fig. 3** Toxicities of three different concentrations of IM14 BF<sub>4</sub> for wheat (*Triticum aestivum*) expressed as growth inhibition [%] compared to untreated controls ( $\pm$  SD, n = 3) for the reference soil Lufa 2.2 and the soils with varying concentrations of kaolinite and smectite. Columns sharing the same letters do not differ significantly within each substance concentration, otherwise  $P \leq 0.05$  (Post-Hoc, Bonferroni).

**Table 1** Toxicities of IM12 BF<sub>4</sub>, IM14 BF<sub>4</sub>, IM18 BF<sub>4</sub> for wheat (*Triticum aestivum*) expressed as growth inhibition [%] ( $\pm$  SD = standard deviation, n = 3) for the reference soil Lufa 2.2 and the soils with varying concentrations of kaolinite and smectite; n.d. = not determined

Substance	Concentration [mg/kg dw soil]	Reference soil Lufa 2.2	Lufa with 10% clay (+ kaolinite)	Lufa with 15% clay (+ kaolinite)	Lufa with 10% clay (+smectite)	Lufa with 15% clay (+ smectite)
IM12 BF <sub>4</sub>	1000	88 $\pm$ 2.40	81 $\pm$ 1.63	96 $\pm$ 2.62	87 $\pm$ 3.06	90 $\pm$ 0.97
	500	64 $\pm$ 5.66	64 $\pm$ 4.24	70 $\pm$ 3.01	40 $\pm$ 5.63	21 $\pm$ 1.93
	100	14 $\pm$ 5.25	30 $\pm$ 0.95	33 $\pm$ 5.86	17 $\pm$ 3.59	12 $\pm$ 1.79
IM14 BF <sub>4</sub>	1000	82 $\pm$ 3.01	68 $\pm$ 5.95	73 $\pm$ 2.35	72 $\pm$ 11.93	81 $\pm$ 6.46
	500	62 $\pm$ 5.82	45 $\pm$ 6.93	53 $\pm$ 7.14	53 $\pm$ 8.23	19 $\pm$ 6.13
	100	21 $\pm$ 2.53	9 $\pm$ 6.24	23 $\pm$ 4.20	9 $\pm$ 4.32	9 $\pm$ 4.22
IM18 BF <sub>4</sub>	1000	92 $\pm$ 0.66	99 $\pm$ 0.12	94 $\pm$ 1.31	63 $\pm$ 4.39	
	500	82 $\pm$ 2.47	86 $\pm$ 1.01	86 $\pm$ 2.23	10 $\pm$ 10.10	n.d.
	100	59 $\pm$ 0.75	13 $\pm$ 9.93	10 $\pm$ 5.25	8 $\pm$ 3.19	

In general for IM18 BF<sub>4</sub> (Fig. 4) the influence of the clay minerals became more obvious with decreasing substance concentrations. For 1000 and 500 mg/kg dw soil no or only slight differences in toxicity occurred between the reference soil and the soils with added kaolinite. In contrast for all tested substance concentrations the soil with added smectite has a strong reducing effect on the toxicity. This reducing effect became also more pronounced at lower substance concentrations. For 100 mg/kg all clay minerals showed a high toxicity reducing potential, but no differences between kaolinite and smectite were observable.

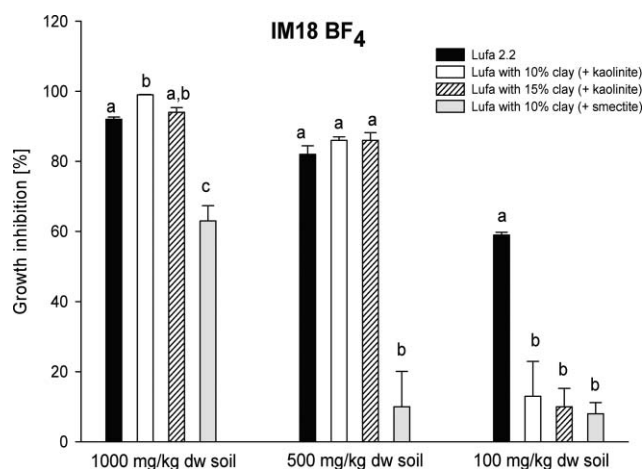


**Fig. 4** Toxicities of three different concentrations of IM18 BF<sub>4</sub> for wheat (*Triticum aestivum*) expressed as growth inhibition [%] compared to untreated controls ( $\pm$  SD,  $n = 3$ ) for the reference soil Lufa 2.2 and the soils with varying concentrations of kaolinite and smectite. Columns sharing the same letters do not differ significantly within each substance concentration, otherwise  $P \leq 0.05$  (Post-Hoc, Bonferroni).

The side chain effect could be proved for the reference soil Lufa 2.2 (Fig. 5), whereas for the different soil mixtures a stagnancy or even a turning back of the side chain effect occurred, *i.e.* the toxicity decreased with increasing alkyl side chain.

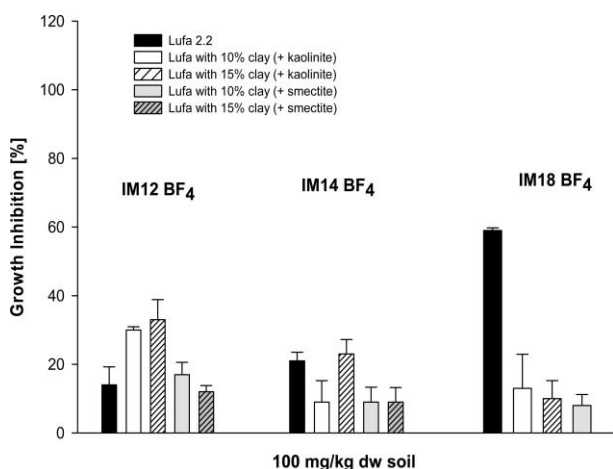


**Fig. 5** Comparison of the toxicities for IM12 BF<sub>4</sub>, IM14 BF<sub>4</sub> and IM18 BF<sub>4</sub> for all investigated soil mixtures at a concentration of 100 mg/kg dw soil expressed as growth inhibition [%] to check for the side chain effect in dependence on different soil properties.

To compare the influence of the soil properties on the toxicity a ratio was calculated for all investigated soil types which relates

the toxicities for the reference soil and the respective toxicities for the varying soil mixtures. An overview on those results is given in the electronic supplementary information.

The obtained results can be summed up as follows:

1. The side chain effect could be proved for the reference soil Lufa 2.2 for IM14 BF<sub>4</sub> and IM18 BF<sub>4</sub>, but not continuously for all tested clay soil compositions. Between IM12 BF<sub>4</sub> and IM14 BF<sub>4</sub> no or only marginal differences in toxicity have occurred for the reference soil. For the clay soils here a reversal of the side chain effect occurred: IM12 BF<sub>4</sub> was more toxic than IM14 BF<sub>4</sub>.
2. The influence of the clay mineral has been strongly dependent on the tested substance concentration.
3. Kaolinite has been able to increase toxicity, *e.g.* for IM12 BF<sub>4</sub> an increase of the kaolinite concentration resulted in an increase of the toxicity.
4. Smectite has shown either no influence or if there had been an influence on toxicity it has a stronger reducing effect than kaolinite

#### The influence of different mixtures of clay minerals on toxicity

The following part shows the results obtained for IM14 BF<sub>4</sub> and IM18 BF<sub>4</sub> influenced by three different mixtures of kaolinite and smectite in varying ratios (Fig. 6).

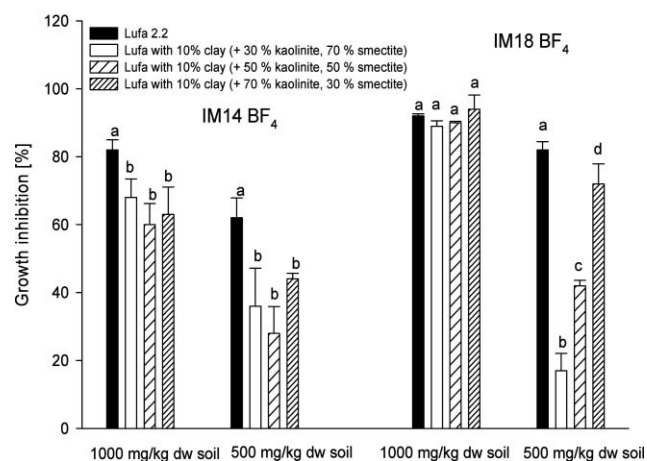


**Fig. 6** Toxicities of two different concentrations of IM14 BF<sub>4</sub> and IM18 BF<sub>4</sub> for wheat (*Triticum aestivum*) expressed as growth inhibition [%] compared to untreated controls (mean  $\pm$  SD,  $n = 3$ ) for the reference soil Lufa 2.2 and the soils with clay mixtures in different ratios at a total clay concentration of 10%. Columns sharing the same letters do not differ significantly and the statistical analysis was performed for each substance concentration separately, significant results are  $P \leq 0.05$  (Post-Hoc, Bonferroni).

For IM14 BF<sub>4</sub> the clay mixtures reduced the toxicity in comparison to the reference soil but no influence of the kaolinite-smectite ratio on the growth inhibition was observable. For IM18 BF<sub>4</sub> a substance concentration dependent influence of the clay minerals was obvious. No differences in toxicity occurred for all tested soils at a substance concentration of 1000 mg/kg dw soil. In contrast for a substance concentration of 500 mg/kg dw soil a clear influence of the clay mineral ratio could be observed: an increase of the kaolinite fraction in the clay mixture resulted in an increase of the observed toxicity. The toxicities for high

**Table 2** Toxicities for IM14 BF<sub>4</sub> and IM18 BF<sub>4</sub> for wheat (*Triticum aestivum*) and cress (*Lepidium sativum*) expressed as growth inhibition [%] (mean ± SD, n = 3) for the reference soil Lufa 2.2 and the soils with 5 and 10% organic matter (C<sub>org</sub>)

Substance	Concentration [mg/kg dw soil]	Growth inhibition [%]					
		Wheat ( <i>Triticum aestivum</i> )			Cress ( <i>Lepidium sativum</i> )		
		Reference soil Lufa 2.2	Lufa with 5% C <sub>org</sub>	Lufa with 10% C <sub>org</sub>	Reference soil Lufa 2.2	Lufa with 5% C <sub>org</sub>	Lufa with 10% C <sub>org</sub>
IM14 BF <sub>4</sub>	1000	82 ± 3.01	43 ± 2.92	23 ± 10.90	100 ± 0	52 ± 4.78	29 ± 0.04
	500	62 ± 5.82	31 ± 1.83	6 ± 7.84	58 ± 6.19	15 ± 6.41	7 ± 0.01
	100	21 ± 2.53	14 ± 2.28	-4 ± 2.75	-3 ± 3.25	-4 ± 12.06	0.3 ± 0.02
IM18 BF <sub>4</sub>	1000	92 ± 0.66	84 ± 1.59	72 ± 3.34	100 ± 0	89 ± 0.75	76 ± 1.38
	500	82 ± 2.47	65 ± 4.02	38 ± 2.32	100 ± 0	73 ± 5.76	33 ± 4.61
	100	59 ± 0.75	1 ± 4.07	11 ± 7.39	83 ± 3.12	8 ± 2.04	-0.2 ± 1.48

smectite contents within the mixture (70% and 50% smectite) are below the toxicities of IM14 BF<sub>4</sub> and so a turning back of the side chain effect is observable. When comparing IM14 BF<sub>4</sub> and IM18 BF<sub>4</sub> at a test concentration of 1000 mg substance kg/dw soil the side chain effect is present for all tested soil compositions: IM18 BF<sub>4</sub> was more toxic than IM14 BF<sub>4</sub> independently from the clay minerals or the clay mineral ratio of the mixtures.

#### The influence of organic matter on toxicity and difference in sensitivity between the two plant species

In general with an increase in the organic matter content a consistent decrease in toxicity could be confirmed (Table 2, Fig. 7). Here the side chain effect could be proved. Additionally differences in sensitivity between the two plant species wheat and cress were observable. For IM14 BF<sub>4</sub> the differences seem to be concentration dependent: at 1000 mg/kg dw soil cress was the more sensitive species and at 100 mg/kg dw it was vice versa. For IM18 BF<sub>4</sub> cress was for the reference soil Lufa and the soil with 5% organic matter more sensitive. At a C<sub>org</sub> concentration

of 10% no differences in sensitivity between the two plant species occurred. For IM14 BF<sub>4</sub> even at high substance concentrations (1000 mg/kg dw soil) a strong reduction in toxicity occurred when the organic matter content was increased: for wheat an increase to a total organic matter content of 5% reduced the toxicity about 50% at 1000 and 500 mg/kg dw soil in comparison to the reference soil. An increase to a total concentration of 10% organic matter resulted in a reduction of the toxicity of approximately 75% for 1000 mg/kg dw soil and at 500 mg/kg dw soil no toxicity was observable anymore. Cress reacted in a similar way apart from the above mentioned differences in species sensitivity. For IM18 BF<sub>4</sub> at 1000 mg/kg dw soil the toxicities were reduced only slightly, but even here the differences were significant (P < 0.01). At 500 mg/kg dw soil the influence of organic matter became stronger, here a reduction of toxicity occurred up to 50% caused by the addition of organic matter (both 5 and 10% organic matter). At 100 mg/kg dw soil no toxicity could be observed anymore for the soils with organic matter addition for both organisms.

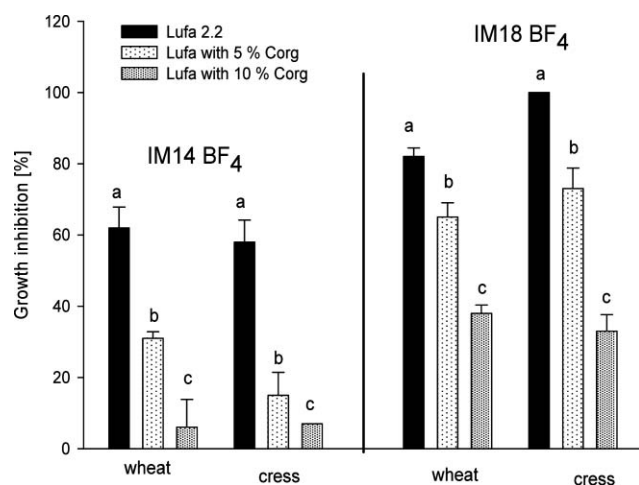


**Fig. 7** Toxicities of IM14 BF<sub>4</sub> and IM18 BF<sub>4</sub> for wheat (*Triticum aestivum*) and cress (*Lepidium sativum*) expressed as growth inhibition [%] compared to untreated controls (mean ± SD, n = 3) for the reference soil Lufa 2.2 and the soils with varying concentrations of organic matter. Columns sharing the same letters do not differ significantly and the statistical analysis was performed for each substance concentration and plant species separately, significant results are P ≤ 0.05 (Post-Hoc, Bonferroni).

#### Discussion

The differences in toxicity observed in the diverse clay soils can be explained by the varying properties of the two-layer and three layer minerals. The most important property of clays is the chemical activity of their surfaces, resulting in a negative surface charge. In general the importance of layer silicate clays to soil properties can be best described by the cation exchange capacity (CEC) which is defined as the ability to absorb and adsorb ionic species in solutions.<sup>37</sup> Three layer minerals, and in this mineral class especially smectites, have the highest CEC in soils.<sup>37</sup> Smectites, representing the most common group, possess the highest chemical and physical activity and ions are usually freely exchanged.<sup>37</sup> The presence of permanently negative charged sites accounts for the ability of many soils to hold cations against leaching, but still in an exchangeable form. Comparing kaolinite and smectite it has to be noticed that kaolinite (being the two layer mineral) has almost no swelling ability and a low sorption potential due to the hydrogen bonds between the two layers.<sup>41,42</sup> In contrast the three layer mineral smectite can expand because here no hydrogen bonds between the single layers are possible. It possesses the ability to shrink and swell, and a (reversible) incorporation of cations, organic molecules or water can occur. Thus smectites are suitable to absorb or



adsorb xenobiotics.<sup>41,42</sup> By definition adsorption is the process of accumulation of chemical species to the surface and absorption is the incorporation of xenobiotics within the clay mineral.<sup>37</sup>

Therefore the differences in toxicity between the reference soil Lufa 2.2 and the soils with kaolinite were small because only a weak adsorption and no absorption occurred. In contrast, for the smectite soils higher interaction potentials were observable because of the possibility for the substances to be adsorbed and absorbed. Owing to the fact that for smectite soils the dominating sorption effect is likely to be based on ionic interactions and not on hydrophobic interactions the observed decreases in toxicity especially for the IM18 BF<sub>4</sub> can be explained with a formation of admicelles on the mineral surface according to Stepnowski *et al.* (2007).<sup>35</sup> They assume that for ionic liquids with increased hydrophobicity (e.g. longer alkyl side chain) the formation of second layers on the clay mineral surface is possible which would explain the lower bioavailability of IM18 BF<sub>4</sub> in the smectite containing soils.

In aquatic systems the side chain effect could be observed even with the shorter side chains, e.g. IM12 and IM14, which means that the EC<sub>50</sub> values for IM12 are higher than for IM14.<sup>32</sup> In contrast there seems to be a "critical" side chain length for the investigated soil systems with respect to interaction with the chemicals because there were either no differences in toxicity between IM12 and IM14 or a reversal of the side chain effect occurred, which means more toxic effects were observed in the soils with kaolinite for IM12 than for IM14.

In general a short side chain seems to increase the mobility of the substances in soils, fewer interactions are possible with the matrix in comparison to ionic liquids with a longer alkyl chain and therefore the influence of the clay minerals is reduced. The results obtained for the clay mineral mixtures were similar in comparison to the singly tested clay minerals kaolinite and smectite. In general for IM14 BF<sub>4</sub> no influence of the clay mixture ratio on toxicity could be observed and therefore no influence of the clay mineral type. However, one exception occurred: the observed toxicities for the added clay mineral mixtures were lower than the toxicities of the reference soil Lufa 2.2 for both tested substance concentrations. In contrast for IM18 BF<sub>4</sub> a saturation of the soils occurred for all investigated clay mixtures at 1000 mg/kg dw soil even for the soil with a high smectite content. This is in contrast to the results for 10% smectite tested singly, resulting in a clear reduction of the toxicity. On the other hand for 500 mg IM18 BF<sub>4</sub>/kg dw soil a clear influence of smectite on the toxicity was observable meaning with an increase of the smectite content in the clay mixture an decrease in toxicity occurred.

For organic matter also a high influence on toxicity was expected in comparison to the clay minerals. Organic matter is a chemically highly diverse mixture of molecules and therefore predictions on fate and performance of ionic liquids are difficult. Humic substances which represent the main part of organic matter being responsible for interactions with chemicals, are mixtures of macromolecule substances with molecular weights between 500 and 100 000 g/mol. Here many functional chemical groups can contribute to the interactions with xenobiotics e.g. hydroxyl, carboxyl or aromatic ring structures.<sup>43-46</sup>

Additionally the formation of chemical complexes can occur between humic acids and clay minerals or the surface of the clay

minerals can be altered by humic acids.<sup>47</sup> In this study a reduced toxicity could be proved for the soils with increased organic matter content for both IM14 BF<sub>4</sub> and IM18 BF<sub>4</sub>. However this reduction in toxicity can be highly variable when testing other types of organic matter from different sources resulting in more or less pronounced toxic effects because the influence of organic matter on toxicity is strongly dependent on type and quantity. For high IM18 BF<sub>4</sub> concentrations (1000 mg/kg dw soil) the reductions in toxicity were only marginal in the soils with increased organic matter content probably based on a saturation of the adsorption capacities of the binding sites. When comparing the toxicity reducing effects of organic matter and smectite for IM18 BF<sub>4</sub> the influence of smectite was very pronounced in comparison to organic matter. The calculated ratio clearly showed for IM18 BF<sub>4</sub> (1000 mg/kg dw soil) in the soil with 10% smectite 68% growth inhibition (in relation to Lufa) whereas for 5% C<sub>org</sub> it was 91% and for 10% C<sub>org</sub> still 78%. For lower substance concentrations this effect was even more pronounced (for details please see electronic supplementary information) For IM14 BF<sub>4</sub> (1000 mg/kg dw soil) this result was vice versa: here the influence of organic matter on toxicity reduction was stronger (5% C<sub>org</sub> = 52% growth inhibition, 10% C<sub>org</sub> = 28% growth inhibition) than the one of smectite (10% smectite soil mixture = 88% growth inhibition).

Additionally differences in sensitivity between the two tested plant species could be observed within this study even though they were not consistent and variable. So at present it is not possible to generate general statements on future testing strategies for monocotyledonous and dicotyledonous plants regarding their species sensitivity. In terms of regulation and hazard assessment the strategy to test representatives from both is furthermore recommended until the remaining uncertainties can be eliminated.

This study was merely performed with laboratory experiments. Such investigations are always limited in their explanatory power because in the field the impact of imidazolium based ionic liquids and therefore the strength of the effects caused is influenced by diverse factors like aging of the substances and soils, acidification of soils (changes in pH-values linked to a changing bioavailability) and temperature as well as biotic factors like community structures and behaviour of e.g. soil invertebrates. Nevertheless the controlled conditions in a laboratory study give important hints for further investigations, and conclusions on undesirable toxic substances are possible. The results here obtained should help to improve the knowledge on the ecotoxicological hazard potential of ionic liquids in order to lead to a better understanding in terms of the design of inherently safer chemicals.

## Conclusions

The objective of this study was to investigate the influence of two different clay minerals, clay mineral mixtures and organic matter content on the toxicity of imidazolium based ionic liquids differing in their alkyl chain length.

In general most ecotoxicological studies focus on the aquatic environment due to an easier performance (lower costs and shorter test duration). But even if, with some exceptions, the results were as expected and the above mentioned hypotheses

could be verified in terms of a prospective hazard assessment for new substance classes a detailed analysis is necessary for the terrestrial environment.

For subsequent studies the structural elements head group and anion of an ionic liquid should be studied in more detail. Here especially for (potentially) toxic anions opposite effects can be expected according to the fact that in the majority of the cases soils are negatively charged matrices.

Additionally a prospective hazard assessment of ionic liquids should not only include some selected standard soils (or even artificial soils *e.g.* OECD soil) but important factors which crucially influence the bioavailability of imidazolium based ionic liquids. For the influence of clay minerals evidence was given that higher clay contents can not be equated with a lower bioavailability/toxicity, especially for low substance concentrations. Further studies should focus on changing environmental conditions influencing the bioavailability and toxicity of substances, *e.g.* aging of the substances, varying pH-values, temperature or formation of humic acid-clay mineral complexes. No consistent differences in species sensitivity could be found for the here analysed compounds, but unless those differences are understood the strategy of testing both monocotyledonous and dicotyledonous plants is recommended.

In general a careful investigation of key structures of ionic liquids in terms of their ecotoxicological hazard potential is advisable to support the development of inherently safer chemicals, reducing the risk for man and the environment.

## Material and methods

The tested ionic liquids were provided by Merck KGaA (Darmstadt, Germany). Cadmiumchloride,  $\text{CaCl}_2 \cdot 2\text{H}_2\text{O}$ , kaolinite and smectite were purchased from the Sigma-Aldrich Cooperation (Germany). The German standard soil LUFA 2.2 was obtained from the Landwirtschaftliche Forschungs- und Untersuchungsanstalt Speyer (Speyer, Germany). Wheat and cress seeds were bought in a health food shop to ensure that the seeds were not treated with any kind of pesticides to exclude mixture effects during the experiments. For the tests with different organic matter content plain flower soil without any fertilisers was used and purchased from a home improvement store.

We used the standardised growth inhibition assay (ISO) with wheat (*Triticum aestivum*) and cress (*Lepidium sativum*).<sup>48</sup>

The determined endpoint is growth inhibition measured as dry weight of the above ground parts of the plants. Wheat (*Triticum aestivum*) and cress (*Lepidium sativum*) were chosen as representatives for monocotyledonous and dicotyledonous plants as requested in the guideline. Test duration is three weeks from sowing. The growth inhibition assay was conducted in plastic plant pots, for wheat 10 seeds were used, and for cress 20. The plants were cultivated in a German standard soil (Lufa 2.2) characterised as loamy sand and with a pH of  $5.6 \pm 0.2$ , a clay content of 7.5% and an organic carbon content of 2.3%. The water content was fixed at 50% of the water holding capacity (48%) with aqueous substance solutions respectively deionised water for the controls. The ionic liquids were solved in 0.01 M  $\text{CaCl}_2$  for spiking the soils and were prepared 24 h before test beginning and stirred to ensure that the ionic liquids are completely dissolved in the aqueous medium. For each test at

least six controls with uncontaminated soil were grown. Within the test each plant pot contained 300 g dry weight (dw) soil and for all substance concentrations three replicates were used. To minimise the waste amount of contaminated soils a toxic reference (cadmium) was used to ensure that the obtained data are valid and a constant quality of the tests was given. The water content was adjusted every second day by weighing. Differently composed soil types were tested in comparison to Lufa 2.2 which was used as a reference soil. For the composition of the different soil types Lufa 2.2 was used as basic substrate and supplemented with the corresponding clay mineral and organic matter concentration. The different clay minerals (kaolinite or smectite) were added to Lufa 2.2 to obtain final soil dry matter concentrations of 10% and 15% of clay. As an organic matter source plain flower soil (Compo Sana Qualitätsblumenerde, Compo GmbH Münster, Germany) was used. The organic matter content was determined (89%) *via* incineration at 500 °C in a muffle furnace. The organic matter was added to Lufa 2.2 to obtain final soil dry matter concentrations of 5% and 10% of organic matter.

To exclude pH effects on plant growth, the pH values of the soil samples were checked at the beginning and the end of the test. For all tested substances pH values ranged in the original pH band of Lufa 2.2. For measuring the pH value 5 g soil and 25 ml 0.01 M  $\text{CaCl}_2$  solution were shaken (150 rpm) for two hours. After sedimentation of the soil samples (at least 4 hours) the pH values were measured. The plants were grown in a phytotron chamber under controlled conditions (temperature 20 °C, 80% humidity) with a 16 hours light and 8 hours darkness cycle.

## Data analysis and data plotting

The presented endpoint is [%] growth inhibition, calculated in relation to the untreated controls. Data are presented as mean  $\pm$  standard deviation (SD). All data achieved in this study were plotted using Sigmaplot Version 10. Statistical analysis was performed by a one-way ANOVA using the Bonferroni multiple comparisons test from the SPSS software package 12, respectively by a two-way ANOVA for the analysis of interactions between clay mineral type and clay concentration. An overview on the results of the performed statistics is given in the electronic supplementary information (ESI).†

## Acknowledgements

The authors thank Prof. Dr. Bernd Jastorff and the whole UFT ionic liquids research group for helpful discussions and support. Furthermore special thanks are given to the Merck KGaA for providing the chemicals and for their generous support within our strategic partnership. The first author especially thanks the Hans-Böckler-Stiftung for funding the work with a PhD scholarship.

## References

- 1 P. Wasserscheid and T. Welton, *Ionic Liquids in Synthesis*, Wiley-VCH-Verlag, Weinheim, 2002.
- 2 T. Welton, *Chemical Reviews*, 1999, **99**(8), 2071–2083.
- 3 F. Endres, *ChemPhysChem*, 2002, **3**(2), 145–154.

- 4 T. Welton, *Coordination Chemistry Reviews*, 2004, **248**(21–24), 2459–2477.
- 5 H. Zhao, *Journal of Molecular Catalysis B: Enzymatic*, 2005, **37**, 16–25.
- 6 B. Jastorff, R. Stormann, J. Ranke, K. Molter, F. Stock, B. Oberheitmann, W. Hoffmann, J. Hoffmann, M. Nuchter, B. Ondruschka and J. Filser, *Green Chemistry*, 2003, **5**(2), 136–142.
- 7 S. Stolte, J. Arning, U. Bottin-Weber, A. Müller, W. R. Pitner, U. Welz-Biermann, B. Jastorff and J. Ranke, *Green Chemistry*, 2007, **9**(8), 760–767.
- 8 S. Stolte, J. Arning, U. Bottin-Weber, M. Matzke, F. Stock, K. Thiele, M. Uerdingen, U. Welz-Biermann, B. Jastorff and J. Ranke, *Green Chemistry*, 2006, **8**(7), 621–629.
- 9 R. J. Bernot, M. A. Brueseke, M. A. Evans-White and G. A. Lamberti, *Environmental Toxicology and Chemistry*, 2005, **24**(1), 87–92.
- 10 R. J. Bernot, E. E. Kennedy and G. A. Lamberti, *Environmental Toxicology and Chemistry*, 2005, **24**(7), 1759–1765.
- 11 D. J. Couling, R. J. Bernot, K. M. Docherty, J. K. Dixon and E. J. Maginn, *Green Chemistry*, 2006, **8**, 82–90.
- 12 K. M. Docherty and C. F. Kulpa, *Green Chemistry*, 2005, **7**(4), 185–189.
- 13 M. T. Garcia, N. Gathergood and P. J. Scammells, *Green Chemistry*, 2005, **7**(1), 9–14.
- 14 B. Jastorff, K. Molter, P. Behrend, U. Bottin-Weber, J. Filser, A. Heimers, B. Ondruschka, J. Ranke, M. Schaefer, H. Schröder, A. Stark, P. Stepnowski, F. Stock, R. Störmann, S. Stolte, U. Welz-Biermann, S. Ziegert and J. Thöming, *Green Chemistry*, 2005, **7**, 362–372.
- 15 A. Latala, P. Stepnowski, M. Nedzi and W. Mroziak, *Aquatic Toxicology*, 2005, **73**(1), 91–98.
- 16 P. Luis, I. Ortiz, R. Aldaco and A. Irabien, *Ecotoxicology and Environmental Safety*, 2006, 1–7.
- 17 M. Matzke, S. Stolte, K. Thiele, T. Juffernholz, J. Arning, J. Ranke, U. Welz-Biermann and B. Jastorff, *Green Chemistry*, 2007, **9**(11), 1198–1207.
- 18 C. Pretti, C. Chiappe, D. Pieraccini, M. Gregori, F. Abramo, G. Monni and L. Intorre, *Green Chemistry*, 2005, **8**(3), 238–240.
- 19 J. Ranke, K. Molter, F. Stock, U. Bottin-Weber, J. Poczobutt, J. Hoffmann, B. Ondruschka, J. Filser and B. Jastorff, *Ecotoxicology and Environmental Safety*, 2004, **58**(3), 396–404.
- 20 A. S. Wells and V. T. Coombe, *Organic Process Research and Development*, 2006, **10**(4), 794–798.
- 21 P. Balczewski, B. Bachowska, T. Bialas, R. Biczak, W. M. Wieczorek and A. Balinska, *J. Agric. Food Chem.*, 2007, **55**(5), 1881–1892.
- 22 J. Pernak, K. Sobaszekiewicz and J. Foksowicz-Flaczyk, *Chemistry-A European Journal*, 2004, **10**(14), 3479–3485.
- 23 R. P. Swatloski, J. D. Holbrey, S. B. Memon, G. A. Caldwell, K. A. Caldwell and R. D. Rogers, *Chem Commun (Camb.)*, 2004, (6), 668–669.
- 24 K. M. Docherty, J. K. Dixon and C. F. Kulpa, *Biodegradation*, 2007, **18**, 481–493.
- 25 M. T. Garcia, E. Campos, J. Sanchez-Leal and I. Ribosa, *Chemosphere*, 1999, **38**(15), 3473–3483.
- 26 N. Gathergood, M. T. Garcia and P. J. Scammells, *Green Chemistry*, 2004, **6**(2), 166–175.
- 27 N. Gathergood, P. J. Scammells and M. T. Garcia, *Green Chemistry*, 2006, **8**(2), 156–160.
- 28 N. Gathergood and P. J. Scammells, *Australian Journal of Chemistry*, 2002, **55**(9), 557–560.
- 29 P. Stepnowski, A. C. Skladanowski, A. Ludwiczak and E. Laczynska, *Human & Experimental Toxicology*, 2004, **23**(11), 513–517.
- 30 M. Alexander, *Environmental Science & Technology*, 1995, **29**(11), 2713–2717.
- 31 T. Frische, K. H. Mebes and J. Filser, *Assessing the bioavailability of contaminants in soils: a review on recent concepts*, Berlin, 2003; Research Report 201 64 214.
- 32 S. Stolte, M. Matzke, J. Arning, A. Bösch, W. R. Pitner, U. Welz-Biermann, B. Jastorff and J. Ranke, *Green Chemistry*, 2007, **9**(11), 1170–1179.
- 33 D. J. Gorman-Lewis and J. B. Fein, *Environmental Science & Technology*, 2004, **38**(8), 2491–2495.
- 34 P. Stepnowski, *Australian Journal of Chemistry*, 2005, **58**, 170–173.
- 35 P. Stepnowski, W. Mroziak and J. Nischtauser, *Environmental Science & Technology*, 2007, **41**(2), 511–516.
- 36 J. J. Beaulieu, J. L. Tank and M. Kopacz, *Chemosphere*, 2007.
- 37 A. Parker and J. E. Rae, *Environmental Interactions of clays*, Springer Verlag, Berlin, Heidelberg, New York, 1998.
- 38 G. Sposito, N. T. Skipper, R. Sutton, S.-H. Park, A. K. Soper and J. A. Greathouse, *Proc. Natl. Acad. Sci.*, 1999, **96**, 3358–3364.
- 39 M. Haitzer, S. Hoss, W. Traunspurger and C. Steinberg, *Chemosphere*, 1998, **37**(7), 1335–1362.
- 40 M. W. Chase, *American Journal of Botany*, 2004, **91**, 1645–1655.
- 41 B. Velde, *Introduction to clay minerals*, Chapman and Hall, London, 1992.
- 42 B. Velde, *Origin and mineralogy of clays*, Springer Verlag, Berlin, Heidelberg, New York, 1995.
- 43 J. R. Burford and J. M. Bremner, *Soil Biology and Biochemistry*, 1975, **7**(6), 389–394.
- 44 C. Chiou, *Theoretical Considerations of the Partition Uptake of Nonionic Organic Compounds by Soil Organic Matter*; Reactions and Movement of Organic Chemicals in Soils. Proceedings of a Symposium of the Soil Science Society of America and the American Society of Agronomy, 1989, pp. 1–29.
- 45 H. Li, B. J. Teppen, D. A. Laird, C. T. Johnston and S. A. Boyd, *Soil Sci. Soc. Am J.*, 2006, **70**(1889), 1895.
- 46 Wei-ping Liu, Zhuo Fang, Hui-jun Liu and Wei-chun Yang, *Journal of Environmental Sciences*, 2002, **14**(2), 173–180.
- 47 S. Hengpraprom, C. M. Lee and J. T. Coates, *Environ. Toxicol. Chem.*, 2006, **25**(1), 11–17.
- 48 ISO Guideline 11269–2: Soil quality - Determination of the effects of pollutants of soil flora - Part 2: Effects of chemicals on the emergence and growth of higher plants; 2003.

# Solar thermochemical reactions: four-component synthesis of polyhydroquinoline derivatives induced by solar thermal energy

Ramadan Ahmed Mekheimer, Afaf Abdel Hameed and Kamal Usef Sadek\*

Received 1st October 2007, Accepted 4th February 2008

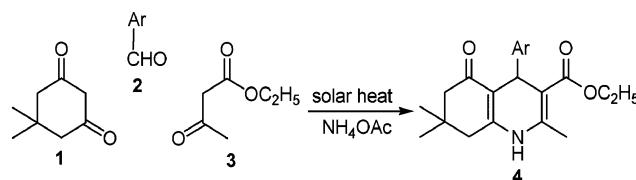
First published as an Advance Article on the web 3rd March 2008

DOI: 10.1039/b715126h

The synthesis of polyhydroquinoline derivatives *via* a four-component unsymmetric Hantzsch reaction induced by solar thermal energy is reported. The process proved to be simple, environmentally friendly, economic and high yielding.

## Introduction

1,4-Dihydropyridines have received considerable attention because of their biological activity.<sup>1</sup> They are among the most widely used drugs for cardiovascular diseases,<sup>2</sup> have a wide range of other pharmacological activities<sup>3,4</sup> and play an important role in CNS-targeted chemical delivery systems.<sup>5</sup> In addition, quinolines exhibit a wide spectrum of activities such as antiplasmodial,<sup>6</sup> antibacterial,<sup>7</sup> antiproliferative,<sup>8</sup> antimalarial,<sup>9</sup> and anticancer properties.<sup>10</sup> Many other biological activities are known<sup>11</sup> which inspired us to search for an improved and green approach for the synthesis of these derivatives. The conventional method for their synthesis involves four-component reaction of an aldehyde with ethyl acetoacetate and ammonia in acetic acid or by refluxing in alcohol. However, these methods suffer from several drawbacks such as long reaction times, use of large quantities of organic solvents and low yields. Recently, several methods have been reported comprising the use of microwave, ionic liquids, TMSCl-MaI, metal triflates and polymers, also Baker's yeast.<sup>12–17</sup> However, the use of high temperature, expensive metal precursors, catalysts that may be harmful to the environment and longer reaction times are disadvantages of such synthesis. Green chemistry has received considerable attention nowadays<sup>18</sup> and we do believe that the nature provides us with many clean and environmentally friendly techniques to achieve our purposes. This encouraged us to think about solar energy as a free energy source. Solar thermal heating overcomes the energy consumption of conventional heating as well as dissipation of energy—typically heat to the environment.<sup>19</sup> It is worth mentioning that solar energy is regarded as a clean reagent<sup>20</sup> and solar transformations proceeded cleanly and no or only minor amounts of side products could be detected. In continuation of our work on the synthesis of azines and fused azines,<sup>21</sup> we reported herein the first attempt to synthesise unsymmetrical polyhydroquinoline derivatives **4** using dimedone (**1**), aryl aldehyde (**2**), ethyl acetoacetate (**3**) and ammonium acetate under the effect of solar heating (Scheme 1).



Scheme 1

## Results and discussion

The structures of the products **4** were confirmed by comparison (TLC) with authentic samples<sup>22</sup> prepared by refluxing the reaction mixture in ethanol for 4–8 hrs. and also by spectral data. In order to examine the effect of substituted aryl aldehydes (**2**) on the reaction rate and the overall yield, various functionalized aryl aldehydes were used under the above reaction conditions. It has been found that the reaction proceeds smoothly to give polyhydroquinolines **4**, in high yields. However, when the aryl substituent was a strong electron withdrawing group (*e.g.* **4h**) prolonged reaction times were required (*cf.* Table 1). This reflects the effect of the nature of substituent on the reactivity of the arylidene derivative supposed to be formed as an intermediate. In order to investigate the exact cause of the reaction, *i.e.* whether it is a thermal or photochemical transformation, we carried out the reaction with **2a–h** in the dark at the same maximum reaction temperature reached during the solar exposure and for the same reaction time. It afforded the same products

Table 1 Solar thermal synthesis of polyhydroquinoline derivatives

Compound	Ar (2)	Time/h	Yield (%)	maximum temp <sup>a,b</sup> reached °C
<b>4a</b>	C <sub>6</sub> H <sub>5</sub>	2.5	92	46
<b>4b</b>	4-HO-C <sub>6</sub> H <sub>4</sub>	2.0	90	48
<b>4c</b>	4-H <sub>3</sub> CO-C <sub>6</sub> H <sub>4</sub>	2.0	92	50
<b>4d</b>	1-naphthyl	2.0	88	48
<b>4e</b>	4-Cl-C <sub>6</sub> H <sub>4</sub>	6.0	87	42
<b>4f</b>	2-furyl	2.0	90	52
<b>4g</b>	4-H <sub>3</sub> C-C <sub>6</sub> H <sub>4</sub>	2.0	88	51
<b>4h</b>	3-O <sub>2</sub> N-C <sub>6</sub> H <sub>4</sub>	12.0	83	40

<sup>a</sup> Compounds **4a–h** were obtained in carrying out the reaction in dark at the same temperature. <sup>b</sup> Reactants were recovered unchanged when carrying out the reaction in dark at room temperature.

Chemistry Department, Faculty of Science, El-Minia University, El-Minia, 61519, Egypt. E-mail: kusadek@yahoo.com; Tel: +2- 086-2364806



obtained under solar heating.<sup>21,22</sup> Likewise, we performed the same reaction with **2a–h** at a low temperature (5 °C) and up to room temperature under the effect of artificial visible light-emitted from a Toshiba low pressure fluorescence lamp (60 W)—and the reactants were recovered, almost unchanged, even when exposure was performed for a longer reaction time. This ruled out the possibility of a solar photochemical reaction.<sup>23–25</sup>

## Conclusions

We have successfully developed an easy, high yielding and versatile method for the synthesis of polyhydroquinolines from the reaction of dimedone, aryl aldehydes,  $\beta$ -ketoester and ammonium acetate catalyzed by free solar thermal energy. The process does not require the use of any expensive or harmful catalysts and thus is a simple, environmentally friendly technique of high yield and produces analytically pure target compounds.

## Experimental

### General procedure


to a solution of an equimolar (0.01 mol) mixture of each of dimedone, aryl aldehyde and ethyl acetoacetate in ethanol (10 ml), in a Pyrex flask, ammonium acetate (1 g) was added. The reaction mixture was exposed to direct sunlight. After 1.5–10 hrs of illumination a precipitate started to form which was completed after the times stated in Table 1. During the solar exposure, the temperature of the reaction mixture reached 40–52 °C (Table 1). The resulting solid product was collected by filtration, washed with EtOH, dried and recrystallized from EtOH to yield **4a–h**. Compounds **4a–g** have been described previously; **4b** ref. 25, **4c** ref. 26, **4f** ref. 14 and **4a**, **4d**, **4e**, **4g** all ref. 17, and our spectral data (IR, <sup>1</sup>H and <sup>13</sup>C-NMR) are substantially identical to those found in literature.

Compound **4h**: Mp: 177–178 °C. <sup>1</sup>H NMR (300 MHz, CDCl<sub>3</sub>):  $\delta$  = 0.93 (s, 3H), 1.07 (s, 3H), 1.22 (t, <sup>3</sup>J = 7.1 Hz, 3H), 2.12–2.42 (m, 7H), 3.69 (q, <sup>3</sup>J = 7.1 Hz, 2H), 5.16 (s, 1H), 6.85 (s, 1H), 7.36 (t, <sup>3</sup>J = 7.9 Hz, 1H), 7.71 (d, <sup>3</sup>J = 7.9 Hz, 1H), 7.98 (m, 1H), 7.99 (m, 1H). <sup>13</sup>C NMR (75 MHz, CDCl<sub>3</sub>):  $\delta$  = 12.9, 18.0, 25.8, 28.1, 31.5, 35.7, 39.5, 49.3, 58.8, 103.7, 109.8, 119.9, 121.6, 127.3, 133.5, 143.4, 146.9, 148.1, 165.7, 194.4. IR (KBr):  $\nu$  = 3282, 3211, 3077, 2960, 1700, 1611 cm<sup>-1</sup>. Found: C, 67.34; H, 6.46; N, 7.45; anal. calcd for C<sub>21</sub>H<sub>24</sub>N<sub>2</sub>O<sub>5</sub>: C, 67.39; H, 6.46; N, 7.48.

## References

- (a) S. Goldman and J. Stoltefuss, *Angew. Chem., Int. Ed. Engl.*, 1991, **30**, 1559; (b) H. Nakayama and Y. Kasoaka, *Heterocycles*, 1996, **42**, 901.

- V. P. Litvinov, *Russ. Chem. Bull.*, 1998, **47**, 2053.
- K. Aouam and A. Berdeaux, *Therapie*, 2003, **58**, 333.
- (a) HIV Protease Inhibition: A. Hilgeroth, *Mini Rev. Med. Chem.*, 2002, **2**, 235; (b) A. Hilgeroth and H. Lilie, *Eur. J. Med. Chem.*, 2003, **38**, 495.
- (a) A. Misral, S. Ganesh, A. Shahiwala and S. P. Shah, *J. Pharm. Sci.*, 2003, **6**, 252; (b) N. Bodor and P. Buchwald, *Drug Discovery Today*, 2002, **7**, 766; (c) L. Prokai, K. Prokai-Tatria and N. Bodor, *Med. Res. Rev.*, 2000, **20**, 367.
- P. Beagley, M. A. L. Blackie, K. Chibale, C. Clarkson, R. Meijboom, J. R. Moss, P. Smith and H. Su, *Dalton Trans.*, 2003, 3046–3051.
- N. Fokialakis, P. Magiatis, L. Chinou, S. Mitaku and F. Tillequin, *Chem. Pharm. Bull.*, 2002, **50**, 413–414.
- P. Fossa, L. Mosti, G. Menozzi, C. Marzano, F. Baccichetti and F. Bordin, *Bioorg. Med. Chem.*, 2002, **10**, 734.
- A. Ryckebusch, R. Derprez-Poulain, L. Maes, M. A. Debreu-Fontaine, E. Mouray, P. Grellier and C. Sergheraert, *J. Med. Chem.*, 2003, **46**, 542.
- L. R. Morgan, B. S. Jursic, C. L. Hooper, D. M. Neumann, K. Thanagaraj and B. Leblanc, *Bioorg. Med. Chem. Lett.*, 2002, **12**, 3407.
- (a) V. Klusa, *Drugs Future*, 1995, **20**, 135; (b) R. G. Bretzol, C. C. Bollen, E. Maester and K. F. Federlin, *Am. J. Kidney Dis.*, 1993, **21**, 54; (c) R. Boer and V. Gekeler, *Drugs Future*, 1995, **20**, 499.
- S.-J. Tu, J.-F. Zhou, X. Deng, P.-J. Cai, H. Wang and J.-C. Feng, *Chin. J. Org. Chem.*, 2001, **21**, 313.
- G. Sabita, G. S. K. K. Reddy, C. S. Reddy and J. S. Yadav, *Tetrahedron Lett.*, 2003, **44**, 4129.
- L. M. Wang, J. Sheng, L. Zhang, J.-W. Han, Z.-Yu. Fan, H. Tian and C.-T. Qian, *Tetrahedron*, 2005, **61**, 1539.
- G. V. M. Sharma, K. L. Reddy, P. S. Lakshmi and P. R. Krishna, *Synthesis*, 2006, 55.
- A. Dondoni, A. Massi, E. Minghini and V. Bertolasi, *Tetrahedron*, 2004, **60**, 2311.
- A. Kumar and R. A. Maurya, *Tetrahedron*, 2007, **63**, 1946.
- (a) P. Tundo, P. Anastas, D. Stc, Black, J. Breen, T. Collins, S. Memoli, J. Miyamoto, M. Polyakoff and W. Tumas, *Pure Appl. Chem.*, 2000, **72**, 1207; (b) P. T. Anastas and J. C. Wagner, *Green Chemistry: Theory and practice*, Oxford University Press, Oxford, 1998.
- (a) J. Bewulf, G. Van, der Vorst, W. Aelterman, B. De Witte, H. Vanbaelen, and H. Van Langenhove, *Green Chem.*, 2007, **9**, 785; (b) A. Lapkin, in *Renewables-Based Technology. Sustainability Assessment*, ed. J. Dewulf and H. Van Langenhove, Wiley, Chichester, 2006, pp. 39–53.
- K.-H. Funken, *Sol. Energy Mater.*, 1991, **24**, 370.
- (a) K. U. Sadek, M. A. El-Maghraby, M. A. Selim and M. H. Elnagdi, *Bull. Chem. Soc. Jpn.*, 1988, **61**, 539; (b) K. U. Sadek, K. Abouhadid and A. H. H. Elghandour, *Liebigs Ann. Chem.*, 1989, 501; (c) R. A. Mekheimer, A. A. Abdel Hameed and K. U. Sadek, *Arkivoc*, 2007, **xiii**, 269.
- Maheswara, V. Siddaiah, J. L. V. Damu and C. V. Rao, *Arkivoc*, 2006, **ii**, 201.
- P. Esser, B. Pohlmann and H.-D. Scharf, *Angew. Chem., Int. Ed. Engl.*, 1994, **33**, 2009.
- M. Oelgemöller, N. Healy, L. de Oliveria, C. Jung and M. Mattay, *Green Chem.*, 2006, **8**, 831.
- A. Schönberg, G. O. Schenck and O. A. Neumüller, *Preparative Organic Photochemistry*, Springer, Berlin, 1968.
- A. Kumar and R. A. Maurya, *Tetrahedron Lett.*, 2007, **48**, 3887.
- S. Ko and C.-Fa. Yao, *Tetrahedron*, 2006, **31**, 7293.



# 2<sup>ND</sup> EUCHEMS CHEMISTRY CONGRESS

2008 SEPTEMBER 16 - 20  
TORINO, ITALY

## CHEMISTRY: THE GLOBAL SCIENCE

### PLENARY LECTURES BY

**Peter AGRE** (Baltimore, USA)  
**Avelino CORMA** (Valencia, Spain)  
**Jean M.J. FRÉCHET** (Berkeley, USA)  
**Robert H. GRUBBS** (Pasadena, USA)  
**Kyriacos C. NICOLAOU** (La Jolla, USA)  
**Martyn POLIAKOFF** (Nottingham, UK)  
**K. Barry SHARPLESS** (La Jolla, USA)

### KEYNOTE LECTURES BY

**Varinder AGGARWAL** (Bristol, UK)  
**Lucia BANCI** (Florence, IT)  
**Matthias BELLER** (Rostock, DE)  
**Richard CATLOW** (London, UK)  
**Ken CAULTON** (Bloomington, USA)  
**Fritz FRIMMEL** (Karlsruhe, DE)  
**Dante GATTESCHI** (Florence, IT)  
**Jana HAJŠLOVA** (Prague, CZ)  
**Dino MORAS** (Illkirch, FR)  
**Ulrich STIMMING** (Munich, DE)  
**Philip TAYLOR** (Geel, BE)  
**Jun-ichi YOSHIDA** (Kyoto, JP)

### SCIENTIFIC COMMITTEE

*Chair* **Hartmut MICHEL** (DE)  
*Co-chair* **Igor TKATCHENKO** (FR)

### ORGANISING COMMITTEE

*Chair* **Giovanni NATILE** (IT)  
*Co-chair* **Francesco DE ANGELIS** (IT)

### LOCAL ORGANISING COMMITTEE

*Chair* **Lorenza OPERTI** (IT)  
*Co-chair* **Salvatore COLUCCIA** (IT)

Special topic symposia:

### ADVANCES IN SYNTHESIS

- Organic Catalysis
- Radical Reactivity in Transition Metal Chemistry
- Reactions under Novel Conditions

### ADVANCES IN UNDERSTANDING

- Chemical Measurement Quality: Societal Impact
- Cutting Edge Chemistry with Computers
- Food Analysis: Pushing Detection Limits down to Nothing

### CHEMISTRY AND LIFE SCIENCES

- Biomolecular Interactions and Mechanisms
- Drug Targeting and Delivery
- Metal Homeostasis

### ENERGY AND INDUSTRY

- Biorefineries and Biotechnologies
- Energy Production & Storage
- New Trends for Agrochemicals

### ENVIRONMENT

- Greening Chemistry
- Greenhouse Gases
- Water Pollutants

### MATERIALS AND DEVICES

- Branched Polymers - Smart Functional Materials
- Nanomaterials
- Porous Materials

### cci ORGANISING SECRETARIAT

**Centro Congressi Internazionale** s.r.l. - Corso Bramante 58/9 10126 Torino - I  
 tel +39 011.2446911 fax +39 011.2446900/44 - info@euchems-torino2008.it

[www.euchems-torino2008.it](http://www.euchems-torino2008.it)

\*EuCheMS, the European Association for Chemical and Molecular Sciences incorporates  
 50 member societies which in total represent some  
 150.000 individual chemists in academia, industry and government in over  
 35 countries across Europe.

# 2nd International Symposium on Green Processing in the Pharmaceutical and Fine Chemical Industries

May 29-30, 2008  
Yale University  
New Haven, CT, USA

"This is the best Green Chemistry Conference that I have attended"- Green Chemistry Lead, Pfizer Inc

"I was somewhat humbled to be among the extraordinarily high caliber of speakers and from which I gained some very useful information"-  
Principal Scientist, J&J

"What a wonderful symposium!" - Professor,  
GeorgiaTech University

## Thank you to our sponsors:



SIGMA-ALDRICH®



## Media Partners

Green Chemistry

Pharmaceutical  
Technology

Pharmaceutical  
MANUFACTURING

Green Chemistry  
LETTERS AND REVIEWS

## Conference Coordination



Guiding Green.

## Objectives

- Create breakthrough innovations with green chemistry to revolutionize the pharmaceutical and fine chemical industries
- Share successes and opportunities to challenge ourselves to achieve greener process design.
- Implement green chemistry solutions through the supply chain

## Program

Organized by Paul T. Anastas, PhD, Chao-Jun Li, PhD, Berkeley W. Cue, Jr., PhD, and Julie B. Manley, CHMM

The program includes speakers representing:

- Research institutes including Warner-Babcock Institute for Green Chemistry and RIKEN
- Corporations including Pfizer Inc, AstraZeneca, Merck & Co., Inc, Schering-Plough Research Institute, BioVerdant, Lonza, DSM, Phoenix Chemicals LTD, Dr. Reddy's, and Novasep.
- Universities including Yale University, McGill University, Carnegie Mellon University, Monash University, University of North Texas, University of Alabama, and Institute for Molecular Science
- Speakers representing Australia, Canada, England, India, Japan, the Netherlands, Switzerland, and the United States.
- In depth technical presentations
- Panel discussion on pharmaceutical lifecycle
- Strong international presence
- Student poster and networking reception

## Registration

(Includes continental breakfast, lunch, and reception)

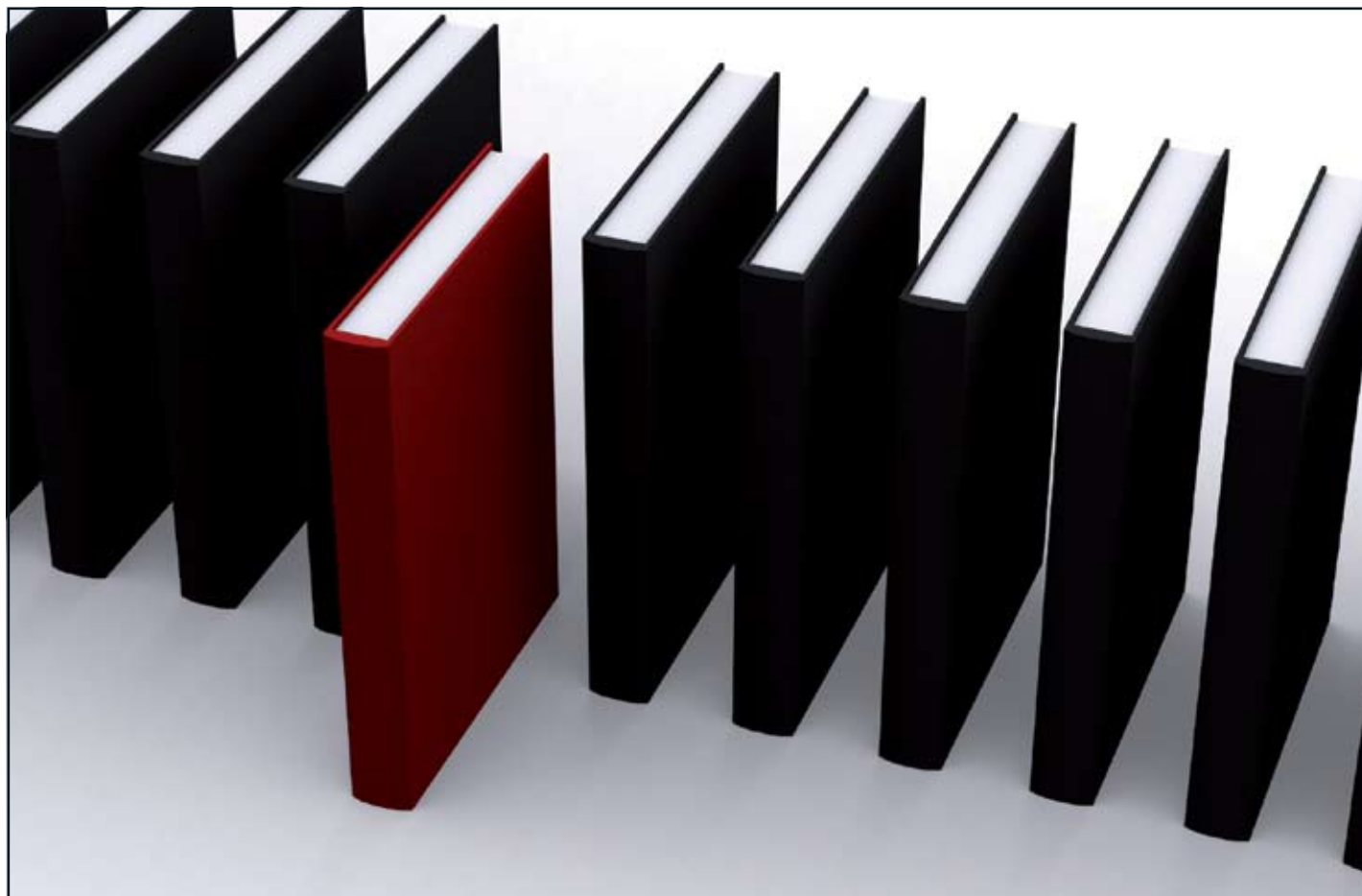
\$500 Industry      \$250 Academia/Gov't/NGO

\$100 Student

## Who should attend

Chemists, Chemical Engineers, Discovery, R&D, & Process Dev. Management, Technical Directors, Senior & Staff Scientists, Academia, Industry, NGOs, & Government

Register online now at [www.GuidingGreen.com/Pharm\\_FineChem.html](http://www.GuidingGreen.com/Pharm_FineChem.html)



## 'Green Chemistry book of choice'



Why not take advantage of free book chapters from the RSC? Through our 'Green Chemistry book of choice' scheme *Green Chemistry* will regularly highlight a book from the RSC eBook Collection relevant to your research interests. Read the latest chapter today by visiting the *Green Chemistry* website.

The RSC eBook Collection offers:

- Over 900 new and existing books
- Fully searchable
- Unlimited access

Why not take a look today? Go online to find out more!

RSC Publishing

[www.rsc.org/greenchem](http://www.rsc.org/greenchem)

Registered Charity Number 207890